AFRRI REPORTS

Third Quarter
1991

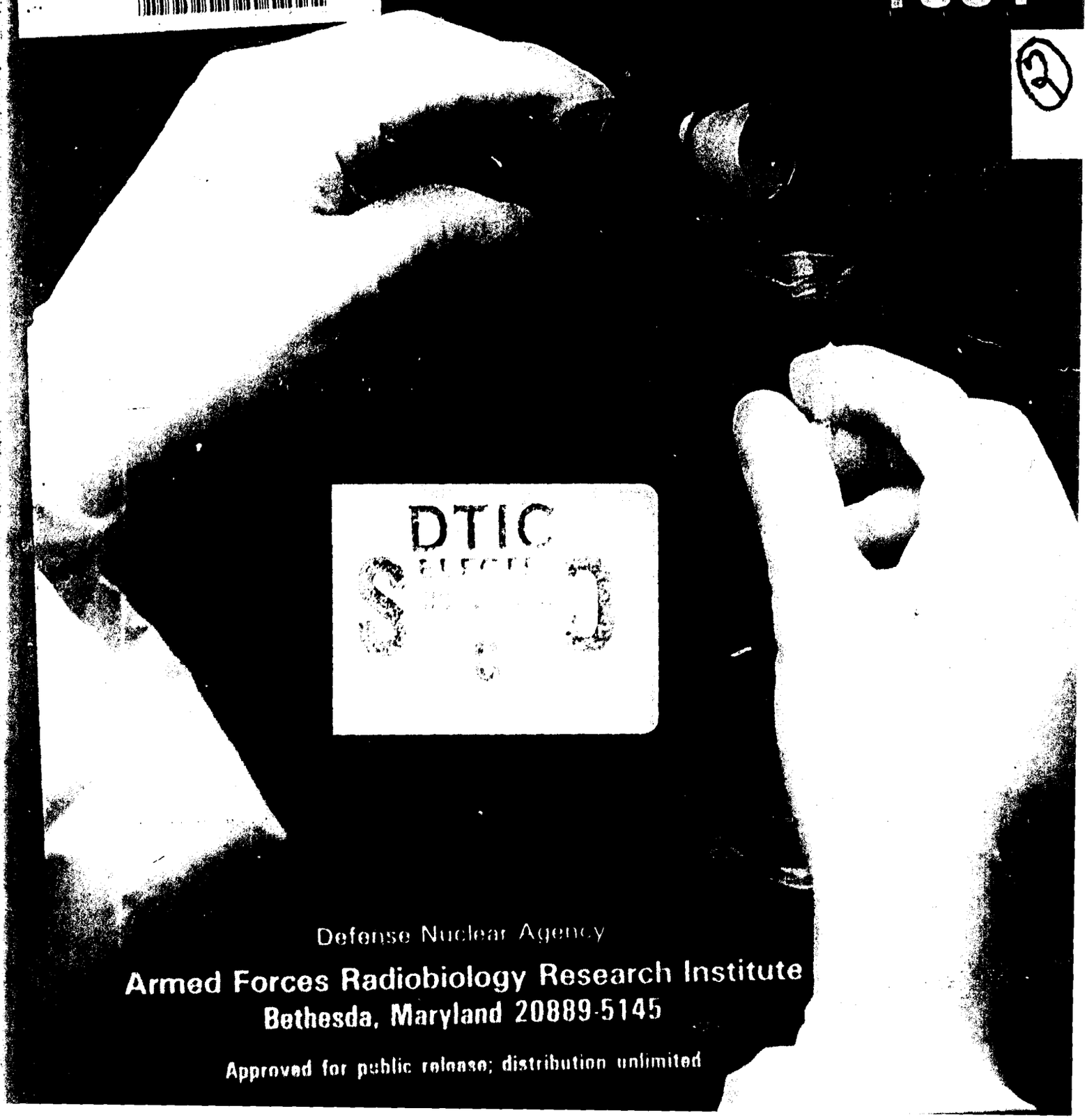

Defense Nuclear Agency

Armed Forces Radiobiology Research Institute
Bethesda, Maryland 20889-5145

Approved for public release; distribution unlimited

REPORT DOCUMENTATION PAGE

Form Approved
OMB No. 0704-0188

1. AGENCY USE ONLY *(Leave blank)*	2. REPORT DATE	3. REPORT TYPE AND DATES COVERED
	1991 October	Reprints/Technical

4. TITLE AND SUBTITLE

AFRRI Reports, Third Quarter 1991

5. FUNDING NUMBERS

PE: NWED QAXM

6. AUTHOR(S)

7. PERFORMING ORGANIZATION NAME(S) AND ADDRESS(ES)

Armed Forces Radiobiology Research Institute
Bethesda, MD 20889-5145

8. PERFORMING ORGANIZATION REPORT NUMBER

SR91-36 - SR91-41

9. SPONSORING/MONITORING AGENCY NAME(S) AND ADDRESS(ES)

Defense Nuclear Agency
6801 Telegraph Road
Alexandria, VA 22310-3398

10. SPONSORING/MONITORING AGENCY REPORT NUMBER

11. SUPPLEMENTARY NOTES

12a. DISTRIBUTION/AVAILABILITY STATEMENT

Approved for public release; distribution unlimited.

12b. DISTRIBUTION CODE

13. ABSTRACT *(Maximum 200 words)*

This volume contains AFRRI Scientific Reports SR91-36 through SR91-41 for Jul-Sep 1991.

14. SUBJECT TERMS

15. NUMBER OF PAGES

81

16. PRICE CODE

17. SECURITY CLASSIFICATION OF REPORT	18. SECURITY CLASSIFICATION OF THIS PAGE	19. SECURITY CLASSIFICATION OF ABSTRACT	20. LIMITATION OF ABSTRACT
UNCLASSIFIED	UNCLASSIFIED	UNCLASSIFIED	UL

CLASSIFIED BY:

DECLASSIFY ON:

CONTENTS

Scientific Reports

SR91-36: Gallin, E. K. Ion channels in leukocytes.

SR91-37: Mickley, G. A., Ferguson, J. L., Mulvihill, M. A., and Nemeth, T. J. Early neural grafts transiently reduce the behavioral effects of radiation-induced fascia dentata granule cell hypoplasia.

SR91-38: Pellmar, T. C., Hollinden, G. E., and Sarvey, J. M. Free radicals accelerate the decay of long-term potentiation in field CA1 of guinea-pig hippocampus.

SR91-39: Samid, D., Miller, A. C., Rimoldi, D., Gafner, J., and Clark, E. P. Increased radiation resistance in transformed and nontransformed cells with elevated *ras* proto-oncogene expression.

SR91-40: Swenberg, C. E., Birke, S., and Geacintov, N. E. Characterization of the interaction of the radioprotector 1-methyl-2-[2-(methylthio)-2-piperidinovinyl]quinolinium iodide with supercoiled DNA.

SR91-41: Vogel, S. N., Henricson, B. E., and Neta, R. Roles of interleukin-1 and tumor necrosis factor in lipopolysaccharide-induced hypoglycemia.

PHYSIOLOGICAL REVIEWS
Vol. 71, No. 3, July 1991
Printed in U.S.A.

Ion Channels in Leukocytes

ELAINE K. GALLIN

Department of Physiology, Armed Forces Radiobiology Research Institute, Bethesda, Maryland

I. Introduction 775
II. Terminology 775
III. Phagocytic Leukocytes 776
A. Macrophages 776
B. Neutrophils 785
IV. Lymphocytes 787
A. T lymphocytes and natural killer cells 788
B. B lymphocytes 799
V. Conclusion 804

I. INTRODUCTION

The purpose of this article is to review the ionic channels that have been characterized in leukocytes and, whenever possible, to discuss their functional significance. This review makes no attempt to provide a comprehensive view of ionic transport mechanisms in leukocytes, nor does it attempt to provide an inclusive summary of the numerous studies done using ion-flux techniques and fluorescence measurements that have examined the role of ionic transport in leukocyte function. Rather, it focuses on the electrophysiological evidence for the existence of specific ionic channels in leukocytes, with the exception of the basophil, which is not covered in this review. (Information on the basophil is more appropriately included in a review of mast cells.) Several recent reviews are available for those interested in a discussion of other transport mechanisms in leukocytes (47, 69, 73, 75, 87).

Because significant progress in this area has depended on the development of the patch-clamp technique by Neher and Sakmann in 1976 (181), the area of investigation is relatively young, the studies covered in this review are just a beginning. Undoubtedly, many channels are yet to be described in leukocytes, and much more will be learned about the relevance of ionic channels to leukocyte function. The observations that the gating of ionic channels can be modulated by phosphorylation and dephosphorylation reactions (217, 246), as well as by a variety of second messengers (132, 217), already have provided an important regulatory link between biochemical events inside leukocytes and ionic channels (72, 73; e.g., see sect. IV*A3*).

II. TERMINOLOGY

Ionic channels are integral membrane proteins that provide low energy pathways for ions to cross cellular membranes, allowing ions to flow passively down their electrochemical gradient at rates exceeding 10^6 ions/s. The high rate of flow of ions through channels and their discrete transitions between open and closed states facilitates the measurement of these transport events (currents) through individual macromolecules. It should be noted that for small currents that are not voltage gated and that have single-channel current amplitudes too small to detect (<1 pA), discriminating between a current through an ionic channel and one produced by carrier-mediated transport can be difficult (151, 164; e.g., see sect. IV*A3*).

If an ion channel is open and the membrane potential (V_m) differs from the electrochemical potential for ion x (E_x, the potential difference at equilibrium), then current will flow into or out of the cell depending on the driving force on x. When V_m is equal to E_x, no current (I) will flow. The current flowing across an ion channel divided by the net electrochemical driving force (V) across the channel is equal to its ion conductance (G), which is expressed in siemens (S) or in reciprocal ohms ($G = I/V$), and is a measure of the ease with which ions flow across the channel. Single-ion channels have conductances in the range of picosiemens (10^{-12} S). Some channels allow current to flow more easily in one direction than in the other direction, a property called rectification. Thus an inwardly rectifying cation channel is one in which cations flow more easily into the cell than out of the cell (conversely, an inwardly rectifying anion channel would allow anions to flow out of the cell more easily than into the cell). In these cases, a plot of the relationship between current and voltage (I-V) will be nonlinear (nonohmic).

Ion channels can be characterized by their conductances, gating properties (factors controlling channel opening and closing), kinetics (rates at which channels open and close), ionic selectivity (differential permeability), and pharmacology (the action of specific agents in

blocking or changing the flow of ions). Furthermore, channel activity can be modified by the presence of competing ions or other molecules, such as GTP-binding proteins or inositol phosphates. Ionic channels have been best characterized in excitable cells where they have been studied for the past 50 years (107). With the advent of the patch-clamp technique, much progress has been made on other cell types, including leukocytes, where ionic channel openings in response to specific chemical ligands (ligand gated), voltage (voltage gated), or both have been described.

Most of the studies discussed in this review used the patch-clamp technique. This technique is extremely versatile because it can be used in a number of recording configurations (103). *1*) the cell-attached patch mode in which single-channel currents are recorded from patches of membrane in intact cells, *2*) two excised-patch modes in which patches of membrane are pulled away from the cell and single-channel currents are recorded with the inside surface of the membrane facing either the bath solution (inside-out patch) or the pipette solution (outside-out patch), and *3*) the whole cell configuration in which currents representing an average of the single-channel currents across the whole cell are measured. In the whole cell configuration, the inside of the cell is perfused with the solution in the patch electrode, this allows the addition of second messengers and other substances to the inside of the cell but also has the disadvantage of washing out intracellular constituents that might modulate the ionic channels being studied (103). This disadvantage has been recently eliminated by a modification of the whole cell configuration, the "nystatin-permeabilized patch" (111). The antibiotic nystatin is added to the pipette solution, reducing the resistance between pipette and cytoplasm. Although this is analogous to whole cell recording, large molecules and even divalent ions do not leave the cell, and second messenger-mediated responses can be observed that do not remain functional in conventional whole cell recording.

III. PHAGOCYTIC LEUKOCYTES

Macrophages, neutrophils, and eosinophils are phagocytic leukocytes that are capable of migrating toward invading microorganisms and/or tumor cells, engulfing them, and ultimately killing them. During these events a number of enzymes, cytokines, toxic oxygen products, and other factors having widespread actions are released. In recent years much has been learned about the physiology of phagocytic cells, including the role of phosphoinositide metabolism, GTP-binding proteins, and protein kinase C in phagocyte activation (10, 256, 269). In addition to these agents, interest in the possible role of ions in stimulus-response coupling in phagocytic cells has resulted in a steady increase in electrophysiological studies that have characterized a number of conductances in these cells. Table 1 contains a list of the ionic conductances in phagocytes. These studies examined neutrophils, macrophages, and related tumor cell lines. Unfortunately, no data exist on the ionic channels in the eosinophil.

A. Macrophages

Macrophages, found in virtually every tissue, originate from bone marrow cells that are released into the blood as monocytes (272). Monocytes circulate in the blood for up to several days until they emigrate into the tissues and mature into macrophages. Macrophages can survive in tissues for months and even possibly years, playing pivotal roles in numerous aspects of host defenses, including processing antigens, killing parasites and tumor cells, ingesting dead or dying cells, and secreting cytokines.

Electrophysiological studies at the whole cell or single-channel level have demonstrated that macrophages exhibit both voltage-gated and Ca gated ionic currents. Four K currents, three Cl currents, and nonselective cation currents have been identified and are described in detail next. Although one laboratory reported action potentials in human monocyte-derived macrophages (165, 283), those events were poorly characterized, and they have not been noted by other investigators. Furthermore, no voltage-dependent Na or Ca currents have been described in macrophages. Both Fc immunoglobulin and ATP receptor-gated ionic conductances have been described in macrophages and are also discussed.

1. Potassium conductances

1) VOLTAGE-DEPENDENT INWARDLY RECTIFYING POTASSIUM CONDUCTANCE. An inwardly rectifying K (K_i) current that activates at voltages negative to −50 mV was first described in intracellular microelectrode studies of mouse spleen and thioglycolate-induced macrophages that had been cultured for several weeks (61, 65). The K_i current has since been characterized in cultured human monocyte-derived macrophages (68, 182), in the murine macrophage-like cell line J774.1 (70), in mouse peritoneal macrophages (212), and in phorbol ester-induced differentiated HL60 cells (a human promyelocytic leukemia cell line) (278). This current is similar to the inwardly rectifying K current characterized in several other cell types, including starfish egg cells (100), frog skeletal muscle (142), heart muscle (80), bovine pulmonary artery endothelial cells (251), and rat basophilic leukemia cells (154).

In macrophages, the K_i current has been best characterized in J774.1 cells, where it has a steep voltage dependence (fractional activation decreased from 66% at −90 mV to 26% at −70 mV) and a time-dependent inactivation (70). Inactivation, which was evident for voltage steps to potentials more negative than −100 mV, followed first-order kinetics and had a rate that increased with membrane hyperpolarization. Whole cell

TABLE 1. *Ion channels in phagocytes*

Channel	Gating	SCG, pS	Blockers	Present In	Reference
			Macrophage		
K channels					
K_o (outward inactivating)	Voltage	16	D 600, TEA, 4-AP, Cs_i, Ba_i	Mouse peritoneal, human blood-derived, human alveolar macrophages; J774.1, P388D1, HL60 cells	70, 183, 290
K_{o2} (outward poorly inactivating)	Voltage		TEA, 4-AP, Cs_i	Human blood-derived macrophages	183
K_i (inwardly rectifying)	Voltage	30*	Ba, Cs, Rb	Mouse peritoneal and spleen, human blood-derived macrophages; J774.1, HL60 cells	68, 70, 211, 278
K_{LCa} (large, Ca and voltage activated)	Ca_i and voltage	240*	CTX, TEA, Cs_i	Human blood derived, human alveolar macrophages	62, 120a, 121, 166
K_{iCa} (inwardly rectifying, Ca activated)	Ca_i	36*	Ba	Human blood-derived, mouse peritoneal macrophages; U937 cells	63, 104, 120a, 121
Cl channels					
Cl_L (large)	Voltage	340	DIDS	U937 cells; mouse peritoneal macrophages	121, 212, 236
Cl_i (intermediate)	Voltage	28	DIDS	U937 cells	121
Cl_s (small)	Voltage	16		U937 cells	121
Cation channels					
Nonselective	Ca_i	Variable	Zn	P388D1 cells; human blood-derived macrophages	155, 183
Fc	Fc-ligand	60		Mouse macrophages	287, 288
			Neutrophil		
K channels					
Outward				Human neutrophils	128
Ca activated	Ca_i			Human neutrophils	128
Cl channels					
Ca activated	Ca_i			Human neutrophils	128
Cation channels					
Nonselective	Ca_i	18-25 4-6		Human neutrophils	276

SCG, single channel conductance under physiological ionic gradients or *115 mM external K (for rectifying channels, largest conductance is given). Ca_i, Cs_i, Ba_i, internal Ca, Cs, and Ba. 4-AP, 4-aminopyridine, CTX, charybdotoxin, DIDS, 4,4-diisothiocyanostilbene-2,2-disulfonic acid; TEA, tetraethylammonium.

K_i currents showing activation and inactivation are shown in Figure 1.1 Removal of external Na reduced (by >50%) inactivation (Fig. 1.1, *bottom*) but did not abolish it, suggesting that some of the inactivation was due to the intrinsic voltage dependence of the channel (176). Voltage-dependent inactivation was verified in single-channel records in the absence of external Na (Fig. 1*B*). As in other cells that display this type of inwardly rectifying K conductance (100, 101), raising extracellular K concentration ($[K]_o$) increased the slope conductance for the inward currents and shifted the voltage dependence to the right, indicating that the activation of the K_i conductance depended on $[K]_o$ (70). Similar results were reported in mouse peritoneal macrophages, where increasing $[K]_o$ from 5 to 110 mM increased the maximum slope of the K_i conductance by a factor of 5.1 (212). External Ba blocked the K_i current in a voltage-dependent manner (170), with complete block occurring at 2.5 mM Ba (70) The K_i current was also reduced by the addition of 1 mM Cs (70).

Single-channel currents, the properties of which correspond to the macroscopic K_i current measured in whole cells, have been described in both J774.1 cells (170) and in human peripheral blood-derived macrophages (68). In both these cell types, single-channel currents were evident in cell-attached patches (145 mM KCl in electrode and normal saline in bath) at zero holding potential (the resting V_m of the cells). Under these conditions the single-channel conductance in cell-attached patches was 29 pS for inward currents, and the extrapolated reversal potential was near E_K. No outward currents were noted at potentials above E_K, indicating either an extreme rectification at the single-channel level or an absence of detectable channel openings positive to E_K. In ventricular heart cells, inward rectification through K_i channels was abolished by removing internal Mg (172). In contrast, the inward rectifier in bovine pulmonary endothelial cells has a voltage- and $[K]_o$-dependent gating mechanism that is distinct from Mg block (251). At potentials more negative than

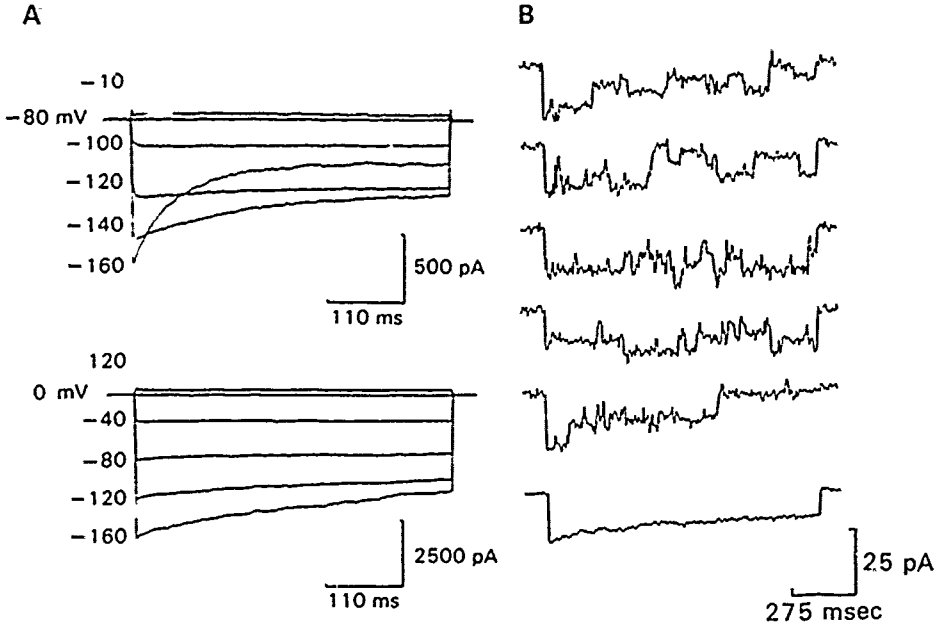

FIG. 1. Inwardly rectifying K (K_i) currents in J774.1 cell. Patch electrode contained (in mM) 145 KCl, 1 $MgCl_2$, 1.1 EGTA, 0.1 $CaCl_2$, and 10 HEPES (pH 7.3). *A*: whole cell currents in response to 440-ms test pulses given every 8 s to potentials shown. *Top*: tracings from cell held at −80 mV and bathed in 150 mM NaCl Hanks' solution. *Bottom*: tracings from cell held at 0 mV and bathed in 150 mM KCl Hanks'. *B*: first 5 current tracings are single-channel currents recorded in cell-attached patch configuration recorded in response to voltage step to −190 mV from holding potential of −30 mV. Bottom tracing is averaged current record for above tracings, comprised of 40 individual tracings. Cell bath is 150 mM KCl Hanks' solution. [From McKinney and Gallin (170).]

120 mV (and in the absence of external Na), averaged single-channel currents showed time-dependent inactivation. The single-channel activity had complex kinetics, manifesting closures of short and long duration that indicated the presence of more than one closed state (170). Single K_i channel currents were blocked by external Ba (2.5 mM) and, like whole cell currents, the single-channel K_i conductance was proportional to the square root of $[K]_o$ (170). The density of K_i channels in J774.1 cells was estimated to be 47 channels/pF or 0.47 channels/μm^2, assuming a specific capacitance of 1 $\mu F/cm^2$ (170).

A) Expression. Macrophages do not always express the K_i conductance. Furthermore, channel expression can be modified by external factors, such as culture conditions. For example, Ypey and Clapham (290) reported that inward rectification was absent in mouse peritoneal macrophages cultured for up to 4 days, whereas previous (65) and subsequent (211) studies on mouse peritoneal macrophages cultured for 5 days or more demonstrated I V relationships with prominent inward rectification. Gallin and Sheehy (70) reported that J774.1 cells that adhered to a glass or plastic surface for ~18 h had a prominent K_i conductance, whereas this conductance was either absent or quite small in cells that adhered for only a few hours. Randriamampita and Trautmann (212) noted that fluid perfusion during whole cell patch-clamp recordings of J774.1 cells reduced the K_i currents. More recently it was demonstrated that the specific K_i conductance (whole cell conductance corrected for leak and normalized to membrane capacitance) of J774.1 cells allowed to adhere for 15 min to 1 h was one-half the specific K_i conductance of long-term (~18 h) adherent cells (171). The increase in specific K_i conductance was associated with a shift in V_m of the cells to more negative potentials, indicating that the K_i conductance participates in setting the cells' resting V_m. These findings are consistent with the earlier observation that block of K_i depolarizes macrophages (70). In J774.1 cells, treatment with the protein synthesis inhibitor cycloheximide abolished the adherence-induced augmentation of the specific K_i conductance, suggesting that the synthesis of new channel protein was required for the upregulation of these channels after adherence (171).

In addition to being affected by culture conditions, two reports indicate that the K_i conductance may be modified by specific agonists. A brief report by Moody-Corbett and Brehm (178) on rat thymus-derived macrophages revealed that the inwardly rectifying current was reduced by acetylcholine and muscarine. Wieland et al. (278) reported that this conductance, present in HL60 cells differentiated to macrophage-like cells with phorbol esters (but absent from HL60 cells that were differentiated to granulocyte-like cells with retinoic acid), was inhibited by the addition of recombinant human colony-stimulating factor I. Further studies are needed to determine the functional relevance of this interesting observation. It should be noted that a recent study by McCloskey and Cahalan (169) demonstrated that in rat basophilic leukemia cells the K_i conductance is inhibited by GTPγS (100 μM) and GppNHp (100 μM), two GTP analogues that activate G proteins. Thus it is possible that colony-stimulating factor I is blocking the K_i conductance in HL60 cells by activating G proteins.

II) LARGE CALCIUM- AND VOLTAGE-ACTIVATED POTASSIUM CONDUCTANCE. Single-channel patch-clamp recordings from human monocyte-derived macrophages that have been grown in culture for 1-6 wk have demonstrated a large-conductance K channel (240 pS in symmetrical K, 110 pS in 150 mM $[Na]_o$/5 mM $[K]_o$) (62, 166). Similar channels are also present in human alveolar macrophages (121) but are absent in J774.1 cells (E. K. Gallin and L. C. McKinney, unpublished observations)

and in the promonocyte cell line U937 (121). Furthermore, activation of U937 cells with recombinant interferon-γ (1,000 U/ml), recombinant interferon-αA (1,000 U/ml), or 12-*O*-tetradecanoylphorbol-13-acetate (TPA, 10 ng/ml) before recording from cells failed to induce the expression of the large-conductance Ca-activated K ($K_{L Ca}$) channels in excised patches (121).

In cell-attached patches from human monocyte-derived macrophages, the $K_{L Ca}$ channel was active only when the patch potential was stepped to very depolarized levels (>80 mV). Excised patch recordings indicated that channel open time increased with both membrane depolarization and increased intracellular Ca concentration ($[Ca]_i$) (62). However, this channel was relatively insensitive to $[Ca]_i$, because at $3 \cdot 10^{-6}$ M $[Ca]_i$ the open-state probability of the channel at +60 mV was only 0.03–0.21 (68). Thus, in the macrophage, large increases in $[Ca]_i$ (>10^{-6} M) are required to activate $K_{L Ca}$ channels at negative membrane potentials. Exposing the extracellular surface of the membrane to 25 nM charybdotoxin [CTX; a proteinaceous component of toxin from *Leiurus quinquestriatus* known to block Ca-activated K channels in other cells (175, 263)] or tetraethylammonium ions (TEACl; 15 mM) abolished $K_{L Ca}$ channel activity (68).

Whole cell currents corresponding to the activity of $K_{L Ca}$ channels have been described in human monocyte-derived macrophages that were perfused intracellularly with a saline solution containing 3×10^{-6} M Ca (68, 183). These currents, activated during voltage steps to potentials >40 mV, were characterized by a noisy baseline (consistent with a large single-channel conductance) and had tail currents that reversed at E_K (60). In addition, either CTX (60) or TEA (68, 183) blocked this current, suggesting that whole cell outward currents represented the activation of $K_{L Ca}$ channels. Randriamampita and Trautmann (212) demonstrated that increasing $[Ca]_i$ from 0.1 to 1 μM increased whole cell currents in both J774.1 cells and mouse peritoneal macrophages and that quinine (0.1–1 mM) markedly reduced these currents. However, unlike the $K_{L Ca}$ conductance in human monocyte-derived macrophages, the whole cell currents they described in J774.1 cells and mouse peritoneal macrophages showed no voltage sensitivity, making it unlikely that they were due to the activation of $K_{L Ca}$ channels.

Membrane hyperpolarizations, reflecting the activation of a Ca-activated K conductance, were first described in macrophages in 1975 (71, see sect. IIIA5ii). A cell-attached patch-clamp study by Ince et al. (117) reported that, during membrane hyperpolarizations induced by microelectrode impalement, the voltage range of activation of the $K_{L Ca}$ channels shifted so that they were open 80% of the time at potentials of 0 to −20 mV. Nevertheless, studies using Ca-indicator dyes have reported $[Ca]_i$ increases after physiological stimulations that are too low (in the range of 0.2–1 μM) (32, 129) to activate $K_{L Ca}$ channels at negative V_m. Therefore it is not clear whether $K_{L Ca}$ channels are normally activated under conditions of physiological stimulation, either the $[Ca]_i$ sensitivity of the $K_{L Ca}$ channels is different in situ from that of the excised patch or these channels open rarely during stimulation. Alternatively, the $K_{L Ca}$ conductance may function in intracellular compartments where $[Ca]_i$ levels may be high.

iii) CALCIUM-ACTIVATED INWARDLY RECTIFYING POTASSIUM CONDUCTANCE. Gallin (63) has demonstrated in cell-attached patches from cultured human macrophages that both ionomycin (Fig. 2) and platelet-activating factor, two substances known to transiently increase $[Ca]_i$, induced bursting channel activity that was very different from $K_{L Ca}$ channel activity. In these studies, the induced currents, which were permeable to K and poorly permeable to Na and Cl, had single-channel conductances (with 150 mM KCl in the pipette) for inward currents of 37 pS; channel activation was independent of voltage. Similar channels have been described in human alveolar macrophages (120a).

The Ca-activated inwardly rectifying K ($K_{i Ca}$) channel in cultured human macrophages can be differentiated from the K_i channel on the basis of its Ca sensitivity, its conductance (37 vs. 29 pS for inward currents), its kinetics (bursting vs. nonbursting), its lack of voltage dependence, and its differing sensitivity to block by external Ba. Three millimolar Ba, a concentration that completely blocked the voltage-dependent K_i channel (170), did not significantly block the $K_{i Ca}$ channel at the resting V_m and produced only a partial block when the patch was hyperpolarized (63).

An inwardly rectifying K channel, the open probability of which was independent of voltage but dependent on $[Ca]_i$, also has been reported in excised inside-out patches from U937 cells (121) and in cell-attached patches from mouse peritoneal macrophages after exposure to 100 μM ATP (104). In contrast to the findings in human macrophages, the single-channel conductance in patches from U937 cells and from mouse peritoneal macrophages was only 25–28 pS at voltages between −40 and 100 mV. Similar Ca-activated inwardly rectifying K channels with single-channel conductances for inward current ranging from 50 to 25 pS have been described in lymphocytes (160), erythrocytes (98), and HeLa cells (227, 228).

Both spontaneous and Ca ionophore-induced oscillatory membrane hyperpolarizations have been recorded in macrophages using intracellular microelectrodes (71, 201), and it is likely that $K_{i Ca}$ channels (rather than $K_{L Ca}$ channels) are responsible for these events because *1*) the $K_{i Ca}$ channel is active at the resting V_m after exposure to ionomycin, whereas the $K_{L Ca}$ channel is not, *2*) the bursting pattern of the $K_{i Ca}$ channel is oscillatory, and *3*) the activity of the $K_{i Ca}$ channel is associated with the oscillatory changes in V_m induced by ionomycin.

As noted in the previous section, Randriamampita and Trautmann (212) reported a linear increase in membrane conductance in whole cell recordings of J774.1 cells and murine peritoneal macrophages obtained under conditions of high $[Ca]_i$, which they concluded was due to a voltage-insensitive Ca-activated K

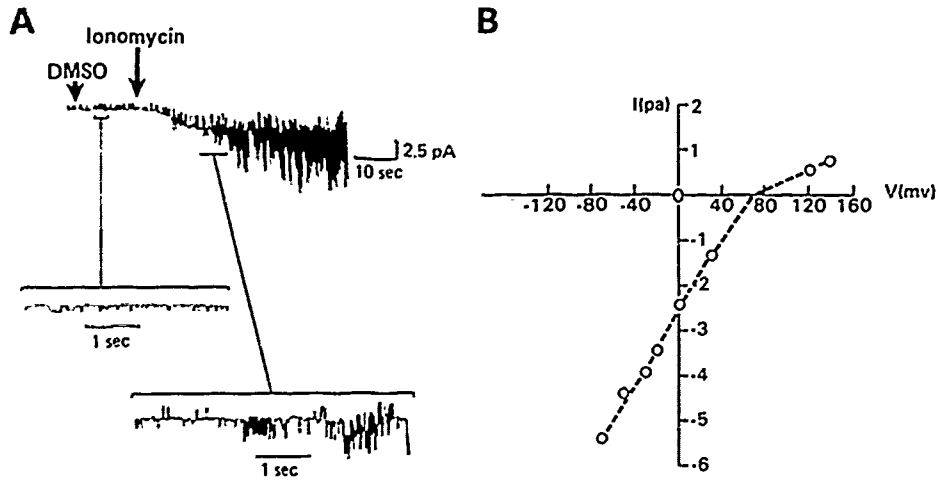

FIG. 2. Ionomycin-induced K channels in human macrophages. *A*, chart recorder tracing of current recorded from cell-attached patch in which cell was exposed first to 0.1 % dimethyl sulfoxide (DMSO) and then 10^{-6} M ionomycin from perfusion pipette. Potential across patch was equal to resting membrane potential, cell was bathed in 150 mM NaCl Hanks' solution. Patch electrode contained 150 mM KCl Hanks' solution. K_i channel activity was evident before exposure of cell to either agent and can be seen in expanded time and voltage scale in middle current tracing. After ionomycin addition, Ca activated inwardly rectifying K ($K_{i,Ca}$) channels were activated and could be seen in expanded time and voltage scale in bottom tracing. *B*, current-voltage (*I-V*) relationship showing inward rectification of ionomycin-induced channels. Single-channel conductance for inward currents = 37 pS. [From Gallin (63).]

conductance. Although it is possible that this conductance was due to the activation of $K_{i,Ca}$ channels, the fact that the conductance reported by Randriamampita and Trautmann (212) showed no rectification argues against this possibility.

IV) INACTIVATING OUTWARD POTASSIUM CHANNEL. An inactivating outward K (K_o) conductance has been described at the whole cell current level in resident mouse peritoneal macrophages (290), cultured human blood-derived monocytes (183, 185), cultured human alveolar macrophages (184), and two macrophage-like cell lines, J774.1 (70, 212) and P388D1 (245). This conductance activated at potentials positive to −30 mV. Current activation had a time course that fit first-order kinetics with a time constant that decreased for steps to more depolarized potentials (183). Inactivation of the K_o current also could be fit by a single exponential with a time constant (~340 ms) that was insensitive to voltage for potentials positive to −20 mV (70). The K_o currents were blocked by extracellular 4-aminopyridine (4-AP, ~5 mM) and by intracellular Ba, Cs, and TEA (70, 183, 290). External TEA (10 mM) also partially blocked the current (290). Similar outward currents have been described in detail in T lymphocytes (17) and are discussed in section IV.*A*. Ypey and Clapham (290) recorded a 16-pS channel in outside-out excised patches under conditions of asymmetric K (140 mM in pipette, 2.8 mM in bath) that, during depolarizing voltage steps, was activated in a time-dependent manner similar to the whole cell K_o currents.

There is no consistent pattern of K_o channel expression across different types of macrophages, it was reported in only 5% of the recordings from cultured blood derived human monocytes, whereas it was noted in 50% of the recordings from cultured human alveolar macrophages (184). Furthermore, for a given type of macrophage, the K_o conductance appears to be variably expressed with time in culture. For example, in J774.1 cells, K_o currents were described in a percentage of cells recorded from 1–8 h after adherence but were rarely present in cells from long-term adherent cultures (70). Ypey and Clapham (290), using resident mouse peritoneal macrophages, reported that K_o conductance was absent during the 1st day after isolation but was present in 96% of cells cultured 1–4 days. Randriamampita and Trautmann (212) also recorded outward currents in mouse peritoneal macrophages cultured for 1–2 days but found that the currents decreased after 5–6 days in culture. Interestingly, in those cells, fluid movement caused by perfusing the bathing medium increased the outward K current (212), whereas the addition of 2 mM *N*-formyl-methionine-leucine-phenylalanine (FMLP, a chemotactic peptide), histamine (20 mM), bradykinin (20 μM), and acetylcholine (50 μM) had no effect on the K_o current (290). (However, it should be noted that mouse macrophages do not respond to FMLP.) Finally, Nelson and colleagues reported that in human blood-derived monocytes, phorbol esters decrease the amplitude of the K_o current (185) and that treating cells for 24 h with bacterial lipolysaccharide (LPS) increased the percentage of cells expressing K_o current from near 0% to 30% (120).

V) POORLY INACTIVATING OUTWARD POTASSIUM CHANNEL. A second outward K conductance has been reported in a whole cell patch-clamp study of cultured human blood-derived monocytes (183). This conductance, noted in the majority of the cells studied, activated at voltages more positive than −10 mV and exhibited no steady-state inactivation for holding potentials of −60 to 0 mV. Inactivation, present for voltage steps

>0 mV, could be fit by a single exponential with a time constant of 951 ms at 10 mV. However, unlike the inactivating K_o conductance, little cumulative inactivation of the poorly inactivating outward K (K_{o2}) conductance was noted. Intracellular Cs blocked the current, as did extracellular TEA (4 mM). This current is similar to the slowly inactivating K_1 conductance that activates at voltages of >0 mV, which has been described in murine T lymphocytes (37; see sect. IV*A1*).

2. *Chloride conductances*

Three different Cl conductances have been described at the single-channel level in excised patch-clamp studies of macrophages. At the whole cell level, Nelson et al. (183) reported an outward current in human monocyte-derived macrophages under conditions where the patch electrode contained either Cs or Na instead of K. The authors concluded that this current was probably a Cl current because *1*) its amplitude was reduced, and its reversal potential shifted when Cl was replaced with the anion aspartate; and *2*) it was blocked by the anion channel blocker 4-acetamido-4′-isothiocyanostilbene-2,2′-disulfonic acid (SITS; 1 mM). However, it is not clear whether this whole cell current corresponds to any of the three Cl channels described in single-channel studies.

I) LARGE-CONDUCTANCE CHLORIDE CHANNEL. A very large-conductance Cl (Cl_L) (180-390 pS) channel was first reported in mouse peritoneal macrophages by Schwarze and Kolb (236) and has been described more recently in excised patches from two macrophage-like cell lines, J774.1 (212) and U937 (121). This channel is very similar to the large Cl channel described in rat skeletal myotubes (9), lymphocytes (12, 167, 195), and other cells. In mouse peritoneal macrophages, Cl_L channel activity was absent in cell-attached patches but became activated when cells were exposed to the Ca ionophore A23187 or when the patch was excised (236). Similar findings were reported by Randriamampita and Trautmann (212) in both mouse peritoneal macrophages and J774.1 cells, where the channel, rarely active in cell-attached patches, was frequently seen in excised patches. In both mouse peritoneal macrophages (236) and U937 cells (121), after excision of the patch a lag occurred before the Cl_L channels were observed. This observation has led Kanno and Takishima (121) to propose the existence of an in situ factor that inhibits these channels.

The Cl_L channels in mouse peritoneal macrophages had a selectivity ratio for Cl over Na of 5.1 (236) and a Cl-to-cation permeability ratio of between 14 and 5 (212). Multiple subconductance states of the Cl_L channel were noted in both mouse peritoneal macrophages (236) and U937 cells (121). In U937 cells the subconductance states were unaffected by the pH buffers *N*-2-hydroxyethylpiperazine-*N*′-2-ethanesulfonic acid (HEPES), tris(hydroxymethyl)aminomethane (Tris), or *N*,*N*-bis(hydroxyethyl)-2-aminoethanesulfonic acid (BES), and neither intracellular pH (pH_i) nor Ca affected the open probability of the channel or the frequency of appearance of the subconductance states (121). Kanno and Takishima (121) reported that in U937 cells, the anion transport blocker 4,4′-diisothiocyanostilbene-2,2′-disulfonic acid (DIDS, 100 μM) produced a flickery block of channel activity, whereas increasing DIDS to 1 mM irreversibly blocked the channel.

The Cl_L channel exhibited complex bursting behavior with at least three kinetically distinguishable nonconducting states (236). Channel activity (in symmetrical saline solution) could be induced by stepping to holding potentials on either side of 0 mV but were inactivated subsequently with the rate of inactivation increasing as the magnitude of the voltage jumps increased (236). Randriamampita and Trautmann (212) reported a somewhat different behavior for the Cl_L channel in both mouse peritoneal macrophages and J774.1 cells in that the probability of channel opening was high at positive potentials (up to 40 mV) and declined at hyperpolarized potentials or when the patch was depolarized beyond 40 mV.

The Cl_L channel has been modeled using two voltage-sensitive gates in series to describe the voltage-dependence of the burst kinetics for the channel (236). Schwarze and Kolb (236) suggested that the voltage-dependent gating properties of the Cl_L channel resemble the properties of voltage-dependent gap junctions and that the Cl_L channel may play a role in intercellular communication. However, octanol, a blocker of gap junction channels, does not block these channels, suggesting that they are not related to gap junction channels (212).

Although cell-attached patch experiments indicated that this channel is quiescent in resting cells, Cl_L channels were elicited by perfusing mouse peritoneal macrophages with zymosan (a particulate fraction of yeast cell wall that macrophages can ingest) during cell-attached patch recordings (125, 258).

II) INTERMEDIATE-CONDUCTANCE CHLORIDE CHANNEL. In addition to the Cl_L channel, two other smaller conductance Cl channels were noted 10 s to several minutes after excising patches from U937 cells (121). In symmetrical 150 mM NaCl, an intermediate Cl channel (Cl_i) that exhibited outward rectification and had a chord conductance of 17 pS between 0 and 100 mV was observed in excise patches. The channel had a Cl-to-Na or K permeability ratio of 4.8, which is similar to the cation/anion selectivity of the Cl_L channel, and although the permeability sequence for anions was not examined in this study, the authors reported that the Cl_i channel was less permeable to $CH_3SO_3^-$ than to Cl (121). Channel activity, which appeared in bursts, decreased with increasing membrane depolarization or hyperpolarization, but channels were generally more active at positive potentials than at negative potentials. Stability plots of channel activity suggested that at least two modes of channel behavior were present. Neither changes in $[Ca]_i$ nor pH_i affected open probability or moding behavior.

In addition, DIDS (10–100 μM) blocked this channel in a dose-dependent reversible manner.

iii) SMALL-CONDUCTANCE CHLORIDE CHANNEL. A small Cl channel with a slope conductance of 15 pS at 0 mV in symmetrical 150 mM NaCl was also noted in excised patches from U937 cells (121). The channel Cl-to-Na permeability ratio was 15.6, thus the small-conductance Cl (Cl_s) channel had a greater anion-to-cation selectivity than the other Cl channels described in macrophages. It also was insensitive to $[Ca]_i$ and was less voltage sensitive tha.. the Cl_t channel.

3. Nonselective cation conductance(s)

Two studies, one measuring single-channel currents and the other measuring whole cell currents, suggested that macrophages possess nonselective cation channels. Lipton (155) described an increase in single-channel activity in cell-attached patches from the murine macrophage cell line P388D1 after exposure to immunoglobulin G2b (IgG2b) or to immune complexes but not after exposure to ascites fluid with IgG2a. Excised patches from cells that had been exposed to antibody revealed similar channel activity that was unaffected by ionic substitutions of Na, K, or Cs. Channel activity with several different conductances was noted, including one ranging from 35 to 45 pS and another ranging from 120 to 150 pS. The reversal potential of the channels under conditions of a fivefold salt gradient across the patch indicated that these channels were permeable to cations but not to anions. Channel activity increased significantly when $[Ca]_i$ was raised, supporting the view that the channels were Ca gated. These observations are quite interesting, but unfortunately, they have not been confirmed or extended.

Slowly activating outward currents were reported in whole cell patch recordings from cultured human blood-derived monocytes during voltage steps to >20 mV (183). These currents were inhibited by external Zn (1–100 μM) and were present when the patch pipette contained Cs, K, or Na. In addition, substitution of Cl for aspartate or gluconate did not alter the current amplitude, leading the authors to conclude that it was a nonselective cation current. Because the currents activated at very positive potentials, it seems unlikely that they represent activation of the channels described by Lipton (155).

4. Conductances induced by specific ligands or cell functions

i) ADENOSINE TRIPHOSPHATE. Extracellular ATP (100–1,000 μM) permeabilizes the membrane of murine macrophages and J774.1 cells to cations (261) or to small (<961 Da) membrane-impermeant molecules, such as Lucifer yellow (262). The enhanced permeability does not involve hydrolysis of ATP by an ecto-ATPase, because addition of Mg (which is required for ATPase activity) inhibited permeabilization, and the poorly hydrolyzable ATP analogue ATPγS (in the presence of 1 mM EDTA) also increased cation efflux (261, 264). Furthermore, by growing J774.1 cells in the presence of ATP, an ATP clone of J774.1 cells was obtained that had normal ecto-ATPase activity but failed to respond to ATP with an increase in permeability (262). Similar ATP-induced permeability changes have also been demonstrated in rat mast cells (30) and in chronic lymphocyte leukemic cells (279).

Whole cell patch-clamp techniques have demonstrated that ATP permeabilization is associated with a rapid membrane depolarization and an increase in membrane conductance (16). Unfortunately, cell-attached patches with ATP in the patch electrode did not reveal single-channel currents (16). Therefore further studies are required to determine whether ATP directly activates a membrane channel or whether it secondarily releases an intracellular signal that opens a channel.

The physiological significance of the ATP-induced conductance is unknown. It is likely that macrophages are exposed to exogenous ATP, because they are often present at sites of cell injury and with cells, such as platelets, the secretory granules of which contain ATP. The ATP-induced permeabilization, therefore, is likely to occur under physiological circumstances and may be important in regulating the subsequent responses of the macrophage.

ii) PHAGOCYTOSIS. Phagocytes ingest particles through receptors for the Fc domain of IgG, as well as through complement receptors or through non-receptor-mediated mechanisms (252). The ionic requirements or signaling events that underlie different kinds of phagocytosis can differ. For example, C3bi[1]-mediated phagocytosis occurs at very low levels of free $[Ca]_i$, whereas Fc-mediated phagocytosis is inhibited by those conditions (144). The role of ionic conductances in phagocytosis has best been studied during Fc-mediated phagocytosis, where evidence exists that ionic conductances are activated during phagocytosis and that the Fc receptor itself may be an ionic channel. However, as discussed next, these results are somewhat controversial.

In the first of a series of studies on the Fc receptor, Young et al. (286), using tetraphenylphosphonium ions (TPP^+) to indirectly monitor V_m, demonstrated that the binding and cross-linking of the γ2b/γ1 Fc receptor by IgG or immune complexes depolarized J774.1 cells. The depolarization required a multivalent Fc ligand and was dependent on external Na. In a related study, in which purified γ2b/γ1-Fc receptors were inserted into lipid vesicles, ligand binding to an Fc receptor containing proteoliposomes increased cation permeability (287). Finally, Young et al. (288) demonstrated that adding ligand to bilayers containing the Fc receptor induced cation-selective ion channels that had a conductance of 60

[1] C3bi is a cleavage product of the third component of complement that binds to the surface of particles as a consequence of complement activation and renders particles recognizable by phagocytic leukocytes, thereby serving as an opsonin.

pS in symmetrical 1 M KCl and that inactivated several minutes after the addition of ligand.

If the Fc receptor complex is an ionic channel, then it follows that ionic currents should be evident during electrophysiological recordings from cells that are internalizing IgG-coated particles or aggregated IgG (aIgG). Several studies directly monitored channel activity in intact macrophages or macrophage membranes before and after addition of aIgG. Nelson et al. (182) recorded whole cell currents as well as single channels in human alveolar macrophages exposed to aIgG. The application of aIgG to cells during whole cell recordings produced an inward current that diminished with successive applications of aIgG, indicating that the response desensitized. In cell-attached patches, channel activity was noted only when the electrode contained aIgG and not when aIgG was applied to the bath. The channels had a unitary conductance of 350 pS in symmetrical 140 mM NaCl Hanks' solution. Changing the permeant cation from Na to K did not affect the reversal potential, indicating that if the channel was a cation channel, it was nonselective. Unfortunately, similar responses have not been noted in patch-clamp studies of J774.1 cells exposed to ligands that bind to and cross-link the Fc receptor (D. J. Nelson, personal communication). In addition, there is a significant difference between the value of conductance obtained in this study (350 pS in physiological saline) and that obtained by Young et al. (288) on the isolated Fc receptor (60 pS in symmetrical 1 M KCl).

The Fc receptor-ligand complex may indirectly activate ionic channels through a second messenger (114, 155). As discussed in section III*A3*, when IgG2b was added to the bath during a cell-attached recording from P388D1 cells, multiple single-channel current amplitudes were evident, representing either several different types of channels or a single-channel type with different subconductance states; the smallest channels had conductances of 35–45 pS and were cation selective (155). Channel activity could be maintained after excision of the patch, and activity was modulated by changes in $[Ca]_i$. Lipton (155) suggested that these channels are activated by $[Ca]_i$ increases that occur after binding and cross-linking of the Fc receptor. Using a similar experimental protocol in patch-clamp recordings from cultured human macrophages, Ince et al. (114) demonstrated transient changes in background current along with the activation of several types of channels with conductances ranging from 26 to 163 pS after ingestion of either IgG-coated or unopsonized latex beads. In this study some of these channels reversed near E_K, but the ionic selectivity of these channels was not investigated.

In contrast to these studies, Randriamampita and Trautmann (212) reported that ion-channel activation does not necessarily occur during Fc-mediated phagocytosis; during whole cell patch-clamp recordings, exposure of murine macrophages to aIgG or to the monoclonal antibody 2.4G2 did not induce membrane currents. In addition, resting V_m values obtained from whole cell recordings immediately after macrophages ingested opsonized erythrocytes were identical to those obtained before phagocytosis. Thus they concluded that Fc-mediated phagocytosis can occur under conditions where no detectable conductances are activated. These findings agree with the observations of Gallin (63) in which intracellular recordings from mouse peritoneal macrophages before and during ingestion of opsonized erythrocytes indicated that phagocytosis occurred without any changes in V_m or input resistance. The discrepancies between these observations and those already discussed indicate that the ionic events associated with Fc-mediated phagocytosis are still unresolved.

5. *Physiological role of ionic conductances*

1) SETTING MEMBRANE POTENTIAL. The resting V_m of the macrophage or of any other cell influences cell function by affecting the gating of voltage-dependent ion channels, the diffusion of ions through non-voltage-gated channels, and the transport of ions and/or substances that use ions as cotransporters. The relationship between resting V_m and ionic permeability has been studied most thoroughly by Ince et al. (116) in human monocytes. Using ion-substitution experiments, they demonstrated that the intracellular content of Na, K, and Cl in human monocytes is 21, 122, and 103 mM, respectively, and that resting V_m is dependent on external K for $[K] > 10$ mM. [It should be noted that the value of 103 mM for $[Cl]_i$ is surprisingly high and differs considerably from the values of 44 and 36 mM for J774.1 and HL60 cells, respectively (173, 216a).[2]] Below 10 mM K the Cl permeability also affected V_m, whereas changing $[Na]_o$ had no effect on resting V_m. Thus in human monocytes and in monocyte-derived macrophages where resting V_m values ranging from −30 mV to −56 mV have been reported (68, 116, 118, 183), both Cl and K conductances/transporters participate in setting V_m. In addition, the Na-K pump contributes between −7 and −11 mV to the resting V_m of macrophages (66).

When present in macrophages, the K_i conductance plays a role in maintaining the V_m close to E_K. Support for this conclusion comes from the finding that macrophages exhibiting this conductance had resting V_m values closer to E_K than macrophages that did not express this conductance (65, 68, 70, 212) and that Ba (2.5 mM), which blocks the K_i conductance, depolarized J774.1 cells by ≥20 mV (70). Furthermore, in J774.1 cells, the presence of this conductance was associated with a shift in the resting V_m to more hyperpolarized levels (171). In macrophages in which the K_i conductance sets the resting V_m, a small inward current that might be produced by the activation of a specific conductance or a nonspecific leak conductance can result in two stable states of resting membrane (−28 and −80 mV) (65). This phenomenon, which is related to the steep voltage dependence of

[2] This discrepancy may be due to the fact that the $[Cl]_i$ in human monocytes was measured in HCO_3-free medium (71a).

the K_i conductance, has also been reported in rat basophilic leukemia cells (154) and in cardiac Purkinje fibers (60) and may be functionally important.

Although the K_i conductance, if present, plays a significant role in setting the resting V_m of the cells, it should be noted that other K conductances may also contribute to the resting V_m. For example, Ypey and Clapham (290) reported that mouse peritoneal macrophages cultured for 24 h displayed only a K_o conductance, not a K_i conductance, and these cells had resting V_m values of −80 to −90 mV (equal to E_K). Because the K_o conductance was reported to activate at potentials positive to −60 mV, it is not clear which K conductance established the resting V_m in these cells.

In macrophages, as in other cell types, V_m affects voltage-dependent ionic conductances and other transport processes that depend on ionic gradients, such as Na-dependent amino acid transport. Several studies have examined the phagocytic ability and the NADPH oxidase activity of macrophages depolarized by high-K medium to determine if a negative V_m is required for these processes. Pfefferkorn (203) reported that J774.1 cells ingest the opsonized protozoan parasite *T. gondii* normally in 120 mM K medium (which depolarizes macrophages to near 0 mV, unpublished observations). Phagocytosis of unopsonized zymosan by murine peritoneal macrophages also occurs normally in high-K medium, although high-K medium does prevent the induction of phospolipase activity that normally occurs after ingestion of zymosan (1). Depolarization by high K does not induce superoxide release in mouse peritoneal macrophages, nor does it interfere with the release of superoxide induced by phorbol myristate acetate (PMA) (123). Similar results were noted when FMLP-induced superoxide release was measured in guinea pig alveolar macrophages depolarized by incubation in 110 mM K/35 mM Na medium. In these cells, increasing $[K]_o$ to 142 mM (and decreasing $[Na]_o$ to 4 mM) decreased superoxide production by 25%, but this decrease was due to the $[Na]_o$ decrease rather than to the increase in $[K]_o$ (110).

II) OSCILLATIONS IN MEMBRANE POTENTIAL. Intracellular microelectrode studies have shown that both human and murine macrophages exhibit spontaneous and electrically or mechanically induced oscillations in V_m from a level of −30 or −40 mV to potentials near E_K (approximately −80 mV) (48, 71). In addition, hyperpolarizations that sometimes oscillate can be induced by addition of Ca ionophores or chemotactic factors (64, 71). Because none of the above treatments dependably induced oscillations in V_m, these events have been difficult to study. More recently, Soldati and Persechini (257) reported that, in the absence of Na, large depolarizing voltage steps reliably induced V_m oscillations in mouse macrophage polykaryons.

Hyperpolarizing membrane oscillations have been ascribed to the activation of a Ca-dependent K conductance, because they involved an increase in conductance, reversed near E_K, were blocked by ethylene glycol-bis(β-aminoethyl ether)-*N*,*N*,*N*′,*N*′,-tetraacetic acid (EGTA), and were induced by either ionomycin (48, 71) or the intracellular injection of Ca (202). The V_m oscillations were not blocked by TEACl (50 mM), but they were blocked by the addition of either quinine (0.2–1.5 mM) or Ba (20 mM) (4, 117). As discussed in section III*A*III, it is likely that the $K_{i\,Ca}$ conductance underlies the V_m oscillations, although it should be noted that Ince et al. (117) reported activation of large-conductance channels (presumably $K_{L\,Ca}$ channels) during mechanical microelectrode-induced hyperpolarizations in human macrophages. Further studies on the effects of pharmacological blockers on both $K_{i\,Ca}$ and $K_{L\,Ca}$ conductances and the V_m oscillations are needed to determine if both these channels play a role in V_m oscillations.

Ince et al. (115) recorded rapid transients immediately after microelectrode impalement and concluded that spontaneous oscillations in V_m were an artifact of recording induced by a leak of external Ca into the cell after impalement by microelectrodes. However, experiments recording currents with patch-clamp electrodes in the cell-attached patch and whole cell configurations (where electrode-induced leak current was negligible) confirmed the presence of spontaneous V_m oscillations (63, see section III*A*III). Interestingly, Kruskal and Maxfeld (129) have demonstrated that spontaneous oscillations in $[Ca]_i$ occur in macrophages after adherence. It is likely that the oscillations in $[Ca]_i$ are linked to the activation of K conductance and that V_m oscillations occur under physiological conditions. However, the functional relevance of these oscillations is not known.

III) CHANGES DURING MATURATION OR AFTER ACTIVATION. Macrophages orginate from bone marrow promonocyte cells that are released as monocytes into the blood where they circulate, leave the circulation (with a half time of 17 h), emigrate into tissues, and mature into resident tissue macrophages (272). Tissue macrophages exposed to microorganisms, LPS, and a variety of cytokines can be activated to exhibit enhanced tumor cell killing and increased secretory responses, and it has been well documented that after activation some of their surface antigens differ from those of monocytes or of resident tissue macrophages (272).

Several studies have indicated that maturation and/or activation can modulate the expression of ionic conductances. In human peripheral blood monocytes the expression of the $K_{L\,Ca}$ channel increased during the first 7 days in culture, a time period during which monocytes mature into macrophages, <5% of cell-attached patches obtained from cells 24 h after plating exhibited this channel, whereas >80% of the patches obtained after 5 days in culture did exhibit this channel (68). If it is true that the $K_{L\,Ca}$ conductance is absent from freshly isolated blood monocytes, then the presence of these channels (in the plasma membrane) must not be required for phagocytosis, chemotaxis, and other functions that are normally carried out by peripheral blood monocytes. However, this observation has not been confirmed in a recent study of whole cell currents in cultured human blood-derived monocytes by Nelson et al. (183). In J774.1 cells, adherence is the trigger for increased channel expression. As discussed in section

III.1.II, a twofold increase in the density of K_i channels occurred during the first 18 h after adherence (171). It is well known that adherence itself can "activate" macrophages to increase responsiveness to a variety of stimuli (31).

The activating stimuli LPS also modulates the expression of ionic currents in macrophages. Jow and Nelson (120; see sect. III.A.IV) showed that treating cultured human peripheral blood-derived macrophages for 24 h with LPS increased the percentage of cells expressing the K_o current from ~0 to ~30%. In contrast, the same treatment in J774.1 cells did not increase the K_o current but decreased the density of K_i channels compared with untreated cells (171). This was due to the fact that LPS-treated J774.1 cells increased their membrane area (as measured by membrane capacitance) more than they increased K_i channel expression.

IV) OTHER POSSIBLE FUNCTIONS. With the exception of the role of the K_i conductance in setting V_m, the role of ionic conductances in macrophage function has not been established. These conductances are likely to serve some of the same functions in phagocytes that they do in other cells. Thus the K_o conductance may be important for restoring V_m to negative values after depolarization. The Ca-activated K conductances may have a similar role after the transient increases in $[Ca]_i$ that occur during phagocytosis (111, 285) and after activation with chemotactic peptides (102). It is also possible that Cl and K conductances play a role in volume regulation in the macrophage, as they do in other cell types (190). Although ion-sensitive microelectrodes used in studies of mouse macrophage polykaryons have demonstrated that $[K]_i$ does not change during spontaneous membrane hyperpolarizations (202), Holian and Daniele (110) demonstrated that there was a 17% decrease in $[K]_i$ in human alveolar macrophages 20 min after stimulation with the chemotactic factor *N*-formyl-methionyl-phenylalanine (FMP). Changes in $[K]_i$ could influence synthetic processes (135, 217, 271) and receptor-mediated endocytosis (134). Intracellular K levels might also modulate the contractile machinery of the macrophage, because the macrophage contains an actin-modulating protein, acumentin, the activity of which is modified by changes in $[K]_i$ (100–200 mM) (259).

Only a few preliminary studies have investigated the effect of pharmacological blockers of ionic conductances on phagocyte functions. In J774.1 cells, Ba (2 mM), which blocks the K_i channel, does not block chemotaxis in response to endotoxin-activated mouse serum, release of hydrogen peroxide after stimulation with PMA, or phagocytosis of opsonized erythrocytes (unpublished observations). Therefore it is unlikely that the K_i conductance plays a crucial role during these events. In alveolar macrophages the extracellular Ca-dependent component of the K efflux stimulated by FMP is blocked by quinine (1 mM), a well-known inhibitor of Ca-activated K channels (110). Quinine also blocked the FMP-induced release of superoxide in these cells, but the inhibitory effect of quinine also occurred under conditions in which the FMP-induced K efflux was absent (low extracellular Ca), indicating that these two effects of quinine were not directly related (110). In human peripheral blood-derived macrophages, TEA (10 mM), which blocks $K_{L\,Ca}$ channels, did not inhibit chemotaxis toward FMLP (unpublished observations). Additional studies examining the effects of blockers should help to clarify the role of ionic conductances in macrophage function.

The observation that buffering $[Ca]_i$ to 1–10 nM in J774.1 cells has no effect on cell spreading or the ingestion of IgG-coated erythrocyte ghosts (46) suggests that Ca-activated ion channels are not required for these events. This is consistent with the lack of $K_{L\,Ca}$ channels in the plasma membrane of freshly isolated human peripheral blood monocytes (68), even though they are capable of carrying out phagocytosis.

B. Neutrophils

Neutrophils, also called polymorphonuclear leukocytes because of their multilobed nucleus, are the most prevalent blood phagocyte. These cells contain numerous secretory granules. After phagocytosis or stimulation with a variety of factors, including leukotriene B_4 and platelet-activating factor (PAF), the contents of these granules are released along with superoxide and other free radicals formed during the oxidative burst. Neutrophils are very motile cells and are often the first cells found at sites of infection. Thus they are very important in phagocytosing and killing invading bacteria.

Although only two electrophysiological studies have been performed on neutrophils, these studies indicate that neutrophils exhibit at least four different ionic conductances. Future studies are needed to further characterize each of these conductances, to determine what additional conductances are present in neutrophils, and to understand their relevance to the large body of information that has accumulated from biochemical, flux, and fluorescence measurements.

1. Potassium conductances

I) OUTWARD POTASSIUM CONDUCTANCE. Whole cell patch-clamp experiments in human neutrophils have demonstrated a current that activated at positive potentials and reversed around −25 mV when NaCl was the predominant salt in the bath and the pipette contained KCl/K-aspartate (128). This current, which had a threshold of activation of −60 mV, was reduced when the pipette concentration of K was reduced but was unaffected by changes in the Cl concentration. Unlike the inactivating K_o current described in macrophages (290), this current showed no inactivation during depolarizing voltage steps up to 4 s. Furthermore, pharmacological studies indicated that the current was not blocked by CTX (1,000 μM), apamin (20 nM), quinine (200 μM), or 4-AP (10 mM). The authors speculated that this channel may be responsible for maintaining the resting V_m (128).

II) CALCIUM-ACTIVATED POTASSIUM CONDUCTANCE. Krause and Welsh (128) also observed that ionomycin produced an increase in outward current that was twofold larger when the pipette contained KCl than when it contained NaCl. When the pipette contained NaCl, changing the bath solution to Na-isethionate abolished the ionomycin-induced current, whereas it only partially decreased the ionomycin-induced current when KCl was in the pipette. These data suggest that human neutrophils have a Ca-activated K conductance (in addition to a Ca-activated Cl conductance described in sect. III*B3*) The presence of a Ca-activated K current was further corroborated by the observation that ionomycin induced outward currents in whole cell patch-clamp recordings done on human neutrophils in symmetric K-aspartate solutions (128).

2. Calcium-activated cation conductance

Von Tscharner et al. (276), using patch-clamp techniques to examine ionic channels during stimulation with the chemotactic peptide FMLP, demonstrated that adding FMLP to the bath during cell-attached patch recordings induced two different Ca-activated cation-nonselective channels. The presence of FMLP in the patch pipette did not increase the probability of channel opening, indicating that the activated channels were not directly coupled to the FMLP receptor. Depleting $[Ca]_i$ by loading cells with fura-2 prevented FMLP-induced channel activation, and treating cells with saponin to increase $[Ca]_i$ activated channels in the absence of FMLP. Thus FMLP-activated channels appeared to be Ca activated Two types of single-channel currents with conductances of 18 25 and 1-6 pS were identified. Ion-substitution experiments indicated that they were equally permeable to K, Na, and Ca. Inositol trisphosphate, which releases Ca from intracellular stores in neutrophils (260), failed to induce the activity of these channels when added to the inside surface of the membrane. (The possible relevance of these channels to FMLP-induced increases in $[Ca]_i$ are discussed in section III*B4*II.)

3. Chloride conductances

In whole cell patch-clamp recordings from human neutrophils exposed to ionomycin, Krause and Welsh (128) reported that substituting isethionate for Cl in the bath decreased (by 80%) the currents in response to positive voltage steps and shifted the reversal potential for the currents to more positive potentials, suggesting that neutrophils also display a Ca-activated Cl conductance. The current that was sensitive to removal of Cl had no apparent voltage sensitivity. Whole cell Cl currents were also described in a preliminary study of human neutrophils by Schumann et al. (235).

4. Physiological role of ionic conductances

I) SETTING RESTING MEMBRANE POTENTIAL. There are no direct electrophysiological measurements of the resting V_m in neutrophils, but measurements with the indirect probes triphenylmethylphosphonium ($TPMP^+$) (240), TPP^+ (179), and the fluorescent dye 3,3'-dipropylthiadicarboxycyanine [$diSC_3(5)$] (255) have yielded resting V_m values for suspended neutrophils of −54, −67, and −53 mV, respectively. From the resting V_m value and ion fluxes, Simchowitz et al. (255) calculated the relative ionic permeability of the neutrophil membrane to K, Na, and Cl to be 10.1.1. They concluded that the small permeability to Na accounts for the deviation of the resting V_m from E_K at physiological $[K]_o$ (4.5 mM), while above 10 mM $[K]_o$, V_m follows E_K. Unfortunately, no data exist about the particular ionic channels that underly resting V_m.

Although it is clear from experiments measuring V_m with voltage-sensitive fluorescent probes that various substances that activate neutrophils produce changes in V_m (238, 268), the events underlying these potential changes are poorly understood, and their relationship to signal transduction is unclear. For example, neutrophils depolarized by high K can still migrate in response to FMLP (179, 248). Although Roberts et al. (221) demonstrated that the number of neutrophils migrating in high-K/low-Na medium is increased, this increase was due to the reduction in extracellular Na and not to the increase in K. Furthermore, data on the relationship between depolarization induced by high K and the oxidative burst have demonstrated both decreases (126) and increases (156) in superoxide generation, and these changes have been attributed to the effects of Na removal rather than to membrane depolarization.

II) OTHER POSSIBLE FUNCTIONS. The Ca-activated conductances described are likely to be activated by the biphasic rise in $[Ca]_i$ that occurs in neutrophils after stimulation by a variety of factors, including FMLP, PAF, and leukotriene B_4 (47, 145, 209). This increase in $[Ca]_i$ has been linked to differential secretion from the three distinct granule populations that are present in neutrophils (145). The early transient $[Ca]_i$ rise is due to a release of $[Ca]_i$ stores, whereas the more sustained $[Ca]_i$ increase requires extracellular Ca and has been attributed to an influx of Ca (3). A stimulus-induced influx of Ca was further corroborated by the observation that extracellular Mn (presumably influxing through Ca-permeable channels) was able to quench the increase in fura-2 fluorescence induced by FMLP, leukotriene B_4, and PAF and that La, Co, and Ni inhibit the influx of Mn (174).

Von Tscharner et al. (276) suggested that intracellular release of $[Ca]_i$ from stores caused the transient activation of Ca-gated cation channels, allowing Ca to flow into the cell. Nasmith and Grinstein (180) tested this possibility by examining FMLP-induced Ca changes under conditions where neutrophils had been loaded with the Ca chelator bis(*o*-aminophenoxy)ethane-*N*,*N*,*N*′,*N*′-tetraacetic acid and demonstrated that

the rise in $[Ca]_i$ that depended on extracellular Ca could still be stimulated by FMLP when intracellular free Ca levels were maintained at or below resting levels. However, Pittet et al. (205) found that the FMLP-stimulated influx of Ca into HL60 cells differentiated into neutrophil-like cells was closely correlated with the rise in $[Ca]_i$ as well as an intracellular accumulation of inositol 1,3,4,5-tetrakisphosphate [Ins-(1,3,4,5)P_4]. They concluded that an elevation of $[Ca]_i$ could activate Ca influx by acting directly on Ca-activated channels, as suggested by von Tscharner et al. (276), or by increasing the production of Ins(1,3,4,5)P_4.

It is possible that the FMLP-induced Ca influx does not occur through ionic channels but occurs through other ion-transport mechanisms. Simchowitz and Cragoe (254) have characterized an electrogenic Na-Ca exchanger in neutrophils that can transport one Ca ion into the cell in exchange for three Na ions. This exchanger is activated by FMLP and may account for some of the observed increase in $[Ca]_i$.[3] Further studies are needed to examine this possibility and to delineate the events that underly the Ca influx.

The early events that follow the binding of FMLP to the membrane include (in addition to increases in $[Ca]_i$) changes in V_m, pH, and the transport of other ions. Studies with fluorescent dyes have shown that FMLP induces an initial depolarization followed by a repolarization that is completed within 8-10 min (141, 240). The FMLP-induced depolarization required a stimulus concentration of at least 10^{-8} M, whereas lower concentrations induced either no change (45) or a slight hyperpolarization (136).

Despite many studies, it is not clear which ionic conductances, if any, are involved in these responses. Decreasing $[Na]_o$ to 20 mM and varying $[K]_o$ from 1 to 100 mM did not change the amplitude of the membrane depolarization, indicating that the depolarization does not involve a Na conductance (238). As noted, von Tscharner et al. (276) proposed that the transient depolarization is caused by an influx of cations through the Ca-dependent cation-nonselective ion channels induced by FMLP. It is plausible that Ca provides a signal leading to depolarization, because it has been demonstrated that an increase in $[Ca]_i$ precedes the depolarization (136). However, Di Virgilio et al. (45) showed that even in Ca-depleted cells where no increase in free-$[Ca]_i$ occurs FMLP can induce a depolarizing response, although it is diminished. Alternatively, it is possible that the membrane depolarization induced by FMLP is due to the FMLP-induced increase in a Cl conductance reported by Schumann et al. (235). It is also possible that the repolarization phase of the FMLP-induced V_m changes involves an additional membrane permeability and that it may be dependent on external Ca (268). Furthermore, FMLP and other activating agents directly stimulate Na-H exchange (89, 253). Although this transport system is not electrogenic, the changes in intracellular Na or pH, which are substantial, could affect ion conductances and/or the Na-K pump (which is electrogenic), thereby producing changes in V_m.

The purpose of the FMLP-induced V_m changes is unclear, because cells can migrate (248) and produce an oxidative burst (110) when depolarized by high K. Nevertheless, the observation that FMLP fails to induce V_m changes in neutrophils from patients with chronic granulomatous disease, a condition in which phagocytes are incapable of producing an oxidative burst (239), supports the view that the membrane depolarization (or events leading to it) is associated with the oxidative burst, even if depolarization is not required for activation of the oxidase. A close association between membrane depolarization and the oxidative burst was also demonstrated in a study that measured FMLP- and PMA-induced V_m changes and superoxide release in HL-60 cells at varying stages of differentiation (124). Similarly, Di Virgilio et al. (45) demonstrated that the dose-response relationship for the FMLP-induced depolarization in neutrophils was identical to the dose-response relationship for FMLP-induced activation of the NADPH oxidase. This study also showed that the increase in $[Ca]_i$, which occurs during FMLP stimulation, is reduced when neutrophils are depolarized and enhanced when they are hyperpolarized during FMLP stimulation. Part of the increase in $[Ca]_i$ requires extracellular Ca and has been attributed to the influx of Ca (3). Therefore the FMLP-induced depolarization may serve to limit the influx of Ca into the cell after stimulation as it does in other cells (208). In addition to limiting the influx of Ca, a recent report by Pittet et al. (214) indicates that membrane depolarization (in the absence of extracellular Ca) diminishes both the release of intracellular Ca and the rise in inositol 1,4,5-trisphosphate [Ins(1,4,5)P_3] that is produced after stimulation of neutrophil-like HL60 cells with FMLP or leukotriene B_4.

IV. LYMPHOCYTES

T, B, and natural killer (NK) lymphocytes participate in a complex series of interactions that underlies the function of the immune system. These include recognition of antigens, cytotoxicity, and lymphokine and antibody secretion (186). Advances in recent years have helped explain how these functions are carried out at the single-cell level (262a). Although questions still remain about lymphocyte ion-transport mechanisms and their functional relevance, considerable progress has been made in identifying the ionic conductances in these cells and characterizing the changes in ionic conductances that occur during lymphocyte activation (18, 20, 72, 73, 87, 152). The conductances described in lymphocytes are listed in Table 2 and are summarized next.

[3] If the Na-Ca exchanger is the major pathway for Ca influx in stimulated neutrophils, then depolarizing the neutrophil should increase the agonist-induced Ca influx. However, Di Virgilio et al. (45) demonstrated that depolarization of FMLP-stimulated neutrophils reduced the Ca influx.

TABLE 2. *Ion channels in lymphocytes*

Channel	Gating	SCG, pS	Blockers	Present In	Reference
K channels					
K_n (n type)	Voltage, Ca	12–18	4-AP, TEA, CTX, quinine, verapamil, D 600, Ni, Hg, La, nifedipine, diltiazem, chlorpromazine, forskolin, trifluorperazine, noxiustoxin	Human and murine T-cells, T-cell lines, cytotoxic T-cells, NK cells, human and murine B-cells	29, 35, 36, 58, 163, 172, 231, 232, 267
K_1 (l type)	Voltage	21–27	TEA, Co	Murine T-cells	24
K_n (n' type)	Voltage	18	CTX	Murine T-cells	148
K_{Ca} (Ca activated)	Ca	25 7 93?	Apamin	Rat thymocytes, human B-cells, human T-cells?, murine B-cells?	20, 95, 159, 160, 168
Na channels	Voltage	20	TTX	Human thymocytes, T-cell lines, murine T-cells	36, 139, 231
Ca channels					
Ca_v (voltage activated)	Voltage			Jurkat 77 6.8 cells, hybridoma cell lines*	52, 57, 59
Ca_{Ins} ($InsP_3$ activated)	$InsP_3$	7	Ca	Human T-cells, Jurkat E6-1 cells	72, 130
Ca_s (small)		<1	Ni, Cd	Jurkat cells	151, 152
Cl channels					
Cl_L (large)	Voltage, PKa	365	Ni, Zn	Thymocytes, T-cells, murine B-cells	12, 19, 167, 230
Cl_s (small)†		~2.6		Murine spleen cells, Jurkat E6-1 cells, human T-cells	19, 147
Cl_A (cAMP activated)	PKa	40		Jurkat E6-1 cells, human T- and B-cells, murine B-cells?	15, 25

SCG, single channel conductance under physiological ionic gradients (for rectifying channels, largest conductance is given). $InsP_3$, inositol trisphosphate, NK, natural killer, PKa, catalytic subunit of protein kinase A. * Hybridoma cell lines constructed from fusion of S194 cells and splenic B lymphocytes. † ATP and hypotonic medium required in patch electrode.

A. T Lymphocytes and Natural Killer Cells

T lymphocytes develop in the thymus and have both effector and regulator functions (262a). As effector cells they participate in graft versus host reactions, cytotoxicity, and delayed hypersensitivity, whereas as cell regulators they either help or suppress the activity of other lymphocytes. Cytotoxic T-cells kill in an antibody-dependent manner a variety of target cells, including those bearing foreign histocompatibility antigens as well as host tumor cells and virally infected cells, which share the same major histocompatibility antigens. In contrast, NK cells are large granular lymphocytes that can kill tumor and virus-infected cells in culture in the absence of antibody. Variations in the surface glycoproteins (i.e., CD_4 and CD_8) of these different lymphocytes correlate with their functional heterogeneity and therefore provide useful phenotypic markers for the different cell types. In vivo T-cell activation is initiated by the binding of specific antigens to the T-cell receptor, whereas in vitro activation can be accomplished using lectins and phorbol esters or monoclonal antibodies against specific surface antigens. The activation of T-cells results in a series of well-studied integrated events that ultimately leads to an increase in DNA synthesis and cell division.

1. Potassium conductances

I) OUTWARD VOLTAGE-GATED POTASSIUM CONDUCTANCE. Outward voltage-dependent K currents were first described in human peripheral blood T lymphocytes by Matteson and Deutsch (163) and by DeCoursey et al. (35) and in murine cytotoxic T-cell clones by Fukushima et al. (58). Similar currents have since been reported in a wide variety of lymphocytes, including immature human thymocytes (230), human helper-inducer T-cells ($T4^+$), suppressor cytotoxic T-cells ($T8^+$), alloreactive-cytotoxic T-cells (36), human NK cells (231), subsets of murine thymocytes (172), a murine noncytolytic T-cell clone (141), and a variety of murine cell lines (36). Only one type of outward voltage-dependent K conductance has been described in human T lymphocytes, whereas three voltage-dependent K conductances have been delineated in murine T lymphocytes. These are *1)* the n (for normal)-type K (K_n) conductance, which is the only voltage-dependent K conductance described in human T lymphocytes (17, 35) and is also present in murine

TABLE 3. *Three types of voltage-dependent K channels in murine T lymphocytes*

	Type n (normal)	Type n' (n-ish)	Type l (large)
Conductance	12-18 pS	18 pS	21-27 pS
Gating			
$V_{1/2}$	−30 mV	−10 mV	0 mV
Use-dependent inactivation	Yes	No	No
Closing rate τ (−60 mV)	30 ms	30 ms	1 ms
Pharmacology			
TEA (K_i)	~10 mM	~100 mM	~0.1 mM
CTX (K_i)	300 pM	<5 nM	Not blocked

$V_{1/2}$, membrane potential at which one-half of the channels are activated, K_i, inhibitory constant. [From Lewis and Cahalan (149).]

lymphocytes (37); 2) the l-type K (K_l) conductance, which is present in large numbers in lymphocytes from the MRL/lpr mouse strain but is also found in T lymphocytes from normal strains of mice (24, 34); and *3)* the type n' (K_n) conductance, which is found in subsets of murine thymocytes (148). A mixture of these channels can be expressed in a given murine T lymphocyte, although one type of channel often predominates (19). Table 3 and Figure 3 summarize some of the characteristics of these voltage-gated K channels.

A) N-type potassium conductance. The K_n conductance is the best characterized ionic conductance in leukocytes. It was first described in whole cell patch-clamp studies of peripheral human blood T lymphocytes (35, 163) and in murine clonal cytotoxic T lymphocytes (58). Under whole cell patch-clamp conditions, K_n currents have a threshold of activation in the −50- to −60-mV range, and the conductance is fully activated above 0 mV. [The threshold for activation for this current may differ in cell-attached recordings (S. C. Lee and C. Deutsch, personal communication).] Similar to delayed rectifying K currents in vertebrate nerve and muscle cells, K_n currents in both human and murine T lymphocytes exhibit sigmoidal voltage-dependent activation kinetics (35, 38, 58, 163) and could be fitted to a Hodgkin-Huxley type n^4j model (17, 38). However, the rate of K_n current deactivation determined from relaxation of tail currents was an order of magnitude slower in lymphocytes than in skeletal muscle (17). When $[K]_o$ was varied, the K_n reversal potential followed the Nernst equation for K, indicating that the current is K selective (17, 58, 165).

The K_n current decreases or inactivates during voltage steps lasting >20 ms. During prolonged depolarization the K_n current inactivates to a steady-state level that, in human T-cells, was half maximal at −70 mV and was complete at almost all potentials that elicited the K_n currents (17), whereas in the murine clonal cytotoxic T-cell line inactivation was absent at −75 mV (58). If the inactivation of K_n currents is state dependent and not voltage dependent, as has been suggested recently for similar channels in rat type II alveolar epithelial cells (34), then these apparent differences in "steady-state" inactivation may be ascribable to a difference in the experimental protocol rather than to actual differences. In addition, recovery from inactivation was much slower than the onset of inactivation during depolarization (17, 38, 58). When pairs of identical pulses separated by different time intervals were used to examine recovery from inactivation, short (80 ms) depolarizing pulses produced a peak current for the second pulse that was smaller than the current at the end of the first pulse (35, 138). This phenomenon of cumulative inactivation has been described in other cells (5, 290). For longer pulses (500-600 ms), recovery time increased and, in the case of human T lymphocytes, was fit by two exponentials with time constants of 10 and 420 s (17). The kinetics of K_n channel inactivation suggest the existence of more than one inactivated state of the channel (17).

Several changes in the K_n current occur during the first 10–15 min after establishing the whole cell patch configuration (17, 40, 58). These include increases in the peak current, the rate of activation, and the rate of inactivation and a −10- to −20-mV shift in the voltage dependence of activation. Similar shifts have been noted in other currents studied using the whole cell patch technique, and it has been postulated that they are due to dissipation of a Donnon potential due to the slow diffusion of large cytoplasmic anions into the pipette (161), although in some cases the voltage shifts are larger than can be accounted for by this mechanism (53). Although junctional potential shifts probably account for some of these changes, several additional factors also may underlie these changes. These include the likely effect of intracellular fluoride on augmenting the rate of K_n inactivation (17) and the removal of inactivation of the K_n conductance when cells are held at −80 or −90 mV. That is, if the resting V_m of intact lymphocytes is −70 mV or less negative (estimates of V_m in unstimulated T lymphocytes obtained using indirect fluorescent probes range from −50 to −70 mV) (87), then the K_n conductance would be partially inactivated at rest.

1) Effects of univalent cations. Ion-substitution studies revealed the following permeability ratio for the K_n conductance: K^+ (1.0) > Rb (0.77) > NH_4 (0.10) > Cs (0.02) > Na (<0.01) (17), which is similar to those reported for other delayed rectifying K channels (106, 218). In high-K medium, the K_n conductance increased, the instantaneous *I-V* relation became inwardly rectifying, and the rate of channel closing (deactivation) slowed (17). Furthermore, peak *G-V* relations indicated that the K_n conductance was activated at potentials 10–20 mV more negative in high-K or high-Rb Ringer than in NH_4-containing or normal Na-containing Ringer, suggesting that permeant cations interact with the gating mechanism of the K_n channel (17).

2) Effects of calcium. Although Cahalan et al. (17) originally reported that changing the $[Ca]_i$ from 10^{-8} to 10^{-6} M (with glutamate or aspartate as the primary internal anion) had no effect on the magnitude of the K_n current, several more recent observations have demon-

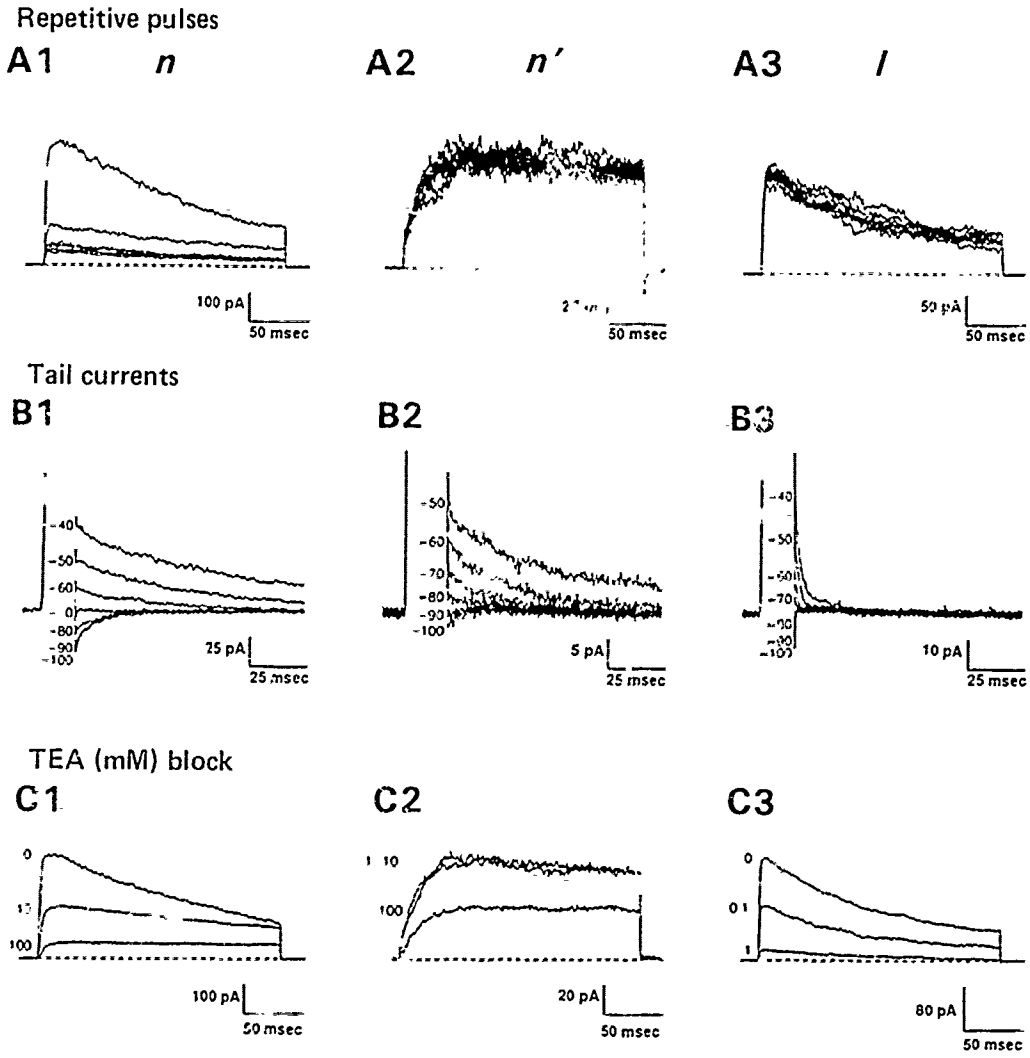

FIG. 3. Characterization of 3 types of thymocyte K currents. *A*: *columns 1–3* represent n, n' and I K currents, respectively. *A*, cumulative inactivation of K current during repetitive depolarization. Voltage stimuli (200-ms pulses from −80 to +30 mV) were delivered at rate of 1/s from holding potential of −80 mV. Seven responses are superimposed. *B*, voltage dependence of K-channel closing rates. Activating pulses of 10–20 ms from holding potential (−80 mV) to +30 mV (currents not shown) were followed by pulses of −100 to −40 mV. *C*, K-channel blockade by tetraethylammonium (TEA). K currents were elicited by pulses from −80 to +30 mV in presence of 0.1–100 mM TEACl. In *C1*, TEA slows apparent inactivation rate of K current, not by unmasking TEA-resistant current component but through direct effect on kinetics of type n channels. Cells were bathed in Ringer solution containing (in mM) 160 NaCl, 4.5 KCl, 2 $MgCl_2$, 1 $CaCl_2$, and 5 Na-HEPES (pH 7.4). Pipette contained (in mM) 134 KF, 11 K_2-EGTA, 1.1 $CaCl_2$, 2 $MgCl_2$, and 10 mM K HEPES (pH 7.2). [From Lewis and Cahalan (148).]

strated that the K_n conductance can be modulated by $[Ca]_i$. First, when the patch pipette contained 10^{-6} M Ca, whole cell currents decreased during the first 5–10 min of recording from human T lymphocytes, whereas they increased during the first 5–10 min of recording when the pipette contained 10^{-8} M Ca (14). Second, adding 1 μM A23187 increased the rate of K_n inactivation and reduced current amplitude by 56%. A similar effect of A23187 on K_n currents was reported in the human Jurkat T-cell line (52). Finally, single-channel recordings of human T-cells obtained in excised inside-out patches indicated that increasing the $[Ca]_i$ from 10^{-8} to 10^{-6} M almost completely blocked channel activity in a reversible manner (14).

Increasing $[Ca]_o$ 10-fold from ~2 to ~20 mM did not increase K_n current amplitude but shifted the *G-V* relationship to more positive potentials (17, 58) and increased the rate of inactivation (36, 94). In Jurkat E6-1 cells the rate of K_n channel inactivation was increased as both internal and external Ca increased, suggesting that Ca can enter open K_n channels from either the inside or the outside. The effects of Ca on K_n channel inactivation are consistent with a model that proposed that Ca binding to a site inside the channel induces a conformational change that inactivates the channel rather than inactivation produced by a direct block by Ca (94).

3) pH effects. Because changes in pH_i occur in lymphocytes after mitogen stimulation (44, 78), clarifying the role of K_n conductance in mitogenesis necessitates examining the effects of pH_i on the K_n conductance. In

whole cell recordings, Deutsch and Lee (42) reported that the conductance is insensitive to external pH (pH_e) until pH_e is lowered below 6.6. In contrast, changing the pH_i from 5.2 to 8.2 increased the average peak K_n current in human T lymphocytes threefold but had no effect on the threshold of activation or on inactivation. Deutsch and Lee (42) described the pH_i dependence of the K_n conductance by a model with two strongly cooperative proton-binding sites with an acidic dissociation constant of 7.15. The threefold increase in whole cell currents was accompanied by an increase in single-channel conductance. However, the increase in single-channel conductance was not sufficient to account for the increase in whole cell peak current, indicating that the number of open channels may also be affected by pH_i. Thus it is possible that alterations in the K_n conductance induced by pH_i changes that occur during the cell cycle may play an important role in proliferation.

4) Temperature effects. Most of the patch-clamp studies in leukocytes have been done at room temperature (~22°C). However, two recent studies on human peripheral T lymphocytes examined the effect of temperature on K_n conductance (138, 194). Changing the temperature from 5 to 12°C increased the K_n current amplitude and the rates of activation and inactivation and shifted the threshold of activation to more negative potentials (194). Both deactivation (the rate of decay of the current on repolarization) and recovery from inactivation were quite temperature sensitive (138). At 37°C, cumulative inactivation did not occur if the interpulse interval was >1–2 s, whereas at 22°C, inactivation was observed with an interpulse interval of 20 s. These changes indicated that increasing the temperature augmented the number of open K_n channels. From the whole cell conductance and Boltzmann fits of the activation and inactivation curves, Pahapill and Schlichter (194) estimated that from −50 to −70 mV (the estimated resting V_m), 5–20 K_n channels would be open at 37°C compared with 3–7 channels at 20°C. The single-channel conductance also increased as temperature increased (138, 194) so that the increase in whole cell conductance at 37°C probably results from increases in both the single channel conductance and open channel probability (194).

5) Single channels. Because T lymphocytes have a very high input resistance (on the order of 20 GΩ), it is possible to record single-channel currents in the whole cell recording configuration (14, 17, 138). In human T lymphocytes, single-channel currents obtained in this manner had conductances of 14–15 and 6–9 pS in normal Ringer solution and 10 and 21 pS in high-K medium (14, 17). In murine T lymphocytes, K_n channels have a conductance of 12 pS (38). Single-channel currents display flicker or rapid closures within bursts, indicating at least two nonconducting states of the channel. In excised patches exposed to symmetrical high-K solutions, I-V relationships of single K_n channels displayed inward rectification, similar to the inward rectification noted in instantaneous I-V relations of whole cell currents in high-K Ringer (17). Unitary current amplitude increased in size as temperature was raised from 22 to 37°C, the most prevalent channel had a conductance of 26 pS at 37°C compared with 11 pS at 22°C (138). The number of K_n channels estimated from the conductance of the single-channel currents and the whole cell conductance is 300–500 and 10–15 channels in human T-cells (17) and resting murine T lymphocytes (38), respectively.

6) Antagonists. Antagonists of the K_n conductance are numerous. They include classic K channel blockers, classic Ca channel blockers, polyvalent cations, and other compounds. The K channel blockers quinine (58, 163), TEA, and 4-AP all reversibly block this conductance when added to the bath with an inhibitory constant (K_i) in human T lymphocytes for quinine, 4-AP, and TEA of 14 μM, 190 μM, and 8 mM, respectively (35). Of these, channel block by TEA has been the best characterized (38, 93). In murine thymocytes, TEA reduced the apparent single-channel amplitude, probably by producing a fast block, the kinetics of which were above the frequency range explored (38). The dose-response relationship for the single-channel block in murine thymocytes was similar to that for blocking macroscopic currents (38). In the human lymphoma line Jurkat E6-1, TEA both reduced the peak K_n current and slowed the time course of decay so that the K_n current integral in the presence of TEA was unchanged (93). These data fit a kinetic scheme in which open K channels blocked by TEA cannot inactivate (93).

The K_n channels also are blocked by a number of agents that inhibit Ca channels. These include polyvalent cations and the Ca channel antagonists diltiazem, verapamil, and nifedipine (23, 36, 38, 250). In human T lymphocytes, the potency sequence of half block for these agents was verapamil (6 μM) > nifedipine (24 μM) > diltiazem (60 μM) (23). Although the potency sequence has not been reported in murine T-cells, these agents also produced half block in concentrations ranging from 4 to 40 mM (38). At intermediate concentrations of verapamil, K_n channels inactivated more rapidly and once inactivated recovered more slowly. Block by verapamil was use dependent, increasing with frequency of channel opening (36, 250). This is similar to the use-dependent block of Ca channels previously described for Ca channel antagonists (137).

Inorganic polyvalent cations reduce the K_n conductance and shift the G-V curve to more positive potentials (36, 38). Divalent cations have been shown to induce similar shifts in G-V relationships of other K conductances (54, 81). In human T lymphocytes the potency sequence for these blockers is Hg > La > Zn > Co > Ba, Cd > Mn, Ca > Sr > Mg (36). In addition, Ni (1 mM) also reduces the K_n current in human T lymphocytes (163). Both Co and La have similar blocking effects on K_n channels in murine T-cells, although murine cells may be somewhat less sensitive to polycation block (38). The interaction of Ba with the K_n channel has been studied in Jurkat E6-1 cells, where it was demonstrated that external Ba enters the open channel, producing a use-dependent block, and is trapped inside the channel when it closes (94).

Other compounds that decrease the K_n conductance are the calmodulin antagonists chlorpromazine and trifluoperazine (19), forskolin (127), retinoic acid (249), and toxins isolated from scorpion venom (210, 226). In human T lymphocytes, forskolin (20 μM) decreased the K_n conductance without changing the voltage dependence and kinetics of inactivation. Surprisingly, the effects of forskolin were not mediated by a rise in adenosine 3',5'-cyclic monophosphate (cAMP), since raising cAMP levels with isoproterenol plus phosphodiesterase or with dibutyryl cAMP had no effect on the K_n conductance (127) and neither did 1,9-dideoxyforskolin, an analogue of forskolin that does not stimulate adenylate cyclase in human lymphocytes (127). There is precedent for a direct block of K channels by forskolin from studies in invertebrate neurons (33).

Charybdotoxin blocked K_n channels in human and murine T lymphocytes with a K_i of ~0.5 nM (210, 226). Because it inhibits the K_n conductance at much lower concentrations than other antagonists, it may be a promising tool for examining the functional relevance of these channels (210). Block by CTX appears to occur when the channel is in either the closed or open state, because it blocked at a holding potential of −80 mV and because there was no indication of recovery during depolarization. Noxiustoxin, purified from *Centruroides noxius* also blocks K_n channels with a K_i of 0.2 nM (226).

Schumann and Gardner (234) reported that the sensory neuropeptide substance P, which stimulates T-lymphocyte proliferation (198) and lymphokine secretion (193), decreases the peak amplitude of the K_n current and accelerates the rate at which the current inactivates in Jurkat E6-1 cells. The effects of substance P could be mimicked by the addition of GTPγS to the pipette. Intracellular application of GDPβS (100-500 μM) blocked the action of substance P, suggesting that GTP-binding proteins may modulate the K_n current (234). However, GTPγS did not have this effect in normal human T-cells (137).

7) Expression in resting cells. With the exception of the T-cell lines CCRF HSB 2 and P12-Ichikawa, K_n channels are present in all T lymphocytes that have been examined (36). Identification of subsets of human T lymphocytes with antibodies indicated that resting T4/Leu3$^+$, T8/Leu2$^+$, and alloactivated cytotoxic T-lymphocytes all expressed K_n channels, although cytotoxic T-cells appear to have more channels (36). Schlicter et al. (232), comparing the expression of K_n channels in immature human thymocytes (negative for the T3 receptor) with channel expression in mature T3$^+$ T cells, found that channel expression in these two groups of cells was similar and concluded that K_n channels are expressed very early in the differentiation process, possibly before thymic processing. The largest number of K_n channels (1,500 channels/cell) has been reported in CCRF CEM 3A cells. Despite the variation in K_n channel numbers in different cell lines, no correlation has been made between the function of different cell lines and K_n channel number (36).

This is not the case in primary murine T lymphocytes, which have only 10-15 K_n channels in the resting mature cell (36). In murine T-cells, there also was a correlation between the type of K channel present and T-cell function, K_n channels predominate in mature thymocyte subsets that are $CD_4^+CD_8^-$ (precursors to helper T-cells), whereas in the mature $CD_4^-CD_8^+$ thymocyte subset that contains precursors to cytotoxic and supressor T-cells, K_i and K_n channels predominate (148, 149). Functionally immature $CD_4^+CD_8^+$ or $CD_4^-CD_8^-$ thymocytes expressed 5- to 10-fold more K_n channels than mature resting thymocytes (148). There also was a correlation between the number of K_n channels and the ability of thymocytes to proceed through the cell cycle (148, 172).

8) Effects of activation. The T-cell activation after in vitro exposure to polyclonal mitogens and cytokines occurs over a period of hours or days and often results in amplification of the K_n conductance. In human T-cells, a 20- to 24-h exposure to the tumor promoter TPA or concanavalin A (ConA) increased K_n conductance 1.7- (40) and 2-fold (163), respectively. In contrast to the slow effects of TPA and ConA, DeCoursey et al. (35) reported that 1 min after exposure of human T lymphocytes to phytohemagglutinin (PHA), the kinetics of K_n channel gating were modified so that the G-V curve was shifted by −15 mV, thus the number of channels open at rest would double. However, subsequent studies on human immature thymocytes and human T lymphocytes have failed to demonstrate these rapid PHA-induced changes in the K_n conductance (138, 232). No effects on the K_n current were noted when isoproterenol, prostaglandin E_2, cAMP analogues, or nucleotides were added to the bath or pipette in human T lymphocytes maintained at 37°C (138).

Although murine resting T lymphocytes have many fewer K_n channels than human T-cells, after stimulation with the mitogen ConA, actively dividing cells of either the helper or suppressor cell variety exhibited a large augmentation in channels (19, 38). This augmentation of the K_n channels is a likely cause for 10- to 15-mV hyperpolarization in murine cells exposed to ConA (122, 271). In the murine noncytolytic T-cell clone L2, exposure to interleukin 2 (IL-2) increased the amplitude of the K currents threefold at 24 h (141). The increased current was maintained for 72 h and paralleled the IL-2-induced augmentation in cell size and DNA synthesis.

9) Cloning. Molecular characterization of the K_n channel has been carried out using probes from Shaker-related K channel genes to screen cDNA libraries from both rats (49) and mice (97). Injection of mRNA encoded by either of the intron-less genes MK3 (97) or RGK5 (49) into *Xenopus* oocytes resulted in the expression of ionic channels with similar biophysical and pharmacological properties to the K_n channel. The amino acid sequence of RGK5 is 60–70% homologous with the Shaker core sequence (19). Using the polymerase chain reaction, Grissmer et al. (97) demonstrated that MK3 is transcribed and expressed in mouse T-cells. In addition, probes prepared from the unique 5'-noncoding region of

MK3 were used to localize MK3 to human chromosome 13 (97).

B) L-type potassium conductance. The K_l channels were first described in T-cells from mice containing two different autosomal recessive mutations, lpr/lpr and gld/gld (24, 31, 96). Both of these mutations result in a lymphoproliferative systemic lupus erythematous (SLE)-like disease that develops early in life. The K_l channels also are found in small numbers in T lymphocytes from control mice (21). The K_l conductance can be distinguished from the K_n conductance in that it activates 30 mV more positive than K_n channels, closes much more rapidly on repolarization, and inactivates more slowly and less completely (37). [Concanavalin A shifted the voltage dependence of K_l channels by about 10 mV, but these channels still opened at more positive potentials than K_n channels (21).] The K_l channels also recover from inactivation more rapidly so that little inactivation accumulates with repetitive pulses. The pharmacological block of K_l channels also differs from K_n channels, they are less sensitive to Co block, are 100 times more sensitive to TEA [mean inhibitory constant ($K_{1/2}$) 50 100 μM] (37), and they are not blocked by CTX (225). Consistent with the whole cell data, single-channel K_l currents are open at more positive potentials and have a larger (21 pS) conductance (37) than K_n channels. Addition of 0.1 mM TEA to the bath reduces single-channel conductance by 50% (37, 149), which is compatible with a rapid open-channel block mechanism like that for K_n channels.

Shapiro (211) has reported that K_l channels are similar to one of the "fast" K conductances called g_{f2} channels in node of Ranvier (50). Unlike K_n currents, but like g_{f2} currents, K_l current activation could not be fitted by Hodgkin-Huxley n^4 kinetics but was well-fitted by a delay followed by a single exponential. Besides similarities in kinetics and voltage dependence, pharmacological agents known to block g_{f2} channels, such as capsaicin (51) and naloxone (112), also block K_l channels (211).

The ionic selectivity of K_l channels to monovalent cations is roughly similar to that for K_n channels, except for a higher Cs permeability (213). For K_l channels, the permeability sequence based on biionic reversal potentials is K > Rb > NH_4, Cs >> Na. The species of permeant ion strongly modulates deactivation kinetics of K_l channels (213). This phenomenon is similar to permeant ion effects on K_n channels (17). The inward NH_4 current was over 10 times that for Cs, even though the permeabilities were nearly identical. This large discrepancy between selectivity and conductance indicates that K_l channels, like most other K channels (108), are multiion pores.

Monoclonal antibodies against specific subsets of T-cells were used to characterize K_l channel expression in both T-cells from healthy mice and T-cells from murine models of SLE, type-1 diabetes mellitus, and experimental allergic encephalomyelitis (21, 96). The T-cells from these diseased mice, which were phenotypically Thy1,2$^+$, CD_4^-, CD_8^-, B220$^+$, and F23.1sp$^+$, displayed a large number of K_l channels, whereas phenotypically similar T-cells from control mice or mice before the onset of the disease did not. Other T-cell subsets from these diseased mice expressed a normal pattern of K channels (21). Thus the abundant expression of the K_l channel may be a marker for the onset of autoimmunity. In developing thymocytes from normal mice, K_l channels were rarely found in $CD_4^-CD_8^-$ or $CD_4^+CD_8^+$ thymocytes but were found on $CD_4^-CD_8^+$ thymocytes, which are destined to become major histocompatibility class I-restricted cytotoxic or supressor T-cells (149). There is no evidence for the existence of K_l channels in human T-cells. However, K_l channels have been reported in the human Burkitt's lymphoma cell line Loucks (242).

C) N'-type potassium conductance. Examination of subsets of developing T-cells from the murine thymus has revealed a K conductance that has the same voltage dependence of activation, closing kinetics, and sensitivity to CTX as the K_n conductance but displayed little cumulative inactivation and was less sensitive to block by TEA ($K_{1/2}$ ~ 100 mM) (148). However, it was blocked by nanomolar concentrations of CTX (226). Corresponding single-channel currents having a conductance of 17 pS have been identified (148). Cell surface-staining techniques revealed that $CD_4^-CD_8^+$ cells destined to become MHC class I-restricted cytotoxic or supressor T-cells most often expressed as K_n channels.

II) CALCIUM-ACTIVATED POTASSIUM CONDUCTANCE. Radioisotope flux and potentiometric dye studies have provided substantial indirect evidence that T lymphocytes possess a Ca-activated K conductance (87, 91, 119, 219, 271). For example, in rat thymic lymphocytes and human peripheral blood mononuclear cells, elevation of $[Ca]_i$ in the submicromolar range by exposure to ionomycin induces a membrane hyperpolarization (measured with fluorescent dyes) that parallels the increase in $[Ca]_i$, depends on the K gradient, and is inhibited by 25 nM CTX (91).

Despite such observations, patch-clamp studies by several different investigators in a variety of T-cells failed to demonstrate Ca-activated K conductances in T-cells until Mahaut-Smith and Schlichter (160) demonstrated the presence of a Ca-activated K conductance in rat thymocytes and human B lymphocytes. In that study, exposing cells to ionomycin induced channel activity in 90% of the cell-attached patches. Two amplitude channels were noted. The smaller (7 pS) channel was not well characterized, but the larger channel had little voltage dependence in the range from 20 to −120 mV applied to the pipette and exhibited inward rectification. Its single-channel conductance was 25 pS for inward currents and 15 pS for outward currents. Channel activity could be retained in a percentage of the patches after excision and increased when $[Ca]_i$ was increased from 100 to 300 nM. However, excision of the patch altered the kinetic behavior and the conductance of the channel, and channel activity frequently disappeared. Similar channel activation has been reported after exposure of rat thymocytes to the mitogen ConA (159).

At this time, it is not clear how widely distributed the Ca-activated K conductance is among T-cells. A pre-

liminary report in Jurkat E6-1 lymphocytes, in which the perforated patch technique (111) was used, demonstrated that ionomycin induces a current that may be a Ca-activated K conductance (95). Further work is needed to determine if this channel is found in most T-cells and whether the previous failure to detect Ca-activated K channels was due simply to washout of the current in the whole cell and excised patch configuration.

2. *Sodium conductance*

Sodium channels with gating properties similar to Na channels in excitable cells have been described in human and murine T lymphocytes (36), in human thymocytes (231), and in several T-cell lines, including Jurkat E6-1, MOLT-4, MOLT-17, CCRF-CEM, CEM-1-3, and K562 cells (36, 139, 232, 284). The Na currents were abolished by replacement of external Na with Cs or TEA, tetrodotoxin (TTX, 100 nM) also reversibly blocked the channels. The Na channels from murine T-cells were less sensitive than human T-cells to TTX block (17, 38). Single-channel currents evident in some whole cell records indicated that the single-channel conductance was 20 pS for human T-cells (17) and 16-18 pS for murine T-cells (38).

Sodium channels are present in only a small percentage (3 of 90 cells) of human resting T lymphocytes (17) but are in as many as one-third of the unstimulated mouse MRL-n strain of T lymphocytes (38). Activation of murine T-cells with ConA did not increase the percentage of cells expressing Na currents but did produce a 10-fold increase in the number of Na channels per cell. However, T-cells from other strains of mice had fewer Na channels. With the exception of murine NK clonal cells and K563 leukemic cells that express a high density of channels, T-cells do not usually contain enough Na channels to generate action potentials (18).

3. *Calcium conductances*

The T-cell receptor/CD_3 ligands or mitogenic lectins induce an increase in $[Ca]_i$ that is essential for subsequent activation events (72, 87, 271). The rise in $[Ca]_i$ has two components, a release of Ca from intracellular stores (2, 113) and an influx of extracellular Ca that is blocked by Ca channel antagonists, such as La (2, 188). Although it has been postulated that the influx of Ca occurs through classic voltage-dependent Ca channels, such channels have only been reported in Jurkat 77 6.8 cells [(52), studies of other Jurkat T-cell lines have failed to confirm this report (36, T. E. DeCoursey, personal communication)]. In those cells, a voltage-gated Ca conductance with slow kinetics, consistent with the behavior of L-type channels (187), was enhanced after exposure to PHA and may mediate the PHA-stimulated rise in $[Ca]_i$ that occurs after PHA stimulation. Patch-clamp studies have failed to demonstrate classic voltage-gated Ca channels in other types of T-cells (17, 58, 163). Thus Ca influx during T-cell activation must be mediated by a non-voltage-gated Ca transport mechanism(s) (72, 152).

Voltage-insensitive inward Ca (or Ba) currents were first described in cell-attached and whole cell recordings from a human cloned helper T-cell line (131). In cell-attached patches with 110 mM Ba in the patch electrode, single-channel currents had a linear I-V curve with an extrapolated reversal potential of ~60 mV and a ~7 pS conductance. They were infrequently open in cell-attached recordings of quiescent cells. However, the probability of opening was increased by bath application of PHA, indicating that PHA was exerting its effect through a second messenger (131). A PHA-stimulated voltage-insensitive current that was blocked by Cd was also noted in whole cell records (131), however, there was little evidence that it was a Ca current. Similar single-channel activity was recorded in human cloned helper T-cells using monoclonal antibodies against the antigen/major histocompatibility complex receptor T3-Ti (CD_3 specific) or the sheep erythrocyte-binding protein T11 (CD_2 specific), demonstrating that a variety of stimuli that increase $[Ca]_i$ activate these channels (72). Although little is known about the pharmacology of this channel, in Jurkat E6-1 cells it could be activated by the Ca agonist BAY K 8644 (289). Moreover, as shown in Figure 4, exposure of the cytoplasmic membrane surface to micromolar concentrations of $Ins(1,4,5)P_3$ activated similar channels in a dose-dependent fashion during excised inside-out patch recordings from human Jurkat E6-1 T-cells (130), suggesting that this Ca-permeable channel is part of a relatively new class of inositol phosphate-sensitive Ca channels (200, 275). In addition, excised patch studies indicate that the channel may be autoregulated by Ca, since elevating $[Ca]_i$ suppressed channel activity (72; Fig. 4).

Lewis and Cahalan (151) have demonstrated that exposure of Jurkat T-cells to PHA-induced oscillations in $[Ca]_i$ depended on $[Ca]_o$ influx and were suppressed by depolarizing the cells with high-K medium. Whole cell patch-clamp recordings from those cells revealed a small (~7 pA in 10 mM intracellular EGTA) voltage-independent Ca current that was activated within seconds of obtaining a whole cell recording. The current was inward at potentials up to 20 mV, did not reverse at voltages up to 100 mV, was diminished by decreasing $[Ca]_o$, and was blocked by 5 mM Ni or 1 mM Cd. Interestingly, this current developed without any notable single-channel activity or increase in baseline noise. Thus the single-channel conductance must be quite small (<1 pS) and may even be due to the activation of an electrogenic pump or exchange mechanism rather than an ion channel. In perforated patch-clamp recordings (obtained by placing nystatin, a pore-forming antibiotic, in the pipette), an oscillating Ca current, the rise and fall of which preceded the oscillations in $[Ca]_i$, could be activated by adding PHA (151). The temporal correlation between the oscillations in $[Ca]_i$ and current activation supports the view that this current was causally related to the $[Ca]_i$ oscillations.

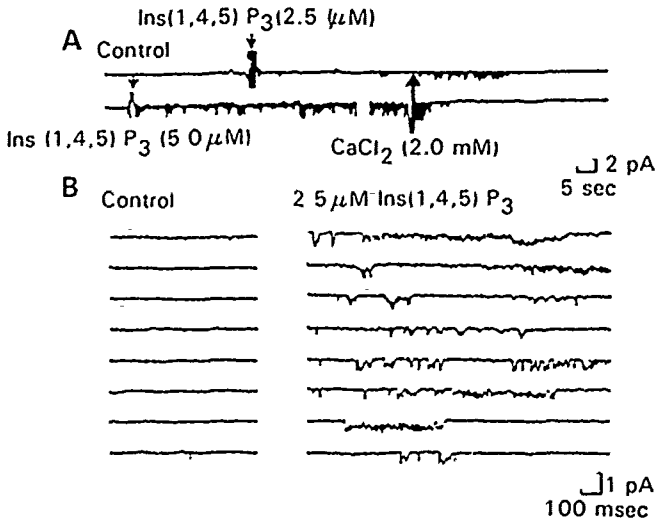

FIG. 4. Single inositol 1,4,5-trisphosphate [Ins(1,4,5)P_3]-induced inward currents recorded from inside-out membrane patch excised from Jurkat cell. Patch pipette contained 110 mM $BaCl_2$, 200 nM tetrodotoxin (TTX), and 10 mM HEPES-KOH (pH 7.3). Membrane patch cytoplasmic surface was bathed in solution containing (in mM) 150 KCl, 0.55 $CaCl_2$, 2 $MgCl_2$, 1.1 EGTA, and 10 HEPES-KOH (pH 7.3). Holding potential was 0 mV. Inward currents are seen as downward deflections from baseline. All records were filtered at 1 kHz. *A*: Ins(1,4,5)P_3 induced inward currents from 1 excised inside-out patch at slow sweep speed. Arrows, addition of Ins(1,4,5)P_3 and $CaCl_2$ to bath. No inward currents were observed in patch for >5 min before addition of Ins(1,4,5)P_3. First break in recording indicates interruption of 1 min during which potential was changed. First bath addition of Ins(1,4,5)P_3 resulted in inward current activity within 10 s of addition to bath. Inward currents appeared for <60 s and then disappeared for period of >4 min. Top and bottom traces were interrupted during this interval. Second application of Ins(1,4,5)P_3 (final concentration 5.0 μM) immediately elicited inward currents that were sustained for 3 min. Interruption in trace indicates a 2-min interval during which membrane potential was changed. Inward currents were abolished by application of $CaCl_2$ (final concentration 2 mM) to internal bathing solution. *B*: Ins(1,4,5)P_3-induced unitary inward currents at higher time resolution with sampling rate of 4 kHz. *Left*, control recordings before application of Ins(1,4,5)P_3. *Right*, inward current traces in presence of 2.5 μM Ins(1,4,5)P_3. [Reprinted by permission from Kuno and Gardner (130) Copyright © 1987 Macmillan Magazines Limited.]

Both the small Ca (Ca_s) current described by Lewis and Cahalan (151) and the Ins(1,4,5)P_3-induced Ca/Ba (Ca_{Ins})-permeable current described by Kuno and Gardner (130) were voltage insensitive and were inhibited by increases in $[Ca]_i$. However, these currents differed in the following ways. *1*) from reversal potential measurements, the Ca_s current is more selective for Ca than the Ca_{Ins} current, *2*) the amplitude of the whole cell Ca_s current was 100-fold smaller than the whole cell Ca_{Ins} current, and *3*) no single channel current fluctuations accompanied Ca_s currents. It is unlikely that these differences reflect differences in experimental protocol, although the study of Lewis and Cahalan (151) was performed in 2 mM extracellular Ca and most of the recordings of Kuno and Gardner (130) were obtained in 110 mM Ba. Further studies are needed to determine if these are related currents or if two different voltage-insensitive Ca transporters exist in T lymphocytes.

A single study on bilayers containing plasma membrane from the human T-cell line REX has shown small (2-3 pS under conditions of symmetrical 100 mM Ca) single-channel Ca or Ba currents that were inhibited by La (199). These currents were induced by adding three different monoclonal antibodies that interacted with the T3-Ti receptors on REX cells but that were not activated by monoclonal antibodies directed against the Ti receptor of different T-cell lines or against the T4 antigen. Because channel activity was present in isolated bilayers, the data suggest a physical link between the T3-Ti receptor and the ionophore and, in contrast to the findings of Gardner (72), argue against the indirect activation of the channels by a second messenger (199). Unfortunately, no data were presented on channel selectivity or voltage dependence. Furthermore, the relationship of these currents to the Ca_{Ins} channels described by Gardner (72) is uncertain.

4. Chloride conductances

1) LARGE CHLORIDE CONDUCTANCE. Single-channel currents of a large-conductance voltage-dependent Cl channel, similar to the Cl_L channels described in macrophages, myotubes (236), and B-cells (12), have been described in whole cell (19) and excised patch (230) recordings from T lymphocytes and thymocytes. Single-channel conductance was ~365 pS. The channel exhibited several subconductance states that had the same voltage sensitivity, ionic selectivity, and block by Zn as the fully conducting channel. The most frequently noted subconductance states were in multiples of 45 pS. Unlike the macrophage, where the anion/cation selectivity of the Cl_L channel was 5:1 (236), in the T-cell this channel was 30 times more selective for Cl than for Na or K (230). Anion selectivity sequences determined from either reversal potentials or conductance ratios produced similar results in contrast to the findings in B lymphocytes, where different selectivity sequences were determined using these two types of measurements (12). The selectivity sequence for the T-cell Cl_L channel was $I > NO_3 > Br, Cl > F$, isethionate, $HCO_3 > SO_4 >$ gluconate, propionate > aspartate (230). As in macrophages (see sect. III*L*2), these channels opened and then closed in a time-dependent manner with excursions of ±20 mV, and the steady-state probability of channel opening fit a bell-shaped curve, fitting a model of a channel with one gate that closes at negative potentials and a second gate that closes at positive potentials (230).

Interestingly, recent observations by Pahapill and Schlichter (195) indicated that channel activity changes dramatically when cells are maintained at 37°C rather than at room temperature. It should be emphasized that all but a few of the patch-clamp studies in leukocytes have been performed at room temperature and that the activity of ionic channels under these conditions may differ from their activity at 37°C. For example, at 37°C, Cl_L channels were active at rest, and activity increased with hyperpolarization.

In excised patches, the Cl_i channel can be activated by the catalytic subunit of protein kinase A plus ATP, indicating that it may be regulated by second messengers (194). The channel was reversibly blocked by Zn or Ni (1 mM) added to the cytoplasmic side of the membrane. Block by Zn was decreased by hyperpolarizing the membrane, suggesting that the cation plugged the channel (230).

II) SMALL CHLORIDE CONDUCTANCE. One study reported that when the patch electrode contained a hypertonic K-aspartate/ATP-containing solution, T lymphocytes exhibited a small Cl (Cl_s) conductance that is absent immediately after establishing the whole cell configuration but then slowly develops (147). This conductance was present in mouse splenic T-cells, Jurkat E6 1-cells, and human T-cells, had an anionic permeability sequence of $NO_3 > Br, Cl, F >$ methanesulfonate > ascorbate > aspartate, and could be reversibly blocked by 2 mM SITS (19, 147). The Cl_s channels were too small to resolve at the single-channel level, but noise analysis resulted in an estimate of 2.6 pS for the single-channel conductance. From this estimate and the measured whole cell conductance, the number of Cl_s channels was estimated to be quite high, on the order of 1,000 (19). Hydrolysis of ATP appears to be required for activation of this conductance, since the current was induced by internal ATP and ATPγS (a nonhydrolyzable ATP analogue) but not by ADP, AMP, or AMP-PCP (147). It was hypothesized that the Cl_s conductance participates in the regulatory volume decrease (RVD) that occurs in lymphocytes exposed to hypotonic conditions. Unfortunately, no subsequent studies have examined this channel or its role in RVD.

III) ADENOSINE 3',5'-CYCLIC MONOPHOSPHATE-DEPENDENT CHLORIDE CONDUCTANCE. Chloride channel activity similar to that described in epithelial cells (277) was reported in excised inside out patches from Jurkat E6 1 cells (25). These single-channel currents were outwardly rectifying in symmetrical solutions and had a slope conductance at 0 mV of 40 pS. Reversal potential shifts produced by changing extracellular Na and Cl concentrations indicated that the Cl to-Na permeability ratio was 10.1. In excised patches the kinetic behavior of the channel was complex, with prolonged bursts interrupted by brief flickers and long closures, channel activation required 10^{-7} M $[Ca]_i$. However, once the channel was activated, lowering $[Ca]_i$ to 10^{-9} M had no affect on channel gating. Similar channel activity could be induced in cell attached patches after exposure to 8-bromo cAMP (25). Furthermore, channel activity was induced when the cytoplasmic surface of excised patches was exposed to the catalytic subunit of cAMP dependent protein kinase plus ATP. Thus this channel appeared to be a cAMP dependent Cl (Cl_A) channel similar to that described in airway epithelial cells (277). In epithelial cells, regulation of the Cl_A channel was reported to be defective in cystic fibrosis (55, 277), and Chen et al. (25) have shown that it is also defective in lymphocytes from cystic fibrosis patients (see sect. IV*B*).

More recently, Bubien et al. (15), using fluorescence digital imaging of the halide-sensitive fluorophore 6-methoxy-*N*-(3-sulfopropyl)quinolinium and whole cell patch clamping, confirmed that both T and B lymphocytes from cystic fibrosis patients lack a Cl current that can be activated by the addition of either cAMP or ionomycin to the cells. They also reported that lymphocytes in G_1 had a significant spontaneous Cl permeability, whereas G_0 and S phase cells had a low Cl permeability (15).

5. *Physiological relevance*

I) SETTING RESTING MEMBRANE POTENTIAL. Estimates of V_m in populations of normal resting mammalian lymphocytes obtained using potentiometric-sensitive dyes and $TPMP^+$ range from −50 to −70 mV (39, 122, 271, 280). These studies indicated that the V_m of lymphocytes was primarily a K diffusion potential (87). From patch-clamp studies, Cahalan et al. (17) estimated in human T-cells that 0.1–2 (of the 300–400) K_n channels are open at the resting V_m. Using a $[K]_i$ of 130 mM (39) and the unitary K_n conductance, Cahalan et al. (17) calculated that the net K efflux through open K_n channels would be 10–400 > 10^{-18} mol/min and concluded that this flux could account for the resting K fluxes measured in lymphocytes by Segel and Lichtman (237). Further support for the involvement of K_n channels in setting the resting V_m comes from the observation that CTX, which blocks K_n channels (226), depolarizes human peripheral blood monocytes under conditions (depleted $[Ca]_i$) in which a Ca-activated K conductance should not be active (91). However, this observation differs from that of Wilson et al. (281), who reported that CTX had no effect on the resting V_m of unstimulated human T-cells. In addition, K_n single-channel currents should be evident in cell-attached patches if they participate in setting the resting V_m, but Deutsch (personal communication) reports a failure to record K_n channels at −70 mV in cell-attached patch experiments. Furthermore, even though K_n channels may contribute to the resting V_m in T-cells that have high numbers of K_n channels, this is less likely for cells that exhibit fewer K_n channels, such as resting mature murine T lymphocytes. The observations that CTX has little effect on the resting V_m of rat thymocytes (91) or murine spleen and thymus cell (281) may reflect this possibility.

Because the V_m of quiescent T-cells is significantly less negative than the E_K (which is approximately −90 mV), other permeabilities, such as the Cl or Ca conductances described, must contribute to the V_m. In human cloned T lymphocytes, a voltage-independent Ca-permeable channel has been shown to be open, albeit infrequently, at rest (131) and therefore would tend to depolarize the cells. In addition, the preliminary report by Pahapill and Schlichter (195), indicating that at 37°C human T-cell Cl_i channels are active at rest, implies that these channels contribute to the resting V_m. This seems somewhat surprising for several reasons. First, the basal Cl permeability in human lymphocytes is very low,

and it is unaffected by changing V_m (which would not be the case if Cl transport occurred via a voltage-dependent conductive pathway) (86). Second, Cl_L channels have such a large conductance that they would be expected to overwhelm the K_n conductance, effectively clamping the cell at E_{Cl}. Further studies are required to determine which conductances play a role in setting the resting V_m of the different types of T-cells.

II) RESPONSE TO MITOGENS. Numerous studies have implicated both K and Ca conductances in T lymphocyte proliferation (for reviews see Refs. 72, 87). In contrast, Na transport also is stimulated during mitogenesis, but the main route for Na entry is via the Na-H exchanger (87). This conclusion fits with the observation that TTX had no detectable effect on mitogenic response of T-cells (17). At present, no direct data exist about the function of Cl channels in T-cell proliferation, although DIDS, an anion transport antagonist, inhibited the ability of monoclonal anti-CD_3 complex antibodies to stimulate Ca influx in Jurkat T-cells without affecting Ca release from intracellular stores (222).

A) Potassium channels. Because patch-clamp studies have only recently described Ca-activated K channels in thymocytes, little electrophysiological data exist supporting their role in the proliferative response of T-cells. In contrast, substantial evidence supports a role for voltage-dependent K channels. Three types of evidence indicate that voltage-gated K channels, and in particular K_n channels, play a role in mitogenesis. First, a variety of mitogens increase the K_n current density (14, 38, 40, 141, 163). The current amplification is consistent with reports of mitogen-induced increases in K efflux and membrane hyperpolarization (237, 270). Moreover, the time courses of the augmentation of K fluxes and the K_n conductance are similar. Thus in human cells, both the K_n conductance and K fluxes were increased within minutes of adding mitogen (17, 36), whereas in murine splenic lymphocytes augmentation of the K_n conductance and K fluxes occurred 15 h after ConA addition (38). However, the lack of voltage-gated K channels in the T-cell line CTLL-2 that responds normally to mitogens (36) suggests that these channels are not absolutely required for proliferation. That is, there are different pathways of activation for a given type of T-cell, as well as different types of T-cells, and it is unlikely that the K_n conductance is required for activation in each of these instances.

Second, pharmacological evidence using a diverse group of K_n channel antagonists on a variety of T-cells shows that these agents inhibit DNA and protein synthesis at similar (11, 19, 22, 39, 141, 209), although not always identical, concentrations (225), providing indirect evidence that K_n channels are involved in proliferation. [It should be also noted that if K-channel blockers block in a state-dependent manner (34), then the dose-response relationship of K_n current block at 20 mV (where most of the dose-response relationships have been determined) and the dose-response relationship of block at the resting V_m may differ.] Despite these findings, it has not been proven that the functional effects of the antagonists are actually mediated by K-channel block. For example, K-channel blockers have been shown to directly inhibit Ins(1,4,5)P_3 release from brain microsomes (196). Schell et al. (229) have reported that TEA and 4-AP (at concentrations that inhibit the K_n conductance) inhibit [^{3}H]thymidine and amino acid incorporation in two tumor cell lines that replicate autonomously, suggesting that these agents act on the uptake of nutrients rather than on pathways related to T-cell activation.

Third, support for the involvement of K_n channels in proliferation comes from the observation that T-cells from diseased MRL-lpr/lpr mice that fail to respond to mitogens or antigens do not upregulate the number of K_n channels on their surfaces. Rather, these cells constitutively express 20-fold more K_1 channels on their surfaces than T-cells from MRL-lpr/lpr mice before the onset of the disease (18).

The mechanism by which K channels are involved in T-cell activation is unknown. Phytohemagglutinin increases K current in immature thymocytes, which do not proliferate (231), indicating that although augmentation of the K_n conductance may be necessary, it is not sufficient to induce proliferation. Before voltage-independent Ca channels were described in T-cells, Cahalan and co-workers (17, 22) proposed that Ca influx might occur through voltage-gated K channels. Although it recently has been demonstrated that Ca ions can enter open K channels and cross the membrane to the inside when the channel closes (94), it is unlikely that this mechanism provides a significant route for Ca entry, since K channels fail to conduct in isotonic Ba (232) and stepped depolarization of Jurkat T-cells to 0 mV (which activates K channels) does not detectably alter $[Ca]_i$ (150). Furthermore, indirect evidence that K_n channels are not permeable to Ca is provided by the following observations. *1)* depolarization of human T lymphocytes (thus activating K_n channels) fails to increase $[Ca]_i$ (77), and *2)* K channel antagonists only partially inhibit mitogen-induced $[Ca]_i$ increases (18, 22, 77). Alternatively, voltage-gated K channels may indirectly affect mitogenesis by changing intracellular K levels, since $[K]_i$ has been linked with protein synthesis (135), or they might set the resting V_m, which may affect the mitogen-induced rise in $[Ca]_i$ (76, 188), thereby modulating the proliferative response. Unfortunately, the relationship of V_m to T-cell activation is unclear: Gelfand et al. (76) reported that depolarization with high-K medium inhibited PHA-induced Ca uptake after short-term exposure to mitogen. However, for lymphocytes cultured in high-K medium and continuously exposed to PHA, proliferation was almost normal (43).

B) Calcium channels. It is well established that mitogens produce a rapid increase in $[Ca]_i$ that is partly due to an influx of extracellular Ca (87). The extensive evidence supporting the view that Ca influx and the subsequent rise in $[Ca]_i$ provide an important signal for proliferation has been the subject of other reviews (72, 87, 153) and therefore is not covered in depth here. Although it was originally hypothesized that voltage-

gated Ca channels were responsible for the extracellular Ca-dependent mitogen-induced $[Ca]_i$ rise, it is now believed that they do not play a role in the mitogen-dependent Ca influx, because *1)* they are not detectable in most T-cells (17, 72, 163), *2)* concentrations of Ca channel blockers known to inhibit voltage-dependent Ca channels do not consistently block mitogen-induced Ca increases (72), and *3)* depolarization by high-K medium (which would be expected to increase the influx of Ca through voltage-gated channels) has no effect on $[Ca]_i$ (72, 76, 188). This view has been confirmed by two recent descriptions of voltage-insensitive Ca currents in T lymphocytes (72, 151), supporting the hypothesis that a non-voltage-gated Ca transport process is responsible for the mitogen-induced Ca influx.

Kuno and Gardner (74, 130) suggested that T-cell activation by mitogens results in an $Ins(1,4,5)P_3$ increase that releases Ca from intracellular stores and activates a transmembrane Ca channel (see sect. IV*A3*). Previous observations that mitogens increase the phosphorylation of phosphoinositides and the generation of inositol phosphates activation fit with this hypothesis (113, 270). However, it is not clear which of the two Ca currents, the Ca_{Ins} current described by Gardner et al. (72) or the Ca_s current described by Lewis and Cahalan (151), is responsible for mitogen-induced increase in $[Ca]_i$ or, alternatively, whether the two currents are related (see sect. IV*A3*). By simultaneously measuring $[Ca]_i$ and membrane currents, Lewis and Cahalan (151) demonstrated a temporal relationship between the PHA-induced Ca currents and the oscillations in $[Ca]_i$, thus providing strong evidence that these currents underlie the mitogen-induced Ca oscillations. Agonist-induced or $Ins(1,4,5)P_3$-induced Ca currents similar to those described by Lewis and Cahalan (151) were described in whole cell recordings of rat peritoneal mast cells (164). It should be noted that non-voltage-gated Ca permeable channels have been described only in T-cell lines. Therefore the functional relevance of these channels in normal T-cells must be regarded as speculative.

It has been suggested that the step that requires Ca in mitogenesis is the production of IL-2, because IL-2 production requires both extracellular Ca and an increase in $[Ca]_i$, whereas the expression of IL-2 receptors is independent of the rise in $[Ca]_i$ (176). Further support for this suggestion comes from the observation that exogenous IL-2 can trigger proliferation in IL-2 receptor-bearing cells in the absence of an increase in $[Ca]_i$ (183). Nevertheless, the role of Ca in signal transduction is more complex, since the requirement for extracellular Ca and a rise in $[Ca]_i$ can be eliminated by treating cells with phorbol ester plus mitogens (79). Also, anti-Thy-1 antibody stimulation of IL-2 secretion in a murine T-cell variant missing the T-cell antigen receptor occurs in the absence of any increase in $[Ca]_i$ or phosphatidylinositol hydrolysis (265). Therefore although Ca channels/transporters appear to play an important role in mitogen-induced IL-2 production, Ca-independent modes of signal transduction also are present in the T-cell.

C) Cytotoxicity. Cytotoxicity mediated by either cytolytic T lymphocytes (CTL) or NK cells share several identifiable stages, including a Ca-dependent programming for a lysis stage that has an optimal temperature of 37°C (6, 109, 211). This dependence on extracellular Ca, together with the rise in $[Ca]_i$ after target cell binding to CTL and the immediate decline in $[Ca]_i$ after removal of extracellular Ca, led to the hypothesis that Ca channels play a pivotal role in cell-mediated cytotoxicity (82, 206). Furthermore, the rise in $[Ca]_i$ correlates with a shape change in the CTL cells and a reorientation of cytoplasmic granules (83). Poenie et al. (206) postulated that binding the target cell to the T-cell receptor opens Ca channels activated by secondary events that occur between receptor binding and channel opening. Voltage-dependent Ca channels have not been described in CTL or NK cells (58, 232), and depolarizing CTL with high K failed to induce a rise in $[Ca]_i$ (82). Thus it is likely that voltage-independent Ca channels/transporters similar to those described by Lewis and Cahalan, (151) or Gardner (72, 74) mediate the rise in Ca in the effector cell.

The evidence implicating voltage-gated K channels present in both mouse CTL (58) and NK cells (250) in cell-mediated cytolysis is threefold. First, the amplitude of the CTL K currents in cytotoxic T-cell-target cell conjugates was enhanced by replacing external Mg with Ca (conditions required for the lethal hit to take place) (58). Second, Rb efflux was stimulated when cloned CTL loaded with ^{86}Rb were mixed with appropriate target cells (224). Third, pretreatment of NK cells with verapamil, 4-AP, Cd, and quinidine inhibited killing at doses comparable to those that blocked voltage-gated K channels (232). Furthermore, by adding EDTA and channel blockers at various times during cell killing, Sidell et al. (250) demonstrated that K channels play a role in the Ca-dependent killing phase and particularly in the release of NK cytolytic factor. The K-channel blockers 4-AP and quinidine similarly inhibit cytolysis by lymphokine-activated killer cells (143).

The role of K channels in this phase of cytolysis is unclear. The findings that depolarizing NK cells with high K^+ has no effect on NK-mediated cytolysis and that valinomycin, which should prevent the depolarization produced by K-channel blockers, did not reverse the block of cytolysis by quinidine, verapamil, or 4-AP (233) argue against the possibility that K channels may function indirectly through effects on V_m. It should be noted that cytolytic activity mediated by CTL cells is not inhibited by verapamil (82), demonstrating that there are distinct differences in the mechanisms of cytolysis mediated by these two cell types. In CTL cells, inhibition by 4-AP and TEA of cytotoxicity can be overcome by adding IL-2, suggesting that the importance of K channels in cytotoxicity may be related to their action on IL-2 production (244).

One report implicated Cl fluxes in cell-mediated cytotoxicity (84). In that study, CTL-mediated cytotoxicity was inhibited by isosmotic replacement of Cl with impermeant anions, and stilbene disulfonates blocked cy-

tolysis, providing indirect evidence that anion transport may be involved in delivery of the lethal hit (84).

D) Volume regulation. Exposing lymphocytes to anisotonic medium results in shrinkage or swelling, followed by a regulation back to near normal size even though the cells remain in anisotonic medium (41, 90). In T-cells, the RVD that occurs within 5 min of hypotonic swelling is associated with a loss of both Cl and K and is dependent on an outwardly directed K electrochemical gradient (90). The increase in Cl permeability is at least partly conductive because it is associated with a depolarization, so that V_m approaches E_{Cl} and Cl flux is independent of the concentrations of external anions or internal cations (86). The ATP-dependent Cl_s channels described by Lewis and Cahalan (147) may account for the increase in Cl permeability during RVD because they are osmotically activated (19). On the other hand, the anion permeability sequence of the Cl_L channel in T-cells (230) is identical to the sequence for supporting volume changes in swollen lymphocytes (87) and differs slightly from the permeability sequence for the ATP-dependent Cl_s channel (147). Therefore further studies are required to determine which Cl channel(s) is involved in volume regulation and how changes in cell volume regulate this Cl conductance.

Despite proposals to the contrary (88, 90), neither a Ca conductance nor a Ca-activated K conductance appear to be involved in the RVD response, because RVD does not require extracellular Ca and because $[Ca]_i$ does not increase during RVD (92). Alternatively, it is likely that the voltage-gated K_n channels provide the route for the RVD-associated K efflux, since in the murine T lymphocyte clone L2 the RVD response is correlated with the expression of voltage-gated K channels. Quiescent L2 cells have low levels of K_n channels and show no RVD, whereas L2 cells stimulated with IL-2 to proliferate exhibit an increase in K_n channels and a RVD response (140). Furthermore, RVD is blocked by quinine, TEA, verapamil, and CTX (41, 88, 92, 140) at concentrations that block K_n conductance. It has been suggested that during RVD K_n channels are activated by depolarization induced by either the increase in Cl permeability that occurs during RVD (19) or the activation of stretch-activated nonspecific cation channels (which have been described in other cell types but not in lymphocytes) (41). Interestingly, gadolinium, which blocks stretch-activated channels, also blocks RVD (41). The increase in K permeability during RVD is present in cells depolarized by high K, indicating that the RVD-activated K conductance can be triggered in a voltage-independent manner (92).

Because cells (with the exception of kidney medullary cells) are exposed to a narrow range of tonicity, the physiological significance of RVD is unclear. Deutsch and Lee (41) postulated that volume regulation supports cell cycle progression and that cells may encounter and/or generate local anisotonic conditions. Conversely, Grinstein and Dixon (87) speculated that the system for volume regulation is a vestige from a time when osmoregulation was important.

B. B Lymphocytes

As the effector cells of the humoral limb of immunity, B lymphocytes (which in mammals develop in the adult bone marrow or the fetal liver) synthesize and secrete antibody (262a). Surface immunoglobulin serves as the antigen receptor on the B-cell. The binding of antigen to its receptor initiates a complex series of events leading to cell proliferation and the production of antibody-secreting cells. The end stage of this maturation process is the large plasma cell that can secrete antibody at a rate of ~2,000 molecules/s.

1. Potassium conductances

I) OUTWARD VOLTAGE-GATED POTASSIUM CONDUCTANCE. The major ionic conductance in both murine B-cells immortalized at various stages of differentiation with Abelson murine leukemia virus and in murine and human resting and LPS-stimulated B-cells is an inactivating outward K current similar in its threshold of activation (40 mV) and block by TEA to the K_n channel described in T lymphocytes (29, 266, 267). [A preliminary study has reported K_i channels in a human B-cell-derived lymphoma cell line, Louckes (242).] Sutro et al. (267) reported that human tonsillar B-cells and murine B-cells have 60 and 23 K_n channels/cell, respectively. Their voltage for half activation ranged from - 20 to -28 mV, and its time constant of inactivation was 140 ms (shorter than that of human T-cells) (29, 267). As reported for the K_n channel in human T lymphocytes, increasing $[Ca]_i$ from 10^{-8} to 10^{-6} M decreased the K-current amplitude and increased the rate of current inactivation in murine B-cells (29). In addition, in murine B-cells, like T-cells, the outward K current is blocked by a variety of pharmacological agents, including extracellular verapamil (K_i - 10 μM), cetiedil (K_i - 20 μM), quinine (K_i = 22 μM), 4-AP (K_i = 300 μM), TEA (K_i = 10 mM), and Co or Cd (K_i 10 mM) (29, 267). The mechanism of K_n channel block in B-cells was described in only one preliminary study, which demonstrated that 4-AP blocks open channels and that the K_i of channel block by 4-AP depends on both internal and external pH (28). Thus the ionized form of 4-AP may block from inside the cell. Furthermore, data on rate of 4-AP block and washout of block suggest that two blocked states may exist (25).

A) Modulation of conductance. After treatment with LPS, B-cells increase in size, proliferate, and secrete antibodies. Sutro et al. (267) reported that LPS treatment also doubled the density of K channels in murine B-cells and that the increase in channel density was closely associated with the increase in cell size, that is, cells that failed to increase their cell size did not increase their K_n channel density. However, different results were obtained by Choquet et al. (29), who reported that the K_n conductance (unfortunately channel density was not measured) in murine LPS-treated B-cell blasts did not differ from the conductance in B-cell lines that were

immortalized at earlier stages of differentiation. Thus it is unclear whether the state of immunocompetency of the B-cell influences the presence of the K_n conductance.

Choquet et al. (29) reported that GTP caused a small initial increase in the K_n current, which may reflect the regulation of this conductance by a GTP-binding protein. When the patch pipette contained cAMP (1 mM), theophylline (1 mM, a phosphodiesterase inhibitor), and ATP (5 mM) the outward K_n current was significantly diminished during the first 5 min of recording from murine B-cells (29). Furthermore, adding the adenylate cyclase activator forskolin plus theophylline to the bath also decreased the current and increased the rate of inactivation. These effects were not due to a shift in the G-V relationship for the K_n current or to the induction of an inward current. Also, adding the adenylate cyclase antagonist adenosine (2 mM) suppressed the effect of forskolin. Taken together, these observations suggest that forskolin acts specifically through its action on adenylate cyclase to increase cAMP and that cAMP modulates the K_n conductance in B-cells. As described in section IV*A*III*A*5, forskolin also reduced the K_n conductance in human T-cells, but in these cells cAMP did not appear to modulate the K_n conductance and the effects of forskolin were not mediated by its efffect on adenylate cyclase (127).

In addition to modulation by cAMP, the K_n conductance in murine B-cells can be modulated by serotonin [5-hydroxytryptamine (5-HT)] (27). That is, exposure to 5-HT (10 μM) induced a transient increase in the peak current, as well as a more maintained increase in the rate of current inactivation. After treatment with 5-HT, the cells became refractory to repeated stimulation, even after prolonged washing. The increase in the peak current was transduced by a $5HT_1$ receptor, while the acceleration of inactivation involved $5\text{-}HT_3$ receptors (27).

B) Single-channel currents. Single-channel K currents with the same conductance (17 pS) as the K_n currents in T-cells were reported in both human tonsillar B-cells and mouse splenic B-cells (266, 267). However, they have not been well characterized. McCann et al. (168), studying cell-attached and excised inside-out patches in murine spleenic B-cells, reported two different outward single-channel K currents with conductances of 18 and 30 pS. The 18-pS channel (present in 9% of the patches examined) and the 30-pS channel (present in 3% of the patches) exhibited different voltage sensitivities, the 18-pS channel opened at voltages more depolarized than −20 mV, and the 30-pS channel opened at voltages more depolarized than −60 mV. McCann et al. (168) also reported that both channels were blocked by TEA and Ba, but the blocking concentrations or the conditions of block were not specified. They suggested that the 18- and 30-pS channels correspond to the T-cell K_n or $K_{n'}$ channel and K_1 channel, respectively. However, this suggestion is equivocal because the voltage dependence reported by McCann et al. (168) for the 30-pS channel is very different from that of the T-cell K_1 channel. Further characterization of the K channels present in B-cells is required to determine their relationship to the K channels described in T-cells.

II) CALCIUM-ACTIVATED POTASSIUM CONDUCTANCE. Simultaneous measurements of both $[Ca]_i$ and V_m with fluorescent dyes have demonstrated that either antibodies against surface immunoglobulins (anti-Ig) or ionomycin induce membrane hyperpolarizations in human tonsillar B-cells (157). The anti-Ig-induced membrane hyperpolarization was associated with an increase in $[Ca]_i$ and was abolished by placing cells in high-K medium, strongly suggesting that a Ca-activated K conductance was responsible for the membrane hyperpolarization. Although whole cell patch-clamp recording techniques have not demonstrated a Ca-activated K current in B-cells, two recent studies demonstrated Ca-activated K single-channel currents that may be responsible for the stimulus-induced hyperpolarization in B-cells (160, 168). As discussed in section IV*A*III, Mahaut-Smith and Schlicter (160) demonstrated that exposure of both human tonsillar B-cells and rat thymocytes to ionomycin (in cell-attached patch experiments) induced two single-channel current amplitude fluctuations (7 and 25 pS with 140 mM K in the pipette). The larger channel was inwardly rectifying and had an open-channel probability that was only weakly voltage dependent. The K channel activity that was sensitive to $[Ca]_i$ was also reported in excised patches from these cells (160).

A different Ca-activated K channel was reported recently in 3% of the patches from resting murine B-cells (168). These channels had a conductance of 93 pS and, in cell-attached patches, were observed only after applying large depolarizing potentials. Similar channels were also noted in inside-out patches, where they opened at both positive and negative potentials under conditions of normal physiological gradient with 10^{-8} M $[Ca]_i$. Channel activity increased when $[Ca]_i$ was increased, and adding EGTA inactivated the channel, demonstrating that the channel was sensitive to $[Ca]_i$ (168).[4]

2. *Calcium conductance*

No ligand-dependent voltage-independent Ca channels similar to those described in T-cells (72, 73) have been reported in B-cells. Nor have any voltage-dependent Ca channels been found in murine resting or LPS-activated B-cells (29, 266). Voltage-dependent Ca channels were reported in the murine myeloma cell line S194 (which produces but does not secrete immunoglobulin) and hybridoma cell lines constructed from the fusion of S194 cell and splenic B lymphocytes (13, 56, 59). In these cells, inward Ca currents were activated at potentials greater than −50 mV and peaked at −20 mV. During long (>50 ms) voltage steps, current inactivated with a single exponential time course, the time constant of which decreased as the V_m became more positive, even

[4] A recent study by Brent et al. (14a) indicates that B-cells have yet another type of Ca-sensitive channel, a nonselective cation channel that is inhibited by $[Ca]_i$.

beyond the peak for the inward current. Substituting Na for TEA had no effect on the decay of the inward Ca current. Thus the current decay is not due to the development of an outward current or to a Ca-induced inactivation of the current but probably reflects voltage-dependent inactivation (56, 57). The channel also was permeable to Sr and Ba (permeability sequence = Sr > Ca = Ba) (56) and surprisingly was rather insensitive to block by D 600 and nifedipine (59). The Ca channels in hybridoma cells are similar to the T-type or low-threshold Ca channels in other cells that are less sensitive to organic Ca channel blockers than other Ca channels (180). More recently, Bosma and Sideil (13) demonstrated that both retinoic acid ($K_{1/2}$ = 5 × 10^{-5} M) and octanol (53 μM produced a 40% decrease) blocked the peak voltage-gated Ca currents in a similar (MHY206) hybridoma cell line. In that study, octanal also increased the rate of current inactivation.

Because no other voltage-dependent conductances were present, murine hybridoma cells provided Fukushima and Hagiwara (57) with a model for examining the permeability of monovalent cations through the hybridoma Ca channel. They demonstrated that internal monvalent cations can carry outward currents through Ca channels and that external monovalent cations carry inward currents through the channel when external divalent cations are reduced to the micromolar range. The selectivity of monovalent cations through Ca channels (in the absence of Ca) was Na > K > Rb > Cs. In the presence of Ca or other divalent cations, monovalent cation currents were blocked in a voltage-dependent manner. The data indicated that under normal conditions Ca channels are occupied by divalent cations and are impermeable to monovalent cations. However, when divalent cations are extruded from the channel, the Ca channel becomes permeable to monovalent cations (57).

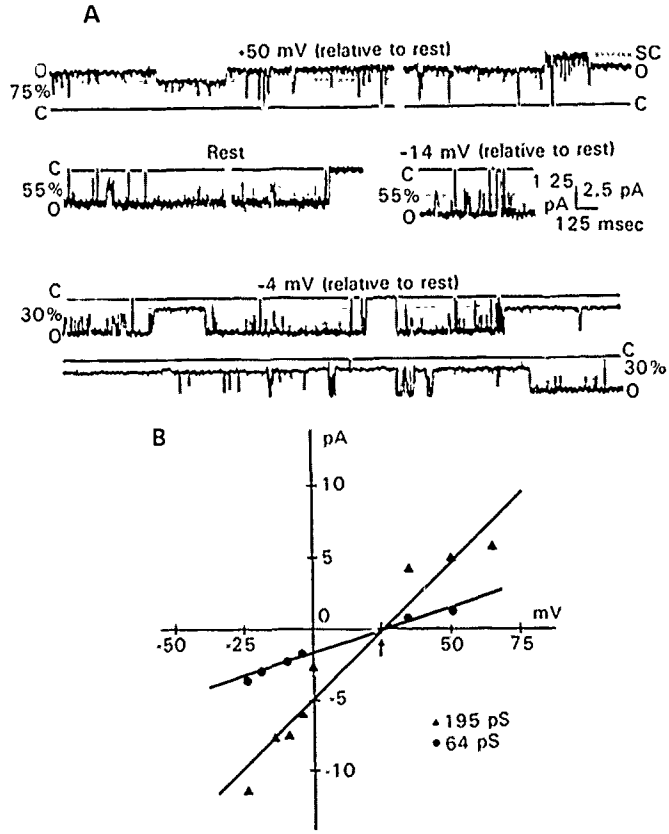

FIG. 5 Cell-attached patch-clamp recording of subconductance levels of large-conductance anion channel in hybridoma cell line constructed from fusion of S194 mouse myeloma cells and mouse splenic B lymphocytes. *A*: records showing various subconductance levels indicated by dotted lines. SC, supraconductance level, C and continuous line, closed level, O, open level. Calibration of 1.25 pA is for currents recorded at rest voltage only, all other refer to 2.5-pA calibration. All voltages are relative to resting potential of cell. *B*: current-voltage relation for currents recorded from different on-cell patch for main open level (195 pS) and 30% subconductance level (64 pS). Reversal is shown at arrow at +25 mV above rest. [From Bosma (12).]

3. *Sodium conductance*

Inward whole cell currents that had a time course of activation and decay similar to Na currents were reported in a single recording from a human tonsillar B-cell (267). Inward single-channel currents having a 17-pS conductance were also observed. Unfortunately, these events were not characterized, so it was not possible to conclude that they represented the activation of Na channels.

4. *Chloride conductance*

I) LARGE-CONDUCTANCE CHLORIDE CHANNEL. A large-conductance anion-permeable channel with multiple conductance levels has been reported in murine splenic B lymphocytes (167) and in an antibody-secreting transformed hybridoma cell line made by fusing a rat myeloma with splenic B lymphocytes (12). The activity of this channel, shown in Figure 5, is similar to the Cl_L channel activity described in macrophages, T lymphocytes, and other cells (9). It was frequently seen in excised inside-out patches, where its conductance in symmetrical NaCl or in physiological solutions was 350-400 pS (12, 167). It was estimated that there were 400-500 channels/hybridoma cell (12). The anion-to-cation permeability ratio was 10.1 in hybridoma cells (12) and 33.1 in murine B-cells (167), thus in B-cells, like T-cells, the Cl_L channel was more selective for anions than the Cl_L channel in macrophages (236). In hybridoma cells, the Cl_L channel permeability sequence for anions was F > I > SCN > Br > Cl > glucuronate > NO_3 > aspartate, which differs from the permeability sequence reported in T-cells (12). Moreover, the conductance sequence in hybridoma cells, which was Cl > SCN = F > Br > NO_3 > I, glucuronate > aspartate, was not the same as its permeability sequence, suggesting that the permeating ions were interacting within the channel (12). Interaction of permeant anions with the channel also was supported by the finding that in mixtures of anions there was an anomalous mole fraction dependence of channel

conductances, that is, a mixture of SCN and Cl (highly permeable anions when present individually) reduced the channel conductance. Mixtures of K and Tl produce a similar effect on the inwardly rectifying K channel in oocytes and other cells (99, 223).

As noted in macrophages and other cells, B-cell Cl_L channel activity is characterized by subconductance levels. These included states that were 10, 30, 55, and 75% of the full conductance level (12). In addition, a supraconductance level of 510 pS was noted, which has not been described in either macrophages or T-cells. The supraconductance level tended to close more frequently than the other levels, suggesting that entry to the closed state was easier from this level (12).

Spontaneous Cl_L channel activity was only noted in 10% of the cell-attached patches from hybridoma cells, but it could occasionally be activated by depolarizing steps (12). In these cases, the conductance levels of the fully opened state and the substates were lower that those in excised patches, probably because intracellular Cl was reduced. In the cell-attached patch, channel open probability increased up to 10 mV (relative to rest) and decreased for depolarizations beyond 10 mV (relative to rest). The behavior of the Cl_L channel changed in three ways after excision. *1)* open probability did not decrease for potentials positive to 10 mV, *2)* the voltage dependence of opening became less steep at negative potentials, and *3)* there was no maintained residence of the channel in the 30% subconductance state. Bosma (12) postulated that these changes may be due to modulation of the channel by cytoplasmic constituents, fitting with the observation in T-cells that the Cl_L channel can be activated by the catalytic subunit of protein kinase A plus ATP (195).

Similar to the Cl_L data in macrophages and T-cells, the gating characteristics of the channel could be modeled by two independent voltage-dependent gates (12). The Cl_L channel was reversibly blocked by cytoplasmic SITS with a K_i of 5.08 mM at 0 mV. The distance of the blocking site in the membrane was estimated (from the voltage dependence of the SITS block) to be 0.37 from the cytoplasmic side. Here DIDS was five times less effective than SITS and anthracene-9-carboxylic acid (1 mM) had no effect on the channel (12).

II) ADENOSINE 3',5'-CYCLIC MONOPHOSPHATE-REGULATED CHLORIDE CHANNEL. Chen et al. (25) demonstrated that normal human Epstein Barr virus (EBV)-transformed (B-cell) lymphoblasts contained a cAMP-dependent Cl (Cl_A) channel similar to that present in Jurkat E6-1 cells (see sect. IV*A4*III). This channel was also present in excised patches from mutant human EBV-transformed lymphoblasts from patients with cystic fibrosis. However, in patches from those cells, regulation by cAMP was defective. A 10-pS Cl channel has also been described in 10% of excised patches from murine splenic B-cells (168). Similar to the cAMP-regulated channel, this Cl channel exhibited outward rectification in symmetrical solution but, unlike the cAMP-regulated channel, $[Ca]_i$ had no effect on channel activity. Further experiments are required to determine if these two 10-pS Cl channel represent different Cl channels.

III) OTHER CHLORIDE CHANNELS. Two other Cl conductances have been reported in patch-clamp studies of murine splenic B-cells, but neither has been well characterized. The first was described in section IV*A4*II and is a Cl_s channel present in both T-cells and B-cells that is slowly activated in whole cell recordings when the patch electrode contains hypertonic medium plus ATP (19, 147). In addition, McCann et al. (168) described a 128-pS Cl channel that was inactive in cell-attached patches but was activated in excised inside-out patches from murine splenic B-cells. The channel had a linear *I-V* relationship in a symmetrical Cl gradient and was voltage-dependent with channel openings increasing as the patch was depolarized beyond −50 mV. It was selective for Cl over cations (Cl-to-Na permeability ratio = 11, Cl-to-K permeability ratio = 8) but was permeable to aspartate (Cl-to-aspartate permeability ratio = 4).

5. *Physiological relevance of ionic conductances*

When activated by a combination of signals that include the binding of antigen and signals from accessory cells and T-cells, the B-cell enlarges, divides, and differentiates into an antibody-secreting cell (186). This process is complex, and the mechanisms of signal transduction that occur during the various stages of activation are not well understood. Moreover, when compared with T-cells, relatively few electrophysiological studies have been done on B-cells, and there are little or no data elucidating the physiological relevance of the ionic conductances that have been described. On the other hand, support for the involvement of ionic channels comes from numerous studies using indirect probes of V_m and Ca (87). A few of these studies are discussed here in terms of their relationship to the electrophysiological data on B-cells, however, the reader is encouraged to refer to other reviews for a more comprehensive discussion (75, 87).

I) SETTING RESTING MEMBRANE POTENTIAL. The resting V_m of mouse spleen B-cells as assessed by two different V_m-sensitive fluorescent dyes is approximately −60 mV and is relatively dependent on K (220). Although it is clear that K conductance(s) plays an important role in setting the resting V_m, no data exist on the relative contribution of any of the other ionic conductances that have been described in B-cells to the resting V_m.

II) B-CELL ACTIVATION. *A) Potassium channels.* Potassium (^{86}Rb) fluxes occur after stimulation of B-cells with anti-Ig (105) or LPS (191), as well as in B-cells activated in the presence of mitogen-stimulated cells (192). As noted, anti-Ig also produced a membrane hyperpolarization in B-cells, supporting the view that K fluxes occur via a conductive pathway (158). Nevertheless, there is little information about the functional importance of K conductances in B-cell activation. Vayu-

vegula et al. (273) reported that verapamil, quinine, 4-AP, and TEA block anti-IgM-induced B-cell proliferation with a potency sequence that is identical to that for K_n-type channels in T-cells. In contrast, Ransom and Cambier (214) reported that TEA (10-100 mM) did not block anti-Ig-induced IA expression in murine B-cells.[5] Furthermore, examination of the K_n conductance in several B-cell lines exhibiting different stages of immunoglobulin secretion demonstrated a lack of correlation between these two phenomena, suggesting that the presence of this conductance is independent of immunocompetency.

If the K_n conductance is important in B-cell activation, then the observations that the K_n conductance is modulated by both $[Ca]_i$ and cAMP are certain to have functional implications since both $[Ca]_i$ (8, 157, 196) and cAMP (189, 191) have been implicated in B-cell activation. The rise in $[Ca]_i$ might also activate Ca-activated K conductance(s), resulting in a membrane hyperpolarization. In addition, the actions of 5-HT on the K_n conductance may also play a role in B-cell activation.

B) Calcium channels. Indirect evidence indicates that voltage-gated Ca channels present in hybridoma cell lines obtained from the fusion of S194 and murine splenic B-cells may be related to immunoglobulin secretion and/or cell proliferation (13, 59). A comparison of the Ca currents in the S194 cell line and in two murine hybridoma cell lines during a 4-day culture period indicated that *1)* the Ca current of secreting hybridomas was larger than the Ca current of nonsecreting S194 cells, *2)* changes in Ca current correlated with the time after the cells were tranferred to fresh medium, and *3)* there were parallel changes in the density of Ca current and immunoglobulin secretion (59). However, a high concentration (100 μM) of D 600 completely blocked both proliferation and antibody production, but it only blocked Ca currents by 37%. In a different hybridoma cell line, Bosma and Sidell (13) demonstrated that retinoic acid, a biologically active metabolite of vitamin A, produces a dose-dependent block of Ca channels in the MHY206 hybridoma cell line that correlated with the ability of retinoic acid to inhibit cell proliferation. Thus the data are suggestive that the Ca current in hybridoma cells may be related to immunoglobulin secretion and/or cell proliferation.

With the exception of S194-derived hybridoma cells, neither ligand-induced or voltage-gated Ca channels have been described in murine and human resting or LPS-stimulated B-cells. However, several observations have indicated that B-cell activation by some stimuli induces a Ca influx and that this influx occurs through Ca channels (87). First, antibodies against the antigen receptor on mouse splenic B lymphocytes induce a rise in $[Ca]_i$ that precedes capping, and removing external Ca diminishes the $[Ca]_i$ increase (208). Similarly, a biphasic increase in $[Ca]_i$ was reported after exposure of human tonsillar B-cells and murine B-cells to anti-Ig antibodies, and removing extracellular Ca inhibited the second more prolonged phase of the $[Ca]_i$ increase (8, 157). [It should be noted that oscillations in $[Ca]_i$ lasting for hours have been demonstrated in single murine B-cells and that in the absence of external Ca the oscillations only persist for several minutes (282).] Second, the addition of Mn, which can permeate Ca channels but quenches the fluorescence of the Ca indicator indo-1, also demonstrated the activation of a Ca permeability after anti-IgM stimulation of human B-cells (157). Third, anti-Ig induced a membrane depolarization in both murine B lymphocytes and human tonsillar B-cells that was dependent on extracellular Ca (157, 213).

Depolarizing B-cells or B-cell tumor cell lines with high-K medium had no effect on the increase in $[Ca]_i$ produced by anti-Ig antibodies (8, 133, 157), indicating that the influx pathway does not involve voltage-gated Ca channels. Furthermore, in the WEHI-231 B-cell line derived from a lymphoma, anti-IgM, which produces a rapid rise in $[Ca]_i$, failed to induce a simultaneous membrane depolarization (which would be expected if a voltage-gated Ca channel was activated). This observation is supported by the absence of voltage-gated Ca currents in patch-clamp studies of resting and LPS-activated B-cells (29, 168). Hence, it is likely that ligand-gated voltage-independent Ca channels are involved in B-cell activation by anti-Ig antibodies. Because B-cell activation induces both phosphoinositide turnover and Ca mobilization (7, 133, 215), a likely candidate would be an $Ins(1,4,5)P_3$-sensitive Ca channel similar to that described in T lymphocytes (72, 73).

Although increasing the influx of Ca with Ca ionophores can result in an activation of B-cells (213, 216), it is not clear at what stage of B-cell activation, if any, influx of Ca (in contrast to release of intracellular Ca stores) is required. For example, although a $[Ca]_i$ increase precedes capping induced by anti-Ig antibodies, cells in Ca-free medium that were depleted of $[Ca]_i$ capped normally without a rise in $[Ca]_i$ (208). Furthermore, not all agents that activate B-cells increase $[Ca]_i$, neither LPS nor PMA, which activate B-cells, induces an increase in $[Ca]_i$ (7). Therefore at least two different activation pathways, one that requires $[Ca]_i$ and one that does not, are present in B-cells.

C) Volume regulation. As described in section IV.A.1.b, the RVD response that occurs after exposure to hypotonic medium involves increased permeability to both Cl and K (for reviews see Refs. 41, 87). Unlike human T-cells, RVD takes ~1 h to occur in human tonsillar B-cells (26). Although swelling in B-cells induces an increase in Cl conductance that is comparable to that noted in T-cells, no augmentation of K permeability occurs (86). However, adding a cation ionophore results in a secondary RVD response in hypotonically stressed B-cells. These observations indicate that the Cl permeabil-

[5] The reason for the discrepancy between these two observations has been clarified by recent studies that demonstrate that TEA blocks B-cell proliferation during the second half of the G_1 phase of the cell cycle, whereas IA expression occurs just before stimulated B-cells enter G_1 (2a, 14a).

ity pathway and the K permeability pathway involved in the RVD response are independent and that the inability of B-cells to undergo RVD is due to a low K permeability.

The absence of an osmotically induced K conductance in human tonsillar B-cells compared with human T-cells may be related to the difference in the number of K_n channels in each cell type, both human tonsillar B-cells and B-cells from peripheral blood have ~20% of the outward K conductance reported in resting human T-cells (40, 267). This correlation between the increase in K permeability after hypotonic stress and the number of K_n channels supports the idea that K_n channels are responsible for the RVD-associated K efflux (see sect. IV*A5*IV).

No direct evidence indicates which Cl conductance is responsible for the Cl flux during RVD. Nevertheless, it is likely that similar pathways for Cl flux are used by both T- and B-cells and that this pathway involves the ATP-dependent Cl_s channels reported in both T- and B-cells (147).

V. CONCLUSION

The objective of this review is to provide readers with a summary of the electrophysiological data describing ion conductances in leukocytes and their potential physiological relevance. Leukocytes contain a diversity of both voltage-gated and/or second messenger-modulated ion channels, and the identifying features of many of these channels are known. Despite considerable progress, a myriad of questions remain, with the most relevant being the relationship of these ion channels to leukocyte function.

Some of the answers to this question are likely to involve the coupling of ion channels to intracellular signaling pathways (130). A prodigious increase in understanding of the biochemical signaling pathways in leukocytes has occurred in parallel with progress in describing ionic conductances in these cells. This increase in knowledge, together with the unique adaptability of the patch-clamp technique to different recording modes, should provide a clarification of the functional relevance of ion channels in leukocytes.

Several other points are salient to a discussion of the physiological relevance of the ion channels described here. First, activation of leukocytes can occur through multiple signaling pathways, and it is likely that ionic conductances, which may be important in one signaling pathway, are not important in others. Second, the relevance of data obtained from tumor cell lines, which vary widely, to normal leukocyte function must be interpreted with caution until it is repeated in normal leukocytes. Third, unlike ion channels in excitable cells, many of the ionic conductances that have been described in leukocytes may have only indirect effects on cell function. That is, by influencing ion homeostasis and membrane potential, ion channels may modulate protein synthesis (135), recycling of receptors (12), or influx of Ca (45, 152) without being directly involved in the signaling pathways.

Furthermore, little is known about the presence of ion channels in intracellular compartments or about the distribution of ion channels on the leukocyte surface during capping, phagocytosis, or other physiological events. The application of molecular biological techniques to the study of leukocyte ion channels will surely provide useful mechanisms to better define the importance of ion channels in leukocyte function and to elucidate how they relate to similar ion channels found in other cell types.

The author wishes to thank Drs. Leslie McKinney, Thomas DeCoursey and Carol Deutsch for critically reading this review.

This work was supported by the Armed Forces Radiobiology Research Institute, Defense Nuclear Agency, under work unit 00020. Views presented in this paper are those of the author; no endorsement by the Defense Nuclear Agency has been given or should be inferred.

REFERENCES

1 ADEREM, A. A., W. A. SCOTT, AND Z. A. COHN. A selective defect in arachidonic acid release from macrophage membranes in high potassium media. *J. Cell Biol.* 99: 1235-1241, 1984.
2. ALCOVER, A., M. J. WEISS, J. F. DALEY, AND E. L. REINHERZ. The T11 glycoprotein is functionally linked to a calcium channel in precursor and mature T-linage cells. *Proc. Natl. Acad. Sci. USA* 83: 2614-2618, 1986.
2a. AMIGORENA, S., D. CHOQUET, J. TEILLAUD, H. KORN, AND W. FRIDMAN. Ion channel blockers inhibit B cell activation at a precise stage of the G1 phase of the cell cycle. *J. Immunol.* 144. 2038-2045, 1990.
3. ANDERSON, T., C. DAHLGREN, T. POZZAN, AND D. P. LEW. Characterization of fMet-Leu-Phe receptor-mediated Ca^{2+} influx across the plasma membrane of human neutrophils. *Mol. Pharmacol.* 30: 437-443, 1987.
4. ARAUJO, E. G., P. M. PERSECHINI, AND G. M. OLIVEIRA-CASTRO. Electrophysiology of phagocyte membrane. role of divalent cations in membrane hyperpolarizations of macrophage polykaryons. *Biochim. Biophys. Acta* 856: 362-372, 1986.
5. ARIGIBAY, J. A., AND O. F. HUTTER. Voltage-clamp experiments on the inactivation of the delayed potassium current in skeletal muscle fibers. *J. Physiol. Lond.* 232. 41-43, 1973.
6 BERKE, G Cytotoxic T lymphocytes. how do they function? *Immunol. Rev.* 72: 5-42, 1983.
7. BIJSTERBOSCH, M. K., C. J. MEADE, G. A. TURNER, AND G. G. KLAUS. B lymphocyte receptors and polyphosphoinositide degradation. *Cell* 41. 999-1006, 1985.
8 BIJSTERBOSCH, M. K., K. P. RIGLEY, AND G. G. KLAUS. Cross-linking of surface immunoglobulin on B lymphocytes induces both intracellular Ca^{2+} release and Ca^{2+} influx: analysis with Indo-1. *Biochem. Biophys. Res. Commun.* 137: 500-506, 1986.
9. BLATZ, A. L., AND K. L. MAGELBY Single voltage-dependent chloride selective channels of large conductance in cultured rat muscle. *Biophys. J.* 43: 237-241, 1983.
10 BOKOCH, G M. Signal transduction by GTP binding proteins during leukocyte activation of phagocytic cells. In: *Current Topics in Membranes and Transport. Mechanisms of Leukocyte Activation*, edited by S. Grinstein and O. Rothstein. New York. Academic, 1990, vol. 35, p. 65-92.
11 BONO, M R., V SIMON, AND M. S. ROSENBLATT. Blocking of human T lymphocyte activation by channel antagonists. *Cell Biochem.* 7: 219-226, 1989.
12. BOSMA, M. M. Anion channels with multiple conductance levels

in a mouse B lymphocyte cell line. *J. Physiol. Lond.* 410: 67–90, 1989.
13. BOSMA, M., AND N. SIDELL. Retinoic acid inhibits Ca^{2+} currents and cell proliferation in a B-lymphocyte cell line. *J. Cell. Physiol.* 135: 317–323, 1988.
14. BREGESTOVSKI, P., A. REDKOZUBOV, AND A. ALEXEEV. Elevation of intracellular calcium reduces voltage-dependent potassium conductance in human T cells. *Nature Lond.* 319: 776–778, 1986.
11a. BRENT, L., J. BUTLER, W. WOOD, AND J. BUBIEN. Transmembrane ion conductance in human B lymphocyte activation. *J. Immunol.* 145: 2381–2389, 1990.
15. BUBIEN, J., K. KIRK, T. RADO, AND R. FRIZZELL. Cell cycle dependence of chloride permeability in normal and cystic fibrosis lymphocytes. *Science Wash. DC* 248: 1416–1419, 1990.
16. BUISMAN, H. P., T. H. STEINBERG, J. FISCHBARG, S. C. SILVERSTEIN, S. A. VOGELZANG, C. INCE, D. L. YPEY, AND P. J. LEIJH. Extracellular ATP induces a large nonselective conductance in macrophage plasma membranes. *Proc. Natl. Acad. Sci. USA* 85: 7988–7992, 1988.
17. CAHALAN, M. D., K. G. CHANDY, T. E. DECOURSEY, AND S. GUPTA. A voltage-gated potassium channel in human T lymphocytes. *J. Physiol. Lond.* 358: 197–237, 1985.
18. CAHALAN, M. D., K. G. CHANDY, T. E. DECOURSEY, S. GUPTA, R. S. LEWIS, AND J. B. SUTRO. Ion channels in T lymphocytes. *Adv. Exp. Med. Biol.* 213: 85–101, 1987.
19. CAHALAN, M. D., AND R. S. LEWIS. Role of potassium and chloride channels in volume regulation of T lymphocytes. In: *Cell Physiology of Blood*, edited by R. Gunn and J. C. Parker. New York: Rockefeller Univ. Press, 1987, p. 281–302.
20. CAHALAN, M. D., AND R. S. LEWIS. Functional roles of ion channels in lymphocytes. *Semin. Immunol.* 2: 107–117, 1990.
21. CHANDY, K. G., M. D. CAHALAN, AND S. GRISSMER. Autoimmune diseases linked to abnormal K channel expression in double negative (CD_4 CD_8) T cells. *Eur. J. Immunol.* 20: 747–751, 1990.
22. CHANDY, K. G, T. E. DECOURSEY, M. D. CAHALAN, AND S. GUPTA. Electroimmunology: the physiological role of ion channels in the immune system. *J. Immunol.* 135: 787–791, 1985.
23. CHANDY, K. G., T. E. DECOURSEY, M. D. CAHALAN, J. McLAUGHLIN, AND S. A. GUPTA. Voltage-gated potassium channels are required for human T lymphocyte activation. *J. Exp. Med.* 160: 369–385, 1984.
24. CHANDY, K. G., T. E. DECOURSEY, M. FISHBACH, N. TALAL, M. D. CAHALAN, AND S. GUPTA. Altered K channel expression in abnormal T lymphocytes from mice with the lpr gene mutation. *Science Wash. DC* 233: 1197–1200, 1986.
25. CHEN, J. H., H. SCHULMAN, AND P. GARDNER. A cAMP-regulated chloride channel in lymphocytes that is affected in cystic fibrosis. *Science Wash. DC* 243: 657–660, 1989.
26. CHEUNG, R. K., S. GRINSTEIN, AND E. W. GELFAND. Volume regulation by lymphocytes. Identification of differences between the two major lymphocyte subpopulations. *J. Clin. Invest.* 70: 632–638, 1982.
27. CHOQUET, D., AND H. KORN. Dual effects of serotonin on a voltage-gated conductance in lymphocytes. *Proc. Natl. Acad. Sci. USA* 85: 4557–4561, 1988.
28. CHOQUET, D., AND H. KORN. Block of K channels by 4-AP depends on opening of channel and pH (Abstract). *Biophys. J.* 57: 116a, 1990.
29. CHOQUET, D., S. D. PRIMI, P. CAZENAVE, AND H. KORN. Cyclic AMP-modulated potassium channels in murine B cells and their precursors. *Science Wash. DC* 235: 1211–1214, 1987.
30. COCKROFT, S., AND B. D. GOMPERTS. The ATP^4 receptor of rat mast cells. *J. Biochem.* 188: 789–798, 1980.
31. COHEN, M., J. RYAN, AND R. ROOT. The oxidative metabolism of thioglycollate-elicited mouse peritoneal macrophages: the relationship between oxygen, superoxide, and hydrogen peroxide and the effect of monolayer formation. *J. Immunol.* 127: 1007–1011, 1981.
32. CONRAD, G. W., AND T. J. RINK. Platelet activating factor raises intracellular calcium ion concentration in macrophages. *J. Cell Biol.* 103: 439–459, 1986.
33. COOMBS, J., AND S. THOMPSON. Forskolin's effect on transient K current in nudibranch neurons is not reproduced by cAMP. *J. Neurosci.* 7: 443–453, 1987.
34. DECOURSEY, T. E. State-dependent inactivation of K^+ currents in rat type II alveolar epithelial cells. *J. Gen. Physiol.* 95: 617–646, 1990.
35. DECOURSEY, T. E., K. G. CHANDY, S. GUPTA, AND M. D. CAHALAN. Voltage-gated K channels in human T lymphocytes. a role in mitogenesis? *Nature Lond.* 307: 465–468, 1984.
36. DECOURSEY, T. E., K. G. CHANDY, S. GUPTA, AND M. D. CAHALAN. Voltage-dependent ion channels in T-lymphocytes. *J. Neuroimmunol.* 10: 71–95, 1985.
37. DECOURSEY, T. E., K. G. CHANDY, S. GUPTA, AND M. D. CAHALAN. Two types of potassium channels in murine T lymphocytes. *J. Gen. Physiol.* 89: 379–404, 1987.
38. DECOURSEY, T. E., K. G. CHANDY, S. GUPTA, AND M. D. CAHALAN. Mitogen induction of ion channels in murine T lymphocytes. *J. Gen. Physiol.* 89: 405–420, 1987.
39. DEUTSCH, C. J., A. HOLIAN, S. K. HOLIAN, R. P. DANIELE, AND D. F. WILSON. Transmembrane electical and pH gradients across human erythrocytes and human peripheral lymphocytes. *J. Cell. Physiol.* 99: 79–94, 1979.
40. DEUTSCH, C., D. KRAUSE, AND S. C. LEE. Voltage-gated potassium conductance in human T lymphocytes stimulated with phorbol ester. *J. Physiol. Lond.* 372: 405–423, 1986.
41. DEUTSCH, C., AND S. C. LEE. Cell volume regulation in lymphocytes. *Renal Physiol. Biochem.* 11: 260–276, 1988.
42. DEUTSCH, C., AND S. C. LEE. Modulation of K^+ currents in human lymphocytes pH. *J. Physiol. Lond.* 413: 399–413, 1989.
43. DEUTSCH, C., AND M. PRICE. Role of extracellular Na and K in lymphocyte activation. *J. Cell. Physiol.* 113: 73–79, 1982.
44. DEUTSCH, C., J. S. TAYLOR, AND M. PRICE. pH homeostasis in human lymphocytes. modulation by ions and mitogen. *J. Cell Biol.* 98: 885–894, 1984.
45. DI VIRGILIO, F., P. D. LEW, T. ANDERSSON, AND T. POZZAN. Plasma membrane potential modulates chemotactic peptide-stimulated cytosolic free Ca^{++} changes in human neutrophils. *J. Biol. Chem.* 262: 4574–4579, 1987.
46. DI VIRGILIO, F., B. C. MEYER, S. GREENBERG, AND S. C. SILVERSTEIN. Fc receptor-mediated phagocytosis occurs in macrophages at exceedingly low cytosolic Ca^{2+} levels. *J. Cell Biol.* 106: 657–666, 1988.
47. DI VIRGILIO, F., O. STENDAHL, D. PITTET, P. D. LEW, AND T. POZZAN. Cytoplasmic calcium in phagocyte activation. In: *Current Topics in Membranes and Transport. Mechanisms of Leukocyte Activation*, edited by S. Grinstein and O. Rothstein. New York: Academic, 1990, vol. 35, p. 180–197.
48. DOS REIS, G. A., AND G. M. OLIVEIRA-CASTRO. Electrophysiology of phagocytic membranes. I. Potassium-dependent slow membrane hyperpolarizations in mice macrophages. *Biochim. Biophys. Acta* 469: 257–263, 1977.
49. DOUGLAS, J., P. OSBORNE, Y. CAI, M. WILKINSON, M. CHRISTIE, AND J. ADELMAN. Characterization and functional expression of a rat genomic DNA clone encoding a lymphocyte potassium channel. *J. Immunol.* 144: 4841–4850, 1990.
50. DUBOIS, J. M. Evidence for the existence of three types of potassium channels in the frog node membrane. *J. Physiol. Lond.* 318: 297–316, 1981.
51. DUBOIS, J. M. Capsaicin blocks one class of K^+ channels in the frog node of Ranvier. *Brain Res.* 245: 372–375, 1982.
52. DUPUS, G., J. HEROUX, AND M. D. PAYET. Characterization of Ca^{2+} and K^+ currents in the human Jurkat cell line. effects of phytohaemagglutinin. *J. Physiol. Lond.* 412: 135–154, 1989.
53. FERNANDEZ, J. M., A. P. FOX, AND S. KRASNE. Membrane patches and whole-cell membranes. a comparison of electrical properties in rat clonal pituitary (GH_3) cells. *J. Physiol. Lond.* 356: 565–585, 1984.
54. FRANKENHAEUSER, B., AND A. L. HODGKIN. The action of calcium on the electrical properties of squid axons. *J. Physiol. Lond.* 137: 218–244, 1957.
55. FRIZZELL, R. A., G. RECHKEMMER, AND R. L. SHOEMAKER. Altered regulation of airway epithelial cell chloride channels in cystic fibrosis. *Science Wash. DC* 233: 558–560, 1986.

56. FUKUSHIMA, Y., AND S. HAGIWARA. Voltage-gated Ca channel in mouse myeloma cells. *Proc. Natl. Acad. Sci. USA* 80: 2240–2242, 1983.
57. FUKUSHIMA, Y., AND S. HAGIWARA. Currents carried by monovalent cations through calcium channels in mouse neoplastic B lymphocytes. *J. Physiol. Lond.* 358: 255–284, 1985.
58. FUKUSHIMA, Y., S. HAGIWARA, AND M. HENKART. Potassium current in clonal cytotoxic T lymphocytes from the mouse. *J. Physiol. Lond.* 351: 645–656, 1984.
59. FUKUSHIMA, Y., S. HAGIWARA, AND R. E. SAXTON. Variation of calcium current during the cell growth cycle in mouse hybridoma lines secreting immunoglobulins. *J. Physiol. Lond.* 355: 313–321, 1984.
60. GADSBY, D. C., AND P. F. CRANEFIELD. Two levels of resting potential in cardiac purkinje fibers. *J. Gen. Physiol.* 70: 729–746, 1977.
61. GALLIN, E. K. Voltage clamp studies in macrophages from mouse spleen cultures. *Science Wash. DC* 214: 158–160, 1981.
62. GALLIN, E. K. Calcium- and voltage-activated potassium channels in human macrophages. *Biophys. J.* 46: 821–825, 1984.
63. GALLIN, E. K. Ionomycin-induced activation of inward-rectifying potassium channels in human macrophages: evidence for a calcium-activated potassium channel with a small unitary conductance. *Am. J. Physiol.* 256 (*Cell Physiol.* 25): C77–C85, 1989.
64. GALLIN, E. K., AND J. I. GALLIN. Interaction of chemotactic factors with human macrophages. Electrophysiology of the response. *J. Cell Biol.* 75: 277–289, 1977.
65. GALLIN, E. K., AND D. R. LIVENGOOD. Inward rectification in mouse macrophages: evidence for a negative resistance region. *Am. J. Physiol.* 241 (*Cell Physiol.* 10): C9–C17, 1981.
66. GALLIN, E. K., AND D. R. LIVENGOOD. Demonstration of an electrogenic Na^+-K^+ pump in mouse spleen macrophages. *Am. J. Physiol.* 245 (*Cell Physiol.* 14): C184–C188, 1983.
67. GALLIN, E. K., AND L. C. MCKINNEY. Potassium conductances in macrophages. In: *Cell Physiology of Blood*, edited by R. Gunn and J. Parker. New York: Rockefeller Univ. Press, 1988, p. 316–32[illegible].
68. GALLIN, E. K., AND L. C. MCKINNEY. Patch-clamp studies in human macrophages: single-channel and whole cell characterization of two K^+ conductances. *J. Membr. Biol.* 103: 55[illegible], 1988.
69. GALLIN, E. K., AND L. C. MCKINNEY. Monovalent ion transport and membrane potential changes during activation in phagocytic leukocytes. In: *Current Topics in Membranes and Transport. Mechanisms of Leukocyte Activation*, edited by S. Grinstein and O. Rothstein. New York: Academic, 1990, vol. 35, p. 127–148.
70. GALLIN, E. K., AND P. A. SHEEHY. Differential expression of inward and outward potassium currents in the macrophage-like cell line J774.1. *J. Physiol. Lond.* 369: 475–493, 1985.
71. GALLIN, E. K., M. WIEDERHOLD, P. LIPSKY, AND A. ROSENTHAL. Spontaneous and induced membrane hyperpolarizations in macrophages. *J. Cell. Physiol.* 86: 653–662, 1975.
71a. GARCIA-SOTO, J., AND S. GRINSTEIN. Determinants of the transmembrane distribution of chloride in T lymphocytes: role of Cl-HCO_3 exchange. *Am. J. Physiol.* 258 (*Cell Physiol.* 27): C1108–C1116, 1990.
72. GARDNER, P. Calcium and T lymphocyte activation. *Cell* 59: 15–20, 1989.
73. GARDNER, P. Patch clamp studies of lymphocyte activation. *Annu. Rev. Immunol.* 8: 231–252, 1990.
74. GARDNER, P., A. ALCOVER, M. KUNO, P. MOINGEON, C. M. WEYAND, J. GORONZY, AND E. L. REINHERZ. Triggering of T lymphocytes via either T3-Ti or T11 surface structures opens a voltage-insensitive plasma membrane calcium-permeable channel: requirement for interleukin 2 gene function. *J. Biol. Chem.* 264: 1068–1076, 1989.
75. GELFAND, E. W. Cytosolic calcium changes during T and B lymphocyte activation: biological consequences and significance. In: *Current Topics in Membranes and Transport. Mechanisms of Lymphocyte Activation*, edited by S. Grinstein and C. Rothstein. New York: Academic, 1990, vol. 35, p. 153–171.
76. GELFAND, E. W., R. K. CHEUNG, AND S. GRINSTEIN. Role of membrane potential in the regulation of lectin induced calcium uptake. *J. Cell. Physiol.* 121: 533–539, 1984.
77. GELFAND, E. W., R. K. CHEUNG, AND S. GRINSTEIN. Mitogen-induced changes in Ca^{2+} permeability are not mediated by voltage-gated K^+ channels. *J. Biol. Chem.* 261: 11520–11523, 1986.
78. GELFAND, E. W., R. K. CHEUNG, AND S. GRINSTEIN. Calcium-dependent intracellular acidification dominates the pH response to mitogen in human T cells. *J. Immunol.* 140: 246–252, 1988.
79. GELFAND, E. W., R. K. CHEUNG, G. B. MILLS, AND S. GRINSTEIN. Mitogens trigger a calcium-dependent signal for proliferation in phorbol-ester treated lymphocytes. *Nature Lond.* 315: 419–420, 1985.
80. GILES, W. R., AND E. F. SHIBATA. Voltage clamp of bullfrog cardiac pacemaker cells: a quantitative analysis of potassium currents. *J. Physiol. Lond.* 368: 265–292, 1985.
81. GILLY, W. F., AND C. A. ARMSTRONG. Divalent cations and the activation kinetics of potassium channels in squid giant axons. *J. Gen. Physiol.* 79: 965–996, 1982.
82. GRAY, L. S., J. R. GNARRA, J. H. RUSSEL, AND V. H. ENGELHARD. The role of K^+ in the regulation of the increased intracellular Ca^{2+} mediated by the T lymphocyte antigen receptor. *Cell* 50: 119–127, 1987.
83. GRAY, L. S., J. R. GNARRA, J. A. SULLIVAN, G. L. MANDELL, AND V. H. ENGELHARD. Spatial and temperal characteristics of the increase in intracellular Ca^{2+} induced in cytotoxic T lymphocytes by cellular antigen. *J. Immunol.* 141: 2424–2430, 1988.
84. GRAY, L. S., AND J. H. RUSSELL. Cytolytic T lymphocyte effector function requires plasma membrane chloride flux. *J. Immunol.* 136: 3032–3037, 1986.
85. GRINSTEIN, S., C. A. CLARKE, A. DUPRE, AND A. ROTHSTEIN. Volume-induced increase of anion permeability in human lymphocytes. *J. Gen. Physiol.* 80: 801–823, 1982.
86. GRINSTEIN, S., C. A. CLARKE, A. ROTHSTEIN, AND E. W. GELFAND. Volume-induced anion conductance in human B lymphocytes is cation independent. *Am. J. Physiol.* 245 (*Cell Physiol.* 14): C160–C163, 1983.
87. GRINSTEIN, S., AND S. J. DIXON. Ion transport, membrane potential, and cytoplasmic pH in lymphocytes: changes during activation. *Physiol. Rev.* 69: 417–481, 1989.
88. GRINSTEIN, S., A. DUPRE, AND A. ROTHSTEIN. Volume regulation in human lymphocytes. Role of calcium. *J. Gen. Physiol.* 79: 849–868, 1982.
89. GRINSTEIN, S., AND W. FURLONG. Cytoplasmic pH regulation in phorbol ester-activated human neutrophils. *Am. J. Physiol.* 251 (*Cell Physiol.* 20): C55–C66, 1986.
90. GRINSTEIN, S., A. ROTHSTEIN, B. SARKADI, AND E. GELFAND. Responses of lymphocytes to anistonic media: volume-regulating behavior. *Am. J. Physiol.* 246 (*Cell Physiol.* 15): C204–C215, 1984.
91. GRINSTEIN, S., AND J. D. SMITH. Ca^{2+} induced charybdotoxin-sensitive membrane potential changes in rat lymphocytes. *Am. J. Physiol.* 257 (*Cell Physiol.* 26): C197–C206, 1989.
92. GRINSTEIN, S., AND J. SMITH. Calcium-independent cell volume regulation in human lymphocytes. *J. Gen. Physiol.* 95: 97–120, 1990.
93. GRISSMER, S., AND M. D. CAHALAN. TEA prevents inactivation while blocking open K channels in human T lymphocytes. *Biophys. J.* 55: 203–205, 1989.
94. GRISSMER, S., AND M. D. CAHALAN. Divalent ion trapping inside potassium channels of human T lymphocytes. *J. Gen. Physiol.* 93: 609–630, 1989.
95. GRISSMER, S., AND M. D. CAHALAN. Ionomycin activates a potassium-selective conductance in human T lymphocytes (Abstract). *Biophys. J.* 55: 245a, 1989.
96. GRISSMER, S., M. D. CAHALAN, AND K. G. CHANDY. Abundant expression of type I K^+ channels. A marker for lymphoproliferative diseases? *J. Immunol.* 141: 1137–1142, 1988.
97. GRISSMER, S., B. DETHLEFS, J. WASMUTH, A. GOLDIN, G. GUTMAN, M. D. CAHALAN, AND K. CHANDY. Expression and chromosomal localization of a lymphocyte K^+ channel gene. *Proc. Natl. Acad. Sci. USA* 87: 9411–9115, 1990.
98. GRYGORCZYK, R., AND W. SCHWARTZ. Properties of the Ca-activated K conductance of human red cells as revealed by the patch clamp technique. *Cell Calcium* 4: 499–510, 1983.

99. HAGIWARA, S., S. MIYAZAKI, S. KRAUSE, AND S. CIANAI. Anomalous permeabilities of the egg cell membrane of a starfish in K^+-Ti^+ mixtures. *J. Gen. Physiol.* 80. 801-824, 1977.
100. HAGIWARA, S., S. MIYAZAKI, AND N. P. ROSENTHAL. Potassium current and the effect of cesium on this current during anomalous rectification of the egg cell membrane of a starfish. *J. Gen. Physiol.* 67: 621-638, 1976.
101. HAGIWARA, S., AND K. TAKAHASHI. The anomalous rectification and cation selectivity of the membrane of a starfish egg cell. *J. Physiol. Lond.* 67. 621-638, 1974.
102. HALLET, M B., AND A. K CAMPBELL Direct measurement of intracellular free Ca^{2+} in rat peritoneal macrophages. correlation with oxygen radical production. *Immunology* 50: 487-495, 1983.
103. HAMILL, O. P., A. MARTY, E. NEHER, B. SAKMANN, AND F. J. SIGWORTH Improved patch-clamp techniques for high resolution current recording from cells and cell-free membrane patches. *Pfluegers Arch.* 391: 85-100, 1981.
104. HARA, N., M. ICHINOSE, M SAWADA, K. IMAI, AND T. MAENO. Activation of single Ca^{2+}-dependent K^+ channel by external ATP in mouse macrophages. *FEBS Lett.* 267. 281-284, 1990.
105. HEIKKLA, R., T. GODAL, A. HENRIKSEN, AND J. G. IVERSEN. Anti-immunoglobulin-induced potassium flux in relation to capping and DNA synthesis. *Exp. Cell Res.* 136. 447-454, 1981.
106. HILLE, B. Potassium channels in myelinated nerve: selective permeability to small cations. *J. Gen. Physiol.* 61: 669-686, 1973.
107. HILLE, B. *Ionic Channels in Excitable Membranes.* Sunderland, MA: Sinauer, 1984.
108. HILLE, B., AND W. SCHWARZ. Potassium channels as multi-ion single file pores. *J. Gen. Physiol.* 72: 409-442, 1978.
109. HISDERODT, J. C., L. J. BRITVAN, AND S. TARGAN. Characterization of the cytolytic reaction mechanism of the human natural killer (NK) lymphocytes: resolution into binding, programming and killer cell-independent steps. *J. Immunol.* 129: 1782-1787, 1982.
110. HOLIAN, A., AND R. DANIELE. Formyl peptide stimulation of superoxide anion release from lung macrophages: sodium and potassium involvement. *J. Cell. Physiol.* 113: 413-419, 1982.
111. HORN, R., AND A. MARTY. Muscarinic activation of ionic currents measured by a new whole-cell recording method. *J. Gen. Physiol.* 92: 145-159, 1988.
112. HU, S., AND N. RUBLY. Effects of morphine on ionic currents in frog node of ranvier. *Eur. J. Pharmacol.* 95: 185-192, 1983.
113. IMOBODEN, J. B., AND J. D. STOBO. Transmembrane signalling by the T cell antigen receptor. *J. Exp. Med.* 161: 446-456, 1985.
114. INCE, C., J. COREMANS, D. YPEY, P. LEIJH, A. VERVEEN, AND R. VAN FURTH. Phagocytosis by human macrophages is accompanied by changes in ionic channel currents. *J. Cell Biol.* 106: 1873-1878, 1988.
115. INCE, C., P. C. LEIJH, J. MEIJER, E. VAN BAVEL, AND D. YPEY. Oscillatory hyperpolarizations and resting membrane potentials of mouse fibroblast and macrophage cell lines. *J. Physiol. Lond.* 352: 625-635, 1984.
116. INCE, C., B. THIO, B. VAN DUIJN, J. VAN DISSEL, D. YPEY, AND P. C. J. LEIJH. Intracellular K^+, Na^+ and Cl^- concentrations and membrane potential in human monocytes. *Biochim. Biophys. Acta* 905: 195-204, 1987.
117. INCE, C., B. VAN DUIJN, D. L. YPEY, E. VAN BAVEL, F. WEIDEMA, AND P. C. J. LEIJH. Ionic channels and membrane hyperpolarization in human macrophages. *J. Membr. Biol.* 97. 251-258, 1987.
118. INCE, C., D. L. YPEY, R. VAN FURTH, AND A. A. VERVEEN. Estimation of membrane potential of cultured macrophages from the fast potential transient upon microelectrode entry. *J. Cell Biol.* 96: 796-801, 1983.
119. ISHIDA, Y., AND T. M. CHUSED. Heterogeneity of lymphocyte calcium metabolism is caused by T cell specific calcium-sensitive potassium channel and sensitivity of the calcium ATPase pump to membrane potential. *J. Exp. Med.* 168. 839 852, 1988.
120. JOW, B., AND D. J. NELSON. Outwardly rectifying K^+ current as a marker of cellular activation in human macrophages (Abstract). *Biophys. J.* 55. 539a, 1989.
120a. KAKUTA, Y., H. OKAYAMA, T. KAWA, T. KANNO, T. OHYAMA, H. SASAKI, T. KATO, AND T. TAKISHIMA. K channels of human alveolar macrophages. *J. Allergy Clin. Immunol.* 81: 460-468, 1988.
121. KANNO, T., AND T. TAKISHIMA. Chloride and potassium channels in U937 human monocyte. *J. Membr. Biol.* 116. 149-161, 1990.
122. KIEFFER, H., A. J. BLUME, AND H. R. KABACK. Membrane potential changes during mitogenic stimulation of mouse spleen lymphocytes. *Proc. Natl. Acad. Sci. USA* 77. 2200-2204, 1980.
123. KITIGAWA, S., AND R. B. JOHNSTON, JR. Relationship between membrane potential changes and superoxide-releasing capacity in resident and activated mouse peritoneal macrophages. *J. Immunol.* 135: 3417-3423, 1985.
124. KITAGAWA, S., M. OHTA, H. NOJIRI, K. KAKINUMA, M. SAITO, F. TAKAKU, AND Y. MIURA. Functional maturation of membrane potential changes and superoxide capacity during granulocyte differentiation. *J. Clin. Invest.* 73. 1062-1071, 1984.
125. KOLB, H.-A., AND J. UBL. Activation of anion channels by zymosan particles in membranes of peritoneal macrophages. *Biochim. Biophys. Acta* 899: 239-246, 1987.
126. KORCHAK, H. M., AND G. WEISSMANN. Stimulus-response coupling in the human neutrophil. Transmembrane potential and the role of extracellular Na^+. *Biochim. Biophys. Acta* 601: 180-194, 1980.
127. KRAUSE, D., S. C. LEE, AND C. DEUTSCH. Forskolin effects on the voltage-gated K conductance of human T cells. *Pfluegers Arch.* 412: 133-140, 1988.
128. KRAUSE, K., AND M. J. WELSH. Voltage-dependent and calcium-activated ion channels in human neutrophils. *J. Clin. Invest.* 85: 491-498, 1990.
129. KRUSKAL, B. J., AND F. R. MAXFIELD. Cytosolic free calcium increases before and oscillates during frustrated phagocytosis in macrophages. *J. Cell Biol.* 105: 2685-2693, 1987.
130. KUNO, M., AND P. GARDNER. Ion channels activated by inositol 1,4,5-triphosphate in plasma membrane of human T-lymphocytes. *Nature Lond.* 326: 301-304, 1987.
131. KUNO, M., J. GORONZY, C. M. WEYAND, AND P. GARDNER. Single-channel and whole-cell recordings of mitogen-regulated inward currents in human cloned helper T lymphocytes. *Nature Lond.* 323: 269-273, 1986.
132. KURACHI, Y. Regulation of G proteins-gated K channels. *News Physiol. Sci.* 4: 158-161, 1989.
133. LABAER, J., R. Y. TSIEN, K. A. FAHEY, AND A. L. DEFRANCO Stimulation of the antigen receptor on WEHI-231 B lymphoma cells results in a voltage-independent increase in cytoplasmic calcium. *J. Immunol.* 137. 1836-1844, 1986.
134. LARKIN, J. M., M. S. BROWN, J. L. GOLDSTEIN, AND R. G. ANDERSON. Depletion of intracellular potassium arrests coated pit formation and receptor-mediated endocytosis in fibroblasts. *Cell* 33: 273-285, 1983.
135. LAU, Y.-T., R. R. YASSIN, AND S. B. HOROWITZ. Potassium salt microinjection into *Xenopus* oocytes mimics gonadotropin treatment. *Science Wash. DC* 240: 1321-1323, 1988.
136. LAZZARI, K. G., P. J. PROTO, AND E. R. SIMONS. Simultaneous measurement of stimulus-induced changes in cytoplasmic Ca^{++} and in membrane potential of human neutrophils. *J. Biol. Chem.* 261: 9710-9713, 1986.
137. LEE, K. S., AND R. W. TSIEN. Mechanism of calcium channel blockade by verapamil, D600, diltiazem and nitrendipine in single dialysed heart cells. *Nature Lond.* 302. 790-794, 1983.
138. LEE, S. C., AND C. DEUTSCH. Temperature dependence of K-channel properties in human T-lymphocytes. *Biophys. J.* 57. 49-62, 1990.
139. LEE, S. C., C. DEUTSCH, AND W. T. BECK. Comparison of ion channels in multidrug-resistant and -sensitive leukemic cells. *Proc. Natl. Acad. Sci. USA* 85. 2019-2023, 1988.
140. LEE, S. C., M. PRICE, M. B. PRYTOWSKY, AND C. DEUTSCH. Volume response of quiescent and interleukin 2-stimulated T-lymphocytes to hypotonicity. *Am. J. Physiol.* 254 (*Cell Physiol.* 23): C286-C296, 1988.
141. LEE, S. C., D. E. SABATH, C. DEUTSCH, AND M. B. PRYTOWSKY. Increased voltage-gated potassium conductance dur-

ing interleukin 2-stimulated proliferation of a mouse helper T lymphocyte clone. *J. Cell Biol.* 102. 1200–1208, 1986.
142. LEECH, C. A., AND P. R. STANFIELD. Inward rectification in frog skeletal muscle fibres and its dependence on membrane potential and external potassium. *J. Physiol. Lond.* 310. 295 309, 1981.
143. LEFEVER, A., A. LIEPINS, AND R. TRUIT. Role of K^+ ion channels in lymphokine-activated killer (LAK) cell lytic function. *Immunopharmacol. Immunotoxicol.* 11: 571–582, 1989.
144. LEW, P. D., T ANDERSON, J. HED, F. DI VIRGILIO, T. POZZAN, AND O STENDAHL. Ca-dependent and Ca-independent phagocytosis in human neutrophils. *Nature Lond.* 315. 509 511, 1985.
145. LEW, P D., A MONOD, F. WALDVOGEL, B. DEWALD, M. BAGGIOLINI, AND T. POZZAN. Quantitative analysis of the cytosolic free calcium dependency of exocytosis from three subcellular compartments in intact neutrophils. *J. Clin. Invest.* 102. 2197-2204, 1986.
146. LEW, P. D., C. WOLLHEIM, F. A. WALDVOGEL, AND T. POZZAN. Modulation of cytosolic free calcium transients by changes in intracellular calcium-buffering capacity: correlation with exocytosis and O_2-production in human neutrophils. *J. Cell Biol.* 99. 1212-1220, 1984.
147 LEWIS, R S., AND M. D CAHALAN. A chloride conductance activated by intracellular ATP hydrolysis in T and B lymphocytes (Abstract). *Biophys. J.* 51: 397a, 1987.
148. LEWIS, R S., AND M D. CAHALAN. Subset-specific expression of potassium channels in developing murine T lymphocytes. *Science Wash. DC* 239: 771–775, 1988.
149 LEWIS, R. S., AND M D. CAHALAN. The plasticity of ion channels: parallels between the nervous and immune sytems. *Trends Neurosci.* 11: 214–218, 1988.
150. LEWIS, R S., AND M D. CAHALAN. Voltage-dependent calcium signaling in single T lymphocytes. *Soc. Neurosci. Abstr.* 14: 298, 1988.
151 LEWIS, R S., AND M. D. CAHALAN. Mitogen-induced oscillations of cytosolic Ca^{2+} and transmembrane Ca^{2+} current in human leukemic T cells. *Cell Regul.* 1: 99–112, 1989.
152. LEWIS, R. S., AND M. D. CAHALAN. Ion channels and signal transduction in lymphocytes. *Annu. Rev. Physiol.* 52: 415–430, 1990.
153. LICHTMAN, A. H., G. S. SEGAL, AND M. A. LICHTMAN. The role of calcium in lymphocyte proliferation (an interpretive review). *Blood* 61: 413–422, 1983.
154. LINDAU, M., AND J M. FERNANDEZ. A patch-clamp study of histamine-secreting cells. *J. Gen. Physiol.* 88: 349–368, 1986.
155. LIPTON, S. Antibody activates cation channels via second messenger Ca^{++}. *Biochim. Biophys. Acta* 856: 59–67, 1986.
156. LUSCINSKAS, F., D. MARK, B. BRUNKHORST, F. LIONETTI, AND E. CRAGOE, JR. The role of transmembrane cationic gradients in immune complex stimulation of human polymorphonuclear leukocytes. *J. Cell. Physiol.* 134: 211–219, 1988.
157. MACDOUGALL, S. L., S. GRINSTEIN, AND E. W. GELFAND. Detection of ligand-activated conductive Ca channels in human B lymphocytes. *Cell* 54. 229–234, 1988.
158. MACDOUGALL, S. L., S. GRINSTEIN, AND E. W. GELFAND. Activation of Ca-dependent K channels in human B lymphocytes by anti-immunoglobulin. *J. Clin. Invest.* 81. 449–454, 1988.
159. MAHAUT-SMITH, M. P., AND M. J. MASON. Ca-dependent K channel activity in rat thymic lymphocytes. effect of mitogenic stimulation (Abstract). *Biophys. J.* 57. 113a, 1990.
160. MAHAUT-SMITH, M. P., AND L. C. SCHLICHTER. Ca^{2+}-activated K^+ channels in human B lymphocytes and rat thymocytes. *J. Physiol. Lond.* 415. 69–83, 1989.
161. MARTY, A., AND E. NEHER. Tight-seal whole-cell recording. In. *Single Channel Recording*, edited by B. Sakmann and E. Neher. New York. Plenum, 1983, p. 107-122.
162. MATSUDA, H., A. SAIGUSA, AND H. IRISAWA. Ohmic conductances through the inwardly rectifying K channel and blocking by internal Mg^{2+}. *Nature Lond.* 325 156–159, 1982.
163. MATTESON, D. R., AND C. DEUTSCH. K channels in T lymphocytes: a patch clamp study using monoclonal antibody adhesion. *Nature Lond.* 307. 468–471, 1984.
164. MATTHEWS, G., E. NEHER, AND R. PENNER. Second messenger-activated calium influx in rat peritoneal mast cells. *J. Physiol. Lond.* 418: 105–130, 1989.
165. MCCANN, F. V., J. J. COLE, P. M. GUYRE, AND J. A. G. RUSSELL. Action potentials in macrophages derived from human monocytes. *Science Wash. DC* 219: 991–993, 1983.
166. MCCANN, F. V., T. M. KELLER, AND P. M. GUYRE. Ion channels in human macrophages compared with the U-937 cell line. *J. Membr. Biol.* 96: 57–64, 1987.
167. MCCANN, F. V., D. C. MCCARTHY, T. M. KELLER, AND R. J. NOELLE. Characterization of a large conductance non-selective anion channel in B lymphocytes. *Cell. Signal.* 1. 31–44, 1989.
168. MCCANN, F. V., D. C. MCCARTHY, AND R. J. NOELLE. Patch-clamp profile of ion channels in resting murine B lymphocytes. *J. Membr. Biol.* 117: 175–188, 1990.
169. MCCLOSKEY, M. A., AND M. D. CAHALAN. G protein control of potassium channel activity in a mast cell line. *J. Gen. Physiol.* 95. 205-227, 1990.
170. MCKINNEY, L. C., AND E. K. GALLIN. Inwardly rectifying whole-cell and single-channel K currents in the murine macrophage cell line J774.1. *J. Membr. Biol.* 103: 41–53, 1988.
171. MCKINNEY, L. C., AND E. K. GALLIN. Effect of adherence, cell morphology, and lipopolysaccharide on potassium conductance and passive membrane properties of murine macrophages J774.1 cells. *J. Membr. Biol.* 116: 47–56, 1990.
172. MCKINNON, D., AND R. CEREDIG. Changes in the expression of potassium channels during mouse T cell development. *J. Exp. Med.* 164: 1846–1861, 1986.
173. MELMED, R., P. KARANIAN, AND R. BERLIN. Control of cell volume in the J774 macrophage by microtubule disassembly and cyclic AMP. *J. Cell Biol.* 90: 761–768, 1981.
174. MERRIT, J., R. JACOB, AND T. HALLAM. Use of manganese to discriminate between calcium influx and mobilization from internal stores in stimulated human neutrophils. *J. Biol. Chem.* 264: 1522-1527, 1989.
175. MILLER, C., E. MOCZYDLOWSKI, R. LATORRE, AND M. PHILLIPS. Charybdotoxin, a protein inhibitor of single Ca-activated K channels from mammalian skeletal muscle. *Nature Lond.* 312: 316-318, 1985.
176. MILLS, G. B., R. K. CHEUNG, S. GRINSTEIN, AND E. W. GELFAND. Increase in cytosolic free calcium concentration is an intracellular messenger for the production of interleukin 2 but not for expression of the interleukin 2 receptor. *J. Immunol.* 134: 1640-1643, 1985.
177. MILLS, G. B., R. K. CHEUNG, S. GRINSTEIN, AND E. W. GELFAND. Interleukin 2-induced lymphocyte proliferation is independent of increases in cytosolic-free calcium concentrations. *J. Immunol.* 134: 2431-2435, 1985.
178. MOODY-CORBETT, F., AND P. BREHM. Acetylcholine reduces inward rectification on thymus-derived macrophage cells in culture. *Can. J. Physiol. Pharamacol.* 65: 348–351, 1986.
179. MOTTOLA, C., AND D. ROMEO. Calcium movement and membrane potential changes in the early phase of neutrophil activation by phorbol myristate acetate. a study with ion-selective electrodes. *J. Cell Biol.* 93: 129–134, 1982.
180. NASMITH, P., AND S. GRINSTEIN. Are Ca^{2+} channels in neutrophils activated by a rise in cytosolic Ca^{2+}? *FEBS Lett.* 221. 95 100, 1987.
181. NEHER, E., AND B. SAKMANN. Single-channel currents recorded from membranes of denervated frog muscle fibers. *Nature Lond.* 260: 779–802, 1976.
182. NELSON, D. J., E. R. JACOBS, J. M. TANG, J. J. ZELLER, AND R. C. BONE. Immunoglobulin G-induced single ionic channels in human alveolar macrophage membranes. *J. Clin. Invest.* 76. 500 507, 1985.
183. NELSON, D. J., B. JOW, AND F. JOW. Whole cell currents in macrophages. I. Human monocyte-derived macrophages. *J. Membr. Biol.* 117: 29–44, 1990.
184. NELSON, D. J., B. JOW, AND K. J. POPOVICH. Whole-cell currents in macrophages. II. Alveolar macrophages. *J. Membr. Biol.* 117: 45–55, 1990.
185. NELSON, D. J., L. RUFER, T. NAKAYAMA, AND J. M. ZELLER.

Phorbol ester block of voltage dependent K current in monocyte-derived macrophages (Abstract). *Biophys. J.* 49: 161a, 1986.
186. NOSSAL, G. J. The basic components of the immune system. *N. Engl. J. Med.* 316: 1320–1325, 1987.
187. NOWYCKY, M. C., A. P. FOX, AND R. W. TSIEN. Three types of neuronal calcium channels with different calcium agonist sensitivities. *Nature Lond.* 316: 440–443, 1985.
188. OETTGEN, H. C., C. TERHOST, L. C. CANTLEY, AND P. M. ROSOFF. Stimulation of the T3 T cell receptor complex induces a membrane-potential-sensitive calcium influx. *Cell* 40: 583–590, 1985.
189. OHARA, J., M. SUGI, M. FUJIMOTO, AND T. WATANABE. Microinjection of macromolecules into normal murine lymphocytes by means of cell fusion. II. Enhancement and suppression of mitogenic responses by microinjection of monoclonal anti-cyclic AMP into B lymphocytes. *J. Immunol.* 129: 1227–1232, 1982.
190. OKADO, Y., AND A. HAZAMA. Volume regulatory ion channels in epithelial cells. *News Physiol. Sci.* 4: 238–242, 1989.
191. OWENS, T., AND J. G. KAPLAN. Increased cationic fluxes in stimulated lymphocytes of the mouse. response of enriched B- and T cell subpopulations to B- and T cell mitogens. *Can. J. Biochem.* 58: 831–839, 1980.
192. OWENS, T., AND J. G. KAPLAN. T-dependent B-cell activation is signalled by an early increase in potassium influx. *Immunobiology* 162: 277–287, 1982.
193. PAEGELOW, I., AND H. WERNER. Immunomodulation by some oligopeptides. *Methods Find. Clin. Pharmacol.* 8: 91–95, 1986.
194. PAHAPILL, P. A., AND L. C. SCHLICTER. Modulation of potassium channels in human T lymphocytes: effects of temperature. *J. Physiol. Lond.* 422: 103–126, 1990.
195. PAHAPILL, P. A., AND L. C. SCHLICTER. Kinase- and temperature-regulated chloride channels in normal human T lymphocytes (Abstract). *Biophys. J.* 57: 394a, 1990.
196. PALADE, P., C. DETTBARN, P. VOLPE, B. ALDERSON, AND A. S. OTERO. Direct inhibition of inositol-1,4,5-trisphosphate-induced Ca^{2+} release from brain microsomes by K^+ channel blockers. *Mol. Pharmacol.* 36: 664–672, 1989.
197. PASTAN, I. H., G. S. JOHNSON, AND W. B. ANDERSON. Role of cyclic nucleotides in growth control. *Annu. Rev. Biochem.* 44: 491–522, 1975.
198. PAYAN, D. G., D. R. BEWSTER, AND E. J. GOETZL. Specific stimulation of human T lymphocytes by substance P. *J. Immunol.* 131: 1613–1615, 1983.
199. PECHT, I., A. CORCIA, M. P. LIUZZI, A. ALCOVER, AND E. L. REINHERZ. Ion channels activated by specific T1 and T3 antibodies in plasma membranes of human T cells. *EMBO J.* 6: 1935–1938, 1987.
200. PENNER, R., G. MATTHEWS, AND E. NEHER. Regulation of calcium influx by second messengers in rat mast cells. *Nature Lond.* 334: 499–504, 1988.
201. PERSECHINI, P. M., E. G. ARAUJO, AND G. M. OLIVEIRA-CASTRO. Electrophysiology of phagocytic membranes, induction of slow membrane hyperpolarizations in macrophages and macrophage polykaryons by intracellular calcium injection. *J. Membr. Biol.* 61: 81–90, 1981.
202. PERSECHINI, P., AND G. OLIVEIRA-CASTRO. Electrophysiology of phagocytic membranes. intracellular K^+ activity and K^+ equilibrium potential in macrophage polykaryons. *Biochim. Biophys. Acta* 899: 213–221, 1987.
203. PFEFFERKORN, L. Transmembrane signalling: an ion-flux-independent model for signal transduction by complexed Fc receptor. *J. Cell Biol.* 99: 2231–2240, 1984.
204. PITTET, D., F. DI VIRGILIO, T. POZZAN, A. MONOD, AND D. LEW. Correlation between plasma membrane potential and second messenger generation in the promyelocytic cell line HL-60. *J. Biol. Chem.* 265: 14246–14263, 1990.
205. PITTET, D., D. P. LEW, G. W. MAYR, A. MONOD, AND W. SCHLEGEL. Chemoattractant receptor promotion of Ca^{2+} influx across the plasma membrane of HL-60 cells. *J. Biol. Chem.* 264: 7251–7261, 1989.
206. POENIE, M., R. Y. TSIEN, AND A. SCHMITT VERHULST. Sequential activation and lethal hit measured by $[Ca^{2+}]_i$ in individual cytolytic T cells and targets. *EMBO J.* 6: 2223–2232, 1987.
208. POZZAN, T., P. ARSLAN, R. Y. TSIEN, AND T. J. RINK. Anti-immunoglobulin, cytoplasmic free calcium, and capping in B lymphocytes. *J. Cell Biol.* 94: 335–340, 1982.
209. POZZAN, T., P. LEW, C. WOLHEIM, AND R. TSIEN. Is cytosolic ionized calcium regulating neutrophil activation? *Science Wash. DC* 221: 1413–1415, 1983.
210. PRICE, M., S. C. LEE, AND C. DEUTSCH. Charybdotoxin inhibits proliferation and interleukin 2 production in human peripheral blood lymphocytes. *Proc. Natl. Acad. Sci. USA* 86: 10171–10175, 1989.
211. QUAN, P., T. ISHIZAKA, AND B. BLOOM. Studies on the mechanism of NK cell lysis. *J. Immunol.* 128: 1786–1791, 1982.
212. RANDRIAMAMPITA, C., AND A. TRAUTMANN. Ionic channels in murine macrophages. *J. Cell Biol.* 105: 761–769, 1987.
214. RANSOM, J. T., AND J. C. CAMBIER. B cell activation. VII. Independent and synergistic effects of mobilized calcium and diacylglycerol on membrane potential and I-A expression. *J. Immunol.* 136: 66–72, 1986.
214. RANSOM, J., AND J. CAMBIER. The dynamics and relationship of K efflux and Ca influx in B lymphocytes after antigen-receptor cross-linking. In: *Cell Physiology of Blood*, edited by R. Gunn and J. Parker. New York: Rockefeller Univ. Press, 1988, p. 241–252.
215. RANSOM, J. T., L. K. HARRIS, AND J. C. CAMBIER. Anti-IgG induces release of inositol 1,4,5-trisphosphate, which mediates mobilization of intracellular Ca stores in B lymphocytes. *J. Immunol.* 137: 708–714, 1986.
216. RESCH, L., D. BOUILLON, AND D. GEMSA. The activation of lymphocytes by the ionophore A23187. *J. Immunol.* 120: 1514–1520, 1978.
216a. RESTREPTO, D., D. KOZODY, L. SPINELLI, AND P. KNAUF. pH homeostasis in promyelocytic leukemia cells. *J. Gen. Physiol.* 92: 489–507, 1988.
217. REUTER, H. Modulation of ion channels by phosphorylation and second messengers. *News Physiol. Sci.* 2: 168–171, 1987.
218. REUTER, H., AND C. F. STEVENS. Ion conductance and ion selectivity of potassium channels in snail neurones. *J. Membr. Biol.* 57: 103–118, 1980.
219. RINK, T. J., AND C. DEUTSCH. Calcium-activated potassium channels in lymphocytes. *Cell Calcium* 4: 463–473, 1983.
220. RINK, T. J., C. MONTECUCCO, T. R. HESKETH, AND R. Y. TSIEN. Lymphocyte membrane potential assessed with fluorescent probes. *Biochim. Biophys. Acta* 595: 15–30, 1980.
221. ROBERTS, R., N. MOUNESSA, AND J. I. GALLIN. Increasing extracellular potassium causes calcium dependent shape changes and facilitates concanavalin A capping in human neutrophils. *J. Immunol.* 132: 2000–2006, 1984.
222. ROSOFF, P. M., C. HALL, L. GRAMATES, AND S. R. TERLECKY. 4,4′-Diisothiocyanatostilbene-2,2′-disulfonic acid inhibits CD3-T cell antigen receptor-stimulated Ca^{2+} influx in human T lymphocytes. *J. Biol. Chem.* 263: 19535–19540, 1988.
223. RUDDY, B. Diversity and ubiquity of K channels. *Neuroscience* 25: 729–749, 1988.
224. RUSSEL, J. H., AND C. B. DUBOS. Accelerated ^{86}Rb (K^+) release from the cytotoxic T lymphocyte is a physiologic event associated with delivery of the lethal hit. *J. Immunol.* 131: 1138–1141, 1983.
225. SABATH, D. E., D. S. MONOS, S. C. LEE, AND C. DEUTSCH. Cloned T cell proliferation and synthesis of specific proteins are inhibited by quinine. *Proc. Natl. Acad. Sci. USA* 83: 4739–4743, 1986.
226. SANDS, S. B., R. S. LEWIS, AND M. D. CAHALAN. Charybdotoxin blocks voltage-gated K^+ channels on human and murine T lymphocytes. *J. Gen. Physiol.* 93: 1061–1074, 1989.
227. SAUVE, R., C. SIMONEAU, R. MONETTE, AND G. ROY. Single channel analysis of the potassium permeability in HeLa cancer cells. evidence for a calcium-activated potassium channel of small unitary conductance. *J. Membr. Biol.* 92: 269–282, 1986.
228. SAUVE, R., C. SIMONEAU, L. PARENT, R. MONETTE, AND G. ROY. Oscillatory activation of calcium-dependent potassium channels in HeLa cells induced by histamine H_1 receptor stimulation. a single channel study. *J. Membr. Biol.* 96: 199–208, 1987.
229. SCHELL, S. R., D. J. NELSON, H. A. FOZZARD, AND F. W. FITCH. The inhibitory effects of K channel-blocking agents on T

lymphocyte proliferation and lymphokine production are nonspecific." *J. Immunol.* 139: 3224–3230, 1987.
230. SCHLICTER, L. C., R. GRYGORCZK, P. A. PAHAPILL, AND C. GRYGORCZYK. A large, multiple conductance Cl channel in normal human T lymphocytes. *Pflugers Arch.* 416: 413–421, 1990.
231. SCHLICTER, L., N. SIDELL, AND S. HAGIWARA. K channels are expressed early in human T cell development. *Proc. Natl. Acad. Sci. USA* 83: 5625–5629, 1986.
232. SCHLICTER, L., N. SIDELL, AND S. HAGIWARA. Potassium channels mediate killing in human natural killer cells. *Proc. Natl. Acad. Sci. USA* 83: 451–455, 1986.
233. SCHLICTER, L. C., AND J. C. MACCOUBREY. Interactive effects of Na and K in killing by human natural killer cells. *Exp. Cell Res.* 184: 99–108, 1989.
234. SCHUMANN, M. A., AND P. GARDNER. Modulation of membrane K^+ conductance by substance P via a GTP-binding protein. *J. Membr. Biol.* 111: 133–139, 1989.
235. SCHUMANN, M. A., D. HELLER, T. TANIGAKI, AND T. A. RAFFIN. Characterization of macroscopic chloride current in human neutrophils (Abstract). *Biophys. J.* 57: 319a, 1990.
236. SCHWARZE, W., AND H. A. KOLB. Voltage dependent kinetics of an anionic channel of large unit conductance in macrophages and myotube membranes. *Pflugers Arch.* 402: 281–291, 1984.
237. SEGEL, G. B., AND M. A. LICHTMAN. Potassium transport in human blood lymphocytes treated with phytohemagglutinin. *J. Cell. Physiol.* 87: 337–344, 1976.
238. SELIGMANN, B., E. GALLIN, D. MARTIN, W. SHAIN, AND J. GALLIN. Interaction of chemotactic factors with human PMN: studies using membrane potential sensitive cyanine dyes. *J. Membr. Biol.* 52: 257–272, 1980.
239. SELIGMANN, B. E., AND J. I. GALLIN. Use of lipophilic probes of membrane potential to assess human neutrophil activation. *J. Clin. Invest.* 66: 493–503, 1980.
240. SELIGMANN, B. E., AND J. I. GALLIN. Comparison of indirect probes of membrane potential utilized in studies of human neutrophils. *J. Cell. Physiol.* 115: 105–115, 1983.
241. SHAPIRO, M. S. Are type "I" K^+ channels in lymphocytes the same as gf2 K^+ channels in frog node of Ranvier? (Abstract). *Biophys. J.* 57: 515a, 1990.
242. SHAPIRO, M. S., AND T. E. DECOURSEY. Two types of potassium channels in a lymphoma cell line (Abstract). *Biophys. J.* 53: 550a, 1988.
243. SHAPIRO, M. S., AND T. E. DECOURSEY. Selectivity and permeant ion effects on gating of the type "I" K channel in lymphocytes (Abstract). *Biophys. J.* 55: 200a, 1989.
244. SHARMA, B. Inhibition of the generation of cytotoxic lymphocytes by potassium ion channel blockers. *J. Immunol.* 65: 101–105, 1988.
245. SHERIDAN, R. E., AND B. M. BAYER. Ionic membrane currents induced in macrophages during cytolysis (Abstract). *Federation Proc.* 45: 1009a, 1986.
246. SHERMAN, M. S., K. SEKIGUCHI, AND Y. NISHIZUKA. Modulation of ion channel activity: a key function of the protein kinase C enzyme family. *Pharmacol. Rev.* 41: 211–237, 1989.
247. SHINOHARA, T., AND J. PLATIGORSKY. Regulation of protein synthesis, intracellular electrolytes and cataract formation in vitro. *Nature Lond.* 270: 406–411, 1977.
248. SHOWELL, H., AND E. BECKER. The effect of external K^+ and Na^+ on the chemotaxis of rabbit peritoneal neutrophils. *J. Immunol.* 116: 99–104, 1976.
249. SIDELL, N., AND L. SCHLICTER. Retinoic acid blocks potassium channels in human lymphocytes. *Biochem. Biophys. Res. Commun.* 138: 560–567, 1986.
250. SIDELL, N., L. SCHLICHTER, S. WRIGHT, S. HAGIWARA, AND S. H. GOLUB. Potassium channels in human NK cells are involved in discrete stages of the killing process. *J. Immunol.* 137: 1650–1658, 1986.
251. SILVER, M. R., AND T. E. DECOURSEY. Intrinsic gating of inward rectifier in bovine artery endothelial cells in the presence and absence of internal Mg^{2+}. *J. Gen. Physiol.* 96: 109–133, 1990.
252. SILVERSTEIN, S., R. STEINMAN, AND Z. COHN. Endocytosis. *Annu. Rev. Biochem.* 46: 669–722, 1977.
253. SIMCHOWITZ, L. Intracellular pH modulates the generation of superoxide radicals by human neutrophils. *J. Clin. Invest.* 76: 1079–1089, 1985.
254. SIMCHOWITZ, L., AND E. J. CRAGOE, JR. Na^+/Ca^{2+} exchange in human neutrophils. *Am. J. Physiol.* 254 (*Cell Physiol.* 23): C150–C164, 1988.
255. SIMCHOWITZ, L., I. SPILBERG, AND P. DE WEER. Sodium and potassium fluxes and membrane potential of human neutrophils. *J. Gen. Physiol.* 79: 453–479, 1982.
256. SNYDERMAN, R., AND R. UHING. Phagocytic cells. stimulus-response coupling mechanisms. In: *Inflammation. Basic Principles and Clinical Correlates*, edited by J. I. Gallin, I. Goldstein, and R. Snyderman. New York. Raven, 1988, p. 309–324.
257. SOLDATI, L., AND P. PERSECHINI. Depolarization of macrophage polykaryons in the absence of external sodium induces cyclic stimulation of calcium-activated potassium conductance. *Biochim. Biophys. Acta* 972: 283–292, 1988.
258. SOMOGYI, R., J. UBL, AND H. A. KOLB. Zymosan and potassium induced activation of single voltage-dependent ion channels in membranes of peritoneal macrophages. In: *Advances in Bioscience*, edited by G. Ricevith. New York. Pergamon, 1987, p. 275–281.
259. SOUTHWICK, F., N. TATSUMI, AND T. STOSSEL. Actimentin, an actin-modulating protein of rabbit pulmonary macrophages. *Biochemistry* 21: 6321–6326, 1982.
260. SPAT, A., P. G. BRADFORD, J. S. MCKINNEY, R. P. RUBIN, AND J. W. PUTNEY. A saturable receptor for ^{32}P-inositol-1,4,5-trisphosphate in hepatocytes and neutrophils. *Nature Lond.* 319: 514–516, 1986.
261. STEINBERG, T. H., A. S. NEWMAN, J. A. SWANSON, AND S. C. SILVERSTEIN. ATP^{4-} permeabilizes the plasma membrane of mouse macrophages to fluorescent dyes. *J. Biol. Chem.* 262: 8884–8888, 1987.
262. STEINBERG, T. H., AND S. C. SILVERSTEIN. Extracellular ATP^{4-} promotes cation fluxes in the J774 mouse macrophage cell line. *J. Biol. Chem.* 262: 3118–3122, 1987.
262a. STOBO, J. D. Lymphocytes. development and function. In: *Inflammation. Basic Principles and Clinical Correlates*, edited by J. I. Gallin, I. M. Goldstein, and R. Snyderman. New York. Raven, 1988, p. 599–612.
263. STRONG, P. N. Potassium channel toxins. *Pharmacol. Ther.* 46: 137–162, 1990.
264. SUNG, S.-S. J., J. D.-E. YOUNG, A. M. ORIGLIO, J. M. HELPLE, H. R. KABACK, AND S. C. SILVERSTEIN. Extracellular ATP perturbs transmembrane ion fluxes, elevates cytosolic $[Ca^{2+}]$, and inhibits phagocytosis in mouse macrophages. *J. Biol. Chem.* 260: 13442–13449, 1985.
265. SUSSMAN, J., M. MERCEP, T. SAITO, R. GERMAIN, E. BONVINI, AND J. ASHWELL. Dissociation of phosphoinositide hydrolysis and Ca^{2+} fluxes from the biological responses of a T-cell hybridoma. *Nature Lond.* 331: 625–627, 1988.
266. SUTRO, J. B., B. VAYUVEGULA, S. GUPTA, AND M. D. CAHALAN. Up-regulation of voltage sensitive K channels in mitogen stimulated B lymphocytes (Abstract). *Biophys. J.* 53: 460a, 1988.
267. SUTRO, J. B., B. VAYUVEGULA, S. GUPTA, AND M. D. CAHALAN. Voltage-sensitive ion channels in human B lymphocytes. *Adv. Exp. Med. Biol.* 254: 113–122, 1989.
268. TATHAM, P. E. R., P. J. DELVES, L. SHEN, AND I. M. ROITT. Chemotactic factor-induced membrane potential changes in rabbit neutrophils monitored by the fluorescent dye 3,3-dipropylthiadicarbocyanine iodide. *Biochim. Biophys. Acta* 602: 285–298, 1980.
269. TAUBER, A., A. KARNAD, AND I. GINIS. The role of phosphorylation in phagocyte activation. In: *Current Topics in Membranes and Transport. Mechanisms of Leukocyte Activation*, edited by S. Grinstein and O. Rothstein. New York. Academic, 1990, vol. 35, p. 469–486.
270. TAYLOR, M. V., J. C. METCALFE, T. R. HESKETH, G. A. SMITH, AND J. P. MOORE. Mitogens increase phosphorylation of phosphoinositides in thymocytes. *Nature Lond.* 312: 462–465, 1984.
271. TSIEN, R. Y., T. POZZAN, AND T. J. RINK. T-cell mitogens cause early changes in cytoplasmic-free Ca^{2+} and membrane potential in lymphocytes. *Nature Lond.* 295: 68–71, 1982.

272. VAN FURTH, R. Phagocytic cells: development and distribution of mononuclear phagocytes in normal steady state and inflammation. In: *Inflammation*, edited by J. Gallin, I. Goldstein, and R. Snyderman. New York: Raven, 1988, p. 281–295.
273. VAYUVEGULA, B., S. GOLLAPUDI, AND S. GUPTA. Inhibition of human B cell proliferation by ion channel blockers. In: *Mechanisms of Lymphocyte Activation and Immune Regulation*, edited by S. Gupta, W. E. Paul, and A. S. Fauci. New York: Plenum, 1987, p. 237–240.
274. VILLEREAL, M. L., AND J. S. COOK. Regulation of active amino acid transport by growth related changes in membrane potential in human macrophages. *J. Biol. Chem.* 253: 8257–8262, 1987.
275. VILVEN, J., AND R. CORONADO. Opening of dihydropyridine calcium channels in skeletal muscle membranes by inositol trisphosphate. *Nature Lond.* 336: 587–589, 1988.
276. VON TSCHARNER, V., B. PRODHOM, M. BAGGIOLINI, AND H. REUTER. Ion channels in human neutrophils are activated by a rise in the free cytosolic calcium concentration. *Nature Lond.* 324: 369–372, 1986.
277. WELSH, M. J., AND C. M. LIEDTKE. Chloride and potassium channels in cystic fibrosis airway epithelia. *Nature Lond.* 322: 467–470, 1986.
278. WIELAND, S. J., R. H. CHOU, AND Q. GONG. Macrophage colony-stimulating factor (CSF-1) modulates differentiation-specific inward rectifying potassium current in human leukemic (HL-60) cells. *J. Cell. Physiol.* 142: 643–551, 1990.
279. WILEY, J. S., AND G. R. DUBYAK. Extracellular adenosine triphosphate increases cation permeability of chronic lymphocytic leukemic lymphocytes. *Blood* 73: 1316–1323, 1989.
280. WILSON, H. A., AND T. M. CHUSED. Lymphocyte membrane potential and Ca^{2+}-sensitive potassium channels described by oxonol dye fluorescence measurements. *J. Cell. Physiol.* 125: 72–81, 1985.
281. WILSON, H. A., D. GREENBLATT, F. D. FINKELMAN, AND T. M. CHUSED. Optical measurements in single cells of membrane potential changes linked to T and B lymphocytes antigen receptors. In: *Cell Physiology of Blood*, edited by R. Geunn and J. Parker. New York: Rockefeller Univ. Press, 1988, p. 253–263.
282. WILSON, H. A., D. GREENBLATT, M. POENIE, F. FINKELMAN, AND R. TSIEN. Crosslinkage of B lymphocyte surface immunoglobulin by anti-Ig or antigen induces prolonged oscillation of intracellular ionized calcium. *J. Exp. Med.* 166: 601–606, 1987.
283. WOEHLCK, H. J., AND F. V. MCCANN. Action potentials in human macrophages are calcium spikes. *Cell Biol. Int. Rep.* 10: 517–525, 1986.
284. YAMASHITA, N., H. HAMADA, T. TSURUO, AND E. OGATA. Enhancement of voltage-gated Na^+ channel current associated with multidrug resistance in human leukemia cells. *Cancer Res.* 47: 3736–3741, 1987.
285. YOUNG, J. D., S. S. KO, AND Z. A. COHN. The increase in intracellular free calcium associated with IgGγ2b/γ1 Fc receptor-ligand interactions: role in phagocytosis. *Proc. Natl. Acad. Sci. USA* 81: 5430–5434, 1984.
286. YOUNG, J. D., J. C. UNKELESS, H. R. KABACK, AND Z. A. COHN. Macrophage membrane potential changes associated with γ2b/γ1 Fc receptor-ligand binding. *Proc. Natl. Acad. Sci. USA* 80: 1357–1361, 1983.
287. YOUNG, J. D., J. C. UNKELESS, H. R. KABACK, AND Z. A. COHN. Mouse macrophage Fc receptor for IgG γ2b/γ1 in artificial and plasma membrane vesicle functions as a ligand-dependent ionophore. *Proc. Natl. Acad. Sci. USA* 80: 1636–1640, 1983.
288. YOUNG, J. D., J. C. UNKELESS, T. M. YOUNG, A. MAURO, AND Z. A. COHN. Role for mouse macrophage IgG Fc receptor as ligand-dependent ion channel. *Nature Lond.* 306: 186–189, 1983.
289. YOUNG, W., J. CHEN, F. JUNG, AND P. GARDNER. Dihydropyridine Bay K 8644 activates T lymphocyte calcium-permeable channels. *Mol. Pharmacol.* 34: 239–244, 1989.
290. YPEY, D. L., AND D. E. CLAPHAM. Development of a delayed outward-rectifying K^+ conductance in cultured mouse peritoneal macrophages. *Proc. Natl. Acad. Sci. USA* 81: 3080–3087, 1984.

Brain Research, 550 (1991) 24–34
Elsevier
ADONIS 0006899391167073

BRES 16707

Early neural grafts transiently reduce the behavioral effects of radiation-induced fascia dentata granule cell hypoplasia

G. Andrew Mickley, J. Leland Ferguson, Maureen A. Mulvihill and Thomas J. Nemeth

Behavioral Sciences Department, Armed Forces Radiobiology Research Institute, Bethesda, MD 20814-5145 (U.S.A.)

(Accepted 15 January 1991)

Key words Ionizing radiation, Rotation, Locomotion, Behavior, Passive avoidance, Transplant, Neural graft, X-ray, Hippocampus, Fascia dentata; Granule cell; Spontaneous alternation

X irradiation of the neonatal rat hippocampus produces a selective hypoplasia of fascia dentata granule cells, locomotor hyperactivity, perseverative movements and deficits in passive avoidance. We previously reported that transplantation of fetal hippocampal tissue into the adult (age 182 ± 4 days) brain produced a partial recovery of these behavioral deficits. Since graft/host interconnections are more prominent when transplants are conducted soon after radiation induced hippocampal damage, in this study we transplanted hippocampal or cerebral cortex neurons when host rats were 33 ± 5 days of age (i.e. only 16 days after radiogenic brain damage). Behavioral evaluations were conducted 80 and 182 days after transplantation or surgical control procedures. In the first test series only, selective components of locomotion (e.g. stereotypy and total distance traveled) and perseverative turning (e.g. mean bout length and turning speed topography) were normalized by the hippocampal grafts. Radiation-induced changes in passive avoidance were less prominent in these studies than in past experiments. Still, transplantation of hippocampal tissue improved performance on this learning task as well. Cerebral cortex grafts did not produce reliable improvements in most behavioral measures. These data suggest that hippocampal grafts placed soon after X-ray induced fascia dentata hypoplasia reduce a broad range of behavioral deficits. However, these benefits are transient and, for the most part, depend on the use of transplant tissues homologous with those damaged.

INTRODUCTION

It is possible to produce selective hypoplasia of the hippocampal granule cells by X-irradiating the partially shielded rat brain. Specificity of damage is assured by conducting the radiation exposure when fascia dentata granule cells are mitotic, but adjacent neurons are mature (and therefore less radiosensitive)[6,28]. This brain damage effectively disrupts major afferents to the hippocampus by eliminating the target cells of the perforant path (from entorhinal cortex). Thus, although the lesion is discrete, it often produces behavioral consequences similar to hippocampectomy[42,43]. Bayer et al.[3], for example, described locomotor hyperactivity, reduced spontaneous alternation in a T-maze and retarded acquisition of a passive avoidance task in rats with early radiation-induced damage of the fascia dentata. More recently, we replicated and extended this work by revealing that rats with hypoplasia of the fascia dentata granule cells also exhibit perseverative spontaneous turning[26] and that behavioral deficits change significantly over time[7,27,43].

The behavioral and neuroanatomical aberrations observed in animals with radiation-induced hippocampal damage can be partially attenuated by transplanting embryonic hippocampal neurons into the young adult fascia dentata[28,40,46,48]. Zimmer and his colleagues[46] described how this fascia dentata hypoplasia and placement of neural grafts causes *secondary* neuroanatomical changes. They report that the hippocampal mossy fiber system is attenuated corresponding to the reduction in granule cells. Further, the perforant pathways from the entorhinal cortex project aberrantly onto the basal dendrites of CA3 hippocampal pyramidal cells in the absence of sufficient target granule cells. These data suggest that the brain's dynamic response to granule cell hypoplasia may produce a transient period in which intervention with transplantation of neural tissue may be beneficial. In fact, Zimmer[46] reported a time-dependent decrease in the growth of host fibers into hippocampal transplants. If grafts were placed 5 or 10 weeks after radiation-induced hypoplasia of fascia dentata granule cells, it was impossible to demonstrate ingrowth of commissural hippocampo dentate fibers into the transplants. Stein et al.[38] also found that brain damaged rats with transplants at 7 or 14 days after cortical lesions

Correspondence G.A. Mickley, Directed Energy Division, Armstrong Laboratory for Human Systems, Brooks AFB, TX 78235-5301, U.S.A.

significantly improved postoperative acquisition of a spatial alternation task. Transplants performed 30 or 60 days postoperatively had no benefit.

The factor of subject age at the time of neural transplantation has also received considerable scrutiny. For example, Stenevi et al.[39] have reported that grafts survive well in neonatal, young postnatal and old rats. Similarly, other data suggest that there is no difference in the growth of the graft in the brains of neonatal, 6-day-, or 9-day-old rat pups[9]. Kaplan et al.[20] also report that there is no qualitative effect of host age on graft morphology nor were there quantitative effects on transplant size, dendritic length or branching frequency within the transplanted tissue. These data may be contrasted with the report of Stein et al.[36] who noted that old (20 months) rats with bilateral lesions of the frontal cortex do not show any behavioral benefits following implants of fetal brain tissue. Further, Zimmer's data[46] (see above) clearly show how host age can alter the nature of host/graft interconnections in the brains of irradiated rats.

In the current study, we grafted embryonic fascia dentata or cerebral cortex neurons into host rats with fascia dentata granule cell hypoplasia. Transplants were performed at age 33 days (i.e. only 16 days after the completion of the radiation treatments). This contrasts with our previous experiments in which we reported partial behavioral recovery in rats receiving hippocampal grafts at approximately 6 months of age (i.e. > 5 months after the initial brain damage). Since graft/host interconnections are more prominent when transplants are conducted in young rats soon after brain damage[46], we hypothesized that a more-complete behavioral recovery might follow from prompt neural transplantation.

MATERIALS AND METHODS

Subjects

Pregnant rats (Crl: CD(SD)BR) obtained from Charles River Laboratories, Kingston, NY, and screened for evidence of disease were housed in a facility accredited by the American Association for Accreditation of Laboratory Animal Care (AAALAC). Temperature and relative humidity in the animal rooms were held at 19–21 °C and 50 ± 10%, respectively, with 10+ air changes/h. Full-spectrum lighting was cycled at 12 h intervals (lights on at 06.00) with no twilight. The 59 male rats used in these experiments came from a total of 18 different litters. On the day of birth (day 1) litters were culled and only 4–8 males/litter were reared together. Based on a random selection process, from 1 to 6 of these rats in each litter were actually used in the experiments reported here. All rats were weaned at the same time (between 23 and 28 days after birth) and then individually housed in micro-isolator, polycarbonate cages on hardwood chip contact-bedding. Rats were given ad-lib Wayne Rodent Blox and water.

Irradiation procedure

Irradiations were conducted as described previously[38]. Briefly, subjects from each litter were randomly assigned to either the X irradiated or the sham-irradiated (control) group. Irradiated rats received collimated X-rays delivered dorsally, in the coronal plane, through a narrow slot in a loose-fitting whole-body lead shield. X-rays were confined to that area of the head previously determined to contain the hippocampus (see ref. 6 for a complete explanation of this procedure). The irradiated rats were exposed to 2 0 Gray (Gy) on postnatal days 1 and 2 (day of birth = postnatal day 1), and to 1.5 Gy on postnatal days 5, 7, 9, 12, 14 and 16 for a total partial-head-only dose of 13 Gy (1 Gy = 100 rads). Doses were determined by using Exradin 0.05 ml tissue-equivalent ion chambers with calibration traceable to the National Institute of Standards and Technology. X-rays were delivered at a rate of 0.49 Gy/min (total irradiation time = 3.0–4.0 min) at a depth of 2 mm in tissue. The sham-irradiated control rats were restrained for the same time period as the irradiated rats but were not exposed to X-rays.

The entire anterior/posterior extent of the hippocampal formation was irradiated as were brain areas dorsal and ventral to this structure (see ref. 32 for a listing of these other brain areas). Brain structures anterior and posterior to the slot in the lead were shielded. At the time of our postnatal radiation exposures the rat brain contained 3 remaining populations of dividing (and therefore radiosensitive) cells: neuronal precursors of granule cells in the hippocampus, cerebellum and olfactory bulbs[1,3,5]. Two of these major neuronal precursor populations (in the cerebellum and olfactory bulbs) were covered by the radio-opaque shielding. Not shielded were the mitotic (radiosensitive) granule cells of the dentate gyrus and the mature neurons in other brain structures residing in the same coronal plane as the hippocampus. This procedure produces selective hypoplasia of granule cells in the dentate gyrus[6,16] while sparing the radioresistant[8,17] mature neurons of other brain structures. The technique has been validated through a variety of neuroanatomical methods[5,16,46]. The rats in the current study were sacrificed at the end of the experiment to allow histological analysis of the brain (see below).

General procedures and experimental groups

Following irradiation or sham-irradiation, rats were allowed to mature for approximately 1 month (mean age 32.9 ± 0.5 (S.E.M.) days) before neural transplantation and sham-surgical procedures were conducted (see Table I). Rats were tested approx. 2.7 months (at mean age of 113 ± 2 (S.E.M.) days) and again at 6.1 months (mean age of 217 ± 3 (S.E.M.) days) after the surgical procedures. See Table I for average ages of rats at the time of each behavioral test.

Thirty-eight experimental rats were irradiated in order to produce hypoplasia of the fascia dentata granule cells. Rats were later randomly assigned to various surgical conditions. Some of these animals received hippocampal grafts (n = 9) or tissue from a non-homologous CNS area (cerebral cortex; n = 11). Other irradiated subjects (n = 7) received no neural grafts but underwent

TABLE I

Average rat age (days ± S.E.M.) at time of transplant surgery/sham surgery and various behavioral tests

Event	*Irradiated**	*Sham-irradiated**
Surgery/sham surgery	32.6 ± 0.6	33.8 ± 0.7
First rotation series	80.2 ± 0.6	80.4 ± 0.8
First passive avoidance	108.9 ± 1.1	107.9 ± 1.3
First locomotion series	146.0 ± 5.2	157.0 ± 8.9
Second rotation series	221.6 ± 2.2	223.4 ± 2.8
Second passive avoidance	192.6 ± 1.4	194.0 ± 1.9
Second locomotion series	230.3 ± 5.6	243.4 ± 8.7

* Subjects were irradiated/sham-irradiated on 8 days during postnatal days 1–16 (day of birth = postnatal day 1). See text for details.

a sham surgical procedure in order to evaluate the effects of our surgical techniques. Additional rats (n = 11) with radiation induced fascia dentata damage received no surgical treatment. Sham-irradiated control rats also underwent a sham-surgical procedure (n = 12) or experienced no surgery (n = 9).

Behavioral tests

During each test series we recorded performance on 3 primary behavioral measures: locomotor activity, spontaneous rotation and passive avoidance (see below and Table I). Rats with fascia dentata granule cell hypoplasia perform poorly on passive avoidance tasks by readily moving into an area in which they have recently been shocked[6,26,27]. These subjects have enhanced levels of spontaneous locomotor hyperactivity[6,17] and become fixated on some motor response patterns. In particular, they exhibit perseverative turning (in a bowl apparatus) and are less likely to reverse their direction of rotation[26,27]. A brief description of the behavioral tests used in this study follows (see ref. 28 for more details).

Locomotor activity. Locomotor behaviors were automatically recorded using Digiscan Animal Activity Monitors, Model DCM-16 (Omnitech Electronics, Columbus, OH). Monitors consisted of a square acrylic activity arena (40 × 40 × 30 cm) and an array of infrared horizontal and vertical sensors 1 inch (2.54 cm) apart. Horizontal and vertical sensors were positioned 1.3 and 11.0 cm, respectively, above the floor of the cage. Measurements were made in a Digiscan activity monitor for at least two, 1-h periods separated by 1 week or more. The following activity parameters were recorded during the lighted portion of the dark-light cycle. (1) total distance traveled, a measure of horizontal locomotion that goes beyond infrared beam break counts, taking into account diagonal movements, and computes actual distance traveled, (2) vertical activity, total number of beam interruptions that occurred in the vertical sensor (these beam breaks reflected rearing and high sniffing movements), (3) stereotypic movements, number of occurrences of quick (< 1 s) repetitive breaks of the same horizontal beam.

Spontaneous rotation. Rotation was measured in one of two opaque, sound-insulated, 60-cm diameter plastic hemispheres (bowls). Rotation within the hemisphere was inevitable since this was the primary gross movement permitted by the shape of the apparatus. Circling was measured through a projector-drive cable clipped to a wide rubber band around the rat's thorax[15]. We recorded the time and direction of each quarter turn in each of 6 30 min sessions, at approximately the same time during the light portion of the day, for 6 consecutive days.

Passive avoidance. Passive avoidance was measured within a shuttle box comprised of two adjacent compartments (each 22 × 22 × 22 cm) separated by a black plastic guillotine door. Leads from a Coulbourn Instrument's (Lehigh Valley, PA) constant-current shocker (Model E13-04) were connected to the floor bars in the goal compartment but not to the bars in the start compartment.

Three to 7 days before training, rats were given daily rations of 5 g of Wayne Rodent Blox and 1-5 g of highly palatable breakfast cereal (Froot Loops, Kellogg Company, Battle Creek, MI). For 2 to 4 days before training, each rat was allowed to fully explore the shuttle box (with cereal in a food tray) for 15–45 min. Body weight on the first day of training averaged 87% of subject weight for the week prior to food reduction. During training (15 trials each day) the rat was placed in the start compartment with the divider door closed. After 5 s the door was raised and a timer started. The trial ended either when the rat grasped a Froot Loop or in 2 min. Between training trials, the rat was returned to its home cage for 30 s. Avoidance testing was started when a rat both averaged less than 10 s per trial to grasp the food during a training session and, on the first 5 trials of the following day, had a median latency to grasp the food in 10 s or less.

Avoidance training/testing consisted of initiating a regular training trial as usual. However, when the rat's 4 feet were in the goal box, the experimenter administered a 0.25 mA scrambled footshock until the rat retreated to the safe side. The rat was then returned to its home cage for 60 s. This procedure was repeated on subsequent trials except that the floor on the food side of the chamber was continuously electrified. The critical latency measured was the time for each rat to cross onto the shock grid. A trial was terminated if the rat either crossed onto the food/shock side of the chamber (registering a decrease in resistance across the rods) or stayed on the safe side for 120 s. The session (and test) was ended when the rat remained in the safe area for 120 s on 3 consecutive trials or after 20 test trials.

Surgery, fetal graft preparation and injection

Twelve of the sham-irradiated rats and 27 of the irradiated animals underwent a surgical procedure at approx. 33 days of age. The animals were injected with atropine sulfate (0.4 mg/kg, i.p.) and then anesthetized with sodium pentobarbital (50 mg/kg, i.p.). Using aseptic techniques (see ref. 28), a 20 gauge stainless steel cannula was stereotaxically directed toward the dentate gyrus of the hippocampal formation in each brain hemisphere using the following coordinates. 3.5 mm posterior to bregma, 1.6 mm lateral to the midline, 4.0 mm below the skull[35]. Donor tissues (see below) were cut into approx. 0.027 mm^3 fractions and 3 or 4 of the pieces were suspended in tissue culture medium (Dulbecco's Modified Eagle Medium, Whittaker M.A. Bioproducts, Walkersville, MD) and injected into each side of the host brain. The total injection volume was 3.0–4.0 μl. Some of our subjects underwent a sham-surgical procedure and were treated as described above except that no fetal tissue was injected into the brain along with the tissue culture medium.

Donor CNS tissue used for transplantation was dissected from E20–21 day rat fetuses while the dam was maintained under deep anesthesia (sodium pentobarbital, 55 mg/kg, i.p.) (see methods previously described by Stenevi et al.[30] and Mickley et al.[28]). Donor tissue was taken from either the dentate gyrus of the hippocampus or from the cerebral cortex. The hippocampal tissue used for transplantation consisted predominantly of the granule cells (and precursors) from fascia dentata. However, interneurons and cells from CA3 were also present in many of the grafts.

Histology

After behavioral testing was completed, our rats were anesthetized and perfused with heparinized saline followed by 10% buffered formalin. Brains were embedded in paraffin, serially sectioned (6 μm) (in the sagittal plane) and then stained with Cresyl violet and luxol Fast blue[24]. The brains of all subjects receiving neural transplants were reviewed by one of us (G.A.M.) who was blind to the behavioral results. During this review we confirmed the presence/absence of the grafts, evaluated graft morphology and determined the neuroanatomical location of the neural transplants.

All brains also received a preliminary review to confirm radiation-induced damage to the dentate gyrus. In addition, many (irradiated, n = 17, sham-irradiated, n = 17) non-transplanted brains were analyzed in more detail. A single section (approx. 1.9 mm lateral to the midline)[37] was used for this analysis. We counted the total number of granule cells that could be visualized in this section (see ref. 28 for more details on this procedure). Using an imaging system (Bioquant System IV, R&M Biometrics, Inc., Nashville, TN) we also derived the area of the dentate gyrus, computed the cellular density of the structure and the thickness of the granule cell layer. In order to confirm that the shielding of other brain areas was sufficient, we also counted granule cells in a 0.048 mm^2 area in the cerebellum and olfactory bulb. Further, we evaluated the sparing of another more mature, and therefore less radiosensitive, hippocampal structure by counting the thickness of the CA1 pyramidal cell layer that was dorsal to the dentate and directly in the path of the X-radiation.

Brains with neural grafts were further analyzed by estimating the volume of the transplants. Using the Bioquant Imaging System, we made measurements of graft areas within every 8th brain section throughout the full extent of the transplants. Estimates of graft volumes were calculated by multiplying the area of the transplant (visualized in each section) by the thickness of tissue between the

sections sampled (7 sections × 6 μm/section = 42 μm) and then summing these scores for each graft. When more than one transplant was visualized in a particular brain, the individual graft volumes were added to get a total transplant volume for that subject.

Data analysis

Locomotor activity was collected in fifteen 4-min bins and then summed during each test session. Locomotor counts were then averaged over the two 1-h test sessions to get the single score per parameter (i.e. total distance traveled, vertical activity, stereotypic movements) used in our analysis.

Spontaneous perseverative rotation was quantified by recording the bout length each time before a reversal in turning direction was made. The mean turning bout length for each of the 6 daily test sessions was computed by dividing the total quarter turns (in either the dominant or non-dominant direction) by the number of bouts of quarter turns (without reversal of direction) in that session. Statistical comparisons were computed using each rat's average bout-length score. This was the mean of the daily bout lengths for the 6 sessions in the test series. In order to conduct an analysis of turning speed we calculated the percent of total quarter turns that was represented by quarter turns of different durations (1–30 s, in 1-s bins; also durations > 30 s). These speed calculations were made over the 6, 30-min daily test sessions.

We assessed performance on the passive avoidance task by analyzing the time spent in the safe compartment before moving onto the shock grid. Of primary interest was the number of trials it took subjects to meet the criterion of staying in the safe area for 3 consecutive 120-s periods on the test day. Rats that required < 20 trials to meet this criterion were assigned a score equal to the number of the third consecutive 120-s trial. Rats that required > 20 trials to meet this criterion were assigned a score of 20.

We accomplished group comparisons within a particular test series by using *t*-tests[44]. In circumstances where multiple group comparisons would significantly increase the probability of a Type I error, the α (0.05 for a 1-tail test, unless otherwise stated) was partitioned according to the procedure of Bonferroni[29]. When assumptions of homogeneity of variance could not be met by using the raw data we transformed the scores to logarithms. Unless otherwise stated, the performance of transplanted rats was compared to that of sham-surgery controls. When sham-surgery and no-surgery treatments produced behavioral results that were not significantly different (α = 0.05), these groups were sometimes combined for analysis.

RESULTS

Histological confirmation of fascia dentata granule cell hypoplasia

Exposure of a portion of the neonatal cerebral hemispheres to fractionated doses of ionizing radiation produced a selective reduction in granule cells of the hippocampal dentate gyrus while sparing other brain areas (see Table II). Specifically, irradiation of the neonatal rat hippocampus produced a statistically significant 86% (t_{32} = 12.43, $p < 0.001$) depletion in the number of dentate granule cells. Similarly, both the areas and the granule cell densities of the irradiated dentate gyri were significantly reduced compared to those of the control rats (t_{32} = 12.8, $P < 0.001$ and t_{32} = 8.65, $P < 0.001$, respectively). The specificity of this damage is illustrated by the sparing of the pyramidal CA1 neurons that were directly in the path of the X-rays. Irradiation produced no significant change in the thickness of the CA1 pyramidal cell layer, yet the thickness of the dentate granule cell layer was significantly reduced (t_{32} = 10.95, $P < 0.001$).

TABLE II

Histological data derived from analysis of sagittal sections of rat brain

Numbers are means and (in parentheses) S.E.M.s

Anatomical parameter	*Irradiated (n = 17)*	*Sham-irradiated (n = 17)*	*% of Control*
Number of dentate granule cells	226.3 (30.3)*	1537.6 (101.0)	14%[+]
Dentate area (mm^2)	0.9 (0.1)*	2.4 (0.1)	38%
Density of dentate granule cells ($/mm^2$)	253.1 (21.5)*	646.5 (40.1)	39%
Thickness** of dentate granule cell layer	2.2 (0.1)*	6.2 (0.3)	35%
Thickness** of CA1 pyramidal cell layer	2.4 (0.2)	2.4 (0.1)	100%
Density of olfactory bulb granule cells ($/mm^2$)	10213.1 (577.2)	11457.9 (598.4)	89%
Density of cerebellum granule cells ($/mm^2$)	15820.1 (646.7)	18020.8 (624.0)	88%
Cerebellum area (mm^2)	21.8 (0.9)	21.2 (1.3)	103%

* Significantly different (*t*-test) from sham-irradiated, $P < 0.01$.

** Number of cells.

[+] Note that these levels are comparable to those reported by Zimmer et al.[46].

The size (area) of the irradiated rat cerebellum was no different from that of sham-irradiated controls (see Table II). Although there was a trend towards granule cell hypoplasia in the cerebellum and olfactory bulb of irradiated rats (as measured by cell densities of 88% and 89% of control, respectively), this was not a statistically reliable effect (α = 0.01). These data suggest that our X-ray exposure procedures produced damage that was selective for fascia dentata granule cells.

Using multiple correlations we compared several brain histology parameters (derived from rats that underwent sham-surgical or no-surgical procedures, see Table II) with results of our behavioral tests. This analysis revealed statistically significant relationships between hippocampal damage and several measures of performance (see Table III and also ref. 14). For example, on both the first and second postoperative tests, mean bout length was negatively correlated with the number of granule cells in the fascia dentata. That is to say, when there were few granule cells in the dentate, turning bouts increased. On the other hand, correlations between behavioral measures and histological indicators of cerebellar and olfactory bulb cell densities were uniformly not statistically significant. These data point to hippocampal damage as a likely predictor of the behavioral alterations described in this paper.

Graft survival, location, volume and cytology

Three or 4 pieces of fetal tissue were injected into each hemisphere of our experimental subjects. Since individual grafts appeared to fuse together in some cases, it was often difficult to count the number of surviving pieces of transplanted tissue. Transplanted rats with at least one viable graft were included in the data pool for this paper. Using this criterion, 95% (20 out of 21) of rats receiving fetal neural transplants as neonates were observed to have viable grafts at the end of the study (see Fig. 1).

Following histological review of the transplanted brains we divided subjects into 4 categories. (1) animals with hippocampal grafts located either entirely or partially within the hippocampal formation (n = 6) (see ref. 32 for the anatomical limits of this structure), (2) animals with hippocampal grafts entirely out of the hippocampal formation (n = 3), (3) animals with cerebral cortex grafts located either entirely or partially within the hippocampal formation (n = 3), or (4) animals with cerebral cortex grafts located entirely out of the hippocampal formation (n = 8). These groupings were used to determine how graft location influenced the animal's performance on our behavioral measures.

Although cerebral cortex grafts tended to be slightly smaller (mean = 0.67 mm^3 ± 0.1 (S.E.M.)) than did hippocampal transplants (mean = 0.69 mm^3 ± 0.4 (S.E.M.)), this difference in volume was not statistically significant. Our analysis of graft volume revealed that most of our transplants were quite small relative to the grafts reported to grow under a variety of other circumstances[10,11]. However, the graft volumes in this study were similar to those graft volumes we observed in adult rats with fascia dentata damage that also received grafts[28]. Similarly, the volumes of the grafts located inside the hippocampal formation did not differ from those located outside this structure. We found no significant correlations between graft volume and post-surgical changes recorded on the spontaneous rotation or locomotor activity measures.

TABLE III

Correlations between behavioral and neuroanatomical data for irradiated and sham-irradiated rats receiving sham-surgical procedures or no surgical treatment

Anatomical parameters	*Behavioral measures**			
	Bout length		*% Turns <1 s*	
	Test 1	*Test 2*	*Test 1*	*Test 2*
Fascia dentata granule cell number	−0.519**	−0.388**	0.424**	0.379**
Fascia dentata granule cell density	−0.528**	−0.376**	0.454**	0.460**
Olfactory bulb granule cell density	−0.343	−0.270	0.100	0.210
Cerebellum granule cell density	−0.290	−0.080	−0.070	0.306

* Mean bout length and mean percent quarter turns of <1 s duration are represented for postoperative tests 1 and 2.
** = $P < 0.05$, df = 32.

Locomotor activity

As we described previously[26,27], radiation-induced hypoplasia of fascia dentata granule cells produced an initial locomotor hyperactivity in the horizontal plane (t_{17} = 2.12, P = 0.02) and increased stereotypic behaviors (t_{17} = 3.28, $P < 0.002$), while sparing the vertical activity of rats that underwent sham surgical procedures. These behavioral changes were most evident during the first behavioral test series. Compared to irradiated rats that had sham surgery, irradiated subjects with hippocampal transplants showed a significant reduction in both total distance traveled (t_{14} = −1.99, P = 0.03) and stereotypy (t_{14} = −3.32, P = 0.002) at the time of the first postoperative test (see Fig. 2). Cerebral cortex grafts did not significantly attenuate changes in either of these measures of locomotor hyperactivity.

Graft-induced behavioral benefits did not persist, however. During the second postoperative test series, rats with hippocampal damage and grafts exhibited levels of horizontal activity and stereotypic behavior that were comparable to those recorded from irradiated rats that underwent sham surgery. It should be noted, however, that radiation-induced locomotor hyperactivity was not a reliable phenomenon during the second test series (see also ref. 27). At this time, rats with hippocampal damage exhibited levels of horizontal activity and stereotypic behavior that were not statistically higher than those recorded from sham-irradiated rats. Thus, the benefits of hippocampal grafts observed during the first test series may be interpreted as an accelerated recovery of locomotion rather than a transient benefit of the hippocampal transplants.

We demonstrated previously how graft location can modulate the behavior of rats with hippocampal damage[28]. In the current study however, the horizontal and stereotypic movements of rats with transplants within the hippocampal formation was not significantly different from that observed in rats with grafts located outside the hippocampus.

Spontaneous rotation

We observed in the present (see Fig. 3) and previous studies[26,27] that radiation-induced hippocampal damage caused rats to make long bouts of turns (without reversals) in a plastic hemisphere. Once they began moving, in either direction, irradiated rats perseverated in that turning to an extent significantly greater than the

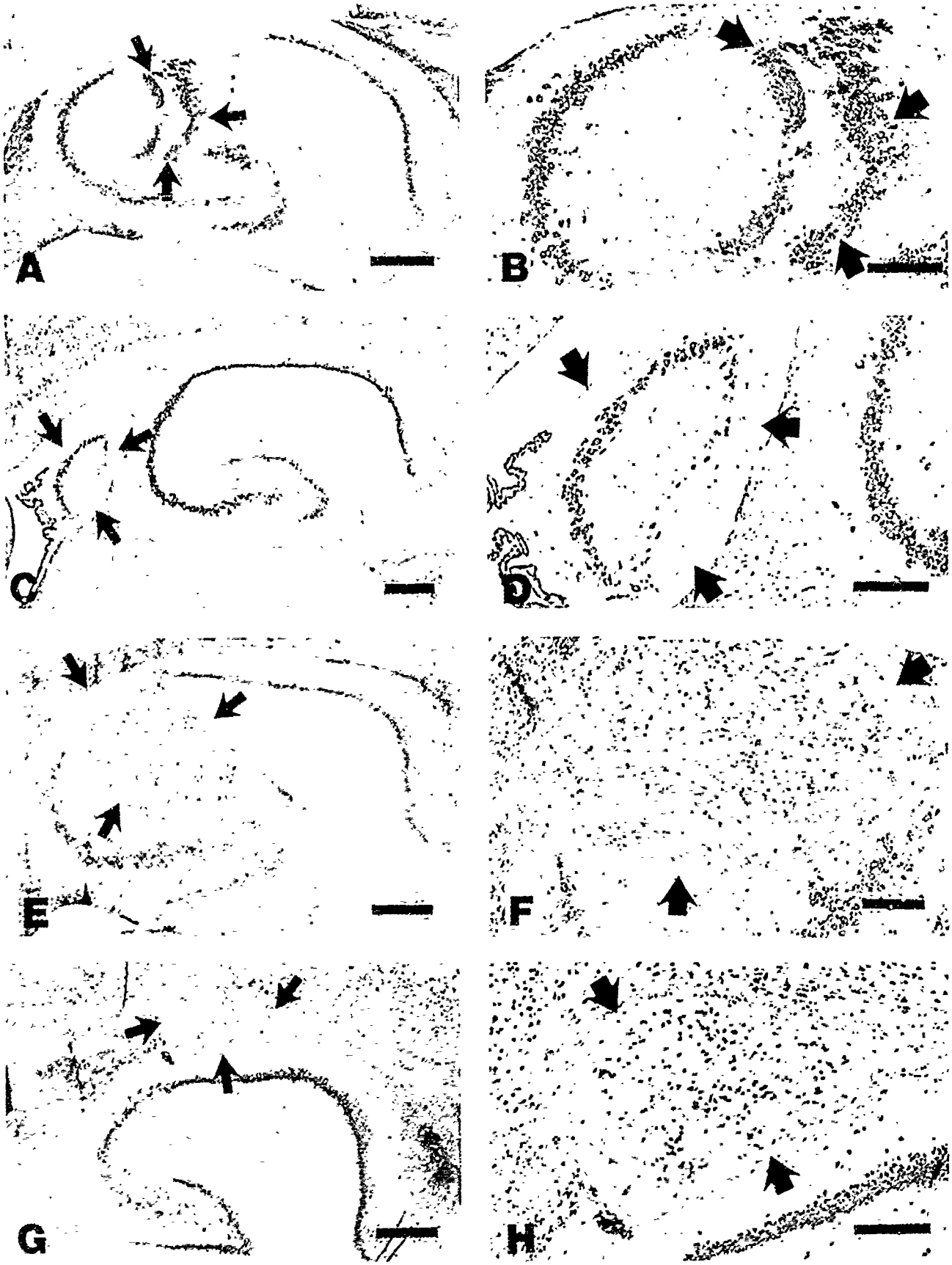

Fig. 1. Examples of fetal brain transplants residing in an adult host brain. Micrographs on the right represent a higher magnification of the graft seen in the adjacent section to the left. Neural grafts from the hippocampus (including fascia dentata granule cells) were placed in the damaged hippocampal formation (A,B). The granule cells in these neuronal grafts often exhibited the laminar organization of the dentate gyrus (A,B,C,D). On the other hand, the cells in cerebral cortex grafts showed little organization (E,F,G,H). Sometimes both hippocampal tissue transplants (C,D) and cortical grafts (G,H) were found outside of the host hippocampal formation in the lateral ventricle or cerebral cortex. Arrows point to the grafted tissue. Calibration bars on the left micrographs represent 500 μm the bars on the right micrographs represent 250 μm.

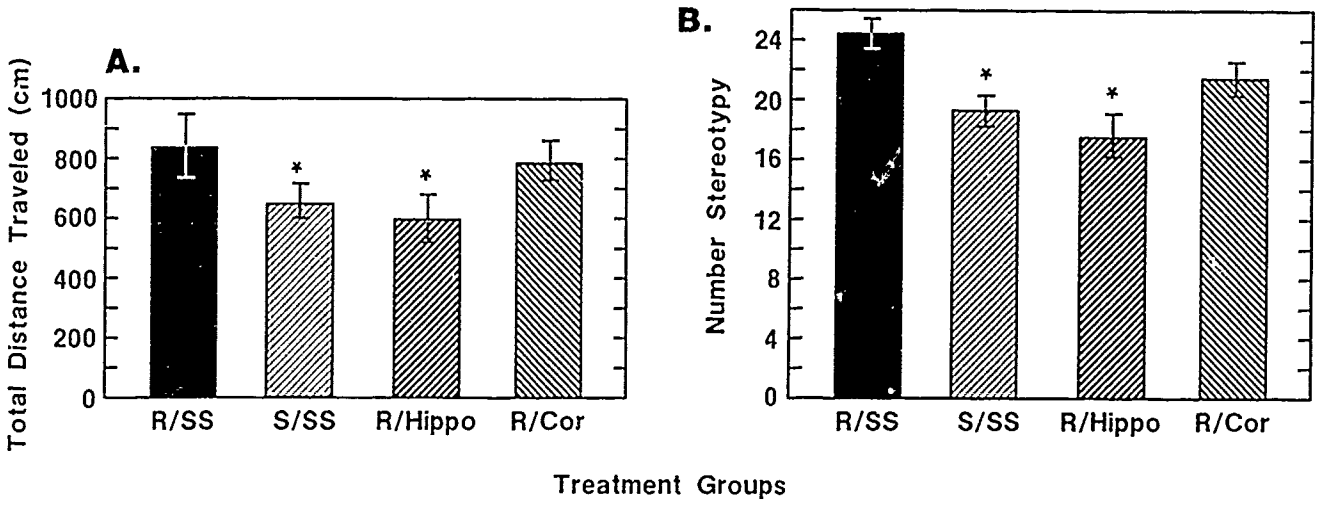

Fig. 2. Mean total distance traveled (in cm) (A) and number of stereotypic movements (B) exhibited by rats during the first behavioral test series. Irradiated rats with fascia dentata granule cell hypoplasia (R/SS – irradiated/sham surgery) show locomotor hyperactivity on these measures as compared to sham irradiated subjects (S/SS – sham-irradiated/sham surgery). Hippocampal grafts significantly (* – $P < 0.05$) reduce these parameters of radiogenic locomotor hyperactivity to levels not different from S/SS controls. Variance indicators represent S.E.M.s.

sham-irradiated subjects ($t_{17} = 4.13$, $P < 0.001$, first postoperative test, $t_{17} = 2.76$, $P = 0.007$, second postoperative test). During the first postoperative test series, rats with hippocampal damage and grafts showed a significant reduction in perseverative turning as compared to irradiated animals that underwent sham-surgical procedures ($t_{14} = -2.64$, $P = 0.01$). Grafts found to be located inside or outside the hippocampus produced similar reductions in perseverative turning. Cortical transplants did not statistically reduce the radiation-induced perseverative responses of our subjects. While the perseverative turning of rats with hippocampal damage persisted during the final behavioral test, neither hippocampal nor cortical grafts significantly reduced these movements.

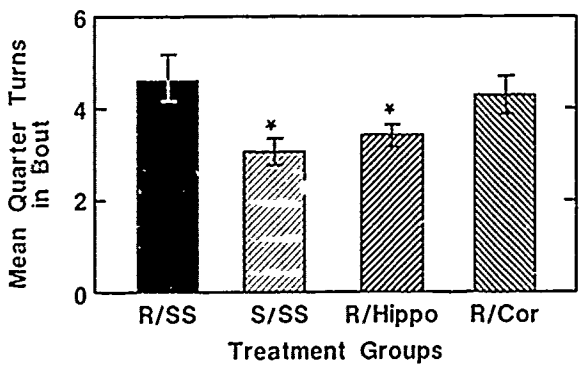

Fig. 3. Mean turning bout length (quarter turns) of rats moving in a plastic hemisphere during the first test series. Irradiated rats with fascia dentata granule cell hypoplasia and sham surgical treatments (R/SS) perseverate in their movements (i.e. continue turning in the same direction once a movement is initiated) to an extent significantly greater (* – $P < 0.05$) than sham-irradiated control animals (S/SS – sham irradiated/sham surgery). Irradiated rats with hippocampal grafts (R/Hippo), but not cerebral cortex grafts (R/Cor), show a significant attenuation of perseverative spontaneous turning. Variance indicators represent S.E.M.s.

Although rats with radiation-induced hypoplasia of fascia dentata granule cells show a locomotor hyperactivity in the form of increased horizontal distances traversed and enhanced stereotypic behaviors, the movement speed of these animals does not generally exceed that of sham-irradiated controls[17]. However, a further analysis of movement speed[14] in the plastic rotation hemispheres has revealed that our rats with hippocampal damage exhibited a lower proportion of quarter turns with durations of < 1 s than did our sham-irradiated subjects (sham-surgery or no surgery controls) ($t_{35} = -2.47$, $P = 0.01$, for the first postoperative test series; and $t_{35} = -2.06$, $P = 0.02$ for the second postoperative test series). In addition, during the first test series only, the irradiated rats had a higher proportion of quarter turns with durations of > 30 s ($t_{35} = 2.25$, $P = 0.03$). Thus, hippocampal granule cell hypoplasia seems to reduce the number of very quick movements while increasing the number of slow turning movements (Fig. 4).

Neural grafts normalized somewhat the topography of turning speed in our brain damaged animals. During the first test series, irradiated rats with either hippocampal or cerebral cortex transplants exhibited significantly more rapid (< 1 s) quarter turns than did rats with similar brain damage but no transplants (i.e. sham surgery or no surgery) ($t_{24} = -2.02$, $P = 0.027$ and $t_{36} = 1.84$, $P = 0.038$, respectively) (Fig. 4). The proportion of these rapid quarter turns in irradiated rats with hippocampal transplants was not significantly different from those observed in sham-irradiated control subjects. Neither

hippocampal nor cortical grafts significantly altered the reduced rapid turning observed during the second test series in rats with fascia dentata granule cell hypoplasia. Similarly, during the first test series only, the long quarter turns (i.e. > 30 s) exhibited in greater number by rats with fascia dentata damage were significantly reduced in rats with either hippocampal grafts ($t_{24} = 2.19$, $P = 0.02$) or cerebral cortex grafts ($t_{26} = 2.58$, $P = 0.01$). These data suggest that neural grafts are capable of producing transient reductions in the effects of hippocampal granule cell hypoplasia on turning speed.

Passive avoidance

Our previous experience with rats having hypoplasia of fascia dentata granule cells revealed that these subjects had deficits in the performance of a passive avoidance task[26,27,28]. Irradiated rats tended to move out of a safe area into a compartment where they had once been shocked more quickly than did sham-irradiated controls. During the first postoperative behavioral test series, irradiated subjects in the current study also tended to take more trials (mean = 19.0 ± 1 S.E.M.) to meet the established learning criterion (see Materials and Methods section) than did sham-irradiated rats (mean = 16.8 ± 1.3 S.E.M.). However, the difference between these groups was not statistically significant ($P > 0.05$).

Nevertheless, irradiated rats with hippocampal transplants learned the passive avoidance task more readily (mean trials to criterion = 13.7 ± 1.7 S.E.M.) than did the rats with fascia dentata damage that underwent sham surgery ($t_{14} = -2.45$, $P = 0.01$). Irradiated subjects with cortical grafts also showed a tendency towards improved passive avoidance performance (mean trials to criterion = 15.7 ± 1.5 S.E.M.) but this was not a statistically significant effect. These effects of transplants were not observed during the second postoperative test.

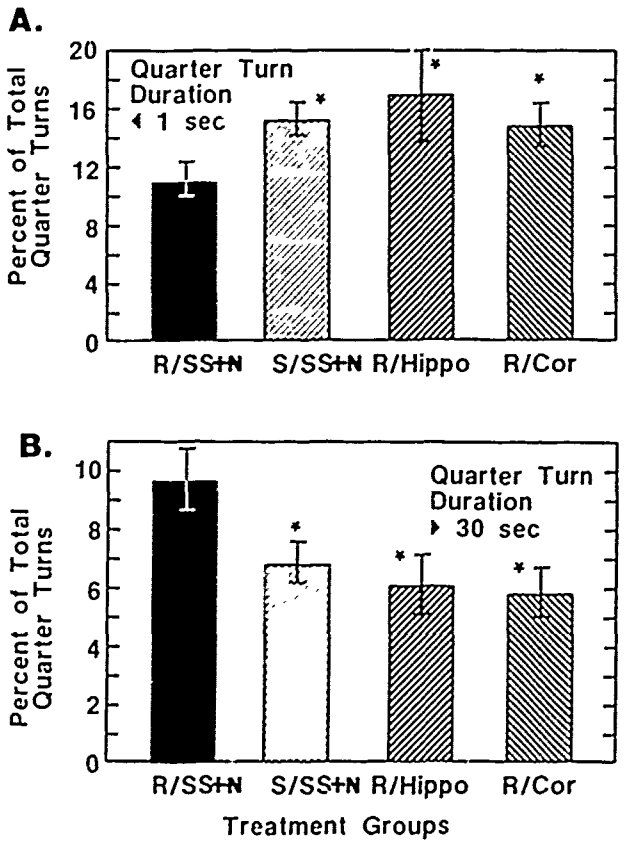

Fig. 4. Mean percent of quarter turns recorded (during the first test series) in the rotation apparatus that are either short (< 1 s) (A) or long (> 30 s) (B) durations. Rats with fascia dentata hypoplasia (R/SS+N = Irradiated/no surgery or sham surgery controls) exhibit fewer quarter turns of short duration and more quarter turns of long duration than sham irradiated control rats (S/SS+N = sham irradiated/sham surgery or no surgery controls). Hippocampal (R/Hipp) or cerebral cortex (R/Cor) transplants significantly (* = $P < 0.05$) attenuate these behavioral changes in irradiated rats. Variance indicators represent S.E.M.s.

DISCUSSION

In this study measures of spontaneous locomotor hyperactivity, perseveration and turning speed reliably accompanied X-ray induced hippocampal damage. Independent of their final location in the host brain, hippocampal tissue transplants caused significant improvements in these behavioral aberrations. Most of these graft-induced benefits were transient, however, since they were confined to the first test series. Transplant tissue homologous with that damaged by the X-rays (i.e. hippocampal granule cells) was consistently effective in reducing behavioral deficits whereas non-homologous tissue from cerebral cortex only reduced aberrations in certain components of turning speed.

These data are consistent with previous reports showing that animals with homologous tissue grafts frequently exhibit postlesion behavioral recovery superior to that observed after non-homologous brain tissue transplants[25]. Woodruff et al.[45] report, for example, that rats with hippocampal tissue grafts transplanted into a hippocampal lesion site, performed better on an operant task requiring slow response rates than did subjects receiving non-homologous grafts of fetal hindbrain tissue. Reports also indicate that a neural graft survives best when transplanted into its corresponding region of origin in the host brain[18]. However, it must be noted that functional benefits of non-homologous neural grafts have also been observed[28,37]. These data suggest that there may be some gradient of homology that modulates the functional recovery offered by neural grafts[28].

The anatomical source of transplanted neurons influenced our various performance measures in different ways. Unlike other radiation-induced behavioral changes

that benefited only from the grafting of hippocampal tissue, aberrations of turning speed were attenuated by transplants from either fascia dentata or cerebral cortex. One possible explanation for this finding is that the hippocampus does not play a significant or exclusive role in the adjustment of movement speed. In general this may be true. Little change in the overall speed of movements accompanies hippocampal damage[13]. Except for very rapid (< 1 s) and very slow (> 30 s) movements, the percent of other turning movement speeds remains intact following fascia dentata granule cell hypoplasia (see current data and ref. 14). Contrary to this hypothesis, however, we report here that the degree of fascia dentata hypoplasia is well correlated with the percent of rapid turns in our bowl apparatus (see Table III). These data suggest a stronger relationship between hippocampal damage and movement speed than was previously appreciated.

Data from the current study cannot fully explain why there are selective behavioral benefits of neural grafts derived from different sources in the central nervous system. Putative mechanisms for the functional benefits of neural transplants have taken many forms. Grafts may provide: (1) new neural interconnections, (2) normalization of available neurotransmitters, (3) stimulation of trophic factors (e.g. nerve growth factor), and/or (4) replacement of glia that may offer structural support for neuronal growth, metabolism of excitotoxins or other functions[2,9,30,31]. It may be the case that *either* hippocampal or cerebral cortex grafts can provide a particular rearrangement of physiological or neuroanatomical factors that results in the normalization of radiation-induced aberrations in turning speed topography, whereas, *only* hippocampal tissue provides the particular pattern of factors that is sufficient to reduce perseverative movements. These hypotheses await empirical testing.

The reliability of the anatomical and behavioral changes following our X-irradiation procedure[3,6,7,26,28] suggests some of the advantages of this technique. Still, we do not fully understand the physiological changes that accompany the use of X-rays to produce selective hypoplasia of fascia dentata granule cells and how these changes may alter graft growth and functionality. For example, no data are currently available regarding the levels and kinetics of neurotrophic factors present in X irradiated neonatal brain tissues. Thus, we do not know the extent to which NGF (or other factors known to facilitate transplant growth[21]) enhanced the behavioral benefits reported here. On the other hand, we know with some certainty that the prompt transplantation of neural tissues following hippocampal X irradiation places relatively few morphological constraints on the growth pattern of the transplanted neurons[10]. Zimmer et al.[47,48] have described the compensatory interconnections formed by entorhinal cortical neurons that project to a dentate gyrus with a reduced population of granule cells. By shortening the time in which reactive host cell growth can occur, more space is allowed for transplanted neurons[46]. Conversely, there is less room for graft/host reinnervation when long latencies separate brain damage and transplantation procedures. By discovering more about the timing of X-ray induced neurotrophic factor release and by manipulating the time between the production of granule cell hypoplasia and neural transplantation (and thereby manipulating the expected neural interconnections possible) it may be possible to validate some of the postulated mechanisms of graft-induced functional recovery listed above.

The results of the current study contrast in several ways with our previous work in which rats with fascia dentata granule cell hypoplasia received grafts as young adults (182 ± 4 days, i.e. > 5 months after brain injury)[28]. In these initial experiments, demonstration of behavioral recovery was task-dependent and more strongly influenced by the final location of the transplanted tissue in host brain (i.e. in or out of the hippocampus). Transplant-induced recovery of function was sometimes not observed until late in the study (mean age = 351 days). Further, if cortical tissue grafts were found to be located outside the hippocampus, they frequently produced behavioral benefits comparable to those following the grafting of homologous hippocampal tissue.

These data are distinct from those that characterize rats transplanted just 16 days after radiogenic hippocampal damage. Here graft location in the host brain did not influence the behavioral outcomes we recorded. Moreover, there was a remarkable degree of uniformity in the timing of the behavioral recovery (all occurring during the first test series, average age 113 ± 2 days) and the ability of hippocampal tissue transplants to produce this recovery. These findings suggest that the placement of grafts soon after the initial brain damage results in more consistent and predictable (albeit transient) behavioral recovery. Similarly, Kolb et al.[22] and Dunnett et al.[17] have reported quite different behavioral effects of cortical grafts at different postoperative recovery times. The waxing and waning of behavioral recovery in our animals undoubtedly reflects a complicated process that includes the kinetics of graft growth and the compensatory changes that occur in the damaged hippocampus over time.

It should be noted, however, that several procedural differences (in addition to the reduced interval between fascia dentata granule cell hypoplasia and grafting) distinguish the present study from our previous work[28]. By necessity, we could not perform a behavioral baseline

on the young animals used here. Thus, the first postoperative test reflects naive performance on the part of these subjects. This contrasts with our former experiment in which the first postoperative behavioral test was really the second behavioral observation performed (i.e. it followed a preoperative baseline measure). Experimental factors such as the timing of postoperative training, testing and handling have been shown to influence recovery from lesions of the hippocampus[41] and entorhinal cortex[33]. Despite the fact that the postoperative behavioral tests were conducted at approximately the same time following transplantation/sham surgery in both of our experiments, by necessity, the ages of the subjects in the 2 experiments were different. In our initial study, postoperative behavioral tests were conducted at ages 265 ± 5 (S.E.M) and 351 ± 6 days. See Table I for the timing of the behavioral tests in the present experiments. Of course, age at time of surgery also covaried with the procedural change from our previous experiment that reduced the interval between the end of irradiation and the placement of neural grafts. These procedural differences in testing, age at test and age at surgery may have contributed to the behavioral disparities observed between the animals in our 2 studies.

In addition, it may be the case that different mechanisms of recovery are at work in animals that receive grafts at different stages of development. The organization and milieu of the preadolescent brain are quite different from that of the adult[1,4]. The enhanced plasticity of the young brain[21,34,46,47] may help explain why the behavioral recovery of the animals in the current study was less dependent on graft location and more consistent over a variety of behaviors. Further, the transience of the behavioral phenomena we observed, and the fact that ectopic grafts mediated recovery of functions comparable to those following grafts located inside the hippocampus, suggests that neural interconnections may not be critical to the transplant effects reported in our young animals. Future studies should focus on the kinetics of neurotrophic factors, neurotransmitter release or the anatomy of neuronal interconnections that might offer an explanation regarding the mechanism(s) underlying the behavioral phenomena reported here.

Acknowledgements. We thank Drs. Paul Reier and Herman Teitelbaum who contributed to the conceptualization of these experiments. The authors recognize the excellent technical assistance provided by Mr. Mark Postler, Ms. Diane Pickle, Ms. Barbara A. Barrett, Ms. Sonya Longbotham and Ms. Brenda Cobb. The dosimetry and irradiations were performed by Mr. V. Scott Hawkins and Mr. Ernest Golightly. Statistical advice was provided by Mr. William Jackson. We thank Ms. Lilly Heman-Ackah and Dr. George Parker for their excellent histological assistance. This research was supported by the Armed Forces Radiobiology Research Institute, Defense Nuclear Agency, under work unit 4340. Views presented in this paper are those of the authors; no endorsement by the Defense Nuclear Agency has been given or should be inferred. Research was conducted according to the principles enunciated in the 'Guide for the Care and Use of Laboratory Animals' prepared by the Institute of Laboratory Animal Resources, National Research Council.

REFERENCES

1 Altman, J. and Das, G.D., Autoradiographic and histological evidence of postnatal hippocampal neurogenesis in rats, *J. Comp. Neurol.*, 124 (1965) 319–336.
2 Azmitia, E.C. and Bjorklund, A., (Eds.), *Cell and Tissue Transplantation into the Adult Brain, Vol. 495*, New York Academy of Sciences, New York, 1987, pp. 1–813.
3 Bayer, S.A., Brunner, R.L., Hine, R. and Altman, J., Behavioural effects of interference with the postnatal acquisition of hippocampal granule cells, *Nature New Biol.*, 242 (1973) 222–224.
4 Bayer, S.A. and Altman, J., Hippocampal development in the rat: cytogenesis and morphogenesis examined with autoradiography and low level X irradiation, *J. Comp. Neurol.*, 158 (1974) 55–80.
5 Bayer, S.A. and Altman, J., Radiation induced interference with postnatal hippocampal cytogenesis in rats and its long term effects on the acquisition of neurons and glia, *J. Comp. Neurol.*, 163 (1975) 1–20.
6 Bayer, S.A. and Peters, P.J., A method for X-irradiating selected brain regions in infant rats, *Brain Res. Bull.*, 2 (1977) 153–156.
7 Brunner, R.L., A cross-sectional study of behavior at 3 ages after neonatal X irradiation of the hippocampus, *Behav. Biol.*, 22 (1978) 211–218.
8 Casarett, G.W., *Radiation Histopathology, Vol. II*, CRC Press, Boca Raton, 1980.
9 Cotman, C.W., Nieto Sampedro, M. and Whittemore, S.R., Relationships between neurotrophic factors and transplant host integration. In A. Björklund and U. Stenevi (Eds.), *Neural Grafting in the Mammalian CNS*, Elsevier, Amsterdam, 1985, pp. 169–178.
10 Cotman, C.W. and Kesslak, J.P., The role of trophic factors in behavioral recovery and integration of transplants. In D.M. Gash and J.R. Sladek (Eds.), *Transplantation into the Mammalian CNS, Progress in Brain Research, Vol. 78*, Elsevier, Amsterdam, 1988, pp. 311–319.
11 Dalrymple-Alford, J.C., Kelche, C., Cassel, J.C., Toniolo, G., Pallage, V. and Will, B.E., Behavioral deficits after intrahippocampal fetal septal grafts in rats with selective fimbria-fornix lesions, *Exp. Brain Res.*, 69 (1988) 545–558.
12 Dunnett, S.B., Ryan, C.N., Levin, P.D., Reynolds, M. and Bunch, S.T., Functional consequences of embryonic neocortex transplanted to rats with prefrontal cortex lesions, *Behav. Neurosci.*, 101 (1987) 489–503.
13 Ferguson, J.L., Mulvihill, M.A., Nemeth, T.J. and Mickley, G.A., Radiation-induced hippocampal damage produces locomotor hyperactivity and spontaneous perseverative turning but not enhanced turning speed, *Soc. Neurosci. Abstr.*, 13 (1987) 1333.
14 Ferguson, J.L., Mickley, G.A. and Nemeth, T.J., An analysis of turning speed in rats with radiation-induced hippocampal damage, in press.
15 Greenstein, S. and Glick, S.D., Improved automated apparatus for recording rotation (circling behavior) in rats or mice, *Pharmacol. Biochem. Behav.*, 3 (1975) 507–510.
16 Hicks, S.P., Radiation as an experimental tool in mammalian developmental neurology, *Physiol. Rev.*, 38 (1958) 337–356.
17 Hicks, S.P. and D'Amato, C.J., Effects of ionizing radiations on

mammalian development. In D.H.M. Woollam (Ed.), *Adv. Teratol.*, Logos Press, London, 1966, pp. 195–250.
18 Heuschling, P., De Paermentier, F. and Van den Bosch de Aguilar, P., Topographical distribution in the adult rat brain of neurotrophic activities directed to central nervous system targets, *Dev. Brain Res.*, 38 (1988) 9–17.
19 Iversen, S.D. and Dunnett, S.B., Functional compensation afforded by grafts of foetal neurones, *Prog. Neuropsychopharmacol. Biol. Psychiatry*, 13 (1989) 453–467.
20 Kaplan, A.S., Gash, D.M., Flood, D.G. and Coleman, P.D., A golgi study of hypothalamic transplants in young and old host rats, *Neurobiol. Aging*, 6 (1985) 205–211.
21 Kalil, K. and Reh, T., Regrowth of severed axons in the neonatal central nervous system: establishment of normal connections, *Science*, 205 (1979) 1158–1161.
22 Kolb, B., Reynolds, B. and Fantie, B., Frontal cortex grafts have opposite effects at different postoperative recovery times, *Behav. Neural Biol.*, 50 (1988) 193–206.
23 Kromer, L.F., Factors in neural transplants which influence regeneration in the mature mammalian central nervous system, In A. Bjorklund and U. Stenevi (Eds.), *Neural Grafting in the Mammalian CNS*, Elsevier, Amsterdam, 1985, pp. 309–318.
24 LaBossiere, E., *Histological Processing for the Neural Sciences*, Charles C. Thomas, Springfield, 1976.
25 Mickley, G.A., Teitelbaum, H. and Reier, P.J., Fetal hypothalamic brain grafts reduce the obesity produced by ventromedial hypothalamic lesions, *Brain Research*, 424 (1987) 239–248.
26 Mickley, G.A., Ferguson, J.L., Nemeth, T.J., Mulvihill, M.A. and Alderks, C.E., Spontaneous perseverative turning in rats with radiation induced hippocampal damage, *Behav. Neurosci.*, 103 (1989) 722–730.
27 Mickley, G.A., Ferguson, J.L., Mulvihill, M.A. and Nemeth, T.J., Progressive behavioral changes during the maturation of rats with early radiation induced hypoplasia of fascia dentata granule cells, *Neurotoxicol. Teratol.*, 11 (1989) 385–393.
28 Mickley, G.A., Ferguson, J.L., Nemeth, T.J. and Mulvihill, M.A., Neural grafts attenuate behavioral deficits produced by early radiation induced hypoplasia of fascia dentata granule cells, *Brain Research*, 509 (1990) 280–292.
29 Miller, G., *Simultaneous Statistical Inference*, 2nd edn., Springer, Berlin, 1981, pp. 6–8.
30 Nieto Sampedro, M., Whittemore, S.R., Needels, D.L., Larson, J. and Cotman, C.W., The survival of brain transplants is enhanced by extracts from injured brain, *Proc. Natl. Acad. Sci. U.S.A.*, 81 (1984) 6250–6254.
31 Nieto Sampedro, M. and Cotman, C.W., Growth factor induction and temporal order in central nervous system repair. In C.W. Cotman (Ed.), *Synaptic Plasticity*, Guilford Press, New York, 1985, pp. 407–455.
32 Paxinos, G. and Watson, C., *The Rat Brain in Stereotaxic Coordinates*, Academic Press, Sidney, 1982.
33 Ramirez, J.J., Labbe, R. and Stein, D.G., Recovery from perseverative behavior after entorhinal cortex lesions in rats, *Brain Research*, 459 (1988) 153–156.
34 Saitua, F. and Alvarez, J., Do axons grow during adulthood? A study of caliber and microtubules of sural nerve axons in young, mature, and aging rats, *J. Comp. Neurol.*, 269 (1988) 203–209.
35 Sherwood, N.M. and Timiras, P.J., *A Stereotaxic Atlas of the Developing Rat Brain*, 1st edn., University of California Press, Berkeley, 1970.
36 Stein, D.G., Labbe, R., Firl, A. and Mufson, E.J., Behavioral recovery following implantation of fetal brain tissue into mature rats with bilateral, cortical lesions. In A. Bjorklund and U. Stenevi (Eds.), *Neural Grafting in the Mammalian CNS*, Elsevier, Amsterdam, 1985, pp. 605–614.
37 Stein, D.G., Labbe, R., Attella, M.J. and Rakowsky, H.A., Fetal brain tissue transplants reduce visual deficits in adult rats with bilateral lesions of the occipital cortex, *Behav. Neural Biol.*, 44 (1985) 266–277.
38 Stein, D.G., Palatucci, C., Kahn, D. and Labbe, R., Temporal factors influence recovery of function after embryonic brain tissue transplants in adult rats with frontal cortex lesions, *Behav. Neurosci.*, 102 (1988) 260–267.
39 Stenevi, U., Kromer, L.F., Gage, F.H. and Björklund, A., Solid neural grafts in intracerebral transplantation cavities. In A. Bjorklund and U. Stenevi (Eds.), *Neural Grafting in the Mammalian CNS*, Elsevier, Amsterdam, 1985, pp. 41–49.
40 Sunde, N., Laurberg, S. and Zimmer, J., Brain grafts can restore irradiation-damaged neuronal connections in newborn rats, *Nature*, 310 (1984) 51–53.
41 Tilson, H.A., Harry, G.J., Nanry, K., Rogers, B., Peterson, J., Jensen, K. and Dyer, R., Experiential factors in the expression of hypermotility produced by intradentate colchicine: lack of effect of GM1 ganglioside on colchicine-induced loss of granule cells and mossy fibers, *J. Neurosci. Res.*, 17 (1987) 410–416.
42 Wallace, R.B., Kaplan, R.F. and Werboff, J., Behavioral correlates of focal hippocampal X-irradiation in rats, *Exp. Brain Res.*, 24 (1976) 343–349.
43 Wallace, R.B., Graziadei, R. and Werboff, J., Behavioral correlates of focal hippocampal X-irradiation in rats II, *Exp. Brain Res.*, 43 (1981) 207–212.
44 Winer, B.J., *Statistical Principles in Experimental Design*, McGraw-Hill, New York, 1971, pp. 30–35, 149–260, 397–402.
45 Woodruff, M.L., Baisden, R.H., Whittington, D.L. and Benson, A.E., Embryonic hippocampal grafts ameliorate the deficit in DRL acquisition produced by hippocampectomy, *Brain Research*, 408 (1987) 97–117.
46 Zimmer, J., Sunde, N. and Sorensen, T., Reorganization and restoration of central nervous connections after injury: a lesion and transplant study of the rat hippocampus. In B.E. Will, P. Schmitt and J.C. Dalrymple-Alford (Eds.), *Brain Plasticity, Learning and Memory*, Plenum, London, 1985, pp. 505–518.
47 Zimmer, J., Laurberg, S. and Sunde, N., Non-cholinergic afferents determine the distribution of the cholinergic septohippocampal projection: a study of the AChE staining pattern in the rat fascia dentata and hippocampus after lesions, X-irradiation, and intracerebral grafting, *Exp. Brain Res.*, 64 (1986) 158–168.
48 Zimmer, J., Poulsen, P.H., Blackstad, Th.W. and West, M.J., Radiation-induced reduction of the rat dentate gyrus. Compensatory cellular and connectional changes, *Soc. Neurosci. Abstr.*, 13 (1987) 1602.

Neuroscience Vol. 44, No. 2, pp. 353–359, 1991
Printed in Great Britain

0306-4522/91 $3.00 + 0.00
Pergamon Press plc
IBRO

FREE RADICALS ACCELERATE THE DECAY OF LONG-TERM POTENTIATION IN FIELD CA1 OF GUINEA-PIG HIPPOCAMPUS

T. C. PELLMAR,*† G. E. HOLLINDEN*‡ and J. M. SARVEY§

*Physiology Department, Armed Forces Radiobiology Research Institute, Bethesda, MD 20889-5145, U.S.A.

§Department of Pharmacology, Uniformed Services University of the Health Sciences, Bethesda, MD 20814-4799, U.S.A.

Abstract – Free radicals have been implicated in a number of pathological conditions. To evaluate the neurophysiological consequences of free radical exposure, slices of hippocampus isolated from guinea-pigs were exposed to hydrogen peroxide which reacts with tissue iron to generate hydroxyl free radicals. Long-term potentiation, a sustained increase in synaptic responses, was elicited in field CA1 by high frequency stimulation of an afferent pathway. We found that 0.002% peroxide did not directly affect the responses evoked by stimulation of the afferent pathway but did prevent maintenance of long-term potentiation. Short-term potentiation and paired-pulse facilitation were not affected by peroxide treatment. Peroxide was less effective if removed following high frequency stimulation and was ineffective if applied only after high frequency stimulation. Input/output analysis showed that the increase in synaptic efficacy was reduced with peroxide treatment. Changes in the enhanced ability of the synaptic potential to generate a spike were less apparent.

These data show that the interference of free radicals with long-term potentiation may contribute to pathological deficits. It is possible that intracellular calcium regulation is disrupted by peroxide treatment. A number of second messenger systems involved with long-term potentiation are potential targets for free radical attack.

Long-term potentiation (LTP) is a persistent increase in monosynaptic efficacy following a high frequency train. Because the potentiation can last for hours or even days *in vivo*,[31] this electrophysiological phenomenon has been considered to be a correlate of memory and learning. The biochemical changes that underlie LTP are complex, possibly involving a number of second messenger systems.[17,20,22,30,32]

Free radicals and active oxygen compounds (e.g. peroxide, superoxide and hydroxyl radicals) are normally generated with cellular metabolism but are well controlled by intrinsic enzyme systems and antioxidants.[7,10,12,13] Under certain pathological conditions, this delicate balance can be disrupted. Free radicals are thought to contribute to a number of diseases such as ischemic injury, aluminum toxicity, Alzheimer's disease and Down's syndrome,[7,9,12,16,23,35,41] all of which affect cognitive processes.

Previous studies have shown that free radicals can interfere with neuronal electrophysiology.[27–29] Hydroxyl radicals can be generated *in vitro* through the Fenton reaction; peroxide reacts with iron intrinsic to the tissue to produce this very reactive free radical. Hydroxyl radicals attack membrane lipids and cellular proteins, which disrupts cell function. Exposure of a hippocampal slice to peroxide ($\geq$0.005%) decreases synaptic responses, decreases orthodromic spike generation[27] and increases spike frequency adaptation.[27] Free radical scavengers (dimethylsulfoxide, Trolox-C) and an iron chelator (deferoxamine) prevent most of the peroxide damage,[29] suggesting that hydroxyl radicals, and not the peroxide itself, are the reactive oxygen species. Colton *et al.*[6] used a similar model and found that peroxide reduced the potentiation occurring 15 min after high frequency stimulation.

This paper examines the actions of free radicals on LTP.

EXPERIMENTAL PROCEDURES

Male Hartley (Harlan Sprague–Dawley, Inc., Indianapolis, IN) guinea-pigs (250–300 g) were anesthetized with isoflurane and euthanized by cervical dislocation. The brain was removed and chilled by submersion in ice cold artificial cerebrospinal fluid (aCSF: NaCl 124 mM, KCl 3 mM, $CaCl_2$ 2.4 mM, $MgSO_4$ 1.3 mM, K_2PO_4 1.24, $NaHCO_3$ 26 mM, glucose 10 mM, equilibrated with 95% O_2/5% CO_2). Hippocampi were dissected out, sliced on a McIlwain tissue chopper to a nominal thickness of 415 μm and incubated in a holding chamber at room temperature for at least 90 min.

Peroxide solutions were made fresh daily from 50% concentrate (Fisher). Most experiments used a peroxide concentration of 0.002% (720 μM). Previous studies[27–29] on hippocampal slices used concentrations between 0.005% (1.8 mM) and 0.01% (3.6 mM). The 0.002% concentration was chosen for the present study because at this level peroxide had no direct effects on electrophysiological potentials in the brain slice. These concentrations of peroxide

†To whom correspondence should be addressed.
‡Present address. Patent and Trademark Office, Group 120, 2011 Jefferson Davis Highway, Arlington, VA 22202, U.S.A.

Abbreviations. aCSF, artificial cerebrospinal fluid, HFS, high frequency stimulation, I/O, input/output, LTP, long term potentiation, PSP, postsynaptic potential, STP, short-term potentiation.

are comparable to those used as a model of free radical damage to electrophysiological events in cardiac tissue (100 μM–10 mM).[11,14]

For electrophysiological recording, a slice was placed in a laminar flow submersion chamber (Zbicz design)[40] and perfused with aCSF at 30 C. A bipolar stimulating electrode was positioned in the stratum radiatum of field CA1 to stimulate afferent pathways. Glass microelectrodes (2 N NaCl) were placed in the s. radiatum of field CA1 to record the afferent volley and the population postsynaptic potential (population PSP) and in the s. pyramidale to record the population spike. The magnitude of the population spike was calculated from the mean of the early and late positivities minus the maximal negativity. The population PSP was quantified from the maximum negative slope early in the synaptic response. Signals from the microelectrodes were recorded with WPI high gain d.c. amplifiers and then digitized, stored and analysed on an LSI 11.23 minicomputer.

For 30 min, baseline recordings were made to ensure stability of the tissue. If the recordings deviated substantially from the initial values or developed secondary population spikes, the experiment was terminated. The slice was stimulated (0.2 Hz) at an intensity sufficient to produce a half maximal response. Averages of four responses were stored at 5-min intervals.

In most experiments, perfusion of peroxide was started after this equilibration period and continued for the duration of the experiment. After 30 min, a high frequency stimulus (HFS; 100 Hz, 1 s) was delivered at the half maximal stimulus amplitude. Following HFS, data collection continued for another 60 min. In most experiments, data continued to be stored every 5 min. In experiments used for the exponential curve fitting, data were collected more frequently and were not averaged, in order to allow accurate representation of the time course. In some experiments, the perfusion of peroxide was either delayed [illegible] HFS or terminated immediately after HFS. Some slices were untreated (i.e. never exposed to peroxide). In control experiments, no HFS was delivered and the actions of peroxide alone were followed. The timing of the experiments was identical in all other respects. In two of the 78 slices, HFS failed to cause even short-term potentiation (STP; i.e. potentiation that develops immediately and decays within 15 min), these two experiments were not included in the analysis.

Input/output (I/O) curves were generated before and after HFS in peroxide-treated and untreated slices using a range of stimulus intensities (0.0–0.5 mA, 200 μs). Three relationships were examined using the averages from eight experiments, population spike vs afferent volley, population PSP vs afferent volley and population spike vs population PSP. The third relationship (population spike vs population PSP) was also evaluated for each individual experiment. I/O curves were generated 30 min prior to HFS and 60 min following HFS. The timing was designed to prevent any influence of STP, sometimes produced by generating the I/O curve, on the LTP evoked by HFS. Since the pre-HFS time point coincided with the application of peroxide, the peroxide concentration was not at its peak. This is not a concern since peroxide at the concentration used does not change the I/O curves (data not shown). Data for the I/O curves were analysed as previously described.[39] In brief, best-fit sigmoid curves were determined for both pre- and post-HFS data. For each curve, a parameter was computed from the maximal y-value divided by the x-value at half maximal y. Changes in this parameter have been effective in evaluating changes in I/O curves.

Paired-pulse facilitation was studied by using two identical stimuli (200 μs) separated by intervals from 10 to 200 ms. The stimulus strength was adjusted to produce approximately a half maximal population spike. Amplitude of the second population spike was expressed as a percentage of the first population spike. Facilitation was evaluated in normal aCSF and 30 min after perfusion with 0.01% peroxide.

Data are expressed as mean values ± standard errors. Student's t-test was used for comparisons of two predetermined sets of data. Analysis of variance was used to evaluate differences among more than two treatment groups. For all statistical analyses, a probability level of $P < 0.05$ was considered to reflect significance.

RESULTS

Peroxide at a concentration of 0.002% had no direct effect on the amplitude of the population spike, even after a 90 min exposure (Fig. 1) ($n = 4$). Yet, this concentration of peroxide significantly impaired the ability of HFS to produce LTP. In untreated slices ($n = 17$), HFS caused an immediate increase in the population spike to 285 ± 14% of control amplitude. Within 15 min, this amplitude fell to 238 ± 13% of control and sustained that level for the remainder of the experiment. All 17 slices showed potentiation of at least 130% of control 60 min following HFS. In slices treated with peroxide ($n = 16$), there was also an early enhancement of the amplitude (270 ± 15%) which was not significantly different from potentiation in untreated slices (t-test, $P > 0.05$). In contrast to untreated tissue, however, by 30 min the amplitude was only 185 ± 13% and by 60 min only 124 ± 14%. The amplitude of population spikes in peroxide-treated slices did not establish a plateau but slowly fell throughout the measurement period (Fig. 1A). Only five of 16 slices showed population spike amplitudes of 130% of control or greater at 60 min post-HFS. At 60 min post-HFS, the population spike amplitudes of treated and untreated slices were significantly different from one another (t-test, $P < 0.05$). The inset in Fig. 1A shows sample traces from treated and untreated slices. The population spike in untreated slices showed a substantial increase in amplitude that was sustained for 60 min. Potentiation was not sustained in peroxide-treated slices and the population spikes before and 60 min after HFS are nearly the same size.

A similar pattern was evident with the population PSP (Fig. 1B). In untreated slices the magnitude of the early slope of the population PSP was increased to 284 ± 26% of control with a decline to 203 ± 20% of control within about 15 min. The increase was sustained for the remainder of the experiment (202 ± 28% at 60 min post-HFS). At 60 min after HFS, in 13 of 17 slices the population PSP was at least 130% of control amplitude. Sample traces before and 60 min following HFS in untreated slices show a sustained enhancement of the synaptic response. Treatment with 0.002% peroxide prevented the maintained increase in the PSP. By 60 min post-HFS the population PSP was nearly the same as during the control period. The initial increase was 261 ± 30% and declined to 129 ± 17% after 60 min. Only five of 16 slices showed population PSPs that

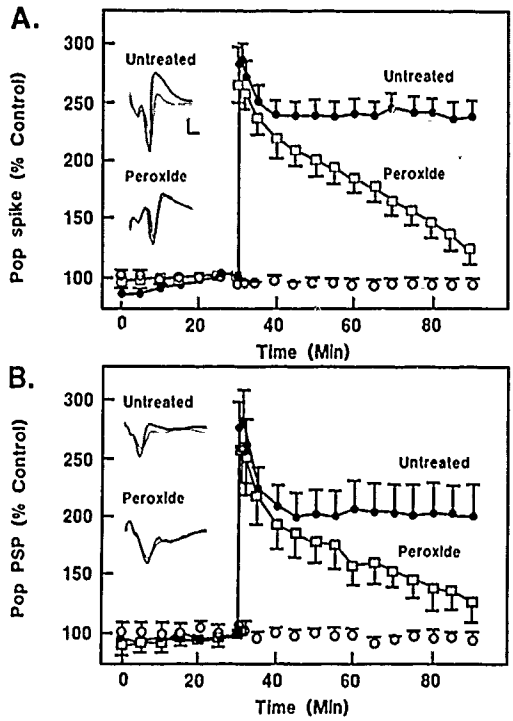

Fig. 1. Hydrogen peroxide (0.002%) prevents the maintenance of LTP. (A) Amplitude of population spike expressed as percentage of control plotted vs time. Error bars show standard error of the mean for each time point. Open circles, population spike in tissue treated with peroxide but not stimulated with HFS ($n = 4$). Open squares: peroxide present, HFS applied at 30 min time point ($n = 16$). Closed circles, untreated tissue, HFS at $t = 30$ min ($n = 17$). Insets show sample traces from individual experiments. Light trace is from before HFS while bold trace occurred 60 min after HFS ($t = 90$ min). Calibration: 1 mV, 2 ms. (B) Changes in population PSP with time. Symbols same as in A. Insets show sample population PSPs from same experiments as in A. light trace from before HFS, bold trace from 60 min post-HFS. Same calibration as in A.

were at least 130% of control. Sample traces show very little difference between synaptic responses recorded prior to HFS and responses 60 min following HFS in peroxide-treated slices. At 60 min post-HFS, treated and untreated population PSPs were statistically different from one another (t-test, $P < 0.05$).

A higher concentration of peroxide (0.005%) was tested with HFS on three slices. As previously observed,[29] this concentration had a direct effect to decrease both the synaptic response and the population spike. HFS elicited early potentiation of both population spike amplitude and population PSP slope. Within about 30 min, however, the responses were back to control level and continued to decline. Population spike potentiation fell to only $105 \pm 28\%$ of control within 30 min. At 45 min post-HFS, the average population spike was $58 \pm 23\%$ of control. The synaptic response was similarly reduced very quickly.

Paired-pulse facilitation was evaluated with 0.01% peroxide ($n = 3$; data not shown). Facilitation was maximal at an interstimulus interval of 30 ms, $302 \pm 50\%$ in untreated slices and $297 \pm 28\%$ in peroxide-treated slices. In agreement with Colton *et al.*,[6] facilitation was unaffected by peroxide at all interstimulus intervals tested (10–200 ms).

Peroxide might prevent LTP by interfering with its induction or its expression. To distinguish between these possibilities, peroxide was applied at different times during the process. Table 1 illustrates the change in population spike 60 min after HFS with four experimental treatments: (1) untreated ($n = 17$), (2) treated with peroxide throughout the experimental period ($n = 16$), (3) treated with peroxide before and up to 10 min after HFS ($n = 16$) and (4) treated with peroxide only after HFS (5–60 min post-HFS; $n = 9$). Analysis of variance showed that potentiation in slices treated with peroxide throughout (treatment 2) was significantly less than in untreated slices (treatment 1, $P < 0.05$). When peroxide was removed after HFS (treatment 3), population spike amplitude was not maintained at the level of untreated slices but decayed more slowly than in slices with continued exposure to peroxide (treatment 2); potentiation was not statistically different from that in either of the first two treatments. When peroxide was applied only after HFS (treatment 4), potentiation of the population spike was sustained as in untreated slices. Analysis of synaptic potentials at 60 min post-HFS showed a similar pattern (data not shown): peroxide following HFS was ineffective while peroxide removed after HFS was only partly effective in reducing LTP.

In the previous series of experiments, the potentiation following HFS was evaluated at only one stimulus intensity, kept constant throughout the experiment. In an effort to evaluate the change in the response to a range of stimulus strengths, I/O curves were generated 30 min prior to HFS and 60 min after HFS. As seen in Fig. 2, in untreated slices ($n = 8$), HFS increased the ability of the afferent volley to elicit a population spike throughout the

Table 1. Timing of peroxide application affects amount of potentiation resulting from high frequency stimulation

Treatment	Percentage increase in population spike (±S.E.M.)
(1) Untreated	137.5 ± 14.5
(2) Peroxide throughout	24.0 ± 13.6*
(3) Peroxide before and during HFS	85.5 ± 16.8
(4) Peroxide after HFS	136.1 ± 16.4

Measurements show percentage increase in population spike 60 min after HFS compared to control. The population spike from untreated tissue shows significant potentiation. Treatment with peroxide (0.002%) throughout the experiment prevented sustained potentiation. *Analysis of variance, $P < 0.05$. Application of peroxide before and during HFS but washed out within 5 min prevented some but not all potentiation ($P < 0.05$). Application of peroxide only after HFS did not affect potentiation ($P < 0.05$).

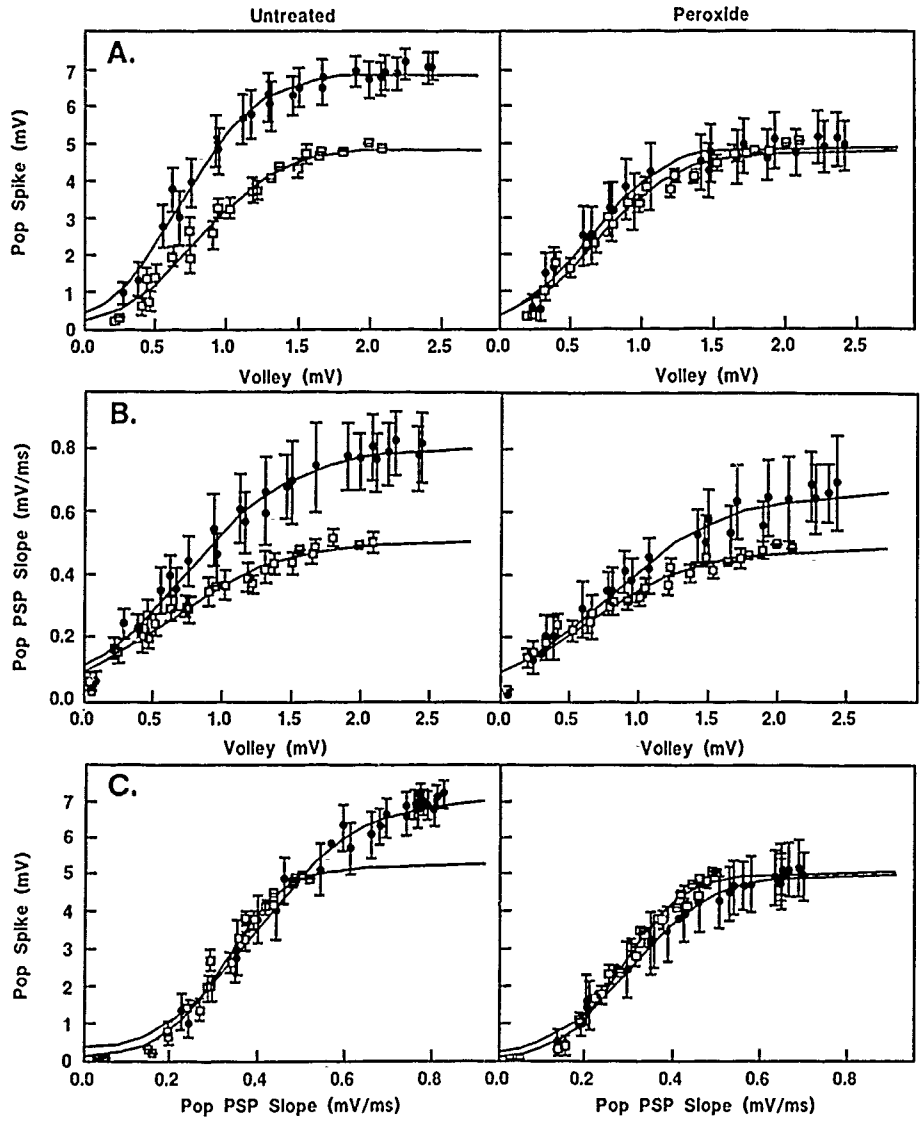

Fig. 2. I/O curves obtained from tissue treated with 0.002% peroxide ($n = 8$, right) and untreated ($n = 8$, left) Curves obtained 30 min prior to HFS (open squares) and 60 min after HFS (closed circles) in both conditions (A) Plot of population spike vs volley shows significant enhancement of population spike following HFS in untreated tissue which is not evident in peroxide-treated tissue. (B) Plot of population PSP vs volley shows enhancement of synaptic response in untreated tissue which is less dramatic with peroxide treatment. (C) Plot of population spike vs population PSP shows only minimal changes in E/S coupling both in treated and untreated tissue.

range of stimulus intensities (166 ± 9%). In tissue treated with 0.002% peroxide ($n = 8$), this enhancement is greatly reduced (112 ± 7%). HFS also increased the ability of the afferent volley to evoke a synaptic potential in untreated slices (134 ± 13%) (Fig 2B). Peroxide decreased this potentiation (105 ± 11%) (Fig. 2B). The third set of graphs (plot of population spike vs population PSP) provides an indication of the ability of the synaptic potential to evoke a spike, also called E/S coupling. Other authors[12,17] have shown that E/S coupling is sometimes enhanced with LTP. Andersen *et al.*[2] reported that only 50% of their slices showed this phenomenon. In the present experiment, there was no obvious change in this relationship following LTP in the average response of eight untreated slices (109 ± 5%), yet four of eight of these slices did show enhanced E/S coupling (i.e. greater than 20% increase) in agreement with Andersen *et al.*[2] In peroxide-treated slices, there is also no E/S enhancement in the averaged curves (94 ± 4%) and only two of eight treated slices showed enhancement.

Potentiation following HFS can be resolved into components by evaluating the time constants of decay of the response back to baseline.[24] In each of the eight treated and eight untreated slices in the experiment above, data at additional time points were collected to provide a more accurate represen-

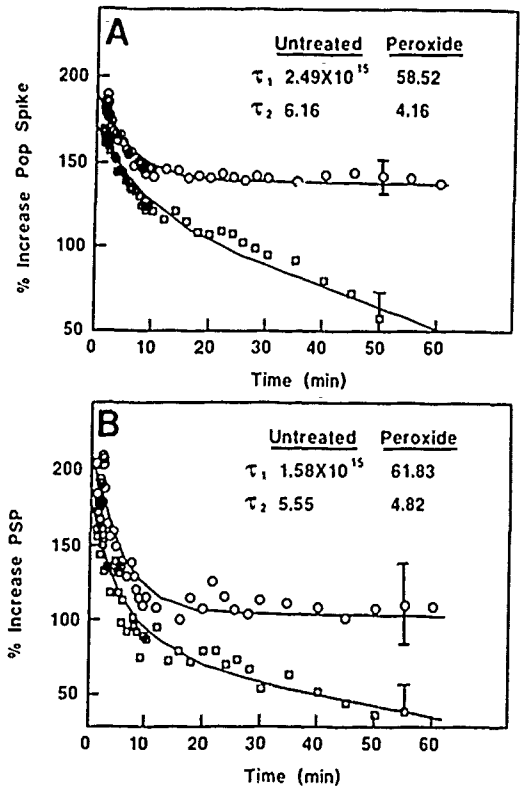

Fig. 3. Curves describing the sum of two exponential processes were fitted to the data for the decay of potentiation of the population spike (A) and the population PSP (B) both with (open squares) and without (open circles) peroxide treatment. HFS given at time = 0. Calculated time constants (min) shown in insets. Details of curve fitting in text. Points represent averages from eight experiments. One representative error bar is shown for each curve.

tation of changes in the amplitude of the population spike and the population PSP with time. The percentage increase in response was plotted vs time, with time = 0 at the time of HFS (Fig. 3). The four resultant curves (population spike and population PSP, with and without peroxide treatment) are described by the equation for the sum of two exponentials:

$$\% \text{ change} = a \cdot \exp(-t/\tau_1) + b \cdot \exp(-t/\tau_2),$$

where a, b, τ_1 and τ_2 are evaluated for the best fit to the experimental data with a routine (FITFUNCTION) in the analytical package RS/1 (BBN Software Product, Cambridge, MA). τ_1 and τ_2 are the time constants for the slow and fast components of the curve, respectively. a and b are weighting constants for the two exponentials and were insensitive to peroxide. While the computed values seem to fit the data very well, we do not assume that they are necessarily unique solutions to the equation. The time constants of decay of potentiation of the population spikes of the best fit curves were 2.49×10^{15} and 6.16 min in untreated tissue and 58.52 and 4.16 min in peroxide-treated slices. It is obvious that the slower time constant is decreased by peroxide treatment, whereas the faster time constant is not much affected. The time constants for the synaptic response showed a similar effect. In untreated slices the calculated time constants were 1.58×10^{15} and 5.55 min and in peroxide-treated slices they were 61.83 and 4.82 min. Again, the slow time constant is greatly decreased by treatment with peroxide while the faster time constant is not. Thus, the late phase of LTP appears to be selectively altered by peroxide.

DISCUSSION

The electrophysiological effects of peroxide on field potentials in hippocampal slices have been shown to be mediated by free radicals.[29] In the present study, we demonstrate that peroxide interferes with LTP at concentrations that do not affect unpotentiated synaptic transmission. The I/O curves show that free radicals predominantly impair potentiation of the synaptic response and have much less effect on spike generation (E/S coupling). This contrasts with higher concentrations of peroxide, which significantly reduced both synaptic efficacy and E/S coupling.[27] The decreased synaptic potentials in previous studies were hypothesized to be a consequence of reduced transmitter release.[28] Free radical effects on LTP, a complex neuronal process, may involve other mechanisms.

HFS induces at least two phases of potentiation, the later one being LTP. The early phase has been referred to as STP.[24,33,36] Our results in untreated tissue suggest that LTP does not decrement measurably. While the calculated time constant may not be an accurate assessment of the extended time course, it does make the point that in untreated tissue, LTP is a sustained process. In contrast, in peroxide-treated tissue, decay of LTP has a time constant of only about 1 h. On the other hand, the earlier component of potentiation, with a time constant of 5–6 min, is not very sensitive to peroxide. This component is likely to correspond to what McNaughton[24] called potentiation, which has a time constant around 1.5 min *in vivo*. Temperature sensitivity can account for much of the quantitative difference in the time constant between his experiments and the present results.

Analysis of the time constants of decay revealed that only the late phase of potentiation was affected by peroxide while the early decay was unchanged. Previous studies have shown that STP and LTP have very different mechanisms. Several authors[19,24,42] have suggested that STP reflects an increase in the probability of transmitter release, most likely due to an increase in presynaptic calcium. Similarly, paired-pulse facilitation is caused by an increase in the probability of transmitter release. In contrast, it has been suggested that enhanced calcium entry at presynaptic terminals is not the mechanism for

LTP.[24,25] LTP does not appear to entail an increase in the probability of transmitter release, instead McNaughton[24] hypothesized that the presynaptic component of synaptic enhancement in LTP could reflect an increase in the number of quanta available for release or an increase in the number of binding sites for vesicles. Since STP and paired-pulse facilitation are unaffected by peroxide exposure, it is unlikely that free radicals are interfering with presynaptic calcium entry. In fact, voltage clamp studies in hippocampal pyramidal cells have shown that sustained high threshold calcium currents[27] and transient low threshold calcium currents (unpublished data) are insensitive to peroxide. Other steps in the release process need to be considered as possible peroxide-sensitive sites.

Induction of LTP also requires calcium postsynaptically,[8,21,26] but only within 5 min of HFS.[34] It is possible that peroxide is interfering with a postsynaptic calcium-dependent process. Remote calcium spikes in hippocampal neurons show an increased threshold with exposure to peroxide[27] and calcium-dependent processes in a number of cell types are reportedly sensitive to free radical damage.[4,5,8,14,15]

Peroxide must be present during induction of LTP to be effective. Yet its action is to prevent maintenance of the potentiation. This suggests that peroxide is interfering with some process during the induction phase of LTP required to fully express the potentiation. Recent reports[17,20,22,30] show that a number of second messenger systems must similarly be available during HFS for LTP to occur. Blocking postsynaptic protein kinase C or calmodulin II kinase prevents the induction of LTP; STP is evident, but by 30 min post-HFS the responses are back to control levels.[20,22] As with peroxide, the time of application of kinase inhibitors is critical. Intracellular injection of the blockers in the postsynaptic cell after HFS has no effect In these experiments it is not possible to remove the blockers after injection, which complicates comparison with our experiments in which removal of peroxide was less effective than continued exposure. It is possible that peroxide is interfering with one of the several second messenger systems thought to be involved with LTP.

Recent studies[1a,38] suggest that the oxidation/reduction state of the *N*-methyl-D-aspartate affects its electrophysiological response. In a number of neuronal preparations, dithiothreitol, a sulfhydryl reducing agent, caused long-term enhancement of the response to *N*-methyl-D-aspartate.[1a] This effect could be reversed by oxidation with dithio-bis-nitrobenzoic acid. Tauck and Ashbeck[38] reported that dithiothreitol, at a concentration that had no direct effects on the synaptic potential, was able to enhance LTP. It is possible that the free radicals formed in the present study oxidize the *N*-methyl-D-aspartate receptor, decrease its contribution to the synaptic response even with HFS and thereby reduce the expression of LTP.

Hydrogen peroxide reacts with tissue iron to generate hydroxyl free radicals. While free radicals are constantly formed in healthy tissue, the intrinsic antioxidant systems keep them in check. However, under pathological conditions, free radical generation can exceed the tissue's ability to control them. Our study suggests that under such conditions, LTP, and perhaps memory processes, can be disrupted.

Acknowledgements—This work was supported by the Armed Forces Radiobiology Research Institute, Defense Nuclear Agency, under work unit 00105. Views presented in this paper are those of the authors, no endorsement by the Defense Nuclear Agency has been given or should be inferred. Research was conducted according to the principles enunciated in the "Guide for the Care and Use of Laboratory Animals" prepared by the Institute of Laboratory Animal Resources, National Research Council.

REFERENCES

1. Abraham W. C., Bliss T. V. P. and Goddard G. V. (1985) Heterosynaptic changes accompany long-term but not short-term potentiation of the perforant path in the anaesthetized rat. *J. Physiol., Lond.* 363, 335–349.
1a. Aizenman E., Lipton S. A. and Loring R. H. (1989) Selective modulation of NMDA responses by reduction and oxidation. *Neuron* 2, 1257–1263.
2. Andersen P., Sundberg S. H., Sveen O., Swann J. W. and Wigstrom H. (1980) Possible mechanisms for long-lasting potentiation of synaptic transmission in hippocampal slices from guinea pigs. *J. Physiol., Lond.* 302, 463 482.
3. Barrington P. L., Meier C. F. Jr and Weglicki W. B. (1989) Abnormal electrical activity induced by H_2O_2 in isolated canine myocytes. In *Oxygen Radicals in Biology and Medicine* (eds Simic M. G., Taylor K A., Ward J. F. and von Sonntag C.), pp. 927–932. Plenum Press, New York.
4. Bellomo G., Jewell S. A., Thor H. and Orrenius S. (1982) Regulation of intracellular calcium compartmentation studies with isolated hepatocytes and t-butyl-hydroperoxide. *J. biol. Chem.* 79, 6842–6846.
5. Braughler J. M. (1988) Calcium and lipid peroxidation. In *Oxygen Radicals and Tissue Injury* (ed Halliwell B.), pp. 99–104. FASEB, Bethesda, MD.
6. Colton C. A., Fagni L. and Gilbert D. (1989) The action of hydrogen peroxide on paired-pulse and long-term potentiation in the hippocampus. *Free Radical Biol. Med.* 7, 3–8.
7. Demopoulos H. B., Flamm E., Seligman M. and Pietronigro D. D. (1982) Oxygen free radicals in central nervous system, ischemia and trauma. In *Pathology of Oxygen* (ed. Autor A. P.), pp. 127 155. Academic Press, New York
8. Forman H. J., Dorio R. J. and Skelton D. C. (1987) Hydroperoxide-induced damage to alveolar macrophage function and membrane integrity, alterations in intracellular-free Ca^{++} and membrane potential. *Archs Biochem. Biophys.* 259, 457–465.

9. Fraga C. G., Oteiza P. I., Golub M. S., Gershwin M. E. and Keen C. L. (1990) Effects of aluminum on brain lipid peroxidation. *Toxic. Lett.* **51**, 213–219.
10. Fridovich I. (1978) The biology of oxygen radicals. *Science* **201**, 875–880.
11. Goldhaber J. I., Ji S., Lamp S. T. and Weiss J. N. (1989) Effects of exogenous free radicals on electromechanical function and metabolism in isolated rabbit and guinea pig ventricle. *J. clin. Invest.* **83**, 1800–1809.
12. Halliwell B. (1987) Oxidants and human disease: some new concepts. *FASEB J.* **1**, 358–364.
13. Halliwell B. and Gutteridge J. M. C. (1984) Oxygen toxicity, oxygen radicals, transition metals and disease. *Biochem. J.* **219**, 1–14.
14. Hayashi H., Miyata H., Watanabe H., Kobayashi A. and Yamazaki N. (1989) Effects of hydrogen peroxide on action potentials and intracellular Ca^{2+} concentration of guinea pig heart. *Cardiovasc. Res.* **23**, 767–773.
15. Hyslop P. A., Hinshaw D. B., Schraufstatter I. U., Sklar L. A., Spragg R. G. and Cochrane C. G. (1986) Intracellular calcium homeostasis during hydrogen peroxide injury to cultured P388D_1 cells. *J. cell. Physiol.* **129**, 356 366.
16. Jeandel C., Nicolas M. B., Dubois F., Nabet-Belleville F., Penin F. and Cuny G. (1989) Lipid peroxidation and free radical scavengers in Alzheimer's Disease. *Gerontology* **35**, 275–282.
17. Lovinger D. M., Wong K., Murakami K. and Routtenberg A. (1987) Protein kinase C inhibitors eliminate hippocampal long-term potentiation. *Brain Res.* **436**, 177–183.
18. Lynch G., Larson J., Kelso S., Barrionuevo G. and Schottler F. (1983) Intracellular injections of EGTA block induction of hippocampal long-term potentiation. *Nature* **305**, 719–721.
19. Magleby K. L. and Zengel J. E. (1975) A quantitative description of tetanic and post-tetanic potentiation of transmitter release at the frog neuromuscular junction. *J. Physiol., Lond.* **245**, 183–208.
20. Malenka R. C., Kauer J. A., Perkel D. J., Mauk M. D., Kelly P. T., Nicoll R. A. and Waxham M. N. (1989) An essential role for postsynaptic calmodulin and protein kinase activity in long-term potentiation. *Nature* **340**, 554 557.
21. Malenka R. C., Kauer J. A., Zucker R. S. and Nicoll R. A. (1988) Postsynaptic calcium is sufficient for potentiation of hippocampal synaptic transmission. *Science* **242**, 81–84.
22. Malinow R., Schulman H. and Tsien R. W. (1989) Inhibition of postsynaptic PKC or CaMKII blocks induction but not expression of LTP. *Science* **245**, 862–866.
23. Martins R. N., Harper C. G., Stokes G. B. and Masters C. L. (1986) Increased cerebral glucose-6-phosphate dehydrogenase activity in Alzheimer's Disease may reflect oxidative stress. *J. Neurochem.* **46**, 1042–1045.
24. McNaughton B. L. (1982) Long-term synaptic enhancement and short-term potentiation in rat fascia dentata act through different mechanisms. *J. Physiol., Lond.* **324**, 249–262.
25. Muller D. and Lynch G. (1989) Evidence that changes in presynaptic calcium currents are not responsible for long-term potentiation in hippocampus. *Brain Res.* **479**, 290–299.
26. Obenaus A., Mody I. and Baimbridge K. G. (1989) Dantrolene-Na (Dantrium) blocks induction of long-term potentiation in hippocampal slices. *Neurosci. Lett.* **98**, 172–178.
27. Pellmar T. C. (1986) Electrophysiological correlates of peroxide damage in guinea pig hippocampus *in vitro*. *Brain Res.* **364**, 377–381.
28. Pellmar T. C. (1987) Peroxide alters neuronal excitability in the CA1 region of guinea-pig hippocampus *in vitro*. *Neuroscience* **23**, 447–456.
29. Pellmar T. C., Neel K. L. and Lee K. J. (1989) Free radicals mediate peroxidative damage in guinea pig hippocampus *in vitro*. *J. Neurosci. Res.* **24**, 437–444.
30. Reymann K. G., Brodemann R., Kase H. and Matthies H. (1988) Inhibitors of calmodulin and protein kinase C block different phases of hippocampal long-term potentiation. *Brain Res.* **461**, 388–392.
31. Sarvey J. M. (1988) Hippocampal long-term potentiation. In *Sensitization in the Nervous System* (eds Kalivas P. and Barnes C. D.), pp. 47–80. Telford Press, Caldwell, NJ.
32. Sarvey J. M., Burgard E. C. and Decker G. (1989) Long-term potentiation: studies in the hippocampal slice. *J. Neurosci. Meth.* **28**, 109–124.
33. Scharfman H. E. and Sarvey J. M. (1985) Postsynaptic firing during repetitive stimulation is required for long-term potentiation in hippocampus. *Brain Res.* **331**, 267–274.
34. Segal M. and Patchornik A. (1989) Modulation of $[Ca]_i$ by a caged EGTA affects neuronal plasticity in the rat hippocampus. *Soc. Neurosci. Abstr.* **15**, 166.
35. Sinet P. M. (1982) Metabolism of oxygen derivatives in Down's Syndrome. *Ann. N.Y. Acad. Sci.* **396**, 83–94.
36. Stanton P. K. and Sarvey J. M. (1984) Blockade of long-term potentiation in rat hippocampal CA1 region by inhibitors of protein synthesis. *J. Neurosci.* **4**, 3080–3088.
37. Taube J. S. and Schwartzkroin P. A. (1988) Mechanisms of long-term potentiation: EPSP/spike dissociation, intradendritic recordings and glutamate sensitivity. *J. Neurosci.* **8**, 1632–1644.
38. Tauck D. L. and Ashbeck G. A. (1990) Glycine synergistically potentiates the enhancement of LTP induced by a sulfhydryl reducing agent. *Brain Res.* **519**, 129–132.
39. Tolliver J. M. and Pellmar T. C. (1987) Ionizing radiation alters neuronal excitability in hippocampal slices of the guinea pig. *Radiation Res.* **112**, 555–563.
40. Zbicz K. L. and Weight F. F. (1985) Transient voltage and calcium-dependent outward currents in hippocampal CA3 pyramidal neurons. *J. Neurophysiol.* **53**, 1038–1058.
41. Zola Morgan S., Squire L. R. and Amaral D. G. (1986) Human amnesia and the medial temporal region: enduring memory impairment following a bilateral lesion limited to field CA1 of the hippocampus. *J. Neurosci.* **6**, 2950–2967.
42. Zucker R. S. (1989) Short-term synaptic plasticity. *A. Rev. Neurosci.* **12**, 13–32.

(*Accepted* 28 *January* 1991)

RADIATION RESEARCH 126, 244–250 (1991)

Increased Radiation Resistance in Transformed and Nontransformed Cells with Elevated *ras* Proto-oncogene Expression

DVORIT SAMID, ALEXANDRA C. MILLER,* DONATA RIMOLDI, JEFFREY GAFNER,* AND EDWARD P. CLARK*,[1]

*Pathology Department, Uniformed Services University of The Health Sciences, and *Radiation Biochemistry Department, Armed Forces Radiobiology Research Institute, Bethesda, Maryland 20889*

SAMID, D., MILLER, A. C., RIMOLDI, D., GAFNER, J., AND CLARK, E. P. Increased Radiation Resistance in Transformed and Nontransformed Cells with Elevated *ras* Proto-oncogene Expression. *Radiat. Res.* 126, 244–250 (1991).

The cellular Ha-*ras* oncogene, activated by missense mutations, has been implicated in intrinsic resistance to ionizing radiation. This study shows that the overexpression of the unmutated gene (proto-oncogene) may also be involved in how the cells respond to radiation. The experimental system consisted of mouse NIH 3T3-derived cell lines which carry multiple copies of a transcriptionally activated human c-Ha-*ras* proto-oncogene. Both tumorigenic (RS485) and revertant nontumorigenic subclones (PR4 and 4C3) which have high levels of *ras* expression exhibited a marked increase in radioresistance as measured by D_0 compared to control NIH 3T3 cells. Other nontransformed cells with elevated levels of *ras* (phenotypically revertant line 4C8-A10) also had a significantly increased resistance to radiation, further indicating an association between *ras* and radioresistance. The increased radioresistance of the RS485 and phenotypic revertants could not be explained by a differential expression of the *myc* or metallothionein I genes or by variations in cell cycle. The correlation between increased *ras* proto-oncogene expression and radioresistance suggests that the *ras* encoded p21, a plasma membrane protein, may participate in the cellular responses to ionizing radiation.

INTRODUCTION

Understanding the molecular mechanisms of intrinsic radioresistance is fundamental to the development of potent chemical radioprotectors and the design of more effective cancer radiotherapy protocols. Recent studies have demonstrated a correlation between radioresistance of human tumors and the expression of specific oncogenes, namely, the *ras* and *raf* oncogenes (*1, 2*). Using DNA-mediated gene transfer techniques, it has been shown that the activated *raf* may contribute to radioresistance in skin fibroblasts from cancer-prone individuals (*1*) and in tumors of the head and neck (*2*). Furthermore, transfected *raf* and genes of the *ras* family (Ha-, Ki-, or N-*ras*) that are activated by missense mutations all induced a radioresistant phenotype in recipient rodent cells (*3–5*). This was in contrast to activated *myc, fes,* and *abl* oncogenes, which had no effect on the response to radiation (*6*). Research efforts extending these observations demonstrated that the inhibition of *raf* expression by antisense RNA is sufficient for restoring radiosensitivity in human squamous carcinoma cells (*7*). It appears, therefore, that specific oncogenes may play a role in intrinsic radioresistance.

Thus far, studies on the cellular Ha-*ras* and radioresistance have focused primarily on the mutated gene (EJ-*ras*), which encodes for a 21-kDa protein (p21) with a glycine to valine substitution (*8*). However, mutations in *ras* are rather infrequent in spontaneous human tumors (*9–11*). In contrast, quantitative changes in Ha-*ras* are commonly found in a wide variety of human neoplasms (*11, 12*). Being interested in the potential role of p21 in radioresponses of normal and malignant tissues, we chose to concentrate on the wild-type p21. Our interest was prompted by early findings indicating that an interaction of a cell membrane component with exogenous (or endogenous) thiols may be necessary to maintain the cellular response to radiation (manuscript in preparation). The cellular $p21^{ras}$, a G-like protein with guanine nucleotide binding and GTPase activities, is localized on the inner side of the plasma membrane (*12*) and is thought to participate in the transduction of extracellular signals through hydrolysis of phosphoinositides or the activation of protein kinase C (*13–16*). Considering its strategic localization and function, we speculated that cellular p21 may be involved in the control of radiation responses.

The studies described here were designed to determine the relationship between the expression of Ha-*ras* proto-oncogene and cellular sensitivity to ionizing radiation. The experimental system consisted of NIH 3T3-derived cell lines which express the human c-Ha-*ras*1 gene transcriptionally activated by a retroviral long-terminal repeat (LTR) control element. Tested cultures included the neoplastically transformed cell line RS485 (*17*) and phenotypi-

[1] To whom correspondence should be addressed.

0033-7587/91 $3.00

cally revertant nontumorigenic subclones (PR4, 4C8A10, 4C3) obtained after long-term treatment with interferon-α/β (IFN-α/β) (*18–20*). The mouse cell lines, which varied in their tumorigenic phenotype and p21 biosynthesis (*18–20*), provided a suitable system for correlative studies focusing on *ras* expression in different genetic and phenotypic backgrounds. The results indicated a tight correlation between radiation sensitivity and *ras* that was independent of the oncogene-induced neoplastic transformation.

METHODS

Cells, Interferon Treatment, and Transfection with cDNA

NIH 3T3 subclones were propagated in Dulbecco's modified Eagle's medium supplemented with 2 m*M* glutamine, 10% heat-inactivated fetal calf serum (GIBCO Laboratories, Grand Island, NY), 100 U/ml penicillin, and 100 μg/ml streptomycin (Sigma, St. Louis, MO). Exponentially growing cells were used in all experiments. The cell line RS485 was originally derived by transforming NIH 3T3 cells (*21*) with the 2.9-kb *Sac*I fragment of the human c-Ha-*ras*1 proto oncogene ligated downstream from the LTR of Harvey murine sarcoma virus (*17*). The isolation and characterization of IFN α,β induced RS485-revertant clonal line 4C3 and its subclone PR4 have been described previously (*18–20, 22*). The 4C8-A10 subclone was isolated from interferon-induced revertant 4C8 cells (*18*) grown in the absence of interferon for 2–3 months. The phenotypically reverted 4C3, PR4, and 4C8-A10 cells contain the transforming *ras* DNA but have lost the ability to proliferate in semisolid agar or in recipient athymic mice ((*18*) and unpublished data). The 4C3 cells were propagated in the continuous presence of 200 IU/ml of mouse L-cell IFN-α/β (sp act 10^8 IU/mg, a gift from M. Pauker, Medical College of Pennsylvania) and irradiated in the absence of interferon (see below). Control cultures included the parental NIH 3T3 cell line as well as the subclones designated N_0, N_1, N_2, N_6, and N_{12} (*23*), obtained by transfection with pSV_2neo (*24*). DNA coprecipitation with calcium phosphate, transfection of cells, and selection of transformants were as described previously (*18*).

Analysis of Mitotic and Labeling Indices

To determine the percentage of cells in S phase, a monoclonal antibody technique was used (*25, 26*). The mitotic fraction was determined by a modification of the percentage labeled mitoses technique (*27, 28*). For both procedures, cells were collected on ice, fixed with 1% Na-citrate/1% glacial acetic acid, and centrifuged onto slides. The slides were treated with RNase to remove any RNA and then stained with propidium iodide. To determine the labeling index, cultures were treated with 0.1 m*M* bromodeoxyuridine (BrdUrd) and 0.01 m*M* fluorodeoxyuridine for 30 min to allow for incorporation into DNA. Cells were collected as above onto slides. Following treatment with 0.9% NaOH, the slides were rinsed with PBS and treated with the double antibody fluorescence technique, using the BrdUrd monoclonal antibody (Becton–Dickinson, Mt. View, CA) and the IgG-biotin-streptavidin-FITC conjugated antibody (TAGO, Inc., Burlingame, CA). This allowed for visualization of those cells in S phase that incorporated the BrdUrd (*26, 28*). Unless otherwise stated, all reagents were obtained from Sigma Chemical Co. Statistical tests are listed below.

Radiobiology

Cellular response to radiation was assessed by the cell survival assay. Cells were counted with a Coulter counter (Hialeah, FL) and plated onto 60-mm-diameter culture dishes in appropriate numbers 4–16 h before radiation treatment to allow for cell attachment. Phenotypically revertant 4C3 cells, normally maintained with continuous treatment of interferon (200 IU/ml), did not have interferon present in the medium during radiation treatment. Cells were treated as a monolayer in complete medium under aerobic conditions and given a total dose of 2 to 10 Gy unilaterally at 0.99 Gy/min from an Atomic Energy of Canada Limited, Theratron-80 cobalt-60 source. Prior to each exposure, the dose rate was measured at the irradiation distance using a 5.0-cc tissue-equivalent ionization chamber with a 4-mm build-up cap manufactured by Exradin, Inc. The ionization chamber used has a calibration factor traceable to the National Institute of Standards and Technology (*29*). The dosimetry measurements were performed following the AAPM Task Group 21 protocol for the determination of the absorbed dose from high-energy photon and electron beams (*29*). Following irradiation, cells were returned to the incubator for 10 days to allow for colony formation and then fixed with methanol and stained with 1% crystal violet. Colonies with more than 50 cells were counted as survivors and only plates with more than 15 colonies were counted.

Northern Blot Analysis and DNA Probes

Cytoplasmic RNA was extracted from exponentially growing cells and separated by electrophoresis in 1% agarose–formaldehyde gels as described (*30, 31*). RNA blotting onto nitrocellulose filters, hybridization with radiolabeled DNA probes, and autoradiography were performed according to standard procedures (*30, 31*). The probes, a *Sac*I 2.9-kb fragment of the human c-Ha-*ras*1 gene and a fragment of the c-*myc* gene spanning the third exon, were obtained from Oncor (Gaithersburg, MD). The probe for metallothionein I (MT-1) transcripts was a *Bgl*II/*Eco*RI fragment (spanning the three exons) derived from the 4-kb *Eco*RI mouse genomic clone of MT-1 (*22*) (gift from D. Hamer, National Cancer Institute, Bethesda, MD). ^{32}P-labeled DNA probes were prepared using a random primed DNA labeling kit (Boehringer-Mannheim, Germany).

Statistical Analysis of Data

Survival curves. Survival curves were fitted by a computer program provided by N. Albright (*32*). This program calculates survival levels and their corresponding weights. The program assumes that the variability in the colony counts is due to random errors. The corresponding weights are based on a Poisson distribution for the number of colony counts and their variations. This program fits different mathematical models to the survival data using those calculated survival levels and associated weights. This is accomplished by an iteration of the weighted least squares and by estimating the covariances of the survival curve parameters and the corresponding confidence limits. The D_0, D_q, and n were calculated by this program. No significant differences in the values for D_0, D_q, and n were observed when the data were fitted to several statistical models, so we chose to fit the data by the repair saturation model. In Figs. 2 and 3 and Table I, each data point represents the mean ± SE from 3–12 experiments with three plates per each point.

Labeling and mitotic indices. Data were analyzed by the Kruskal–Wallis test, which is a nonparametric one-way analysis of variance (*33, 34*). Data represent the mean ± SE of four experiments with three plates per data point.

RESULTS

The malignant RS485 cells, transformed by a transcriptionally activated c-Ha-*ras* proto-oncogene, produce large amounts of *ras* mRNA (Fig. 1) and encoded p21 protein compared to parental 3T3 cells (*18, 22*). Similarly, elevated *ras* expression is characteristic of the nontumorigenic, phenotypically revertant PR4 cells (Fig. 1). The RS485 and

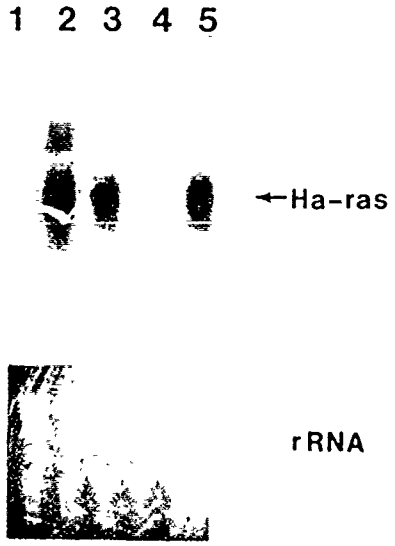

FIG. 1. Northern blot analysis of *ras*-specific mRNA. Cytoplasmic RNA (40 μg) from: Lane 1, NIH 3T3; Lane 2, RS485; Lane 3, PR4; lane 4, 4C3 cells continuously maintained on 200 IU/ml of IFN-α/β; and Lane 5, RS485 cells treated with 200 IU/ml of IFN-α/β for 72 h prior to radiation. One week after IFN-α,β treatment of the 4C3 cells was discontinued, the levels of *ras* mRNA were comparable to those shown in Lane 5 as measured by densitometric analysis. (Top) Hybridization with a ^{32}P-labeled Ha-*ras* probe. The Ha-*ras* RNA was undetectable in NIH 3T3 cells. (Bottom) The ribosomal RNA indicates the relative amounts of RNA loaded in each lane.

PR4 cells both exhibited a marked increase in radioresistance compared to control cultures (Fig. 2) as determined by their D_0 and D_q values. The values for RS485 were D_0 – 1.79 ± 0.12 Gy and D_q – 2.82 ± 0.19 Gy, and for PR4, D_0 1.70 ± 0.14 Gy and D_q – 2.63 ± 0.19 Gy. In contrast, the

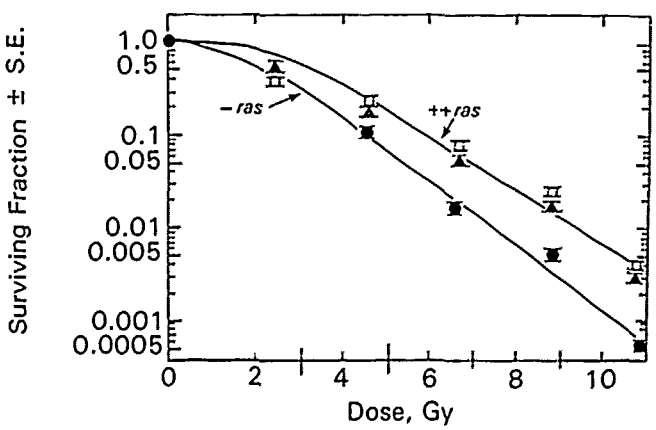

FIG. 2. The association of *ras* expression with resistance to ionizing radiation. Survival curves designated with [−*ras*] or [++*ras*] represent cells with negligible or high *ras* expression, respectively. Data represent the mean ± SE from 5–15 experiments. RS485 (□), PR4 (▲), NIH 3T3 (●). Error bars smaller than the symbol have been omitted.

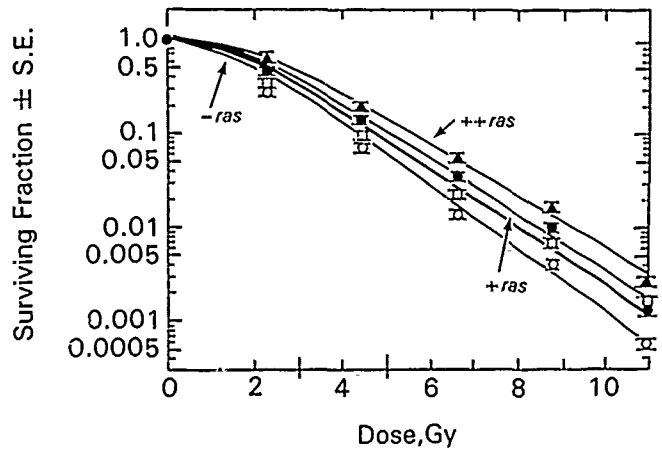

FIG. 3. Dose-dependent correlation between *ras* expression and radioresponse. Cells with varying levels of *ras* expression were exposed to ionizing radiation. Data represent the mean ± SE from 4–15 experiments. PR4 (▲); 4C3 (●); 4C8A10 (□); NIH 3T3 (○). Error bars smaller than the symbol have been omitted.

parental NIH 3T3 cells had a D_0 of 1.27 ± 0.09 Gy and a D_q of 1.63 ± 0.20 Gy. The increased radioresistance observed with the *ras* transformants and phenotypic revertants was not due to the transfection process per se since there was no significant difference in the D_0's between cells transfected with the bacterial neo^r gene (clones N_0, N_1, N_2, N_6, N_{12}) and the parental NIH 3T3 cells. The neo^r transfected NIH 3T3 subclones had D_0 values ranging from 1.12 ± 0.14 to 1.38 ± 0.14 Gy, which were not statistically different (*33, 34*) from the D_0 values previously reported for NIH 3T3 cells (*5, 6, 35*). These data indicate that a significant increase in radioresistance is associated with overexpression of *ras* and is independent of neoplastic transformation by this proto-oncogene.

In revertant 4C3 cells, *ras* expression can be modulated by IFN-α/β treatment (*20*). This allowed further examination of the relationship between *ras* and radioresistance within the same cellular system. Continuous treatment of 4C3 cells with 200 IU/ml of IFN-α/β was associated with a four- to eightfold reduction in the levels of *ras* mRNA (Fig. 1) as compared to RS485 and PR4 cells. Our previous studies showed that the levels of p21 *ras* closely follow those of the *ras* mRNA (*19, 22*). The 4C3 cells irradiated immediately after cessation of IFN-α/β treatment exhibited only a slight reduction in radioresistance (D_0, 1.59 ± 0.09 Gy; D_q, 2.53 ± 0.09 Gy) when compared to RS485 or PR4 cells (Fig. 3). One week later, at which time *ras* expression was fully restored in 4C3 cells, cellular radioresistance was also fully restored (Table 1), indicating a link between *ras* and radiation response.

It could be argued, however, that the changes observed in the radiation response of 4C3 cells were related to a pertur-

bation of the cell cycle by IFN-α/β. While this may be the case with high concentrations of IFN-α/β (>1000 IU/ml) (*36*), the concentration used in our studies (200 IU/ml) has had no significant effect on cell proliferation and resulted in negligible cellular toxicity in previous studies (*19, 36*). Furthermore, a similar IFN-α/β treatment of RS485 cells for 72 h prior to irradiation, which had no effect on *ras* expression, also had no effect on the response to radiation (D_0, 1.80 ± 0.12 Gy; D_q, 2.84 ± 0.20 Gy). Labeling and mitotic index measurements of both the IFN-α/β-treated RS485 and 4C3 cells showed that this dose of IFN-α/β had no effect on the proportion of cells in S (LI, 0.40 ± 0.04) or M (MI, 0.045 ± 0.004) phase. Therefore, it appears that alterations in radiosensitivity of 4C3 cells were associated with modulation of *ras* expression.

Even though *ras* expression was somewhat reduced in interferon-treated 4C3 cells, the cells still exhibited markedly increased resistance to radiation compared to parental NIH 3T3 cells, suggesting a possible required threshold for *ras* p21 to induce cellular radioresistance. In agreement, the phenotypically revertant clonal line 4C8-A10, which exhibits intermediate levels of *ras* constitutively (without IFN-α/β treatment), also had increased radioresistance with D_0 and D_q values of 1.65 ± 0.07 and 2.56 ± 0.09 Gy, respectively (Fig. 3). A summary of the relationship among *ras* expression, cell phenotype, and radiation sensitivity is presented in Table I.

It is well documented that sensitivity to radiation varies during the cell cycle, with S-phase cells being relatively radioresistant (*37, 38*). Strict statistical examination of the data showed, however, that there was no significant difference in the fraction of cells in S phase in NIH 3T3 cells, RS485 cells, and the revertant cultures, as indicated by their labeling indices (Fig. 4). Thus the differential radiosensitivity in these cell lines is not due to differences in cell cycle.

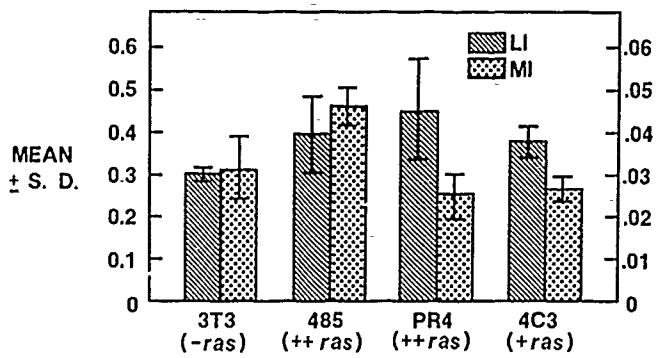

FIG. 4. Labeling (LI) and mitotic (MI) indices of NIH 3T3-derived cells. Samples were processed as described under Methods. Data represent the mean ± SE from three experiments with three samples per experiment. Statistical analysis was done as described under Methods section. Group 1, NIH 3T3; Group 2, RS485; Group 3, PR4; Group 4, 4C3. The labeling index is on the y axis and the mitotic index is on the y^2 axis.

TABLE I
Relationship of *ras* Proto-oncogene Expression to Radioresistance

Cell line[a]	*ras* level[b]	Tumorigenicity[c]	Radioresistance[d] D_0 ± SE (Gy)
NIH 3T3	<0.1	0/12	1.27 ± 0.09
RS485	6	9/9	1.79 ± 0.12
PR4	6	0/6	1.70 ± 0.14
4C3 (IFN)	1	0/11	1.59 ± 0.09
4C3 (w/o IFN)	6	0/6	1.72 ± 0.10
4C8-A10	1	0/6	1.65 ± 0.07

[a] Number of survival experiments per cell line: NIH 3T3, RS485, PR4—12; 4C3 (IFN), 4C8A10—6;4C3 (w/o IFN)—3.

[b] Data were obtained from Northern blot analysis, and the values are the relative absorbance of the bands measured by densitometric analysis of the blots.

[c] Number of mice that developed tumors after sc injection of 5 × 10^5 cells ((*19, 21*), by permission).

[d] D_0, dose required to reduce the number of surviving cells to 37% on the exponential portion of the survival curve.

Since recent reports focusing on *ras* and radioresistance in other cellular systems have shown that increased radioresistance also correlated with increased expression of other genes including metallothionein (MT)[7] and *myc* (*4, 40*), we examined their expression in our cells. Northern blot analyses showed no correlation between cellular sensitivity to radiation and the expression of either c-*myc* (Fig. 5) or MT (Fig. 6) genes. The levels of c-*myc* mRNA were comparable in NIH 3T3, PR4, and RS485 cells, regardless of their differential *ras* expression and radioresistance. Expression of MT was comparable in the RS485 and control NIH 3T3 cells despite their differential radioresistant phenotype (Fig. 6, Lanes 1 and 3). Furthermore, the MT mRNA levels were significantly lower in PR4 cells compared to RS485 cells, yet the two cell lines exhibit essentially the same high radioresistance. The findings that PR4 cells are not tumorigenic and show no elevation in MT expression despite the large amounts of p21 *ras* produced suggest that the induction of neoplastic transformation, modulation of MT expression, and an increase in radioresistance may occur via different mechanisms in cells with activated *ras*.

DISCUSSION

The cellular *ras* oncogenes in their mutated form have been implicated in intrinsic radioresistance. We show here that quantitative changes in expression of the *ras* proto-on-

[7] M. J. Renan, P. I. Dowman, and G. Blekkenhorst, Radiosensitivity of *ras*-transformed cells. Effects of metallothionein induction. Presented at the Thirty-Seventh Annual Meeting of the Radiation Research Society, Seattle, WA, 1989.

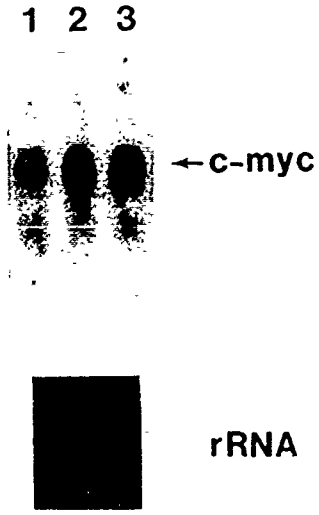

FIG. 5. Northern blot analysis of *myc*-specific mRNA. Cytoplasmic RNA (25 μg) was isolated from exponentially growing cells. Lane 1, NIH 3T3, Lane 2, PR4, Lane 3, RS485. (Top) Results of hybridization with a ^{32}P-labeled c-*myc* probe. Arrow indicates the 2.4-kb c-*myc* mRNA. (Bottom) rRNA, as in Fig. 1. The same amount of RNA was loaded in each lane.

cogene are correlated with changes in cellular response to ionizing radiation. Using NIH 3T3-derived cells that carry the human Ha-*ras* proto-oncogene (cell line RS485 and its IFN-α/β-induced phenotypic revertants) it was demonstrated that. (a) cellular response to ionizing radiation is independent of neoplastic transformation by *ras*, (b) there is a correlation between *ras* expression and radioresistance (as defined by the D_0 and D_q values) with a possible threshold requirement for the *ras*-encoded protein, and (c) agents which affect *ras* expression may also affect cellular radiosensitivity (Table I).

The malignant RS485 and phenotypically revertant cell lines contain multiple copies of the c-Ha-*ras* proto-oncogene that are under the control of the Harvey-MuSV LTR (*17, 18*) and consequently produce large amounts of p21 (*18, 19*). These cultures exhibited a marked increase in radioresistance compared to control NIH 3T3 cells. The results for RS485 are in agreement with those recently reported by Pirollo *et al.* (*6*). In contrast to our findings with the RS485-derived cells, independent studies with another NIH 3T3 subclone (NN192), transformed by the rat Ha-*ras* proto-oncogene driven by the Moloney-MuSV LTR, showed no increase in intrinsic radioresistance (*3*). Although the two cellular systems differ with respect to their transfected *ras* DNA, the differential response to ionizing radiation is more likely to be related to quantitative differences in *ras* expression. Our studies suggest that there is indeed a threshold level of *ras* expression required for the cellular radioresistance observed in these studies. Moreover, we have recently observed a dose-dependent association between *ras* expression and increased radioresistance in human osteosarcoma cells (manuscript in preparation).

Since others have suggested that response to radiation among NIH 3T3 subclones may vary even prior to transfection due to genetic instability (*39, 40*), we tested five additional neo^r NIH 3T3 subclones. Our data showed no significant heterogeneity with respect to radioresponse. The D_0 values obtained for the NIH 3T3 subclones are similar to that obtained by Chang's laboratory (*6*), but appear slightly lower compared to values obtained by others (*3, 5, 35, 42*). A strict statistical analysis (*33, 34*) and comparison of the values reported by these laboratories showed, however, that those data are not significantly different from our own in spite of differences in experimental techniques, dosimetry, and dose rate, as well as the statistical model chosen to fit the data.

We further demonstrated that the differential radiosensitivity observed in cells with high *ras* expression is not related to clonal variations. This was shown by modulating *ras* expression in revertant 4C3 cells and examining the correlation between radioresistance and *ras* expression under a uniform genetic background. In these studies, *ras* expression was modulated using IFN-α/β treatment. Treatment of 4C3 cells with 200 IU/ml of murine IFN-α/β caused a partial reduction (four- to eightfold) in *ras* gene transcription and p21 biosynthesis (this study, *18, 20*). Interestingly, this IFN-α/β treatment of 4C3 cells was not associated with restoration of radiation sensitivity, while it might appear that there was a slight restoration of radiation sensitivity, statistical analysis demonstrates that this was not the case. Perhaps additional experiments would have demonstrated a dose-dependent relationship between *ras* expression and radiation resistance. While high concentrations of IFN-α/β (>1000 IU/ml) could alter radiation re-

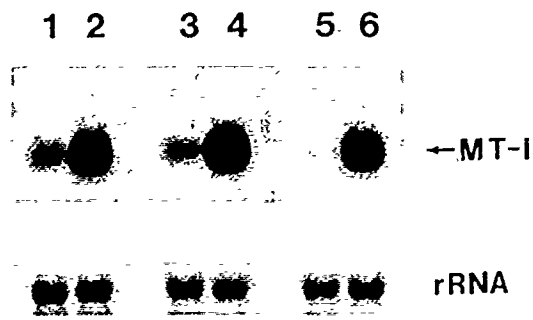

FIG. 6. Northern blot analysis of metallothionein I (MT-I) transcripts in uninduced and Cd^{2+}-induced cells. Samples were 25 μg of cytoplasmic RNA from uninduced (Lanes 1, 3, 5) and Cd^{2+} induced cultures (Lanes 2, 4, 6). NIH 3T3, Lanes 1 and 2; RS485, Lanes 3 and 4; and PR4, Lanes 5 and 6. (Top) Results of hybridization with a ^{32}P-labeled MT probe. Arrow indicates the 0.6-kb MT-specific mRNA. MT induction resulted from cellular exposure to 5 μ*M* CdSO for 10 h. (Bottom) rRNA, as in Fig. 1.

sponse via a cell-cycle effect (*36, 37*), the concentrations of IFN-α/β used (200 IU/ml) had no significant effect on cell proliferation and viability. Furthermore, a similar IFN-α/β treatment of RS485 cells, which did not affect *ras* expression (*20*), had no effect on the cellular response to radiation, suggesting that the changes in radiation sensitivity in our studies may be related to the modulation of *ras* expression.

Although the tight correlation between *ras* expression and radioresistance suggests a role for the *ras*-encoded p21 protein in cellular response to radiation, other contributing factors should be considered. Cellular radiosensitivity is known to vary during the cell cycle, with cells in the S phase being relatively radioresistant (*38, 39*). The observed increase in radioresistance cannot, however, be explained by a cell-cycle effect, because analysis of the labeling and mitotic indices showed no significant difference in tested cell lines, regardless of the level of *ras* expression. Increased radioresistance that is independent of cell cycle was also observed in EJ-*ras*-transformed primary rat embryo fibroblasts (*4, 5*). In some of these studies, however, a significant increase in radioresistance was observed only after transfection with both EJ-*ras* and a viral *myc* oncogene (*4, 40*). Since *myc* expression is cell cycle-dependent (*43, 44*) and our studies involved asynchronous cell populations, no conclusions regarding the involvement of endogenous c-*myc* in radioresistance of the NIH 3T3-derived cells can be reached. In another study with N-*ras* transformed cells, it has been proposed that enhanced radioresistance is related to elevation in metallothionein expression.[2] Such a correlation was not observed in our cellular system. Despite a marked difference in MT expression between RS485 and PR4 cells, these cultures exhibited a similar elevation in radioresistance. Moreover, in cell lines with a comparable MT expression but differential *ras* expression (i.e., the RS485 and parental NIH 3T3), the radiation response reflected the increased *ras* proto-oncogene expression.

Considering these results, it appears that quantitative changes in *ras* expression closely correlate with radiation response. Constitutive overexpression of *ras* is characteristic of a variety of human cancers. If an abundance of *ras* p21 protein is needed for the maintenance of the radioresistant phenotype, then a decrease in *ras* expression might enhance killing of tumor cells by radiation. Alternatively, radioprotection of normal cells might be achieved through the controlled induction of *ras*. This hypothesis is currently under investigation.

ACKNOWLEDGMENTS

The authors thank the reviewers of this paper for their helpful comments. This research was supported in part by the Armed Forces Radiobiology Research Institute under Research Work Unit 00150 and NIH Grant R03 EY08220-01. The views presented are those of the authors and do not reflect the official views of the Department of Defense or the U.S. Government.

RECEIVED. August 9, 1990, ACCEPTED. December 10, 1990

REFERENCES

1. E. H. CHANG, K. F. PIROLLO, Z. Q. ZOU, H. Y. CHEUNG, E. L. LAWLER, R. GARNER, L. WHITE, W. B. BERSTEIN, J. W. J. FAUMENI, and W. A. BLATTNER, Oncogenes in radioresistant, noncancerous skin fibroblasts from a cancer-prone family. *Science* 237, 1036–1039 (1987).
2. U. KASID, A. PFEIFER, R. R. WEICHSELBAUM, A. DRITSCHILO, and G. E. MARK, The *raf* oncogene is associated with a radiation-resistant human laryngeal cancer. *Science* 237, 1039–1041 (1987).
3. M. D. SKLAR, The *ras* oncogenes increase resistance of NIH 3T3 cell to ionizing radiation. *Science* 239, 645–647 (1988).
4. W. G. MCKENNA, M. C. WEISS, B. ENDLICH, C. C. LING, V. J. BAKANAUSKAS, M. L. KELSTEN, and R. J. MUSCHEL, Synergistic effect of the v-*myc* oncogene with H-*ras* on radioresistance *Cancer Res* 50, 97–102 (1990).
5. T. J. FITZGERALD, S. HENAULT, M. SAKAKEENY, M. A. SANTUCCI, J. H. PIERCE, P. ANKLESARIA, K. KASE, I. DAS, and J. S. GREENBERGER, Expression of transfected recombinant oncogenes increases radiation resistance of clonal hematopoietic and fibroblast cell lines selectively at clinically low dose rate. *Radiat. Res.* 122, 44–52 (1990).
6. K. F. PIROLLO, R. GARNER, S. Y. YANG, L. LI, W. A. BLATTNER, and E. H. CHANG, *Raf* involvement in the simultaneous genetic transfer of the radioresistant and transforming phenotypes. *Int. J. Radiat. Biol.* 55, 783–796 (1989).
7. U. KASID, A. PFEIFER, T. BRENNAN, M. BECKETT, R. R. WEICHSELBAUM, A. DRITSCHILO, and G. E. MARK, Effect of antisense c-*raf*-1 on tumorigenicity and radiation sensitivity of a human squamous carcinoma. *Science* 243, 1354–1356 (1989).
8. D. J. TABIN, S. M. BRADLEY, C. L. BORGMANN, R. A. WEINBERG, A. G. PAPAGEORGE, E. M. SCOLNICK, R. DHU, D. R. LOWY, and E. H. CHANG, Mechanism of activation of a human oncogene. *Nature* 300, 143–149 (1982).
9. A. P. FEINBERG, M. J. DROLLER, S. B. BAYLIN, and B. D. NELKIN, Mutation affecting the 12th amino acid of the c-Ha-*ras* oncogene product occurs infrequently in human cancer. *Science* 220, 1175–1177 (1983).
10. A. THOR, P. HORAN HAND, D. WUNDERLICH, A. CARUSO, R. MURRARO, and J. SCHLOM, Monoclonal antibodies define differential *ras* gene expression in malignant and benign colonic diseases. *Nature* 311, 562–564 (1984).
11. J. L. BOS, The *ras* gene family and human carcinogenesis. *Mutat. Res.* 195, 255–271 (1988).
12. M. BARBACID, *ras* genes. *Annu. Rev. Biochem.* 56, 779–927 (1987).
13. M. J. O. WAKELMAN, S. A. DAVIES, M. D. HOUSLAY, I. MCKAY, C. J. MARSHALL, and A. HALL, Normal p21 N-*ras* couples the bombesin and other growth factor receptors to inositol phosphate production. *Nature* 323, 173–176 (1986).
14. L. F. FLEISCHMAN, S. B. CHAWALA, and L. CANTLEY, *Ras* transformed cells: Altered levels of phosphatidylinositol-4,5-biphosphate and catabolites. *Science* 231, 407–410 (1986).
15. A. WOLFMAN and I. G. MACARA, Elevated levels of diacylglycerol and decreased phorbol ester sensitivity in *ras*-transformed fibroblasts. *Nature* 325, 359–361 (1987).

16. C. J. MARSHALL, The *ras* oncogenes. *J. Cell Sci. Suppl.* 10, 157–169 (1988).

17. E. H. CHANG, M. E. FURTH, E. M. SCOLNICK, and D. R. LOWY, Tumorigenic transformation of mammalian cells induced by a normal human gene homologous to the oncogene of Harvey murine sarcoma virus. *Nature* 297, 479–483 (1982).

18. D. SAMID, L. H. CHANG, and R. M. FRIEDMAN, Biochemical correlates of phenotypic reversion in interferon-treated mouse cells transformed by a human oncogene. *Biochem. Biophys. Res. Commun.* 119, 21–28 (1984).

19. D. SAMID, L. H. CHANG, R. M. FRIEDMAN, Z. SCHAFF, and J. J. GREENE, Biological and morphological characteristics of phenotypic revertants appearing in interferon-treated mouse cells transformed by a human oncogene. *J. Exp. Pathol.* 2, 211–216 (1985).

20. D. SAMID, D. M. FLESSATE, and R. M. FRIEDMAN, Interferon-induced revertants of *ras*-transformed cells: Resistance to transformation by specific oncogenes and retransformation by 5-azacytidine. *Mol. Cell. Biol.* 7, 2196–2200 (1987).

21. J. F. JAINCHILL, S. A. AARONSON, and G. J. TODARO, Murine sarcoma and leukemia viruses: Assay using clonal lines of contact-inhibited mouse cells. *J. Virol* 4, 549–553 (1977).

22. D. RIMOLDI, D. SAMID, D. M. FLESSATE, and R. M. FRIEDMAN, Transcriptional Inhibition of Ha-*ras* in interferon-induced revertants of *ras*-transformed mouse cells. *Cancer Res.* 48, 5157–5162 (1988).

23. D. RIMOLDI, V. SRIKANTAN, V. L. WILSON, R. H. BASSIN, and D. SAMID, Increased sensitivity of nontumorigenic fibroblasts expressing *ras* or *myc* oncogenes to malignant transformation induced by 5-aza-2'-deoxycytidine. *Cancer Res.* 51, 324–330 (1991).

24. P. J. SOUTHERN and P. BERG, Transformation of mammalian cells to antibiotic resistance with a bacterial gene under control of the SV40 early region promoter. *J. Mol. Appl. Genet.* 1, 327–341 (1982).

25. H. G. GRATZNER, Monoclonal antibody to 5-bromo and 5-iododeoxyuridine: A new reagent for detection of DNA replication. *Science* 218, 474–475 (1982).

26. A. RAZA, H. D. PREISLER, G. L. MAYERS, and R. BANKERT, Rapid enumeration of S-phase cells by means of monoclonal antibodies. *N. Engl. J. Med.* 310, 991–993 (1984).

27. J. W. GRAY, J. H. CARVER, Y. S GEORGE, and M. L. MENDELSOHN, Rapid cell analysis by measurement of the radioactivity per cell in a narrow window in S-phase (RCSi). *Cell Tissue Kinet.* 10, 97–104 (1977).

28. J. K LARSEN, B MUNCH-PETERSEN, J. CHRISTIANSEN, and K. JORGENSEN, Flow cytometric discrimination of mitotic cells: Resolution of M, as well as G_1, S, and G_2 phase nuclei with mithramycin, propidium iodide, and ethidium bromide after fixation with formaldehyde. *Cytometry* 7, 54–63 (1986).

29. Task Group 21, Radiation Therapy Committee, American Association of Physicists in Medicine, Protocol for the determination of the absorbed dose from high-energy photon and electron beams. *Med. Phys.* 10, 1–30 (1983).

30. T. MANIATIS, E. F. FRITSCH, and J. SAMBROOK, *Molecular Cloning.* 1st ed. Cold Spring Harbor Laboratory, Cold Spring Harbor, NY, 1982.

31. H. LEHRACH, D. DIAMOND, J. M. WOZNEY, and H. BOEDTKER, RNA molecular weight determinations by gel electrophoresis under denaturing conditions. A critical reexamination. *Biochemistry* 16, 4743–4767 (1977).

32. N. ALBRIGHT, Computer analysis of cell survival. *Radiat. Res.* 112, 331–340 (1987).

33. W. H. KRUSKAL, A nonparametric test for the several sample problem. *Ann. Math. Statist.* 23, 525–540 (1952).

34. W. H. BEYER, *CRC Handbook of Tables for Probability and Statistics.* 1st ed. Chemical Rubber Co., Cleveland, OH, 1966.

35. J. F. HARRIS, A. F. CHAMBERS, and A. S. K. TAM, Some *ras*-transformed cells have increased radiosensitivity and decreased repair of sublethal radiation damage. *Somatic Cell Mol. Genet.* 16, 39–48 (1990).

36. P. KENG, Effect of interferon on radiosensitivity. *Cancer Res.* 48, 351–356 (1985).

37. K. PAUCKER, K. CANTELL, and W. HENLE, Effect of interferons on cell proliferation. *Virology* 17, 324–334 (1962).

38. W. K. SINCLAIR and R. A. MORTON, X-ray sensitivity during the cell generation cycle of cultured chinese hamster cells. *Radiat. Res.* 29, 450–474 (1966).

39. E. J. HALL, J. M. BROWN, and J. CAVANAUGH, Radiosensitivity and the oxygen effect measured at different phases of the mitotic cycle using synchronously dividing cells of the root meristem of *Vicia faba*. *Radiat. Res.* 35, 622–634 (1968).

40. C. C. LING and B. ENDLICH, Radioresistance induced by oncogenic transformation. *Radiat. Res.* 120, 267–279 (1989).

41. E. KATZ, Heterogeneity in transformation efficiency of NIH 3T3 cells as determined by transfection with oncogenes. *Eur. J. Cell Biol.* 42, 231–236 (1986).

42. U. N. KASID, R. R. WEICHSELBAUM, T. BRENNAN, G. E. MARK, and A. DRITSCHILO, Sensitivities of NIH/3T3 clonal cell lines to ionizing radiation: Significance for gene transfer studies. *Cancer Res.* 49, 3396–3400 (1989).

43. H. M. LACHMAN and A. I. SKOULTCHI, Expression of c-*myc* changes during differentiation of mouse erythroleukaemia cells. *Nature* 310, 592–598 (1984).

44. A. B. PARDEE, J. CAMPISIS, H. E. GRAY, M. DEAN, and G. SONENSHEIN, Cellular oncogenes, growth factors, and cellular growth control. In *Mediators in Cell Growth and Differentiation* (R. J. Ford and L. Abby, Eds.), Vol. 1, pp. 219–258. Raven Press, New York, 1985.

RADIATION RESEARCH 127, 138–145 (1991)

Characterization of the Interaction of the Radioprotector 1-Methyl-2-[2-(methylthio)-2-piperidinovinyl]quinolinium Iodide with Supercoiled DNA

CHARLES E. SWENBERG, SHERYL BIRKE,*,[1] AND NICHOLAS E. GEACINTOV*,[1]

*Radiation Biochemistry Department, Armed Forces Radiobiology Research Institute, Bethesda, Maryland 20889-5145, and *Chemistry Department and Radiation and Solid State Laboratory, New York University, New York, New York 10003*

SWENBERG, C. E., BIRKE, S., AND GEACINTOV, N. E. Characterization of the Interaction of the Radioprotector 1-Methyl-2-[2-(methylthio)-2-piperidinovinyl]quinolinium Iodide with Supercoiled DNA. *Radiat. Res.* 127, 138–145 (1991).

The interaction of the radioprotector 1-methyl-2-[2-(methylthio)-2-piperidinovinyl]quinolinium iodide (VQ) with linear and supercoiled pIBI30 DNA was studied by flow linear dichroism spectroscopy, equilibrium dialysis, circular dichroism, and UV absorption spectroscopy. The negative linear dichroism spectra of VQ–DNA complexes throughout the 220–500 nm wavelength region, a red shift in the VQ main absorption band (at 452 nm) of 1–2 nm upon binding to DNA, and a concentration-dependent unwinding of supercoiled DNA suggest that the primary mode of interaction of VQ with DNA (at least at low concentrations) is intercalative in nature. A least-squares analysis of the equilibrium dialysis binding of VQ to supercoiled DNA using the McGhee–von Hippel equation gives an association constant $K = 7300 \pm 300\ M^{-1}$, and an exclusion number n in the range of 3.3–5.3. The lower value of n is obtained when effects of polyelectrolytes are also taken into account. Because quinolinium iodide derivatives with different substituents and DNA binding affinities can be synthesized, this family of compounds could be employed to probe relationships, if any, between radioprotective efficacy and DNA binding affinity.

INTRODUCTION

Numerous chemicals have been investigated for their radioprotective ability. The most widely studied class of antiradiation compounds are the aminothiols, initially synthesized by the U.S. Army Medical Research and Development Command at Walter Reed Institute (*1*). The mechanism at the molecular level (*2, 3*) by which aminothiols confer protection is not known with certainty, although a number of possibilities have been suggested, including free radical scavenging (*4, 5*), hydrogen atom exchange (*6*), enhancement of DNA repair (*7*), and activation of cellular enzymatic processes (*8*). Studies by Zheng *et al.* (*9*) and Smoluk *et al.* (*10*) have demonstrated the importance of the interaction of molecules of the radioprotective compounds with DNA.

Recently Foye and co-workers (*11, 12*) have introduced a new class of radioprotective compounds, the bis-methylthio- and methylthioamino-derivatives of 1-methylquinolinium iodide and 1-methylpyridinium-2-dithioacetic acid. Although not investigated as extensively as the aminothiols, these compounds have been reported to provide reasonable protection to mice at drug doses much lower (below 10 mg/kg) than those required for aminothiols (150–600 mg/kg) administered intraperitoneally. In addition, several compounds in this class have been shown to exhibit significant antileukemic activity (*13*). Detailed studies of the interactions of these quinolinium derivatives with DNA, similar to those carried out with WR-1065 and WR-2721 (*9, 10*), have not been performed. However, these compounds have been shown to bind to DNA and to inhibit polymerase activity (*14*).

Because the effectiveness of radioprotective agents may depend on their physical binding to DNA (*9, 10*), we investigated the physicochemical characteristics of the interaction of the radioprotector 2-[methylthio]-2-piperidino derivative of 1-methyl-2-vinyl quinolinium iodide (VQ) with supercoiled DNA (plasmid pIBI30). Linear dichroism measurements provide evidence that the interaction of this compound with DNA is primarily intercalative in nature. This conclusion is supported by the observation that the noncovalent binding with supercoiled DNA produces a concentration-dependent unwinding of the superhelical turns. The possible importance of complex formation of radioprotective agents with DNA is discussed.

MATERIALS AND METHODS

Plasmid pIBI30 (2926 base pairs) was isolated from *Escherichia coli* by alkaline lysis methods (*15*). The 260/280 nm absorbance ratio of all super-

[1] Research at New York University supported by the Office of Health and Environmental Research, Department of Energy, Grant DE-FG02-86ER60405.

0033-7587/91 $3.00

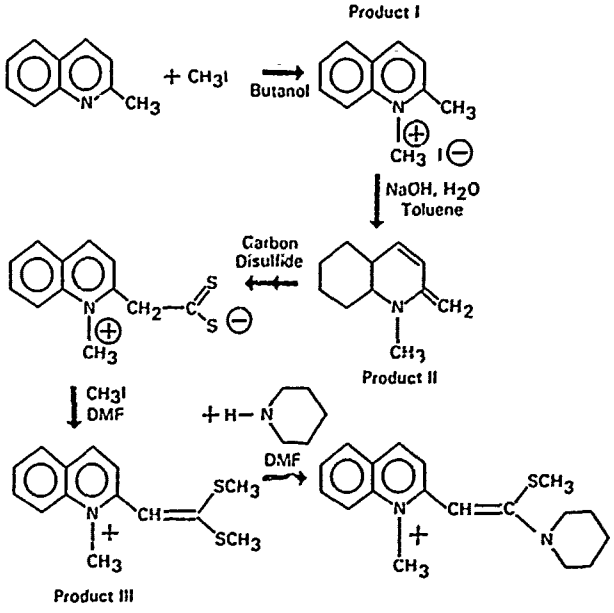

FIG 1. Synthesis of 1-methyl-2-[2-(methylthio)-2-piperidinovinyl]-quinolinium iodide.

coiled DNA samples was at least 1.85, which is indicative of a low protein contamination.

The radioprotector VQ was synthesized following closely the approach described by Foye *et al.* (*11, 13*). All reagents were obtained from Aldrich Chemical Company. Initially 50 g (0.35 mol) of quinoline and 49.7 g (0.35 mol) of iodomethase were added to 260 ml of 1-butanol and were refluxed for 4 h and then cooled in an ice bath for 30 min. The yellow product (1-methylquinolinium iodide, MW = 285.12, product I in Fig. 1) was collected by vacuum filtration and washed with 1-butanol. 1-Methylquinolinium iodide (35.0 g, or 0.123 mol) was dissolved in 100 ml of H_2O to which 500 ml of toluene was added, followed by 36 g of 50% (NaOH). The solution was stirred 1 h at room temperature, and the toluene phase was subsequently decanted into a beaker containing K_2CO_3. After 10 min, the toluene was transferred to a 1-liter round-bottom flask, 14.05 g (0.185 mol) of CS_2 was added, and the flask shaken vigorously, stoppered, and left overnight at room temperature. The green product was collected by vacuum filtration and resuspended in 100 ml of dimethylformamide (DMF) with 52.3 g (0.37 mol) of CH_3I, and stirred overnight at room temperature. The yellow-green precipitate was collected by vacuum filtration, washed with acetone, and then recrystallized from water. About 4.0 g of the bronze crystals, collected by vacuum filtration, was dissolved in 65 ml of DMF with 0.937 g (0.011 mol) of piperidine. The flask was sealed with a drying tube and stored at 35°C for 6 days. Toluene was then carefully added (approximately 425 ml) until the solution turned dark orange, and was stored at 20°C until orange crystals were observed to grow. Crystals (final product) were collected by vacuum filtration and recrystallized from 2-propanol (mp 193–195°C). The yields of 1-methylquinolinium iodide, product III, and the final product were, respectively, 35, 4.4, and 1.2% of the starting chemical, quinoline. The identities of the intermediate products, as well as that of the final product, were analyzed by proton NMR spectroscopy.

All equilibrium dialysis and linear dichroism experiments were conducted at 4°C in TE buffer (5 m*M* Tris, 1 m*M* EDTA, pH 7.9).

The principles of the linear dichroism technique have been discussed in detail by Frederieq and Houssier (*16*). Our layout of the linear dichroism experiment, which is based on a hydrodynamic orientation of the DNA in aqueous solutions in a Couette cell, is shown in Fig. 2. The Couette cell consists of two concentric quartz cylinders, a stationary outer cylinder, and a rotating inner cylinder (*17*). The inner diameter of the outer stationary cylinder is 26 mm, while the outer diameter of the rotating inner cylinder is 25 mm. The aqueous DNA solution is placed in the 0.5-mm annular space, and rotation of the inner cylinder causes a partial alignment of the DNA molecules with their long axes parallel to the flow lines in a plane perpendicular to the axis of rotation. The linear dichroism (LD) is defined by

$$LD \propto A_{\parallel} - A_{\perp}, \qquad (1)$$

where $A_{\parallel}$ and $A_{\perp}$ are the absorbances of the solutions measured with the polarization vector of the light beam oriented either parallel or perpendicular, respectively, to the direction of flow. This flow linear dichroism system requires a sample volume of approximately 1.5 ml. in this work, DNA concentrations of 7.5×10^{-5} to 1.5×10^{-4} *M* (expressed in concentrations of phosphate) were utilized since reasonable signal/noise ratios were obtained at these concentrations. Absolute linear dichroism values were obtained by calibrating the linear dichroism apparatus as described by Breton *et al.* (*18*).

The equilibrium dialysis experiments were performed by placing 2 ml of a pIBI30 DNA solution (175 μM) in dialysis bags (Spectra/Por, 6000–8000 molecular weight cut-off, Spectrum Medical Industries, Inc., Los Angeles, CA) which were suspended in 6.0 ml of solutions of different concentrations of VQ. Dialysis was carried out for 4 days at 4°C; the absorbance spectra both in and out of the dialysis bags were then determined at the same temperature using a Hewlett-Packard 8451 diode array absorption spectrophotometer. The concentration of free VQ was calculated from the absorbance at 452 nm using a molar extinction coefficient of 45,000 M^{-1} cm^{-1}.

Thermal denaturation measurements were performed using a Hewlett-Packard 8450 diode array spectrophotometer equipped with an HP89100A temperature control station. The temperature was increased 0.5°C/2.5 min, the absorbance at 260 nm was measured once a second for 30 s, and the average was then recorded. Samples (50 μM pIBI30 DNA) were mixed with a magnetic stirrer throughout the experiment. All solutions were deoxygenated by purging with either argon or nitrogen, and the cuvettes were capped tightly with a rubber septum.

The circular dichroism spectra were recorded using a Jasco DP-501N CD instrument. The signal-averaged spectra were recorded at ambient temperature (20°C) from 200 to 500 nm at 0.2-nm intervals in 1-cm pathlength cells under a constant flow of nitrogen gas. The data were transferred to a VAX/VMS computer system, baseline-corrected, and plotted using RS/Explore software. Molar ellipticity values are based on calibrations using the Jasco standard ammonium *d*-10-camphorsulfonate solutions.

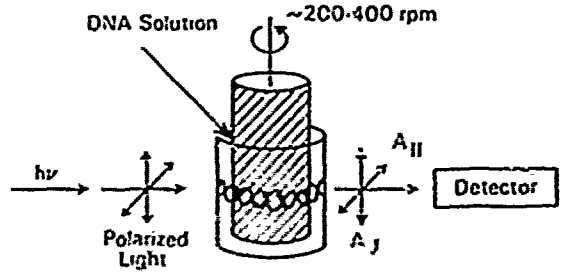

FIG. 2. Schematic of the flow linear dichroism apparatus (see text for details).

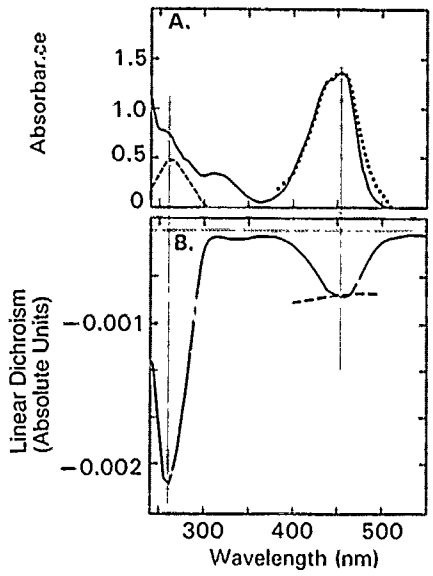

FIG. 3. (A) Absorption spectrum of a dialyzed (solid line) VQ–DNA solution (contents of a dialysis bag, DNA concentration 175 μM, bound VQ concentration 8 8 μM (r_b = 0 05), free VQ concentration 66 μM). Dashed line: absorption spectrum of the DNA solution (175 μM) in the absence of VQ. Dotted curve: absorption spectrum of VQ bound to DNA (obtained by subtracting an absorption spectrum of the solution outside of the dialysis bag from the absorption spectrum of the contents of the dialysis bag, and normalized at the maximum of the overall absorption spectrum of VQ (bound + free) to allow for easy comparison (B) Solid line. linear dichroism spectrum of the contents of the dialysis bag (only bound VQ molecules contribute to the linear dichroism spectrum). Dashed line: reduced linear dichroism spectrum (LD/A, in arbitrary units) within the 400–500 nm absorption band of VQ; the LD/A values were calculated using the absorption spectrum of bound VQ molecules (dotted curve in part A). The absorption spectra were determined using a 0.4-cm light path length.

RESULTS

Linear Dichroism

Figure 3A shows a typical absorption spectrum of the supercoiled DNA (dashed line) and of a dialyzed solution of VQ and DNA (solid line), this solution represents an aliquot withdrawn from the contents of a dialysis bag containing DNA, as well as free and bound VQ molecules, which had been equilibrated against a solution containing only free VQ molecules outside the dialysis bag. The dotted line in Fig. 3A represents the difference absorption spectrum (inside − outside the dialysis bag), and is thus due solely to VQ molecules bound to the DNA, this spectrum, normalized to the absorption spectrum of the solution inside the dialysis bag for ease of comparison, is somewhat broader on the long-wavelength side, and was used to calculate the reduced linear dichroism spectrum (see Fig. 3).

The linear dichroism spectrum of the VQ–DNA solution (Fig. 3A, solid line) is shown in Fig. 3B. Because the planes of the DNA bases tend to be tilted perpendicular to the flow lines, the linear dichroism signal within the DNA absorption band (below 300 nm) is negative in sign, as is evident in Fig. 3B. Intercalated planar molecules also display a negative linear dichroism signal within their own absorption bands if the transition moments are parallel with those of the DNA bases. Below 300 nm there is an overlap of the DNA and VQ absorption bands and linear dichroism signals. However, the broad absorption and linear dichroism band centered near 450 nm is due uniquely to DNA-bound VQ molecules since free ligand molecules do not contribute to the linear dichroism spectrum. Since the linear dichroism spectrum between 400 and 500 nm is negative in sign, the transition moment of VQ tends to be tilted perpendicular to the flow direction. While the polarization of this transition dipole moment has not been determined explicitly, it is reasonable to assume that this transition, because of its obvious π–π^* origin, is polarized within the plane of the aromatic ring system. Since the planes of the DNA bases also tend to be tilted perpendicular to the flow direction (*19*), the negative linear dichroism band in the 400–500 nm region is consistent with (but does not necessarily prove) an intercalative complex conformation. This hypothesis can be tested further by comparing the relative magnitudes of the reduced linear dichroism, LD/A (LD and A are the magnitudes of the linear dichroism and absorbance signals, respectively), evaluated within the DNA absorption band at 258 nm and within the VQ absorption band at 452 nm. The reduced linear dichroism is defined as (*17, 19*)

$$\mathrm{LD}/A = \tfrac{3}{2}\langle 3\cos^2\theta - 1\rangle F, \qquad (2)$$

where F ($0 \leq F \leq 1$) describes the degree of orientation of the DNA in the hydrodynamic flow gradient, while θ denotes the angle formed by a vector along the flow direction and the oriented molecular transition dipole moment. For homogeneous binding (when all of the bound molecules are characterized by the same absorption spectrum and the same value of θ), the reduced linear dichroism is expected to be independent of wavelength within the absorption band between 400 and 500 nm (assuming that the electronic transition moment giving rise to this absorption band is also homogeneous). The wavelength dependence of LD/A calculated from the linear dichroism signal and the absorbance of the bound VQ molecules (dotted curve in Fig. 3A) is shown in Fig. 3B (dashed line). The reduced linear dichroism does not vary by more than 10–15% within the indicated wavelength region, suggesting that there is one major and primary binding site (*14*), the small decrease in the magnitude of LD/A with increasing wavelength suggests nevertheless that minor proportions of bound VQ molecules with nonintercalative conformations may also be present.

The orientation of the VQ transition moment vector rela-

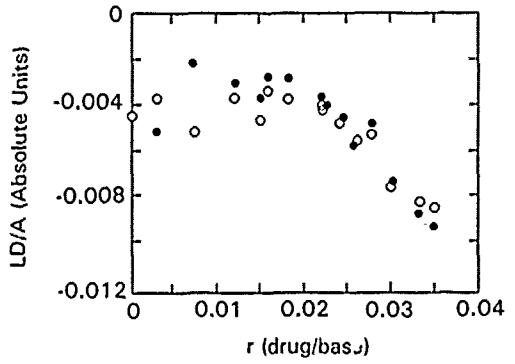

FIG. 4. Reduced linear dichroism spectra evaluated at (○) 258 nm within the DNA absorption region, $(LD/A)_{258}$, and at (●) 452 nm within the VQ absorption region, $(LD/A)_{452}$, as a function of the binding ratio, r_b = (bound VQ)/(DNA nucleotide). The concentration of DNA-bound VQ molecules was determined by equilibrium dialysis, and the DNA concentration in these experiments was 250 μM.

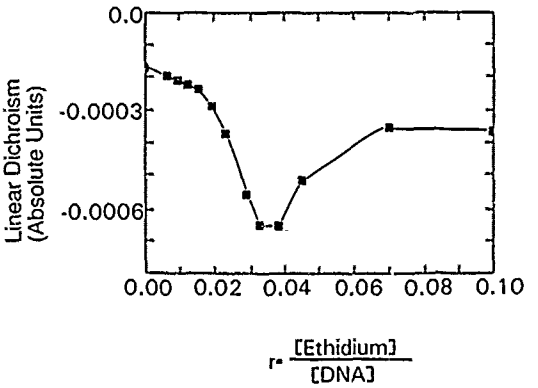

FIG. 5. Changes in superhelicity of pIBI30 supercoiled DNA as a function of added ethidium bromide measured by the flow linear dichroism method. The linear dichroism signals were measured at 258 nm. The DNA concentration was 0.19 mM. In this range of molar [ethidium]/[DNA nucleotide] ratios, at least 95% of the added ethidium molecules are bound to the DNA (*20*).

tive to the average orientation of the in-plane transition moments of the DNA bases can be estimated by evaluating the ratio R which is defined as

$$R = \frac{(LD/A)_{452}}{(LD/A)_{258}} = \frac{\langle 3\cos^2\theta_{VQ} - 1\rangle_{452}}{\langle 3\cos^2\theta_{DNA} - 1\rangle_{258}} \approx 1.0, \quad (3)$$

where $(LD/A)_{452}$ and $(LD/A)_{258}$ are the reduced linear dichroism values determined at 452 and 258 nm, respectively. When the R-ratio is equal to unity, the in-plane polarized transition dipole moments of the nucleic acid bases and those of bound drug molecules are tilted at the same average angle with respect to the flow direction, as expected for an intercalative complex. The R-ratio is, within experimental error, constant and equal to unity for the entire range of r_b values (bound VQ molecules/nucleotide) utilized in these experiments (Fig. 4), thus further supporting the intercalation model of binding of VQ to DNA.

The results depicted in Fig. 4 also demonstrate that the magnitude of the linear dichroism signal increases with increasing level of binding when $r_b \geq 0.02$. As was demonstrated earlier (*20*), this behavior is exhibited by the classical intercalator ethidium bromide (EB), which is known to cause unwinding upon binding to supercoiled DNA by an intercalation mechanism (*21*). As the EB binding ratio is increased from $r_b = 0$ to $r_b = 0.04$, the unwinding causes the hydrodynamic volume of the supercoiled molecules to increase, thus leading to a larger, negative linear dichroism signal (*20*).

In the case of pIBI30, the EB-induced minimum in the linear dichroism signal is achieved at $r_b = 0.035 \pm 0.003$, corresponding to complete relaxation of super coils and the formation of covalently closed, relaxed circular DNA. When $r_b > 0.035$, a rewinding of the DNA is observed, which causes the linear dichroism signal to diminish when the EB concentration is increased further (*20*). A typical ethidium–pIBI30 supercoiled DNA titration curve measured by the flow linear dichroism method (*20*) is shown in Fig. 5. In the case of VQ, the rewinding effect was not observed within the ranges of VQ concentrations utilized in our experiments (Fig. 4). At the highest VQ binding ratio used, $r_b = 0.035$, the magnitude of the linear dichroism signal is only ≈ 2.5 larger than in the absence of drug when $r = 0$. The difference between the magnitudes of the LD/A data points at $r = 0$ and in the region of $r = 0.01$–0.02 is deemed too small to be significant. The scatter in the 452-nm data points at low values of r are consistent with the errors in the measured absorbances at low values of VQ. The use of VQ concentrations corresponding to $r \geq 0.04$–0.05 is difficult because of the high absorbances of the solutions which interfere with the accurate recording of the linear dichroism signals. However, in EB unwinding experiments, the signals of completely relaxed pIBI30 are 3.5–4.0 greater than those of the supercoiled form (Fig. 5, for exam-

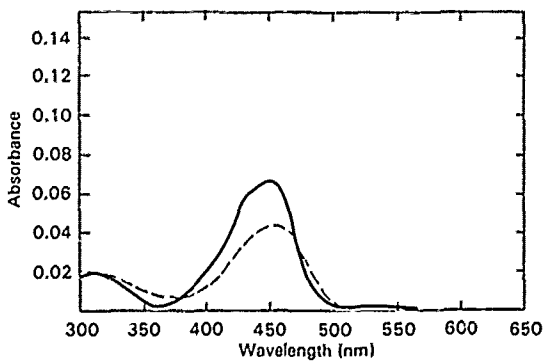

FIG. 6. Absorption spectra of free VQ (2 μM) in TE buffer solution (solid line), and in the presence of an excess of DNA (1.2 mM, dashed line).

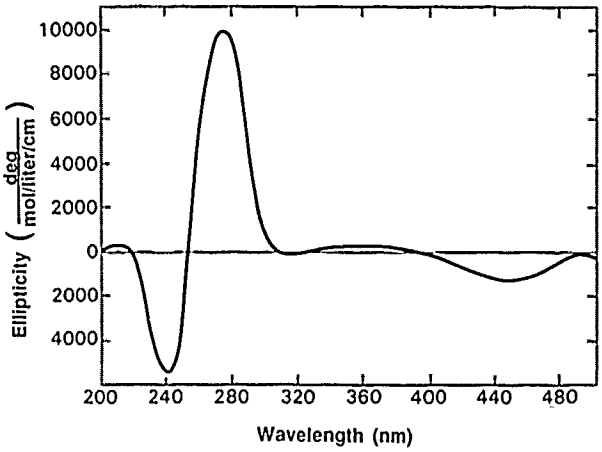

FIG. 7. Circular dichroism spectrum (molecular ellipticity vs wavelength) of supercoiled DNA (200 μM) with 50 μM of VQ in TE buffer minus the circular dichroism spectrum of 50 μM of VQ in TE buffer. Molecular ellipticity is the ellipticity (in degrees) divided by the molar concentration (mol/liter) per unit path length (cm).

ple). We therefore conclude that VQ is not as effective as EB in unwinding supercoiled DNA.

Absorption and Circular Dichroism

Typical absorption spectra of a 2 μM VQ buffer solution and the same solution containing an excess of DNA (1.2 mM) are shown in Fig. 6. Under these conditions, there is a decrease observed in the molar extinction coefficient of VQ of 35% (hypochromic effect) and a small red shift in the absorption maximum (at most 1–2 nm). These results are consistent with intercalative binding (*19*) and suggest that an appreciable fraction of the VQ molecules is bound to the DNA (see Fig. 6).

A circular dichroism spectrum of VQ–DNA complexes is shown in Fig. 7. In the absence of DNA, the VQ solutions did not exhibit any measurable circular dichroism signal. However, in DNA solution ([VQ] = 50 μM, [DNA] = 200 μM), a prominent negative circular dichroism signal cent red at 452 nm is observed. It is apparent that the circular dichroism spectrum is induced in nature, since it has a shape resembling the inverted absorption spectrum. It has been shown (*22*) that both the sign and the magnitude of the induced circular dichroism for DNA intercalators depend on (1) the lateral displacement of the intercalator relative to the surrounding base pairs at the intercalation site, (2) the orientation of the intercalator transition moment in the plane parallel to those of the base pairs, and (3) the particular base pairs surrounding the molecule. Thus the circular dichroism spectrum shown in Fig. 7 is consistent with an intercalative interaction mode since an isolated long-wavelength electric-dipole transition of a DNA intercalator should have the same shape and position as that of the corresponding absorption band. The negative sign of the circular dichroism spectrum could be indicative of the orientation of the transition moment (*22, 23*) relative to the in-plane transition moments of the nucleotide base pairs.

Equilibrium Dialysis

The calculations of the fractions of VQ molecules bound to DNA, from which the r_b ratios shown in Fig. 4 were deduced, were obtained from equilibrium dialysis measurements at 4°C. In these experiments, the concentrations of free VQ molecules (C_f) were deduced from the absorption spectra of the dialysates, while the concentration of bound VQ molecules was calculated from the total concentration and the values of C_f. These binding data were analyzed in terms of the McGhee–von Hippel equation (*24*), which takes into account the number (n) of binding sites (base pairs) which are not available to a second ligand molecule after the binding of the first ligand. A typical plot (r/C_f versus C_f, where r is now defined as the number of ligand molecules bound per base pair) is shown in Fig. 8; the equilibrium dialysis data from which this plot was calculated are presented in Table I. The dashed line in Fig. 8 is a theoretical fit of the McGhee–von Hippel equation (*24*):

$$\frac{r}{C_f} = K(1 - nr)\left(\frac{1 - nr}{1 - (n-1)r}\right)^{n-1}, \qquad (4)$$

where K is the association constant. This multiple-site exclusion model provides a reasonable fit to the data with K

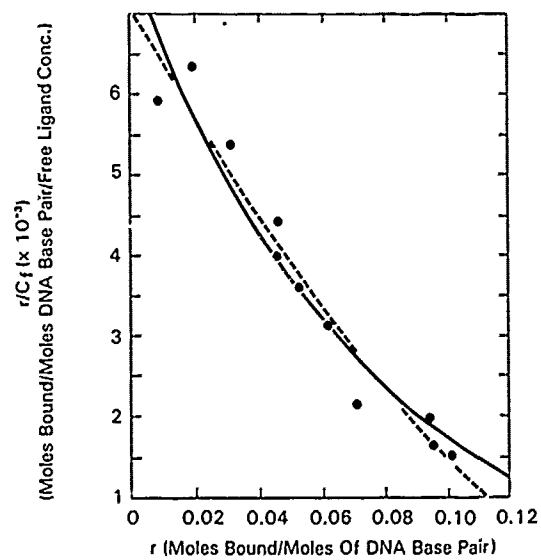

FIG. 8. Scatchard plot denoting the number of moles free VQ ligand (C_f) versus r (moles VQ bound per base pair). The solid circles denote the experimental points. The solid line is a least-squares fit of Eq. (5) to the experimental data points with $\xi(0) = 4.2$, $K = 7600\ M^{-1}$, and $n = 3.1$. The dashed line represents a least-squares fit of Eq. (4) to the data points with $K = 7100\ M^{-1}$ and $n = 5.3$.

TABLE I

Concentrations of Free (C_f) and Bound (C_b) VQ Molecules in a Typical Dialysis Experiment Performed at 4°C, at a Fixed DNA Concentration (175 μM Nucleotide Concentration, or 87.5 μM Concentration of Base Pairs); These Data Were Used to Construct the Scatchard Plot in Fig. 8

C_f (μM)	C_b (μM)
1.41	0.730
3.00	1.67
5.78	2.73
10.3	4.00
11.4	4.00
14.6	4.60
19.7	5.40
32.7	6.20
46.7	8.20
57.3	8.30
65.6	8.80

= 7100 M^{-1} expressed in moles of base pairs and n = 5.3 (see dashed curve in Fig. 8).

Since the DNA molecule is negatively charged, we expect that there is, in addition to the effects of multiple-site exclusion, a polyelectrolytic contribution to the drug–DNA interaction which gives rise to anticooperative binding effects. For univalently charged drug–DNA intercalative binding in the presence of an excess of univalently charged salt ions, Friedman and Manning (*25*) and Friedman *et al.* (*26*) have shown that

$$\frac{r}{C_f} = K\left(\frac{2+r}{2-r}\right)^{-\{2+2/\xi(0)\}} \times 10^{\{1.302r/\xi(0)(2-r)+2.604r/(1+r)\}} \times (1-nr)\left(\frac{1-nr}{1-(n-1)r}\right)^{n-1}, \quad (5)$$

where $\xi(0)$ is the charge density parameter of the polyion in the absence of bound ligands.

$$\xi(0) = q^2/\epsilon k_B T b,$$

where q is the charge of an electron, ϵ is the bulk dielectric constant of the liquid, k_B is Boltzmann's constant, and b is the charge spacing on the polyion chain. The solid curve in Fig. 8 is a least-squares fit of Eq. (5) to the data treating the exclusion parameter n and the association constant K = 7600 M^{-1} as variables with $\xi(0)$ = 4.2. It is evident that the polyelectrolytic contribution to binding is quite small, although its inclusion does lower the inferred magnitude of n to a more realistic value representative of intercalative binding. This value of n (~3) suggests that a bound ligand molecule excludes the binding of other ligands from the two nearest neighbor base pairs.

Melting Curves

Thermal denaturation curves (not shown) for VQ (50 μM) interacting with supercoiled pIBI30 DNA (50 μM) in TE buffer give an increase in T_m of 2.5°C. This is quite small as compared to the stabilization provided by external (primarily) electrostatic binding molecules such as putrescine. For example, Morgan *et al.* (*27*) reported an increase in T_m (ΔT_m) of 28.5°C for calf thymus DNA (25 μM) in the presence of 50 μM putrescine in 1.5 mM NaCl solutions. A ΔT_m of 2.5°C for VQ–DNA is similar in magnitude to the value of 7.5°C for 1-methyl-2-bis[(2-methylthio)-vinyl]quinolinium iodide (product III in Fig. 7) reported by Foye *et al.* (*14*), and is consistent with the corresponding association constant. We conclude that VQ does not appear to enhance the stability of DNA significantly.

DISCUSSION

Our spectroscopic data provide evidence that VQ interacts with DNA primarily by intercalation with an association constant $K \approx 7300 \pm 300\ M^{-1}$, which is much smaller than that of ethidium bromide–DNA (K(EB) $\approx 10^5$–10^6 M^{-1}, depending on experimental conditions (*28, 29*)). The value of K for VQ is similar to those reported by Foye *et al.* (*30*) for several *N*-heterocyclic substituted aminoethyl disulfides at similar ionic strengths, and a factor of 10 less than the binding of 1-methyl-2-bis[2-(methylthio)-vinyl]quinolinium iodide (product III, Fig. 1); furthermore, it is interesting to note that the DNA binding constant decreases by a factor of 70 when a methyl group is present at the 6-position of the quinolinium ring of product III (*14*). Thus a small substituent on the aromatic quinolinium ring system can exert a profound influence on the noncovalent DNA association constant.

It is not known whether binding of radioprotective agents to DNA is or is not important in determining their efficiencies as radioprotectors. Foye *et al.* (*14*) studied the binding to calf thymus DNA of a series of aminoalkyl thiosulfates and heterocyclic aminoethyl disulfides and concluded that DNA binding for this class of compounds was not a requirement for radioprotective efficiency. However, Ward (*2*) came to the opposite conclusion for aminothiols by noting that their radioprotective effects are observed at relatively low aminothiol concentrations (2–5 mM); based on known aminothiol-hydroxyl radical scavenging rate constants, comparable radioprotective effects would be expected at much higher concentrations (50 mM) of radioprotectors. Ward (*2*) speculated that aminothiols, especially those with positive charges (*9*) which tend to associate with the negatively charged DNA, are able to concentrate near the DNA molecules, thus providing high local concentrations of these radioprotective agents for effective scavenging of radicals produced by ionizing radiation. Thus radicals formed

on the DNA can be quenched by hydrogen atom transfer, and hydroxyl radicals produced in the aqueous environment can be prevented from reaching the DNA molecules by these large local concentrations of radioprotective agents. This hypothesis is supported by the observation that negatively charged aminothiols have low radioprotective efficacies (*9, 10*).

Significant radioprotection in the case of whole-body γ irradiation of mice (10 Gy) was observed at doses of VQ of ~2.5 mg/kg, i.e., at dose levels 50–100 times smaller than those required for typical aminothiol derivatives (*11*). It was therefore concluded that these two different classes of compounds exert their radioprotective effects by different mechanisms.

The apparent DNA binding affinities of VQ and the aminothiol WR-1065 appear to be similar (*10*). Because of the relatively low value of K (=7300 ± 300 M^{-1}, expressed in concentrations of base pairs), a substantial fraction of VQ molecules are not associated with DNA under the conditions of the dialysis experiments (DNA concentration 175 μM, total VQ concentration in the range of 10–400 μM). If, *in vivo*, there is an analogous distribution of VQ molecules between DNA and other macromolecular binding sites and in the free state, VQ molecules can scavenge radicals when they either are associated directly with DNA molecules or are located relatively far from DNA molecules. The rate of scavenging of hydroxyl radicals by VQ is not known, although it certainly cannot be larger than the diffusion-limited value of 1.3×10^{10} mol^{-1} dm^3 s^{-1} for glutathione reported by Quintiliani *et al.* (*31*). AT physiological pH values, VQ is positively charged. Its concentration within the immediate neighborhood of DNA is thus expected to be significantly higher than in the bulk phase; in contrast, the oxidized form of glutathione is negatively charged and its concentration is expected to be low near the DNA molecule (*32*). For these reasons, radical scavenging by VQ is expected to be significantly lower than scavenging by glutathione in the bulk phase, however, within the 2-to-3-nm water layer surrounding the DNA, radical scavenging by VQ rather than by glutathione is likely to be more important. Because only those hydroxyl radicals which are formed within the immediate vicinity (2–3 nm) of DNA are of importance for creating DNA damage (*10*), even small concentrations of VQ (relative to glutathione) could be significant as hydroxyl radical scavengers in cellular radioprotection. Furthermore, 1-methyl-2-[2-(methylthio)-2-piperidinovinyl]quinolinium iodide is a molecule that is capable of undergoing a variety of reactions in addition to free radical addition. The methylthio-piperidinovinyl moiety is essentially a ketene thioaminal and is capable of undergoing addition reactions with both nucleophiles and electrophiles, as well as cycloaddition reactions in a manner analogous to those of ketene aminal and thioketal. Hydrolysis of this moiety to the ketene form could then readily undergo reactions with water, amino, hydroxyl, and other chemical groups. Nucleophilic addition is also possible on the quinolinium ring, with the 2- and 4-positions being the most reactive. Reactions at these sites, however, would not be as likely under physiological conditions.

Finally, the possibility of designing VQ molecules with different substituents, and thus different DNA-binding affinities (*14*), suggests that this series of molecules could be used to test the importance of DNA binding in radioprotection, and thus provide some clues to the molecular mechanisms involved.

ACKNOWLEDGMENTS

The authors thank Dr. Eric Holwitt for the synthesis of 1-methyl-2-[2-(methylthio)-2-piperidinovinyl]quinolinium iodide, and Ms. Colleen Loss for preparation of the plasmid DNA.

RECEIVED: October 29, 1990; ACCEPTED: March 12, 1991.

REFERENCES

1. D. L. KLAYMAN and E. S. COPELAND, Radioprotective agents. In *Kirk-Othmer. Encyclopedia of Chemical Technology* (M. Grayson, Ed.), 3rd ed., Vol. 19, pp. 801–832. Wiley, New York, 1982.
2. J. F. WARD, Chemical aspects of DNA radioprotection. In *Radioprotectors and Anticarcinogens* (O. F. Nygaard and M. G. Simic, Eds.), pp. 73–85. Academic Press, New York, 1983.
3. J. F. WEISS AND M. G. SIMIC, *Pharmacology and Therapeutics*. Vol. 39. *Perspectives in Radioprotection*. Pergamon, New York, 1988.
4. T. L. PHILLIPS. Rationale for initial clinical trials and future development of radioprotectant, *Cancer Clin. Trials* 3, 165–173 (1980).
5. See, for example, W. O. FOYE, In *Burger's Medicinal Chemistry* (M. E. Wolff, Ed.), 4th ed., pp. 14–54. Wiley, New York, 1981.
6. R. E. DURAND, Radioprotection by WR-2721 *in vitro* at low oxygen tensions. Implications for its mechanism of action. *Br. J. Cancer* 47, 387–392 (1983).
7. E. RIKLIS, R. KOL, M. GREEN, A. PRAGER, R. MARKO, and M. MINTSBERG, Increased radioprotection attained by DNA repair enhancement. *Pharmacol. Theor.* 39, 311–322 (1988).
8. L. A. HOLWITT, L. KODA, and C. L. SWENBERG, Enhancement of topoisomerase I-mediated unwinding of supercoiled DNA by the radioprotector WR-33278. *Radiat. Res.* 124, 107–109 (1990).
9. S. ZHENG, G. L. NEWTON, G. GONICK, R. C. FAHEY, and J. F. WARD, Radioprotection of DNA by thiols: Relationship between the net charge on a thiol and its ability to protect DNA. *Radiat. Res.* 114, 11–27 (1988).
10. G. D. SMOLUK, R. C. FAHEY, and J. F. WARD, Equilibrium dialysis studies of the binding of radioprotector compounds to DNA. *Radiat. Res.* 107, 194–204 (1986).
11. W. O. FOYE, R. W. JONES, P. K. GHOSHAL, and B. ALMASSIAN, Anti-radiation compounds. 20:1-Methylquinolinium (and pyridinium)-2-dithioacetic acid derivatives. *J. Med. Chem.* 30, 57–62 (1987).
12. W. O. FOYE and J. M. KAUFFMAN, Antileukemic activity of 2-bis-(2-methyl-thio)-vinyl-1-methylquinolinium iodides. *J. Pharm. Sci.* 69, 477–480 (1980).
13. W. O. FOYE, Y. H. KIM, and J. M. KAUFFMAN, Synthesis and anti-

leukemic activity of 2-[2-(methylthio)-2-aminovinyl]-1-methylquinolinium iodides. *J Pharm Sci* 72, 1356–1358 (1983).

14. W. O. FOYE, O. VAJRAGUPTA, and S. K. SENGUPTA, DNA-binding specificity and RNA polymerase inhibitory activity of bis(aminoalkyl)anthraquinones and bis(methylthio)vinylquinolinium iodides. *J Pharm. Sci* 71, 253–257 (1982).
15. F. M. AUSUBEL, R. BRENT, R. E. KINGSTON, D. D. MOORE, J. G. SEIDMAN, J. A. SMITH, and K. STRAHL (EDS.), *Current Protocols in Molecular Biology*, pp. 1.71–1.74. Wiley–Interscience, New York, 1989.
16. E. FREDERICQ and C. HOUSSIER, *Electric Dichroism and Electric Birefringence*. Oxford Univ. Press, Oxford, 1973.
17. N. E. GEACINTOV, V. IBANEZ, M. ROUGÉE, and R. V. BENSASSON, Orientation and linear dichroism characteristics of porphyrin–DNA complexes. *Biochemistry* 26, 3087–3092 (1987).
18. J. BRETON, M. MICHEL-VILLAZ, and G. PAILLOTIN, Orientation of pigments and structural proteins in the photosynthetic membrane of spinach chloroplasts: A linear dichroism study. *Biochim. Biophys. Acta* 314, 42–56 (1973).
19. B. NORDÉN and F. TJERNÉLD, High sensitivity linear dichroism as a tool for equilibrium analysis in biochemistry stability constant of DNA–ethidium bromide complex. *Biophys. Chem.* 4, 191–198 (1976).
20. C. E. SWENBERG, S. E. CARBERRY, and N. E. GEACINTOV, Linear dichroism characteristics of ethidium- and proflavine-supercoiled DNA complexes. *Biopolymers* 29, 1735–1744 (1990).
21. M. WARING, Variation of the supercoils in closed circular DNA by binding of antibiotics and drugs. Evidence for molecular models involving intercalation. *J. Mol. Biol.* 54, 247–279 (1970).
22. R. LYNG, I. HARD, and B. NORDÉN, Induced CD of DNA intercalators. Electric dipole allowed transitions. *Biopolymers* 26, 1327–1345 (1987).
23. M. KUBISTA, B. AKERMAN, and B. NORDÉN, Induced circular dichroism in non-intercalative DNA-drug complexes. Selection rules for structural applications. *J. Phys. Chem.* 92, 2352–2356 (1988).
24. J. D. MCGHEE and P. H. VON HIPPEL, Theoretical aspects of DNA–protein interactions. Cooperative and non-cooperative binding of large ligands to a one-dimensional homogeneous lattice. *J. Mol. Biol.* 86, 469–489 (1974).
25. R. A. G. FRIEDMAN and G. S. MANNING, Equilibria with application to the intercalation of drugs into DNA. *Biopolymers* 23, 2671–2714 (1984).
26. R. A. G. FRIEDMAN, G. S. MANNING, and M. A. SHAHIN, The polyelectrolyte correction to the site exclusion numbers in drug–DNA binding. In *Chemistry and Physics of DNA–Ligand Interactions* (N. R. Kallenbach, Ed.), pp. 37–64. Academic Press, New York, 1988.
27. J. E. MORGAN, J. W. BLANKENSHIP, and H. R. MATTHEWS, Association constants for double-stranded and single-stranded DNA with spermine, spermidine, putrescine, diaminopropane, N^1- and N^8-acetylspermidine and magnesium. Determination from analysis of the broadening of thermal denaturation curves. *Arch. Biochem. Biophys.* 246, 225–232 (1986).
28. J. B. LEPECQ and C. PAOLETTI, A fluorescent complex between ethidium bromide and nucleic acids. Physical-chemical characterization. *J. Mol. Biol.* 27, 87–106 (1967).
29. C. HOUSSIER, B. HARDY, and E. FREDERICQ, Interaction of ethidium bromide with DNA. Optical and electrooptical study. *Biopolymers* 13, 1141–1160 (1974).
30. W. O. FOYE, M. M. KARKARIA, and W. H. PARSONS, Antiradiation compounds XVII. Binding ability of radiation-protective *N*-heterocyclic aminoethyl disulfides and thiosulfates to DNA. *J. Pharm. Sci.* 69, 84–86 (1980).
31. M. QUINTILIANI, R. BADIELLO, M. TAMBA, A. ESFANDI, and G. GORIN, Pulse radiolysis of glutathione. *Int. J. Radiat. Biol.* 32, 195–204 (1977).
32. G. D. SMOLUK, R. C. FAHEY, and J. F. WARD, Interaction of glutathione and other low-molecular weight thiols with DNA. Evidence for counterion condensation and coion depletion near DNA. *Radiat. Res.* 114, 3–10 (1988).

INFECTION AND IMMUNITY, July 1991, p. 2494–2498
0019-9567/91/072494-05$02.00/0

Vol. 59, No. 7

NOTES

Roles of Interleukin-1 and Tumor Necrosis Factor in Lipopolysaccharide-Induced Hypoglycemia

STEFANIE N. VOGEL,[1]* BETH E. HENRICSON,[1] AND RUTH NETA[2]

Department of Microbiology, Uniformed Services University of the Health Sciences, 4301 Jones Bridge Road,[1] and Experimental Hematology, Armed Forces Radiobiology Research Institute,[2] Bethesda, Maryland 20814

Received 11 January 1991/Accepted 15 April 1991

In this study, hypoglycemia induced by injection of lipopolysaccharide (LPS) or the recombinant cytokine interleukin-1α or tumor necrosis factor alpha (administered alone or in combination) was compared. LPS-induced hypoglycemia was reversed significantly by recombinant interleukin-1 receptor antagonist.

Among the varied responses elicited by administration of lipopolysaccharide (LPS) in vivo is a modulation of glucose metabolism, which in mice results in dose-dependent hypoglycemia (reviewed in references 18, 21, 22, and 30). LPS is also known to induce cytokines, among which are interleukin-1 (IL-1) and tumor necrosis factor (TNF), and both of these have been demonstrated to induce hypoglycemia when administered to mice in vivo (3, 4, 7, 8, 15, 21, 22, 25). Thus, it has been hypothesized that IL-1 and TNF act as probable intermediates in LPS-induced hypoglycemia. However, we recently demonstrated that administration of a rabbit polyclonal immunoglobulin prepared against recombinant murine TNF to mice failed to block LPS-induced hypoglycemia, under conditions in which a highly significant inhibition of serum colony-stimulating factor (CSF) activity was observed (27). In the present study, we attempted to determine the role of IL-1 in mediating LPS-induced hypoglycemia. Our results demonstrate that a recombinant IL-1 receptor antagonist (rIL-1ra) reversed significantly the hypoglycemia induced by LPS, even when administered 3 days prior to LPS challenge, suggesting that IL-1 is an intermediate in this process.

(Portions of this work were carried out by B. E. Henricson in partial fulfillment of the requirements for the Ph.D. degree from the Uniformed Services University of the Health Sciences, Bethesda, Md.)

Female mice, 5 to 6 weeks of age, were used for all experiments. The following strains were used during the course of this study: C3H/HeN (National Cancer Institute, Frederick, Md.), and C57BL/6J, C3H/OuJ, and C3H/HeJ (Jackson Laboratories, Bar Harbor, Maine). The experiments reported herein were conducted according to the principles set forth in *Guide for the Care and Use of Laboratory Animals* (16a). Mice were injected intraperitoneally with 0.5 ml of pyrogen-free saline (Abbott Laboratories, North Chicago, Ill.), 25 μg of *Escherichia coli* K235 LPS (prepared by the phenol-water extraction method of McIntire et al. [17]), or the indicated concentrations of recombinant murine IL-1α (rIL-1α; kindly provided by Peter Lomedico, Hoffmann-LaRoche, Inc., Nutley, N.J.) or recombinant human TNF-α (rTNF-α; kindly provided by Abla Creasey, Cetus Corporation, Emeryville, Calif.). rIL-1ra was the generous gift of Robert Thompson (Synergen, Inc., Boulder, Colo.). All dilutions of LPS, cytokines, or rIL-1ra were prepared in pyrogen-free saline. Levels of blood glucose in serum samples (pooled from two to six mice per treatment per experiment) were measured by using a glucose oxidase reagent kit (Sigma Chemical Co., St. Louis, Mo.), modified exactly as described elsewhere (13). A glucose standard curve was included in each assay. All data were analyzed by two-tailed Student's *t* tests.

The capacities of LPS (25 μg), rIL-1α (500 ng), and rTNF-α (7.5 μg) to induce hypoglycemia were first compared. For this initial series of experiments, the doses of LPS, rIL-1α, and rTNF-α chosen were based on previous experience in which these three reagents were compared for their ability to induce comparable CSF activity (26). The data in Fig. 1 confirm and extend previous work using these three inducers of hypoglycemia: injection of LPS leads to a statistically significant depression of blood glucose levels by 4 h after injection. In contrast, both rIL-1α and rTNF-α induced a significant degree of hypoglycemia by 2 h after administration, although the hypoglycemic response to rIL-1α was significantly greater than that induced by rTNF-α at 2 h ($P = 0.007$).

These findings were further extended by analyzing the effects of the recombinant cytokines administered at various doses, alone or in combination, on blood glucose levels obtained 6 h after injection (Table 1). Both rIL-1α and rTNF-α induced dose-dependent decreases in blood glucose; however, when administered in combination, a more profound state of hypoglycemia was observed, resulting in a maximum decrease in blood glucose of ~50%. Certain dose combinations (i.e., IL-1 at 100 ng plus TNF at 5 μg, IL-1 at 500 ng plus TNF at 5 μg, and IL-1 at 100 ng plus TNF at 7.5 μg) were synergistic and resulted in hypoglycemia which is significantly greater than one would predict from the sum of the decreases observed following injection of either cytokine individually ($P < 0.001$). This pattern of induction of hypoglycemia by rIL-1α and/or rTNF-α was also observed in LPS-hyporesponsive C3H/HeJ mice under conditions in which 25 μg of LPS failed to induce a significant decrease in blood glucose levels (data not shown).

Given the fact that LPS has been demonstrated to induce both IL-1 and TNF in vivo (reviewed in references 19 and

* Corresponding author.

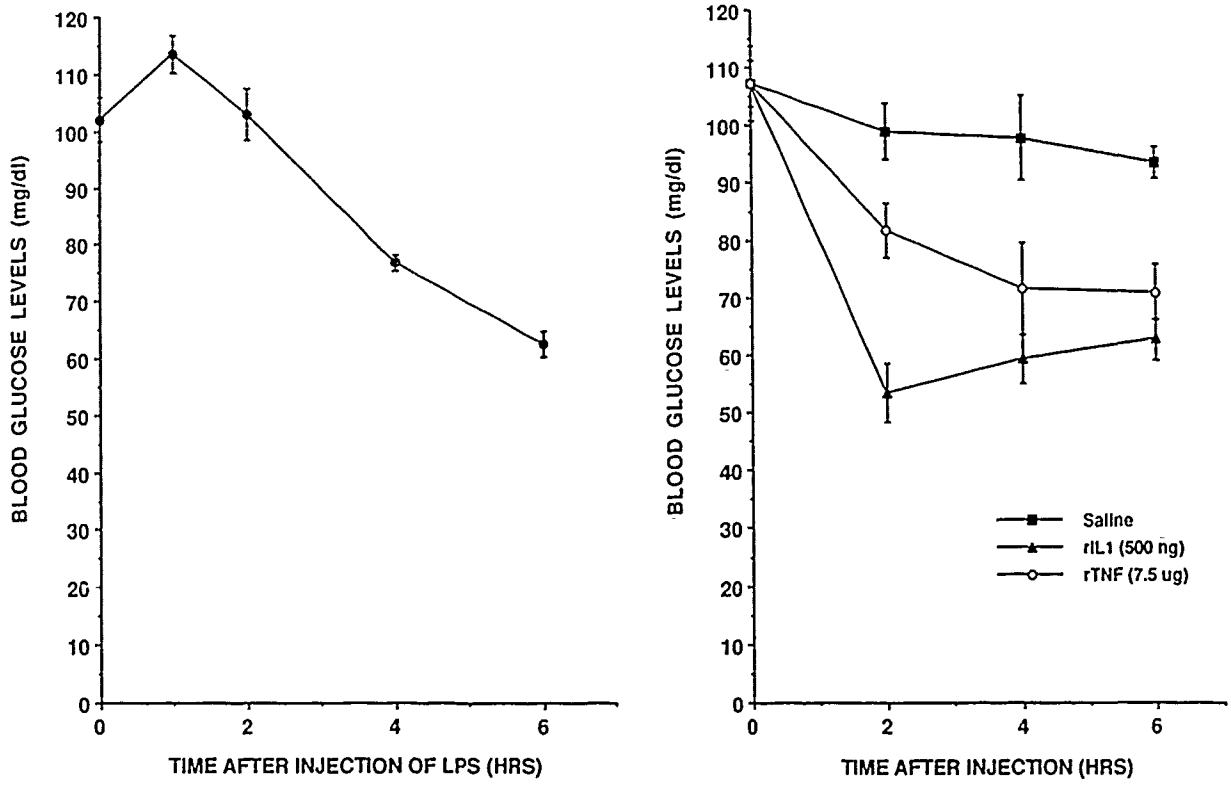

FIG. 1. Effect of administration of LPS, rIL-1α, and rTNF-α on blood glucose levels in mice. Groups of mice (C57BL/6J, C3H/HeN, and C3H/OuJ, two to five mice per treatment per experiment) were injected with 25 μg of LPS (left panel) or saline, rIL-1α (500 ng), or rTNF-α (7.5 μg) (right panel). Serum samples were collected and pooled at the indicated times after injection, and blood glucose was measured as described in the text. The results represent the arithmetic means ± standard errors of the means of 4 to 12 separate experiments for each data point. For LPS, levels of blood glucose were significantly different ($P < 0.05$) from saline controls at 4 and 6 h after injection. Levels of blood glucose were significantly different from saline controls at 2, 4, and 6 h after injection of either rIL-1α or rTNF-α.

28) and since both of these cytokines (either alone or in combination) induce hypoglycemia faster than LPS (Fig. 1), it has been hypothesized that both of these cytokines mediate the hypoglycemia induced by LPS. However, unless a specific LPS-mediated effect is blocked with a cytokine-specific antagonist, it cannot be presumed that the cytokine in question is indeed an intermediate in the response being studied. For example, we recently observed that administration of a monospecific anti-murine rTNF-α antibody to mice failed to block LPS-induced hypoglycemia, even at concentrations that were 10 times higher than that required to ablate LPS induced serum TNF (27), reduce LPS-induced CSF activity significantly (27), and neutralize in vivo all of the TNF activity produced in the spleens and sera of tumor-bearing mice injected with 25 μg of LPS (20). Thus, it was concluded that TNF-α may not serve as an intermediate in the induction of hypoglycemia by LPS, even though its exogenous administration results in a significant decrease in blood glucose levels (3, 4, 25).

Recently, a human rIL 1ra was cloned and purified (10). This protein binds to high affinity murine IL-1 receptors (6, 12) and has been shown to inhibit IL 1-induced prostaglandin E_2 and collagenase secretion from synovial cells in vitro (2). We have used this reagent to inhibit significantly LPS-induced CSF activity, as well as the induction of early endotoxin tolerance by LPS, in vivo (14). Table 2 illustrates the effects of simultaneous or prior administration of rIL-1ra on LPS-induced hypoglycemia. Separate groups of mice were injected on day 0 with either saline (treatment groups A to D) or the rIL-1ra (treatment group E). Three days later, individual groups were challenged with saline (treatment group A), LPS only (treatment group B), rIL-1ra only (treatment group C), or both LPS and rIL-1ra (treatment group D). This experimental design was chosen so that we could concurrently assess both the simultaneous and long-term efficacy of the rIL-1ra in this system (treatment group D versus group E). The dose of rIL-1ra (300 μg) used in this study was based on two in vivo observations. (i) this concentration of rIL-1ra was found to result in a highly significant reduction of LPS-induced CSF activity and early endotoxin tolerance in vivo (14), and (ii) in preliminary experiments, 300 μg of rIL-1ra was found to reverse the hypoglycemia induced by 300 ng of rIL-1α from 45 to 91% of the saline control. As shown in Table 2, 25 μg of LPS induced the expected level of hypoglycemia (~54% of the saline control, compare treatment groups A and B). Injection of rIL-1ra (300 μg) only (treatment group C) had no effect on blood glucose levels. However, when the rIL-1ra and LPS were administered simultaneously (treatment group D), blood glucose levels were significantly higher than when mice were treated with LPS only. Thus, rIL-1ra partially, but significantly, reverses the hypoglycemia induced by LPS. LPS-induced hypoglycemia was reversed to the same extent even if the rIL-1ra was administered 3 days prior to LPS (treatment group E), and the extent of the reversal with rIL-1ra is comparable to that observed in mice rendered

TABLE 1. Effects of combined treatment with rIL-1α and rTNF-α on levels of blood glucose[a]

Treatment	Blood glucose level (% of saline controls) [n]	P value
Saline	100.0 ± 2.9 [8]	
IL-1		
10 ng	87.8 ± 6.0 [5]	0.066 (NS[b])
100 ng	80.2 ± 4.9 [7]	0.003
500 ng	70.0 ± 6.5 [7]	0.001
TNF		
5 μg	88.5 ± 6.8 [7]	0.128 (NS)
7.5 μg	80.0 ± 5.9 [7]	0.007
IL-1 (10 ng) + TNF (5 μg)	75.4 ± 5.8 [4]	0.002
IL-1 (100 ng) + TNF (5 μg)	52.3 ± 6.2 [6]	<0.001
IL-1 (500 ng) + TNF (5 μg)	48.1 ± 3.7 [4]	<0.001
IL-1 (10 ng) + TNF (7.5 μg)	68.8 ± 4.3 [4]	<0.001
IL-1 (100 ng) + TNF (7.5 μg)	54.4 ± 5.4 [5]	<0.001
IL-1 (500 ng) + TNF (7.5 μg)	48.9 ± 4.1 [6]	<0.001
LPS (25 μg)	58.6 ± 5.5 [4]	<0.001

[a] Groups of mice were injected with saline, LPS, or the indicated concentrations of rIL-1α and/or rTNF-α. Mice were bled 6 h later, and the level of blood glucose was measured in pooled samples as described in Materials and Methods. Results represent the arithmetic means ± standard errors of the means of *n* separate experiments per treatment group. The level of significance (*P*), determined by comparison by Student's *t* test with the saline treatment group, is provided.

[b] NS, not significant.

endotoxin tolerant by injection of LPS 3 days prior to challenge with LPS (treatment group F). Significant reversal of LPS-induced hypoglycemia in mice which have been rendered endotoxin tolerant has been reported previously (13). Simultaneous treatment of mice with a higher concentration (600 μg) of rIL-1ra and 25 μg of LPS was no more efficacious in the reversal of hypoglycemia than that observed with 300 μg of rIL-1ra, and the inhibition observed with 150 μg of rIL-1ra was found not to be statistically significant (data not shown).

Since TNF-α has been shown to induce IL-1 at high concentrations (9), the capacity of the rIL-1ra to antagonize TNF-induced hypoglycemia was also examined. Table 3 shows that simultaneous administration of rIL-1ra (300 μg) and LPS (25 μg) results in partial reversal of hypoglycemia (as was seen in the data in Table 2). In contrast, rIL-1ra had no effect on the induction of hypoglycemia by rTNF-α (7.5 μg), whereas the hypoglycemia induced by rIL-1α (500 ng) was reversed completely by simultaneous administration of the inhibitor. These findings suggest that if TNF-α-induced IL-1 is responsible for hypoglycemia, it is either acting intracellularly or through an IL-1 receptor type (e.g., type II) which does not bind the rIL-1ra.

TABLE 2. Effect of rIL-1ra on LPS-induced hypoglycemia

Group	Treatment (day 0/day 3)[a]	Mean blood glucose level ± SEM (mg/dl) [n][b]	P value[c]
A	Saline/saline	105.0 ± 3.1 [12]	
B	Saline/LPS (25 μg)	56.7 ± 3.4 [14]	<0.001, A vs B
C	Saline/rIL-1ra (300 μg)	100.9 ± 5.9 [6]	
D	Saline/LPS + rIL-1ra	79.1 ± 4.6 [3]	0.011, B vs D
E	rIL-1ra (300 μg)/LPS	79.9 ± 3.3 [4]	0.003, B vs E
F	LPS/LPS	80.4 ± 7.1 [10]	0.003, B vs F

[a] Mice (C57BL/6J) were injected on day 0 with saline, rIL-1ra (300 μg), and/or LPS (25 μg) and then challenged 3 days later (day 3) with saline, LPS (25 μg), rIL-1ra (300 μg), or LPS plus rIL-1ra, as indicated. Mice were bled 6 h after the day-3 injection, and blood glucose levels were measured as described in Materials and Methods.

[b] Results represent arithmetic means ± standard errors of the means of blood glucose levels measured on pooled serum samples (four or five mice per treatment group per experiment) from the indicated number (*n*) of individual experiments.

[c] Differences were assessed by unpaired Student's *t* test, and *P* values for specific comparisons are reported.

TABLE 3. Effect of rIL-1ra on LPS-, rTNF-α-, and rIL-1α-induced hypoglycemia

Treatment[a]	Mean blood glucose level ± SD (mg/dl)[b]
Saline	93.9 ± 2.2
LPS (25 μg)	61.5 ± 0.7
LPS (25 μg) + rIL-1ra (300 μg)	72.4 ± 1.2 (*P* = 0.041)
rTNF-α (7.5 μg)	72.6 ± 3.1
rTNF-α (7.5 μg) + rIL-1ra (300 μg)	71.7 ± 0.4 (*P* = 0.765)
rIL-1α (500 ng)	78.7 ± 5.4
rIL-1α (500 ng) + rIL-1ra (300 μg)	96.0 ± 7.0 (*P* = 0.042)

[a] Mice (C57BL/6J; four mice per treatment group) were injected with saline, LPS (25 μg), rTNF-α (7.5 μg), or rIL-1α (500 ng), with or without rIL-1ra (300 μg), as indicated. The mice were bled 6 h later, serum samples were collected, and blood glucose levels were measured as described in Materials and Methods.

[b] Results represent arithmetic means ± standard deviations of blood glucose levels measured in two separate assays of pooled sera from a single representative experiment. Differences were assessed by a paired Student's *t* test, and *P* values for comparison of a specific treatment in the absence and presence of rIL-1ra are provided in parentheses.

Administration of LPS to experimental animals causes a profound carbohydrate "dyshomeostasis" (21, 22, 31) which is dose, time, and species dependent. Typically, one observes in sera or plasma of LPS-injected animals a pattern of initial hyperglycemia, which is followed by a profound hypoglycemia (reviewed in reference 21). The effect of LPS on specific pathways involved in carbohydrate metabolism has also been examined by many, and it appears that the basis for the observed hypoglycemia is multifaceted: inhibition of gluconeogenesis, increased glycogenolysis, increased peripheral glucose oxidation, induction of hyperinsulinemia, and increased glucose tolerance have all been suggested (11, 18, 21, 22, 30). The seminal work of Berry and his colleagues (reviewed in reference 18) provided important insights into the regulation of glucose levels following endotoxin administration. These investigators demonstrated that in response to LPS, a macrophage-derived soluble factor is produced which inhibits gluconeogenesis. This soluble factor was called glucocorticoid antagonizing factor. It is detectable in the serum within 2 h of LPS administration and acts on hepatocytes by blocking corticosteroid-induced phosphoenolpyruvate carboxykinase (PEPCK), a rate-limiting enzyme in the conversion of oxaloacetate to phosphoenolpyruvate during gluconeogenesis. This provided the first evidence that the hypoglycemia induced by LPS could be mediated indirectly by a macrophage-derived soluble factor. However, this may not be the only pathway by which LPS induces hypoglycemia. Recently, Silverstein et al. (23) demonstrated that hydrazine sulfate, a specific inhibitor of gluconeogene-

sis, counteracted the LPS induced decrease in PEPCK activity, however, the mice were still hypoglycemic. This points to the possibility that inhibition of PEPCK activity as a mechanism for disrupting gluconeogenesis may be but one of several pathways in the induction of LPS-induced hypoglycemia. For example, in an earlier study, Snyder et al. (24) reported that LPS induced an increase in the glycolytic enzyme pyruvate kinase, which could also have a net effect of counteracting gluconeogenesis.

Nonetheless, the finding that LPS-induced hypoglycemia could be reproduced in vivo by injection of an LPS-induced, macrophage-derived soluble factor led to the testing of specific LPS-induced cytokines as more purified cytokines, and subsequently, recombinant cytokines became available. Since it is well documented that both IL-1 and TNF are induced very early in response to LPS, some of the initial studies were carried out using partially purified preparations of natural IL-1. For example, in a study by Hill et al. (15), an IL 1 rich preparation was shown to induce hypoglycemia and to decrease PEPCK activity, however, the methods used to purify this material could not have ensured the elimination of other cytokines, such as TNF or IL-6. In a subsequent study, Del Rey and Besedovsky (7) showed that injection of rIL-1 into mice and rats led to hypoglycemia. In mice, this decrease in blood glucose was accompanied by enhanced levels of insulin, glucagon, and corticosterone, whereas in rats, only the last two were enhanced. In rats which were adrenalectomized, rIL-1 induced severe hypoglycemia, as well as hypoinsulinemia, and therefore it was concluded that the effect of IL 1 was independent of its capacity to induce insulin. Subsequently, these investigators showed that rIL 1 induced hypoglycemia in normal animals and exerted normalizing effects in mice rendered diabetic by alloxan treatment and in two insulin resistant, diabetic mouse strains. In these studies, they found a decrease in insulin levels in mice injected with rIL 1 and again concluded that rIL 1 did not cause hypoglycemia by inducing insulin (8). In contrast, Sacco-Gibson and Filkens (21) and Yelich et al. (31) showed that rIL-1 induced in glucose-challenged rats both increased glucose clearance and hyperinsulinemia and that both responses were a clear potentiation of the response to glucose alone. In a subsequent review (22), Sacco-Gibson and Filkens postulated that additional cofactors induced by LPS, such as TNF, might synergize with IL-1 to potentiate hyperinsulinemia. Recently, Bird et al. (5) showed that rIL-1 increased the rate of glycolysis (as measured by increased lactate production) and also caused an increase in hexose transport by increasing the net rate of glucose transporter synthesis in vitro. LPS-induced increases in plasma lactate levels in vivo have also been documented (30, 31).

Since TNF has many of the same biological properties as IL-1 (reviewed in references 16 and 19) and has been shown to induce IL-1 at high doses (10), it is not surprising that rTNF-α was also found to modulate blood glucose levels in both rats and mice (4, 25). Tracey et al. (25) demonstrated that continuous infusion of rTNF-α into rats for 20 min led to a dose dependent induction of hyperglycemia, followed by a profound hypoglycemia ~4 h postinfusion. Bauss et al. (4) subsequently showed that a single injection of rTNF-α into mice led to a decrease in plasma glucose levels in both LPS-responsive and LPS-hyporesponsive mouse strains. In addition, they observed an increase in plasma lactate levels when very high doses of rTNF-α were administered; however, this was not observed in LPS-hyporesponsive C3H/HeJ mice. Bagby et al. (3) found that infusion of culture supernatants which contained LPS-induced monokines into rats which had been made endotoxin tolerant had a much more profound effect on alterations in plasma insulin, glucagon, and catecholamines than administration of rTNF alone, suggesting the possibility of soluble-factor synergy.

The data presented in this report confirm and extend many of these previous findings. It is clear that (i) either rIL-1α or rTNF-α is capable of inducing significant hypoglycemia by 2 h after injection (equivalent to levels induced by LPS at 4 h after injection) and (ii) rIL-1α appears to be more potent, acting somewhat more quickly than rTNF-α (Fig. 1 and Table 1). When injected in combination, rIL-1α and rTNF-α synergize to induce hypoglycemia (Table 1). This finding extends an increasingly growing list of biological effects in which IL-1 and TNF have been found to synergize, death, weight loss, early endotoxin tolerance, hematopoietic changes, radioprotection, and others (29, reviewed in reference 19). The finding that rIL-1ra significantly reversed LPS-induced hypoglycemia (Table 2) directly demonstrates that IL-1, induced by LPS, is an intermediate in the induction of hypoglycemia by LPS. This reversal is incomplete, is induced to the same extent when rIL-1ra is administered simultaneously with or 72 h prior to LPS, and is not augmented by administration of higher doses of rIL-1ra, suggesting strongly that IL-1 is not the only intermediate in this complex process. This notion is further strengthened by the data in Table 3 showing that the rIL-1ra failed to reverse rTNF-α-induced hypoglycemia. Thus, it seems unlikely that hypoglycemia induced by rTNF-α is mediated by elaborated IL-1. However, previous findings that anti-rTNF-α antibody failed to reverse LPS-induced hypoglycemia or corticosterone levels, under conditions in which induction of CSF was significantly inhibited (26), suggest that TNF may not be the additional intermediate in this LPS-induced cascade and that perhaps other cofactors, such as IL-6 (1), participate in the induction of hypoglycemia. However, an alternative explanation may be that anti-rTNF-α antibodies are unable to extravasate into the liver in sufficient quantities to neutralize TNF effects on hepatocytes. The prolonged half-life in the circulation of anti-TNF antibody (several days) supports this possibility. Future experiments using TNF receptor antagonists will be required to address these possibilities.

We thank Hoffmann-LaRoche, Inc. (Nutley, N.J.), Cetus Corp. (Emeryville, Calif.), and Synergen, Inc. (Boulder, Colo.) for their generous gifts of recombinant materials. This study was supported by Naval Medical Research and Development Command protocol 63706.0095.001 (USUHS protocol G173BP), USUHS protocol RO7338, and AFRRI Work Unit 00129.

We thank Bonita M. Bundy for assistance in experiments related to Fig. 1 and Table 1.

REFERENCES

1. Akira, S., T. Hirano, T. Taga, and T. Kishmoto. 1990. Biology of multifunctional cytokines: IL 6 and related molecules (IL 1 and TNF). FASEB J. 4:2860–2867.
2. Arend, W. P., H. G. Welgus, R. C. Thompson, and S. P. Eisenberg. 1990. Biological properties of recombinant human monocyte-derived interleukin 1 receptor antagonist. J. Clin. Invest. 85:1694–1697.
3. Bagby, G. J., C. H. Lang, D. M. Hargrove, J. J. Thompson, L. A. Wilson, and J. J. Spitzer. 1988. Glucose kinetics in rats infused with endotoxin-induced monokines or tumor necrosis factor. Circ. Shock 24:111–121.
4. Bauss, F., W. Droge, and D. N. Mannel. 1987. Tumor necrosis factor mediates endotoxin effects in mice. Infect. Immun. 55:1622–1625.
5. Bird, T. A., A. Davies, S. A. Baldwin, and J. Saklatvala. 1990.

Interleukin 1 stimulates hexose transport in fibroblasts by increasing the expression of glucose transporters. J. Biol. Chem. 265:13578–13583.
6. Bomsztyk, K., J. E. Sims, T. H. Stanton, J. Slack, C. J. McMahan, M. A. Valentine, and S. K. Sower. 1989. Evidence for different interleukin 1 receptors in murine B- and T-cell lines. Proc. Natl. Acad. Sci. USA 86:8034–8038.
7. Del-Rey, A., and H. Besedovsky. 1987. Interleukin 1 affects glucose homeostasis. Am. J. Phys. 253:R794–R798.
8. Del-Rey, A., and H. Besedovsky. 1989. Anti-diabetic effects of interleukin 1. Proc. Natl. Acad. Sci. USA 86:5943–5947.
9. Dinarello, C. A., J. G. Cannon, S. W. Wolff, H. A. Bernheim, B. Beutler, A. Cerami, I. S. Figari, M. A. Palladino, and J. V. O'Connor. 1986. Tumor necrosis factor (cachectin) is an endogenous pyrogen and induces production of interleukin 1. J. Exp. Med. 163:1433–1450.
10. Eisenberg, S. P., R. J. Evans, W. P. Arend, E. Verderber, M. T. Brewer, C. H. Hannum, and R. C. Thompson. 1990. Primary structure and functional expression from complementary DNA of a human interleukin 1 receptor antagonist. Nature (London) 343:341–346.
11. Hamilton, T. A., and D. O. Adams. 1987. Molecular mechanisms of signal transduction in macrophages. Immunol. Today 8:151–158.
12. Hannum, C. H., C. J. Wilcox, W. P. Arend, F. G. Joslin, D. J. Dripps, P. L. Heimdal, L. G. Armes, A. Sommer, S. P. Eisenberg, and R. C. Thompson. 1990. Interleukin 1 receptor antagonist activity of a human interleukin 1 inhibitor. Nature (London) 343:336–340.
13. Henricson, B. E., W. R. Benjamin, and S. N. Vogel. 1990. Differential cytokine induction by doses of lipopolysaccharide and monophosphoryl lipid A that result in equivalent early endotoxin tolerance. Infect. Immun. 58:2429–2437.
14. Henricson, B. E., R. Neta, and S. N. Vogel. 1991. Interleukin-1 receptor antagonist blocks lipopolysaccharide-induced colony-stimulating factor production and early endotoxin tolerance. Infect. Immun. 59:1188–1191.
15. Hill, M. R., R. D. Stith, and R. E. McCallum. 1986. Interleukin 1: a regulatory role in glucocorticoid-regulated hepatic metabolism. J. Immunol. 137:858–862.
16. Hogan, M. M., and S. N. Vogel. 1988. Macrophage-derived cytokines. EOS J. Immunol. Immunopharm. 8:6–15.
16a. Institute of Laboratory Animal Resources, National Research Council. 1985. Guide for the care and use of laboratory animals. DHEW publication no. (NIH) 86-23. National Institutes of Health, Bethesda, Md.
17. McIntire, F. C., W. W. Sievert, G. H. Barlow, R. A. Finley, and A. Y. Lee. 1967. Chemical, physical, and biological properties of a lipopolysaccharide from *Escherichia coli* K235. Biochemistry 6:2363–2372.
18. Moore, R. N., G. M. Shackleford, and L. J. Berry. 1985. Glucocorticoid antagonizing factor, p. 123–150. *In* L. J. Berry (ed.), Handbook of endotoxin, vol. 3. Cellular biology of endotoxin. Elsevier Science Publishing, BV, Amsterdam.
19. Neta, R., T. Sayers, and J. J. Oppenheim. Relationship of tumor necrosis factor to interleukins. *In* J. Vilcek and B. B. Aggarwal (ed.), Tumor necrosis factor, in press. Marcel Dekker, Inc., New York.
20. North, R. J., and E. A. Havell. 1988. The antitumor function of tumor necrosis factor (TNF). II. Analysis of the role of endogenous TNF in endotoxin-induced hemorrhagic necrosis and regression of an established sarcoma. J. Exp. Med. 167:1086–1099.
21. Sacco-Gibson, N. A., and J. P. Filkens. 1988. Glucoregulatory effects of interleukin-1: implications to the carbohydrate dyshomeostasis of septic shock. Prog. Clin. Biol. Res. 264:355–360.
22. Sacco-Gibson, N. A., and J. P. Filkens. 1989. Macrophages, monokines, and the metabolic pathophysiology of septic shock. Prog. Clin. Biol. Res. 286:203–218.
23. Silverstein, R., C. A. Christoffersen, and D. C. Morrison. 1989. Modulation of endotoxin lethality in mice by hydrazine sulfate. Infect. Immun. 57:2072–2078.
24. Snyder, I. S., M. Deters, and J. Ingle. 1971. Effect of endotoxin on pyruvate kinase activity in mouse liver. Infect. Immun. 4:138–142.
25. Tracey, K. J., B. Beutler, S. F. Lowry, J. Merryweather, S. Wolpe, I. W. Milsark, R. J. Hariri, T. J. Fahey III, A. Zentella, J. D. Albert, G. T. Shires, and A. Cerami. 1986. Shock and tissue injury induced by recombinant human cachectin. Science 234:470–474.
26. Vogel, S. N., S. D. Douches, E. N. Kaufman, and R. Neta. 1987. Induction of colony stimulating factor *in vivo* by recombinant interleukin 1α and tumor necrosis factor α. J. Immunol. 138: 2143–2148.
27. Vogel, S. N., and E. A. Havell. 1990. Differential inhibition of lipopolysaccharide induced phenomena by anti-tumor necrosis factor alpha antibody. Infect. Immun. 58:2397–2400.
28. Vogel, S. N., and M. M. Hogan. 1990. The role of cytokines in endotoxin-mediated responses. p. 238–258. *In* J. J. Oppenheim and E. Shevach (ed.), Immunophysiology. role of cells and cytokines in immunity and inflammation. Oxford University Press, Oxford.
29. Vogel, S. N., E. N. Kaufman, M. D. Tate, and R. Neta. 1988. Recombinant interleukin 1α and recombinant tumor necrosis factor α synergize in vivo to induce early endotoxin tolerance and associated hematopoietic changes. Infect. Immun. 56:2650–2657.
30. Wolfe, R. R., D. Elahi, and J. J. Spitzer. 1977. Glucose and lactate kinetics after endotoxin administration in dogs. Am. J. Physiol. 232:E180–E185.
31. Yelich, M. R., H. S. Havdala, and J. P. Filkins. 1987. Dexamethasone alters glucose, lactate, and insulin dyshomeostasis during endotoxicosis in the rat. Circ. Shock 22:155–171.

DISTRIBUTION LIST

DEPARTMENT OF DEFENSE

ARMED FORCES INSTITUTE OF PATHOLOGY
ATTN: RADIOLOGIC PATHOLOGY DEPARTMENT

ARMED FORCES RADIOBIOLOGY RESEARCH INSTITUTE
ATTN: PUBLICATIONS DIVISION

ARMY/AIR FORCE JOINT MEDICAL LIBRARY
ATTN: DASG-AAFJML

ASSISTANT TO SECRETARY OF DEFENSE
ATTN: AE
ATTN: HA(IA)

DEFENSE NUCLEAR AGENCY
ATTN: TITL
ATTN: DDIR

DEFENSE TECHNICAL INFORMATION CENTER
ATTN: DTIC-DDAC
ATTN: DTIC-FDAC

FIELD COMMAND DEFENSE NUCLEAR AGENCY
ATTN: FCFS

INTERSERVICE NUCLEAR WEAPONS SCHOOL
ATTN: RH

LAWRENCE LIVERMORE NATIONAL LABORATORY
ATTN: LIBRARY

UNDER SECRETARY OF DEFENSE (ACQUISITION)
ATTN: OUSD(A)/R&AT

DEPARTMENT OF THE ARMY

HARRY DIAMOND LABORATORIES
ATTN: SLCHD-NW
ATTN: SLCSM-SE

LETTERMAN ARMY INSTITUTE OF RESEARCH
ATTN: SGRD-UL-B1-R

SURGEON GENERAL OF THE ARMY
ATTN: MEDDH-N

U.S. ARMY AEROMEDICAL RESEARCH LABORATORY
ATTN: SCIENTIFIC INFORMATION CENTER

U.S. ARMY ACADEMY OF HEALTH SCIENCES
ATTN: HSHA-CDF

U.S. ARMY CHEMICAL RESEARCH, DEVELOPMENT, AND ENGINEERING CENTER
ATTN: DIRECTOR OF RESEARCH

U.S. ARMY INSTITUTE OF SURGICAL RESEARCH
ATTN: DIRECTOR OF RESEARCH

U.S. ARMY MEDICAL RESEARCH INSTITUTE OF CHEMICAL DEFENSE
ATTN: SGRD-UV-R

U.S. ARMY NUCLEAR AND CHEMICAL AGENCY
ATTN: MONA-NU

U.S. ARMY RESEARCH INSTITUTE OF ENVIRONMENTAL MEDICINE
ATTN: DIRECTOR OF RESEARCH

U.S. ARMY RESEARCH OFFICE
ATTN: BIOLOGICAL SCIENCES PROGRAM

WALTER REED ARMY INSTITUTE OF RESEARCH
ATTN: DIVISION OF EXPERIMENTAL THERAPEUTICS

DEPARTMENT OF THE NAVY

NAVAL AEROSPACE MEDICAL RESEARCH LABORATORY
ATTN: COMMANDING OFFICER

NAVAL MEDICAL COMMAND
ATTN: MEDCOM-21

NAVAL MEDICAL RESEARCH AND DEVELOPMENT COMMAND
ATTN: CODE 40C

OFFICE OF NAVAL RESEARCH
ATTN: BIOLOGICAL SCIENCES DIVISION

DEPARTMENT OF THE AIR FORCE

BOLLING AIR FORCE BASE
ATTN: AFOSR

BROOKS AIR FORCE BASE
ATTN: USAFOEHL/RZ
ATTN: USAFSAM/RZ
ATTN: USAFSAM/RZB

NUCLEAR CRITERIA GROUP, SECRETARIAT
ATTN: WL/NTN

SURGEON GENERAL OF THE AIR FORCE
ATTN: HQ USAF/SGPT
ATTN: HQ USAF/SGES

U.S. AIR FORCE ACADEMY
ATTN: HQ USAFA/DFBL

OTHER FEDERAL GOVERNMENT

BROOKHAVEN NATIONAL LABORATORY
ATTN: RESEARCH LIBRARY, REPORTS SECTION

CENTER FOR DEVICES AND RADIOLOGICAL HEALTH
ATTN: HFZ-110

DEPARTMENT OF ENERGY
ATTN: ER-72 GTN

GOVERNMENT PRINTING OFFICE
ATTN: DEPOSITORY RECEIVING SECTION
ATTN: CONSIGNED BRANCH

LIBRARY OF CONGRESS
ATTN: UNIT X

LOS ALAMOS NATIONAL LABORATORY
ATTN: REPORT LIBRARY/P364

NATIONAL AERONAUTICS AND SPACE ADMINISTRATION
ATTN: RADLAB

NATIONAL AERONAUTICS AND SPACE ADMINISTRATION,
GODDARD SPACE FLIGHT CENTER
ATTN: LIBRARY

NATIONAL CANCER INSTITUTE
ATTN: RADIATION RESEARCH PROGRAM

NATIONAL LIBRARY OF MEDICINE
ATTN: OPI

U.S. ATOMIC ENERGY COMMISSION
ATTN: BETHESDA TECHNICAL LIBRARY

U.S. FOOD AND DRUG ADMINISTRATION
ATTN: WINCHESTER ENGINEERING AND
ANALYTICAL CENTER

U.S. NUCLEAR REGULATORY COMMISSION
ATTN: LIBRARY

RESEARCH AND OTHER ORGANIZATIONS

BRITISH LIBRARY (SERIAL ACQUISITIONS)
ATTN: DOCUMENT SUPPLY CENTRE

CENTRE DE RECHERCHES DU SERVICE DE SANTE DES
ARMEES
ATTN: DIRECTOR

INHALATION TOXICOLOGY RESEARCH INSTITUTE
ATTN: LIBRARY

INSTITUT FUR RADIOBIOLOGIE
ACADEMIE DES SANITATS UND GESUNHEITSWESESNS DER
BW (WEST GERMANY)
ATTN: DIRECTOR

KAMAN TEMPO
ATTN: DASIAC

NBC DEFENSE RESEARCH AND DEVELOPMENT CENTER OF
THE FEDERAL ARMED FORCES (WEST GERMANY)
ATTN: WWDBW ABC-SCHUTZ

NCTR-ASSOCIATED UNIVERSITIES
ATTN: EXECUTIVE DIRECTOR

RUTGERS UNIVERSITY
ATTN: LIBRARY OF SCIENCE AND MEDICINE

UNIVERSITY OF CALIFORNIA
ATTN: LABORATORY FOR ENERGY-RELATED
HEALTH RESEARCH
ATTN: LAWRENCE BERKELEY LABORATORY

UNIVERSITY OF CINCINNATI
ATTN: UNIVERSITY HOSPITAL, RADIOISOTOPE
LABORATORY